NOTE TO USERS

The original manuscript received by UMI contains pages with indistinct and/or slanted print. Pages were microfilmed as received.

This reproduction is the best copy available

UMI

University of Alberta

Characterization of Dimethylsulfoxide, Pyridine N-oxide, and Trimethylamine N-oxide Reductases of *Escherichia coli*

by

Joanne Lisa Simala-Grant

©

A thesis submitted to the Faculty of Graduate Studies and Research in partial fulfillment of the requirements for the degree of Doctor of Philosophy

Department of Biochemistry

Edmonton, Alberta
1998

National Library
of Canada

Acquisitions and
Bibliographic Services

395 Wellington Street
Ottawa ON K1A 0N4
Canada

Bibliothèque nationale
du Canada

Acquisitions et
services bibliographiques

395, rue Wellington
Ottawa ON K1A 0N4
Canada

Your file Votre référence

Our file Notre référence

The author has granted a non-exclusive licence allowing the National Library of Canada to reproduce, loan, distribute or sell copies of this thesis in microform, paper or electronic formats.

The author retains ownership of the copyright in this thesis. Neither the thesis nor substantial extracts from it may be printed or otherwise reproduced without the author's permission.

L'auteur a accordé une licence non exclusive permettant à la Bibliothèque nationale du Canada de reproduire, prêter, distribuer ou vendre des copies de cette thèse sous la forme de microfiche/film, de reproduction sur papier ou sur format électronique.

L'auteur conserve la propriété du droit d'auteur qui protège cette thèse. Ni la thèse ni des extraits substantiels de celle-ci ne doivent être imprimés ou autrement reproduits sans son autorisation.

0-612-29109-X

Canada

University of Alberta
Faculty of Graduate Studies and Research

The undersigned certify that they have read, and recommend to the Faculty of Graduate Studies and Research for acceptance, a thesis entitled Characterization of *Escherichia coli* Dimethylsulfoxide, Pyridine N-oxide, and Trimethylamine N-oxide Reductases of *Escherichia coli*, submitted by Joanne Lisa Simala-Grant in partial fulfillment of the requirements for the degree of Doctor of Philosophy.

Joel H Weiner
Dr. Joel Weiner

Glen Armstrong
Dr. Glen Armstrong

DN Brindley
Dr. David Brindley

Dr. Carol Cass

G Voordouw
Dr. Gerrit Voordouw

Date: March 12, 1998

In appreciation of the most important people in the world,

Steve Simala-Grant and John and Betty Simala.

Abstract

E. coli dimethylsulfoxide reductase (DmsABC) is a trimeric iron-sulfur molybdoenzyme that allows respiratory growth on S- and N-oxides. Absorption and fluorescence spectroscopy was employed, and indicated DmsABC binds molybdopterin guanine dinucleotide (MGD).

A soluble form of DmsABC, missing the membrane anchor (DmsC), is found in the cytoplasm (DmsAB). Examination of the properties of DmsAB, and reconstitution of MGD into apo-DmsAB, confirmed the instability of DmsAB in comparison with DmsABC. These data implicated DmsC in the stabilization of DmsABC.

Determination of the correct initiating Met for DmsA indicated DmsA possesses a leader with a double-arginine consensus, suggested to be important for membrane targeting and translocation of a subset of redox cofactor containing proteins. Examination of DmsABC with truncated, deleted, or mutated double-arginine consensus leader, demonstrated the leader and consensus within, are essential for production of functional enzyme.

Open, closed, and nuclear magnetic resonance spectroscopic assays were examined for use with DmsABC. Investigation suggested dithionite was both a competitive and irreversible inhibitor. The kinetic constants for DmsABC were determined for both the electron donor, and electron acceptor portions of the reaction. This showed DmsABC's very broad electron acceptor specificity for S- and N-oxides and miscellaneous

compounds. This was demonstrated to contrast trimethylamine N-oxide reductase (TorA), as it was shown to reduce only a few N-oxides.

Examination of the crystal structure of dimethylsulfoxide reductase from *Rhodobacter sphaeroides* (DMSOR), and comparison of the homologous DmsA and DMSOR sequences, revealed potential DmsA active site residues. Site-directed mutagenesis was employed to alter these residues in DmsA. Kinetic analysis demonstrated T148, A178, and R217 altered the electron acceptor K_m, suggesting a role in substrate binding. G167 and Q179I decreased the k_{cat} for DMN, and abolished growth on Gly/DMSO, suggesting a role in electron transfer.

Examination of respiratory growth of *E. coli* not expressing DmsABC or TorA, indicated the presence of an additional previously unidentified anaerobically expressed energy conserving terminal reductase. It allowed for anaerobic growth on substituted pyridine N-oxides. The enzyme responsible, pyridine N-oxide reductase, was characterized, and appears to be a cytoplasmic molybdoenzyme.

Acknowledgments

I would like to thank my supervisor Joel Weiner, for providing me with an environment where there was room to grow and develop as a scientist and individual. He provided guidance, while at the same time allowed me to make my own choices. I was given the opportunity to make mistakes, and take responsibility for my actions.

I am grateful to Catherine Trieber, Raymond Turner, and Richard Rothery, for helpful advice and useful discussions during my time in the laboratory. They were more than willing to answer my numerous questions, and aid me in any way they could! In addition, Gillian Shaw provided technical assistance as needed. I have appreciated the efforts of Chantelle Gwozd in editing and improving my thesis, and also Christine Wiebe for reading my introduction.

I am indebted to the following people for their assistance with the following : Colin Bigam and Dr. Sykes, for NMR spectroscopy; Ruthvin Lewis, for synthesis of biotin sulfoxide; Ernst Bergman for a beautiful computer picture in Chapter 7; Dr. Jed Harrison for use of his computer; Marcia Craig and Dr. Holmes for help with, and use of their HPLC; Dr. Randy Irvin for the use of his HPLC; Drs. Brindley and Cass for reviewing my work yearly as part of my committee; and the Group in the Molecular Biology of Membranes for giving me numerous opportunities to present my research .

I would like to acknowledge our collaborators : Dr. Gerard Giordano, and Janine Pommier from the CNRS in Marseille France; Drs Rajagopalan, and Johnson from Duke Medical Center, and Dr. Campbell from Stanford University.

The Department of Biochemistry has provided assistance as needed, and I have appreciated the support I have been given over the years. It has been a pleasure to be part of a department that has so much to offer.

I would like to thank my parents who always believed in me, and ingrained in me the belief that I could achieve anything I set my mind to. I am indebted to them for the moral and financial support they have given me over the years.

My husband Steve has been a wonderful support and source of encouragement over the years! He has continually opened my eyes to true meaning of life. Without him, this endeavor would not have been much fun at all. He makes me laugh and smile, whether I want to or not!

I am very appreciative to the National Science and Engineering Research Council, the Alberta Heritage Foundation for Medical Research, the University of Alberta, and the Department of Biochemistry for financial support.

Table of Contents

Chapter 1 : Introduction

1.1. Introduction 1

1.2. Respiration 2

1.2.1. Energy Transduction 2

1.2.2. Mechanisms of Proton Translocation 2

1.3. Respiration in *E. coli* 4

1.3.1. Modularity of Redox Components 4

1.3.2. Transcriptional Regulation of Respiratory Enzymes 6

1.3.2.1. NarX/L and NarQ/P 8

1.3.2.2. ArcA/B 9

1.3.2.3. FNR 9

1.3.3. Prosthetic Groups in Respiratory Enzymes 10

1.3.3.1. Hemes 10

1.3.3.2. Fe-S clusters 10

1.3.3.3. Moco 12

1.3.4. Translocation of Respiratory Enzymes Across the Cytoplasmic Membrane 14

1.3.5. Transport of Substrates to the Cytoplasm 16

1.3.6. Electron Transport Chain Components 16

1.3.6.1. Q 16

1.3.6.2. Primary Dehydrogenases Using Various Substrates 17

1.3.6.2.1. Proline 17

1.3.6.2.2. Pyruvate 17

1.3.6.2.3. D- and L-lactate 19

1.3.6.2.4. Glucose 19

1.3.6.2.5. Gly-3-P 19

1.3.6.2.6. Succinate 20

1.3.6.2.7. Formate 20

1.3.6.2.8. H_2 21

1.3.6.2.9. NADH 21

1.3.6.3. Terminal Reductases Using Various Substrates 21

1.3.6.3.1. O_2 21

1.3.6.3.2. Nitrite 22

1.3.6.3.3. Fumarate 22

1.3.6.3.4. Nitrate 23

1.3.6.3.5. S- and N-oxides 24

1.4. Bacterial Utilization of S- and N-oxides 25

1.4.1. Ecology of Substrates 25

1.4.2. Bacterial DMSO/TMAO Reduction 26

1.4.3. *Rhodobacter sphaeroides* DMSO Reductase 27

1.4.4. S- and N-oxide Reduction in *E. coli* 28

1.5. DmsABC 30

1.5.1. Bioenergetics of Growth on DMSO 30

1.5.1.1. *In vivo* Electron Donors and Acceptors 30

1.5.1.2. H^+/e^- Ratio and Model for the Generation of a Proton Gradient 30

1.5.2. Molecular Genetics of the *dms* Operon 31

1.5.2.1. Structure and Organization of the *dms* Operon ... 31

1.5.2.2. Other Genes Required for DmsABC 32

1.5.3. Expression of DmsABC....32

1.5.3.1. Expression of Wild-Type Chromosomal DmsABC....32

1.5.3.2. Mutant Chromosomal and Plasmid Encoded DmsABC Expression....33

1.5.4. Enzymology of DMSO Reductase....33

1.5.5. Topological Organization of DmsABC....34

1.5.5.1. Topological Organization of DmsABC with Respect to the Membrane....34

1.5.5.2. Topological Organization of DmsA, DmsB, and DmsC with Respect to Each Other....36

1.5.6. DmsC....36

1.5.6.1. Topology of DmsC....36

1.5.6.2. DmsC Anchors DmsAB to the Membrane....37

1.5.6.3. DmsAB is More Stable in the Presence of DmsC....37

1.5.6.4. DmsC is Responsible for MQ Binding....37

1.5.6.5. The Role of DmsC in Electron and Proton Transfer....38

1.5.7. DmsB....41

1.5.7.1. DmsB is an Fe-S protein....41

1.5.7.2. Mutagenesis of DmsB Cys Residues to Define the Cys Groups (I-IV) that Ligate Each of the Four Fe-S Clusters (1-4)....43

1.5.7.3. Electron Flow Through DmsB....46

1.5.8. DmsA....45

1.5.8.1. DmsABC is a Molybdoenzyme....46

1.5.8.2. DmsA Binds Moco....47

1.5.8.3. Engineering a Novel Fe-S Cluster into DmsA....49

1.5.8.4. Electron Transfer Through DmsA....50

1.5.8.5. The Protein Ligand of Mo 50

1.6. Thesis Objectives 51

1.7. References 54

Chapter 2 : Characterization of DmsAB

2.1. Introduction 83

2.2. Materials and Methods 84

2.2.1. Materials 84

2.2.2. Strains and Plasmids 84

2.2.3. Media and Growth Conditions 86

2.2.4. Preparation of Membrane and Supernatant Fractions 86

2.2.5. Enzyme Assays 86

2.2.6. Separation of Low and High Molecular Weight Fractions 87

2.2.7. Purification of DmsAB 87

2.2.7.1. Ammonium Sulfate Precipitation 88

2.2.7.2. Heat Purification of DmsAB 88

2.2.7.3. Whatman DE-52 Column 88

2.2.8. Stability/Stabilization of DmsAB/DmsABC 89

2.2.9. Reconstitution of DmsAB and NarGH from *moa* and *mob* Mutants 89

2.2.10. Analytical Techniques 89

2.3. Results 90

2.3.1. Localization of DmsAB in Supernatant and Membrane Fractions 90

2.3.2. TMAO Reductase Activity is Found in the High Molecular Weight Fraction.......92

2.3.3. Preliminary Purification of DmsAB.......92

2.3.4. Stability and Stabilization of DmsAB/DmsABC.......94

2.3.5. Attempted Purification of DmsAB.......97

2.3.6. Reconstitution of DmsAB.......100

2.4. Discussion.......100

2.5. References.......105

Chapter 3 : Structural Characterization and Quantitation of the Moco in Purified DmsA

3.1. Introduction.......110

3.2. Materials and Methods.......111

3.2.1. Materials.......111

3.2.2. Strains and Plasmids.......111

3.2.3. Media and Growth Conditions.......112

3.2.4. Purification of DmsABC.......112

3.2.5. Purification of DMSOR.......112

3.2.6. Identification of Moco Structure.......112

3.2.7. Quantitation of MPT in DmsABC.......113

3.2.8. Analytical Techniques.......113

3.3. Results.......113

3.3.1. Identification of Moco Structure in DmsABC.......113

3.3.2. Quantitation of MPT in DmsABC.......115

3.4. Discussion.......118

3.5. References 120

Chapter 4 : Mutation of the DmsA Leader Sequence and Analysis by Growth, Accumulation, and Expression Studies

4.1. Introduction 124

4.2. Materials and Methods 126

  4.2.1. Materials 126

  4.2.2. Strains and Plasmids 126

  4.2.3. Analysis of the DmsA Upstream Region for Leader Peptidase I Cleavage Sites 130

  4.2.4. Site-directed Mutagenesis of the DmsA Leader Sequence 130

  4.2.5. PCR of DmsA and Subsequent Cloning into pMS119EH 130

  4.2.6. Media and Growth Conditions 131

  4.2.7. Quantitative and Qualitative Anaerobic Growth Experiments 131

  4.2.8. Aerobic Expression of DmsABC from the T7 Promoter 132

  4.2.9. Aerobic Expression of DmsABC from the tac Promoter 132

  4.2.10. Preparation of Membrane and Supernatant Fractions 132

  4.2.11. Analytical Techniques 132

4.3. Results 133

  4.3.1. Site-directed Mutagenesis of the Newly Proposed Initiating Met (M^{-}29) for DmsA 133

  4.3.2. Anaerobic Growth of M^{-}29Stop on Gly/DMSO 133

  4.3.3. Anaerobic Accumulation of M^{-}29Stop DmsABC 134

4.3.4. Aerobic T7 Promoter Driven Expression of M^{-}29Stop DmsA and DmsB 136

4.3.5. PCR Mutagenesis and Cloning of DmsABC to Generate DmsA Expressed from the *tac* Promoter Initiating at M^{-}29 or M1 136

4.3.6. Qualitative Anaerobic Growth on Gly/DMSO for DSS301 with pDMSP$_{tac}$M^{-}29 and pDMSP$_{tac}$M1 138

4.3.7. Aerobic Expression of DmsA and DmsB from the *tac* Promoter in pDMSP$_{tac}$M^{-}29 and pDMSP$_{tac}$M1 138

4.3.8. PCR Mutagenesis and Cloning of DmsABC to Generate a Construct Where DmsA is Missing its Leader Sequence 140

4.3.9. Qualitative Anaerobic Growth of DSS301/pDMS119P$_{tac}$A16M on Gly/DMSO 143

4.3.10. Aerobic Expression of DmsA and DmsB from the *tac* Promoter in pDMS119P$_{tac}$A16M 143

4.3.11. Site-Directed Mutagenesis of the Double-Arginine Consensus in DmsA 144

4.3.12. Anaerobic Growth of DSS301/pDMS160R^{-}13D on Gly/DMSO 145

4.3.13. Anaerobic Accumulation of R^{-}13D DmsABC 145

4.3.14. Aerobic T7 Promoter Driven Expression of R^{-}13D DmsA and DmsB 146

4.3.15. Analysis of Potential DmsA Leader Sequences 146

4.3.16. Creation of Cleavage Site Mutants 146

4.3.17. Anaerobic Growth of Cleavage Site Mutants on Gly/DMSO 147

4.4. Discussion 147

4.5. References 154

Chapter 5 : DmsABC Assay Characterization and Development

5.1. Introduction 160

5.2. Methods and Materials 162

5.2.1. Materials 162
5.2.2. Strains and Plasmids 162
5.2.3. Media and Growth Conditions 162
5.2.4. Purification of DmsABC 162
5.2.5. Kinetic Assays 163
5.2.6. Analytical Techniques 165

5.3. Results 165

5.3.1. Dithionite Inhibits DmsABC 165
5.3.2. Glycerol Depresses Apparent K_m and V_{max} Values 169
5.3.3. Apparent K_m and k_{cat} Values for BVH + And $DMNH_2$ 169
5.3.4. DmsABC Kinetic Assay Using NMR Spectroscopy 172

5.4. Discussion 179

5.5. References 181

Chapter 6 : Analysis of the Substrate Specificity of DmsABC

6.1. Introduction 189

6.2. Materials And Methods 190

6.2.1. Materials 190
6.2.2. Strains and Plasmids 190
6.2.3. Media and Growth Conditions 190
6.2.4. Toxicity of DmsABC Substrates as Indicated by Inhibition of Anaerobic Growth 192
6.2.5. Purification of DmsABC 192

6.2.6. Kinetic Analysis 193

6.2.7. Analytical Techniques 194

6.3. Results 194

6.3.1. Utilization of N-oxides by DmsABC 194

6.3.2. Utilization of S-oxides 196

6.3.3. Utilization of Inorganic Anions and Miscellaneous Substrates 198

6.3.4. Inhibition of DmsABC Activity 198

6.3.5. Growth Inhibition by S- and N-oxides 199

6.3.6. Ability of S- and N-oxides to Act as Terminal Electron Acceptors 199

6.3.7. Membrane Permeability of Non-Toxic DmsABC Substrates Unable to Support Anaerobic Growth on Glycerol 200

6.4. Discussion 200

6.5. References 206

Chapter 7 : Modulation of the Substrate Specificity of DmsABC

7.1. Introduction 211

7.2. Materials And Methods 213

7.2.1. Materials 213

7.2.2. Strains and Plasmids 213

7.2.3. Sequence Analysis 213

7.2.4. Molecular Modeling 213

7.2.5. Site-Directed Mutagenesis 215

7.2.6. Media and Growth Conditions 215

7.2.7. Membrane Preparation 215

7.2.8. Kinetic Analysis 217

7.2.9. Analytical Techniques 217

7.3. Results 218

7.3.1. Sequence Analysis, Molecular Modeling, and Primer Design 218

7.3.2. Preparation of Mutants in DmsABC 220

7.3.3. Accumulation of Wild-Type and Mutant DmsABC in DSS301 220

7.3.4. Growth Characteristics of DSS301 Harboring Plasmid Containing Wild-Type or Mutant DmsABC 221

7.3.5. Kinetic Characteristics of Mutant and Wild-type DmsABC with BV 221

7.3.6. k_{cat} for Mutant and Wild-Type DmsABC with Saturating $DMNH_2$ and DMSO 224

7.4. Discussion 225

7.4. References 228

Chapter 8 : Elucidation and Identification of a Previously Uncharacterized Terminal N-oxide Reductase

8.1. Introduction 233

8.2. Materials and Methods 234

8.2.1. Materials 234

8.2.2. Strains and Plasmids 235

8.2.3. Media and Growth Conditions 235

8.2.4. Preparation of Membrane and Supernatant Fractions 237

8.2.5. Enzyme Assays 237

8.2.5.1. Assays for Reductase Activity 238

8.2.5.2. Assays for Electron Donor Activity 238

8.2.5.3. β-lactamase Assays 239

8.2.6. Localization of PNOR Activity 239

8.2.7. Stability of PNOR Activity 240

8.2.7.1. Stability at 4°C 240

8.2.7.2. Stability to Freeze/Thaw 240

8.2.8. PNOR Activity Staining of Native-Polyacrylamide Gels 240

8.2.9. Purification of PNOR 241

8.2.9.1. Heat Purification 241

8.2.9.2. Ammonium Sulfate Precipitation 241

8.2.9.3. Desalting 241

8.2.9.4. MonoQ FPLC 241

8.2.10. Isolation and Analysis of DSS501-3 242

8.2.11. DNA Sequence Analysis 243

8.2.12. Analytical Techniques 243

8.3. Results 244

8.3.1. Ability of Wild-Type and Mutant *E. coli* to Grow on S- and N-oxides in the Presence of Glycerol 244

8.3.2. Anaerobic Growth of DSS501 on Gly/PNO is Abolished by the Addition of Tungstate 246

8.3.3. PNO Does not act as an Electron Sink During Growth on Glucose 246

8.3.4. Expression of PNOR Activity 246

8.3.5. Localization of PNOR Activity 248

8.2.6. Characterization of PNOR Activity 251

8.3.7. Stability of PNOR Activity 255

8.3.8. PNOR Activity is Protein Mediated and is Distinct from DmsABC 255

8.3.9. Purification of PNOR 258

8.3.10. Isolation of a Mutant with Increased PNOR Activity 260

8.3.11. Sequence Analysis of the *E. coli* Chromosome for Previously Unidentified Molybdoenzymes 260

8.4. Discussion 269

8.5. References 278

Chapter 9 : Kinetic Analysis and Substrate Specificity of *E. coli* TorA

9.1. Introduction 285

9.2. Materials and Methods 286

9.2.1. Materials 286

9.2.2. Strains 286

9.2.3. Media Preparation and Crude Extracts 287

9.2.4. Purification of TorA 287

9.2.5. Enzyme Assays and Determination of Kinetic Parameters 287

9.3. Results 288

9.3.1. Kinetic Analysis 288

9.4. Discussion 290

9.5. References 295

Chapter 10 : Conclusions, Discussion, and Future Directions

10.1. Conclusions 298

10.2. Discussion 301

10.2.1. The Role of S- and N-oxide Reductases in Respiratory Growth in *E. coli* 301

10.2.2. Stability of DmsABC 301

10.2.3. Assembly of Moco into DmsABC 302

10.2.4. Double-Arginine Consensus 303

10.3. Future Directions 304

10.3.1. DmsC 305

10.3.2. DmsB 306

10.3.3. DmsA 307

10.3.4. PNOR 308

10.3.5. The Double-Arginine Consensus and the MTT Apparatus 309

10.4. References 310

Appendix : Inability of BisC to Complement a Deletion of DmsABC

A.1. Introduction 317

A.2. Materials and Methods 317

A.2.1. Materials 318

A.2.2. Strains and Plasmids 318

A.2.3. Media and Growth Conditions 318

A.3. Results 319

A.3.1. Anaerobic Growth of DSS501/ pBRBISC352 on Gly/DMSO 319

A.4. Discussion 319

A.5. References 319

List of Tables

Table 1.1. Midpoint Potentials at pH 7.0 ($E_{m,7}$) of Some Electron Donor and Acceptor Couples 7

Table 2.1. *E. coli* Strains and Plasmids Used in This Study 85

Table 2.2. TMAO Reductase Activity in Various Strains and Fractions From Cells Grown Anaerobically on Gly/Fum 91

Table 2.3. Stabilization of DmsAB in HB101/pDMS160 Supernatant 95

Table 2.4. Stabilization of DmsABC 98

Table 2.5. Reconstitution of DmsAB and NarGH Using *moa*$^-$ (AP15) and *mob*$^-$ (RK5208/pDMS160) Supernatants 102

Table 3.1. FormA Fluorescence from Equivalent Amounts of DmsABC and DMSOR 119

Table 4.1. *E. coli* Strains Used in this Study 128

Table 4.2. Plasmids and Phage Used in this Study 129

Table 4.3. Qualitative Anaerobic Growth on Gly/DMSO of DSS301 Transformed with *tac* Constructs 139

Table 5.1. TMAO K_m's for DmsABC, Using Open and Closed Cuvette Assays 166

Table 5.2. TMAO K_m and V_{max} for Purified DmsABC, Using Increasing Concentrations of Glycerol in the Open Cuvette Assay 171

Table 5.3. Electron Donor K_m and k_{cat} for DmsABC, with Saturating Electron Acceptor 173

Table 6.1. Kinetic Parameters for N-oxide Substrates of DmsABC, and Their Ability to Support or Inhibit Growth 191

Table 6.2. Kinetic Parameters for S-oxide Substrates of DmsABC, and Their Ability to Support or Inhibit Growth 197

Table 7.1. Bacterial Strains and Plasmids 214

Table 7.2. Primers for Site-directed Mutagenesis, Mutants Obtained in DmsA, and the Corresponding Residues in DMSOR 216

Table 7.3. Growth Properties and Accumulation of DmsABC Mutants 222

Table 7.4. Kinetic Parameters for DmsABC Mutants with $BVH^{\cdot+}$ or $DMNH_2$ as Electron Donor 223

Table 8.1. *E. coli* Strains Used in this Study 236

Table 8.2. PNOR Specific Activity in DSS501 Grown Anaerobically on Gly/Fum for Increasing Amounts of Time 249

Table 8.3. Effect of the Inclusion of Substituted PNO's on PNOR Activity in DSS501 Grown Anaerobically on Gly/Fum... 250

Table 8.4. Localization of Enzyme Activities in Anaerobically Grown DSS501 252

Table 8.5. PNOR Activity from Anaerobically Grown DSS501 253

Table 8.6. %PNOR Activity Remaining After 21 Hours at 4°C 256

Table 8.7. Sequence from the Complete *E. coli* Genome Homologous to DmsA 262

Table 9.1. Kinetic Parameters for N- and S-oxide Substrates of TorA 289

Table 9.2. Ability of N- and S-oxide's to Inhibit Reduction of TMAO by TorA 291

List of Figures

Figure 1.1. Scalar and Vectorial Mechanisms of Proton Translocation 3

Figure 1.2. Modularity of the *E. coli* Respiratory System 5

Figure 1.3. Structures of [2Fe-2S], [3Fe-4S], and [4Fe-4S] Clusters 11

Figure 1.4. Structures of Moco Derivatives 13

Figure 1.5. Biosynthetic Pathway for Moco in *E. coli* 15

Figure 1.6. Structures of the Oxidized forms of UQ, DMQ and MQ 18

Figure 1.7. Proposed Reaction Mechanism for DMSOR 29

Figure 1.8. Schematic of MQH_2 Binding to DmsC and Electron Transfer to DmsB 40

Figure 1.9. Gene Insertion and Gene Duplication Models for Fe-S Cluster Binding in DmsB 42

Figure 1.10. Blocks of Sequence Homology are Shared Between Prokaryotic Moco Containing Enzymes 48

Figure 2.1. Loss of DmsAB Activity in HB101/pDMS160 Supernatant Over Time at 52 and 62°C 93

Figure 2.2. pH Stability Profile for DmsAB in HB101/pDMS160 Supernatant 96

Figure 2.3. Purification of DmsAB using a Whatman DE-52 Column 99

Figure 2.4. Schematic of DmsAB Reconstitution Using RK5208/pDMS160 and AP15 Supernatants 101

Figure 3.1. Fluorescence Excitation and Emission Spectra of FormA from HB101/pDMS160 (top) and RK5208/pDMS160 (bottom) Membranes 114

Figure 3.2. Absorption Spectra of Oxidized Cam Derivative Prepared from Purified DmsABC in 50 mM Ammonium Acetate (pH 6.8) 116

Figure 3.3. Absorption Spectra of Gentle-FormA Derivative from Purified DmsABC in 50 mM Ammonium Acetate (pH 6.8) 117

Figure 4.1. Schematic of the DmsA Leader Sequence - Growth and Accumulation Data for Leader Sequence Mutants and *tac* Constructs 127

Figure 4.2. Western Blot Analysis for DmsA and DmsB Expressed Anaerobically from Their Natural Promoter for Wild-Type, $M^{-}29$, and $R^{-}13D$ Mutants 135

Figure 4.3. Western Analysis of DmsA and DmsB Expressed Aerobically from the T7 Promoter for Wild-Type, $M^{-}29$Stop and $R^{-}13D$ Mutants 137

Figure 4.4. SDS-polyacrylamide gel of Aerobically Expressed DmsABC from *tac* Promoter Constructs 141

Figure 4.5. Western Analysis of Aerobically Expressed DmsABC from *tac* Promoter Constructs Probed with DmsA Antibody 142

Figure 4.6. Alignment of Amino Acid Sequences of DMSO Reductases from *E. coli* and *H. influenza* 149

Figure 4.7. Double-Arginine Leader Dependent Membrane Targeting and Translocation Model for Cytoplasmic and Periplasmic Proteins 151

Figure 5.1. TMAO K_m and V_{max} Values for Purified DmsABC Using the Closed Cuvette Assay with Increasing Concentrations of Dithionite 168

Figure 5.2. TMAO K_m and V_{max} Values for Purified DmsABC, with Increasing Concentrations of Glycerol in the Assay Buffer 170

Figure 5.3. DmsABC Kinetic NMR Spectra with TMAO as Substrate 175

Figure 5.4. DmsABC Kinetic NMR Spectra Using DMSO as Substrate 176

Figure 5.5. TMA Peaks and Corresponding Integrals Over Time 177

Figure 5.6. TMA Integral Height is Linear With Time, and Two Concentrations of DmsABC 178

Figure 6.1. Structures of Various S- and N-oxides 195

Figure 6.2. K_m Versus k_{cat} for DmsABC Substrates 200

Figure 6.3. K_m Versus k_{cat}/K_m for Substrates of DmsABC........201

Figure 6.4. Comparison of K_m and k_{cat} Values for Various PNO Substrates of DmsABC........202

Figure 7.1. Sequence Alignment of *E. coli* (*dmsA*) and *R. sphaeroides* (*DMSOR*) DMSO Reductases Using GAP........219

Figure 7.2. Modeling of DMSOR Active Site Residues........227

Figure 8.1. Anaerobic Growth of Wild-Type *E. coli* and Selected Mutants on S- and N-oxide Substrates with Glycerol as the Electron Donor and Carbon Source 245

Figure 8.2. Anaerobic Growth of DSS501 on Glucose Minimal Media +/- PNO 247

Figure 8.3. Optimization of PNOR Activity Using Various Buffers at Various pH's for the BV/PNOR Assay........254

Figure 8.4. Native-PAGE, SDS-PAGE, and Western Blot Analysis of DSS501 Supernatant Grown Anaerobically on Gly/Fum........257

Figure 8.5. Alignment of the Amino Acid Sequences for DmsA, orf808A, and orf808B........263-266

Figure 8.6. Alignment of the Amino Acid Sequences for DmsB and orf205 267

Figure 8.7. Alignment of the Amino Acid Sequences for DmsC and orf207 268

Figure 8.8. 5' Untranslated Region for orf1-4 at 35.60 minutes on the *E. coli* Chromosome 270

Figure 9.1. Substrates of TorA Arranged in Order of Increasing K_m Versus k_{cat} Value 293

Figure 9.2. Substrates of TorA Arranged in Order of Increasing K_m Versus k_{cat}/K_m Value 294

Figure A.1. Anaerobic Growth of HB101 and DSS501, With or Without pBRBISC352, on Gly/DMSO Media 320

List of Abbreviations

AMP	adenosine monophosphate
ANO	adenosine N-oxide
APMSF	(4-amidino-phenyl)methane-sulfonyl fluoride
ATP	adenosine triphosphate
BICINE	N,N-bis[2hydroxyethyl]glycine
BisC	*Escherichia coli biotin* sulfoxide reductase
BIS-TRIS	bis-[2-hydroxyethyl]imino-tris[hydroxymethyl]methane; 2-bis[2hydroxyethyl]amino-2hydroxymethyl]-1,3propanediol
BisZ	*Escherichia coli* alternative biotin sulfoxide reductase
bp	base pair
BV	benzyl viologen
BV^{2+}/$BVH^{\cdot +}$	oxidized and reduced benzyl viologen
cam	carboxyamidomethyl
CAPS	3-[cyclohexylamino]propane-sulfonic acid
CHES	2-[N-cyclohexylamino]ethane-sulfonic acid
CMP	cytidine monophosphate
Cu	copper
CydAB	*Escherichia coli* cytochrome *bd* oxidase
CyoABCD	*Escherichia coli* cytochrome *bo* oxidase
CyxAB	*Escherichia coli* cytochrome oxidase
Dld	*Escherichia coli* D-lactate dehydrogenase

DMN/DMNH$_2$	oxidized and reduced 1,2-dimethyl-1,4-napthoquinone
DMS	dimethylsulfide
DmsA	molybdenum cofactor containing subunit of *Escherichia coli* dimethylsulfoxide reductase
DmsAB	soluble catalytic dimer of *Escherichia coli* dimethylsulfoxide reductase
DmsABC	*Escherichia coli* dimethylsulfoxide reductase
DmsB	[4Fe-4S] cluster containing subunit of *Escherichia coli* dimethylsulfoxide reductase
DmsC	membrane anchor subunit of *Escherichia coli* dimethylsulfoxide reductase
DMSO	dimethylsulfoxide
DMSOR	*Rhodobacter sphaeroides* dimethylsulfoxide reductase
DMQ	demethylmenaquinone
DTT	dithiothreitol
DyEDTA	dysprosium ethylenediaminetetraacetic acid
E. coli	*Escherichia coli*
EDTA	ethylenediaminetetraacetic acid
$E_{m,7}$	midpoint potential at pH 7.0
EPPS	N-[2-hydroxyethyl]piperazine-N'[3-propanesulfonic acid]
EPR	electron paramagnetic resonance
FAD/FADH$_2$	oxidized/reduced flavin adenine dinucleotide
FdhF	molybdenum cofactor containing subunit of *Escherichia coli* formate hydrogenlyase/formate dehydrogenase-H

FdhG	molybdenum cofactor containing subunit of *Escherichia coli* formate dehydrogenase-N
FdhGHI	*Escherichia coli* formate dehydrogenase-N
FdoG	molybdenum cofactor containing subunit of *Escherichia coli* formate dehydrogenase-O
FdoGHI	*Escherichia coli* formate dehydrogenase-O
Fe	iron
Fe-S	iron-sulfur
$FMN/FMNH_2$	oxidized/reduced flavin mononucleotide
FPLC	fast protein liquid chromatography
FrdAB	soluble catalytic dimer of *Escherichia coli* fumarate reductase
FrdABCD	*Escherichia coli* fumarate reductase
FrdB	iron-sulfur cluster containing subunit of *Escherichia coli* fumarate reductase
FrdCD	anchor subunits *Escherichia coli* fumarate reductase
Gcd	*Escherichia coli* glucose dehydrogenase
GlpAC	soluble catalytic dimer of *Escherichia coli* anaerobic glycerol-3-phosphate dehydrogenase
GlpACB	*Escherichia coli* anaerobic glycerol-3-phosphate dehydrogenase
GlpB	membrane anchor subunit of *Escherichia coli* anaerobic glycerol-3-phosphate dehydrogenase
GlpD	*Escherichia coli* aerobic glycerol-3-phosphate dehydrogenase
gly-3-P	glycerol-3-phosphate
Gly/DMSO	glycerol dimethylsulfoxide minimal media
Gly/Fum	glycerol fumarate minimal media
Gly/PNO	glycerol pyridine N-oxide minimal media

GMP	guanosine monophosphate
H	hydrophobic
H.	*Haemophilus*
H_2	hydrogen
HEPES	N-[2-hydroxyethyl]piperazine-N'-[2-ethanesulfonic acid
HOQNO	2-n-heptyl-4-hydroxyquinoline-N-oxide
HyaABC	*Escherichia coli* hydrogenase-1
HybABC	*Escherichia coli* hydrogenase-2
HybC	Ni-M containing subunit of *Escherichia coli* hydrogenase-2
imidazole	1,3,diaza-2,4-cyclopentadiene
IMP	inosine monophosphate
IPTG	isopropyl β-D-thiogalactopyranoside
kbp	kilobase pair
kDa	kilodalton
lapachol	2-hydroxy-3-(3-methyl-2-butenyl)-1,4-napthoquinone
LB	Luria-Bertani media
LDAO	N,N-dimethyldodecylamine N-oxide
Lld	*Escherichia coli* L-lactate dehydrogenase
MEKC	micellar electrokinetic chromatography
MES	2[N-morpholino]ethanesulfonic acid
MGD	molybdopterin guanine dinucleotide
Mo	molybdenum
moco	molybdenum cofactor
MOPS	3-[N-morpholino]propanesulfonic acid

MPT	molybdopterin
MQ/MQH_2	oxidized/reduced menaquinone
MsrA	*Escherichia coli* methionine sulfoxide peptide reductase
MTT	membrane targeting and translocation
MV	methyl viologen
MV^{2+}/$MVH\cdot^{+}$	oxidized and reduced methyl viologen
N	negative
N_2	nitrogen
NAD^{+}/NADH	oxidized/reduced nicotinamide adenine dinucleotide
NADPH	nicotinamide adenine dinucleotide phosphate
Nap	*Escherichia coli* periplasmic nitrate reductase
NapA	molybdenum cofactor containing subunit of *Escherichia coli* periplasmic nitrate reductase
NarG	molybdenum cofactor containing subunit of *Escherichia coli* nitrate reductase A
NarGH	soluble dimer of *Escherichia coli* nitrate reductase A
NarGHI	*Escherichia coli* nitrate reductase A
NarH	Fe-S cluster containing subunit of *Escherichia coli* nitrate reductase A
NarI	membrane anchor subunit of *Escherichia coli* nitrate reductase A
NarJ	assembly subunit for *Escherichia coli* nitrate reductase A
NarW	assembly subunit for *Escherichia coli* nitrate reductase Z
NarZ	molybdenum cofactor containing subunit of *Escherichia coli* nitrate reductase Z

NarZYV	*Escherichia coli* nitrate reductase Z
NDH-I	*Escherichia coli* nicotinamide adenine dinucleotide dehydrogenase I
NDH-II	*Escherichia coli* nicotinamide adenine dinucleotide dehydrogenase II
Ni	nickel
Ni-M	nickel-metal
NMR	nuclear magnetic resonance
NrfABCD	*Escherichia coli* nitrite reductase
O_2	oxygen
OD	optical density unit
orf205	open reading frame of 205 amino acids at 35.69 minutes on the *Escherichia coli* chromosome homologous to DmsB
orf207	open reading frame of 207 amino acids at 35.69 minutes on the *Escherichia coli* chromosome homologous to DmsC
orf808A	open reading frame of 808 amino acids at 35.69 minutes on the *Escherichia coli* chromosome homologous to DmsA
orf808B	open reading frame of 808 amino acids at 35.69 minutes on the *Escherichia coli* chromosome downstream of orf808A homologous to DmsA
orf1-4	open reading frame 1 through 4, including orf808A, orf808B, orf205, and orf207, at 35.69 minutes on the *Escherichia coli* chromosome
P	positive
PADAC	7-(thienyl-2-acetamido)-3-[2-(4-N,N-dimethylaminophenyl-azo)-pyridinium methyl]-3-cepham-4-carboxylic acid
PAGE	polyacrylamide gel electrophoresis

PCR	polymerase chain reaction
PhoA	alkaline phosphatase
plumbagin	5-hydroxy-2-methyl-1,4-napthoquinone
pmf	proton motive force
PMSF	phenylmethyl sulfonyl fluoride
PNO	pyridine N-oxide
PNOR	pyridine N-oxide reductase
PoxB	*Escherichia coli* pyruvate oxidase
PutA	*Escherichia coli* proline dehydrogenase
PQQ	pyrroloquinoline quinone
Q	quinone
Q_A	high affinity (non-dissociable) quinone binding site
Q_B	low affinity (dissociable) quinone binding site
Q_H	high affinity (non-dissociable) quinone binding site
Q_L	low affinity (dissociable) quinone binding site
R.	*Rhodobacter*
SdhABCD	*Escherichia coli* succinate dehydrogenase
SDS	sodium dodecyl sulfate
Se-Cys	seleno-cysteine
SNAP	S-nitroso-D/L-acetylpenacillamine
TLCK-HCl	L-1-chloro-3-[4-tosylamido]-7-amino-2-heptanone-HCl
TMA	trimethylamine
TMAO	trimethylamine N-oxide

TorA	*Escherichia coli* trimethylamine N-oxide reductase
TorC	pentaheme subunit of *Escherichia coli* trimethylamine N-oxide reductase operon
TorCAD	operon encoding *Escherichia coli* trimethylamine N-oxide reductase
TorD	membrane anchor subunit of *Escherichia coli* trimethylamine N-oxide reductase operon
TPCK	L-1-chloro-3-[4-tosylamido]-4-phenyl-2-butanone
TRIS	tris[hydroxymethyl]aminomethane
UQ	ubiquinone
UV	ultraviolet
W	tungsten

Chapter 1 : Introduction

1.1. Introduction

Escherichia coli (*E. coli*) can obtain energy using either fermentation or respiration. During fermentation, energy is generated exclusively by substrate level phosphorylation, concomitant with redox-balanced dismutation of substrate. However, much of the energy in reduced substrate is lost. When terminal electron acceptor is present, *E. coli* can switch to respiration, where a proton gradient is produced during the oxidation/reduction reactions. This gradient of protons can be used directly for transport, motility, or by the F_0F_1 ATPase to generate adenosine triphosphate (ATP) [198, 233].

During respiration, *E. coli* expresses primary dehydrogenases, and terminal reductases, and produces membrane soluble quinones (Q) [81]. In the absence of the terminal electron acceptors oxygen (O_2) or nitrate, dimethylsulfoxide (DMSO) reductase (DmsABC) is synthesized [29]. It is a terminal reductase able to reduce S- and N-oxides found in the environment [270], and in the process, energy is conserved as a proton gradient across the membrane [30, 215]. DmsABC has been cloned, sequenced, overexpressed, and purified [27, 31, 270]. It has also been well characterized functionally [29, 30, 214-216, 267, 270, 272] and biophysically [53, 207-210, 244-246], making it an excellent model system for elucidating key features in electron transfer through an electron transport chain protein.

The aim of this introduction is to briefly outline concepts important in respiration, provide an overview of respiration in *E. coli,* and describe our current understanding of the structure and function of DmsABC. At the end of the introduction the aims of the thesis will be outlined.

1.2. Respiration

1.2.1. Energy Transduction

According to Mitchell's chemiosmotic hypothesis, electron transfer through the electron transport chain, from lower to higher redox potential, is coupled to ATP synthesis, by production of a proton gradient across the membrane [178]. The proton gradient is generated by utilizing the free energy available from the oxidation and reduction of substrates. The proton gradient is composed of a concentration gradient of protons (ΔpH), and electrical potential ($\Delta\psi$) due to charge separation. The two components constitute the proton motive force (pmf). The pmf is then utilized directly for solute transport, flagellar rotation, or synthesis of ATP via the F_0F_1 ATPase [81].

1.2.2. Mechanisms of Proton Translocation

In *E. coli,* two different mechanisms are utilized to generate the pmf. Respiratory proteins may utilize one or both of scalar and vectorial proton movement. The scalar mechanism involving Q employs two physically separated half reactions, where protons are first consumed on the negative (N) side of the membrane, and then released on the positive (P) side of the membrane. This is coupled with electron movement. In bacteria, this mechanism requires reduction and oxidation of Q to occur at the cytoplasmic and periplasmic face of the membrane, respectively (Figure 1.1.). Another scalar mechanism employs the production of protons on the periplasmic side of the membrane by chemical reactions. The vectorial mechanism employs the "pumping" of protons from the N to P side of the membrane (Figure 1.1.). Protons generated by the first mechanism are called chemical, scalar, or substrate protons, while protons pumped across the membrane are called vectorial protons [25, 81].

An additional mechanism of proton translocation, the "proton motive Q cycle" has been observed, although not in *E. coli*. Briefly, the oxidation of Q results in separate pathways for the two electrons. One

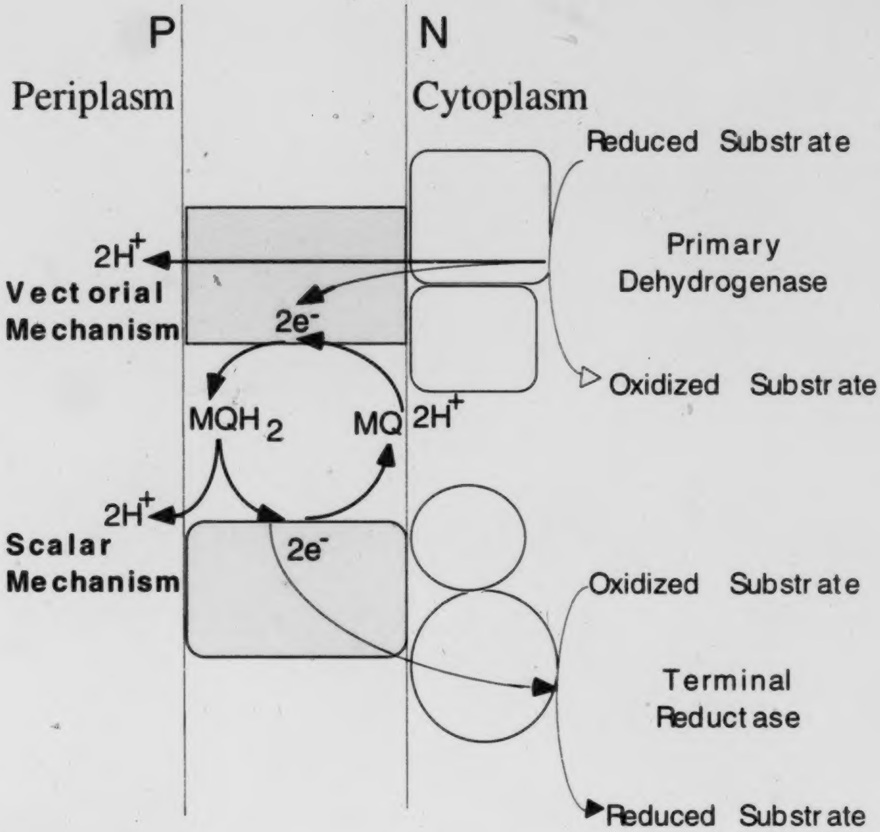
P
Periplasm
N
Cytoplasm
Reduced Substrate
Primary Dehydrogenase
Oxidized Substrate
2H+
Vectorial Mechanism
2e-
MQH2
MQ
2H+
2H+
Scalar Mechanism
2e-
Oxidized Substrate
Terminal Reductase
Reduced Substrate

Figure 1.1.

Scalar and Vectorial Mechanisms of Proton Translocation

In the scalar mechanism of proton translocation Q picks up protons from the cytoplasm and deposits them in the periplasm. This is the result of two physically separate reducing and oxidizing half reactions. Scalar protons are also generated when protons are produced by chemical reactions in the periplasm (not shown). In the vectorial mechanism protons are pumped across the membrane. The negative (N) and positive (P) sides of the membrane are indicated. The subunit structure is not meant to be representative of all primary dehydrogenases and terminal reductases.

continues through the electron transport chain while the other is routed back to oxidized Q. The net result is translocation of four protons for every one net Q oxidized [81, 248].

1.3. Respiration in *E. coli*

1.3.1. Modularity of Redox Components

The *E. coli* respiratory system consists of a modular design composed of fourteen primary dehydrogenases that oxidize substrate, three Q's that transfer reducing equivalents within the membrane, and eleven terminal reductases that reduce substrate [255, 266]. The dehydrogenases and terminal reductases use membrane soluble Q as their common substrate, thus electrons from one dehydrogenase can be utilized by a number of terminal reductases (Figure 1.2.). All respiratory proteins must be linked to the membrane, either via other subunits (i.e. cytochrome C) or on their own, at least transiently, to allow electron transfer to and from the Q pool [255].

Growth conditions alter the synthesis of dehydrogenases, Q's, and terminal reductases by a relatively complex regulatory system. This allows the quantity of each component to be optimized, results in minimal change to adapt to new environmental conditions, and eliminates wasteful synthesis of unneeded protein. In addition, it allows *E. coli* to exploit the oxidation/reduction couple with the largest free energy, allows expression of apparently redundant proteins under different growth conditions, and permits utilization of appropriate enzymes as needed resulting in either the highest growth rate or most efficient growth [81, 255, 257].

The expression of terminal reductases under various growth conditions demonstrates how the cell utilizes the oxidation/reduction couple with the largest available free energy. In the presence of O_2, the

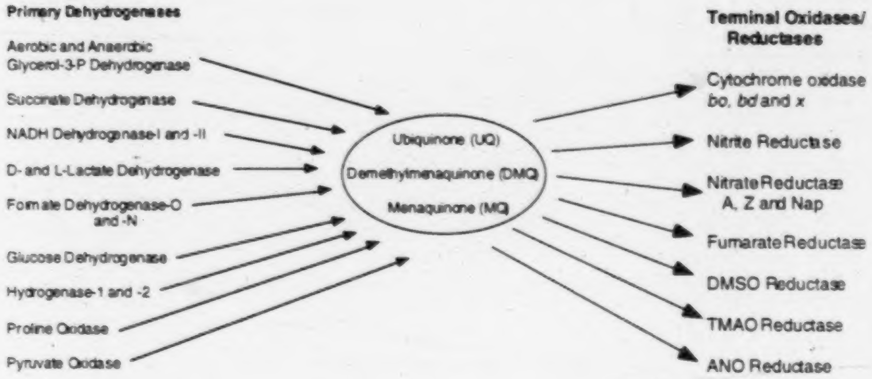
Primary Dehydrogenases
Aerobic and Anaerobic Glycerol-3-P Dehydrogenase
Succinate Dehydrogenase
NADH Dehydrogenase-I and -II
D- and L-Lactate Dehydrogenase
Formate Dehydrogenase-O and -N
Glucose Dehydrogenase
Hydrogenase-1 and -2
Proline Oxidase
Pyruvate Oxidase
Ubiquinone (UQ)
Demethylmenaquinone (DMQ)
Menaquinone (MQ)
Terminal Oxidases/ Reductases
Cytochrome oxidase *bo*, *bd* and *x*
Nitrite Reductase
Nitrate Reductase A, Z and Nap
Fumarate Reductase
DMSO Reductase
TMAO Reductase
ANO Reductase

Figure 12.

Modularity of the *E. coli* Respiratory System

Primary dehydrogenases that donate electrons to the Q pool are shown on the left, the three types of membrane soluble Q's are shown in the middle, and terminal reductases that accept electrons from the Q pool are shown on the right.

electron acceptor with the highest redox potential (Table 1.1), all genes involved in anaerobic respiration and fermentation are repressed. In the presence of nitrate, the electron acceptor with the second highest redox potential, all other anaerobically expressed genes not necessary for respiration on nitrate are repressed [255].

E. coli express a number of apparently redundant respiratory enzymes. More than one protein exists to oxidize the substrates glycerol-3-phosphate (gly-3-P), formate, hydrogen (H_2), and nicotinamide adenine dinucleotide (NADH), and to reduce the substrates O_2, nitrate and trimethylamine N-oxide (TMAO). Proteins with the same substrate specificity may have very similar, or somewhat different functional properties. However, their differential expression achieves particular advantages for the cell. Nitrate reductase-A and -Z are functionally very similar enzymes, but their differential expression may allow the cell to reduce low levels of nitrate as the cell encounters anaerobic conditions prior to synthesis of nitrate reductase-A [34, 105, 108]. The two NADH dehydrogenases may be expressed differentially to allow for a higher growth rate, or more efficient growth, under optimal and sub-optimal growth conditions, respectively. Under high O_2 tension, expression of the uncoupled NADH dehydrogenase increases, whereas under low O_2 tension, expression of the pmf producing NADH dehydrogenase is augmented [232, 234]. This indicates under optimal growth conditions, some efficiency is lost to allow for faster transfer through the electron transport chain, resulting in a higher growth rate [255].

1.3.2. Transcriptional Regulation of Respiratory Enzymes

The superimposition of positive and negative regulation by a number of proteins, results in the fine-tuning of respiratory enzyme expression in response to environmental conditions. Transcriptional regulation of respiratory genes in response to nitrate and nitrite is accomplished by NarX/L and NarQ/P, and anaerobiosis by ArcA/B and FNR. Although less well characterized, a number of other proteins also

Table 1.1.

Midpoint Potentials at pH 7.0 ($E_{m,7}$) of Some Electron Donor and Acceptor Couples

Redox Couple	$E_{m,7}$ (mV)
$H_2/2H^+$	$^{-}414$
$NADH/NAD^+$	$^{-}320$
Glycerol-3-phosphate/Dihydroxyacetone phosphate	$^{-}190$
Menaquinol/Menaquinone	$^{-}74$
Succinate/Fumarate	$^{+}30$
Demethylmenaquinol/Demethylmenaquinone	$^{+}36$
Ubiquinol/Ubiquinone	$^{+}113$
Trimethylamine/TMAO	$^{+}130$
Dimethylsulfide/DMSO	$^{+}160$
$H_2^{-}/1/2O_2$	$^{+}820$

appear to regulate some respiratory genes. Continued study of AppY, IHF, H-NS, Fis, and StpA, will clarify the magnitude and importance of their role in regulating the expression of respiratory enzymes [160, 255, 266].

ArcB/A, NarX/L and NarQ/P are two component regulatory systems. The first protein in the set is a membrane localized sensor kinase, followed by a cytoplasmic response regulator with a DNA binding domain. The membrane sensors autophosphorylate in response to their stimulus. Regulator activity is a function of the ratio of phosphorylation and dephosphorylation by the sensor. Transfer of the sensor phosphate to the response regulator results in DNA binding of the regulator, and modulation of protein expression by interaction with RNA polymerase [6, 57, 233, 255].

1.3.2.1. NarX/L and NarQ/P

NarX/L and NarQ/P mediate complex regulation in response to nitrate and nitrite. They activate genes involved in nitrate and nitrite catabolism, while repressing other anaerobic respiratory and fermentative genes. NarX and NarQ are homologous sensors that respond differently to periplasmic nitrate and nitrite. They mediate dissimilar rates of phosphorylation and dephosphorylation for both homologous regulators NarL and NarP. In addition, NarL and NarP act as both activators and repressors at different gene loci. The differences between NarX and NarQ, and NarL and NarP, result in a complex pattern of regulation. For example, NarL represses, while NarP activates nitrite reductase expression in the presence of nitrate. However, both NarL and NarP activate nitrite reductase expression in the presence of nitrite [81, 238, 255].

The NarL heptanucleotide recognition sequence has been identified. It is present in the 5' untranslated sequence of genes for respiratory enzymes with undefined number, location, orientation and spacing [81, 238, 255]. NarP has affinity for the same or very similar heptanucleotide [251], although binding appears be restricted to inverted repeats with two basepairs in between [66].

1.3.2.2. ArcA/B

Under anaerobiosis, ArcAB is mainly responsible for the repression of genes involved in aerobic metabolism. However, ArcAB also activates a handful of genes in anaerobic metabolism [81, 160]. It has been postulated that ArcB senses redox potential rather than O_2 concentration [110, 113], redox state of the ubiquinone (UQ) pool [6], pmf [37], or anaerobic metabolites [114]. ArcB has a large C-terminus containing an additional cytoplasmic domain found in a subgroup of two-component sensors. As a result, it is possible that more than one signal may affect ArcB function simultaneously. Their superimposition may result in fine tuning of regulation by ArcA/B in response to environmental conditions [112, 160]. The DNA binding site for ArcA has not yet been determined [160]

1.3.2.3. FNR

Under anaerobic conditions, FNR acts as both a transcriptional activator and repressor of genes involved in anaerobic and aerobic metabolism, respectively. FNR belongs to a family of transcriptional regulators that includes the cyclic adenosine monophosphate (AMP) receptor protein [71, 160]. However, FNR contains an additional N-terminal extension with three Cys residues. Along with an additional Cys residue, they are believed to form a [4Fe-4S] cluster in response to low O_2 tension [136, 152]. This results in FNR dimerization, DNA binding, and regulation of transcription [71, 152, 160, 291]. The FNR binding site is a 22 base pair (bp) segment containing an inverted repeat. Negative regulation is generally due to the FNR binding site overlapping with the transcriptional start site resulting in promoter occlusion. The FNR binding site is normally found thirty nucleotides upstream of the transcription initiation site for positively regulated genes [77, 160].

1.3.3. Prosthetic Groups in Respiratory Enzymes

The transfer of electrons through respiratory proteins requires redox centers including the nickel-metal (Ni-M) dinuclear center, polynuclear copper (Cu) sites, flavin adenine dinucleotide (FAD), flavin mononucleotide (FMN), pyrroloquinoline quinone (PQQ), heme, iron-sulfur (Fe-S) clusters, and molybdenum cofactor (moco) [24]. The protein environment surrounding the redox centers alters their redox potential, allowing them to be used for a variety of reactions [151].

1.3.3.1. Hemes

E. coli uses four types of heme involved in one electron transfer reactions [81, 240]. Heme *b* is found in the membrane anchoring subunits of a number of respiratory components, while heme *d* and heme *o*, are associated only with the two terminal oxidases Cyd and Cyo, respectively. In contrast, heme *c* is covalently bound to protein, and is found exclusively in the periplasm, attached to soluble or membrane bound protein [81].

1.3.3.2. Fe-S clusters

The basic [2Fe-2S], [3Fe-4S] and [4Fe-4S] clusters mediate single electron transfer [49]. The iron (Fe) is coordinated to one or two RS^- (generally Cys) and two to three S^{2-} ligands (Figure 1.3.). A number of consensus sequences have been identified that can be used to distinguish Cys residues involved in the ligation of Fe-S clusters. They include three closely spaced Cys's and a distant Cys residue as the final ligand, even if an adjacent Cys near the first three is available. In contrast, Rieske Fe-S clusters use two Cys and two His residues for ligation of the Fe [19]. In addition, unusual clusters involving iron (Fe) have been observed in nitrogenases (molybdenum-Fe) and hydrogenases (Ni-Fe) [101, 261].

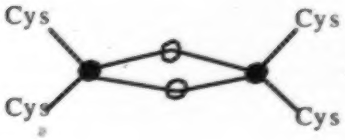
Cys
Cys
Cys
Cys

[2Fe-2S]

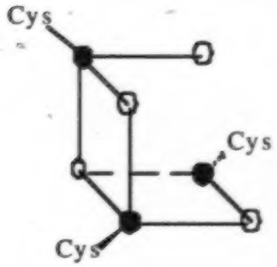

[3Fe-4S]

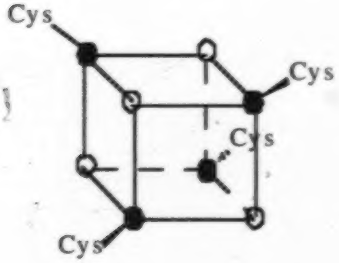
Cys
Cys
Cys
Cys

[4Fe-4S]

Figure 1.3.

Structures of [2Fe-2S], [3Fe-4S], and [4Fe-4S] Clusters

The filled circles represent iron, the open circles represent sulfur, and ligated Cys residues are as indicated.

1.3.3.3. Moco

Molybdenum (Mo) is capable of mediating both one and two electron transfer reactions. This allows it to couple redox centers and substrate with different electron requirements. Mo has been selected by nature for use in two cofactors [52, 97]. The first is the multinuclear M center with seven Fe's and one Mo. It is found in nitrogenase, the enzyme responsible for catalyzing the conversion of nitrogen (N_2) to ammonia [51, 101]. The second Mo containing cofactor is the pterin containing moco, utilized by all other molybdoenzymes [138, 237] (Figure 1.4.). Moco containing enzymes generally catalyze oxygen transfer [97]. The two electron oxidative reaction involves the movement of oxygen from water, to the Mo, and then to substrate [17, 98]. The reductive reaction carried out by these enzymes involves the reverse transfer of oxygen. The function of the pterin is at present speculative. However, it appears to be important in electron transfer, and/or modulation of the redox potential of the Mo [43, 97, 196].

Tungsten (W) and Mo share a number features, including similar atomic radii, electronegativity, and biologically relevant oxidation states [97]. W was shown to be a Mo antagonist in *E. coli*, as growth in the presence of W resulted in inactive molybdoenzymes [120]. However more recently, a number of enzymes have been shown to contain W instead of Mo ligated in the pterin moco. W-substituted moco has been found in acetate-producing, methane-producing, hyperthermophilic, acetylene-utilizing and sulfate-reducing organisms [26, 96, 102, 103, 123, 180, 222, 285]

Moco is highly O_2 labile, and as a result its structure was originally extrapolated from the structural characterization of a number of stable oxidized derivatives [117, 118, 121, 144]. Previously it was thought the structure of moco was identical for all moco containing enzymes. However, it became apparent that moco from some prokaryotic enzymes had a higher molecular weight than expected [133, 146-148, 181]. Eventually it was demonstrated in addition to the

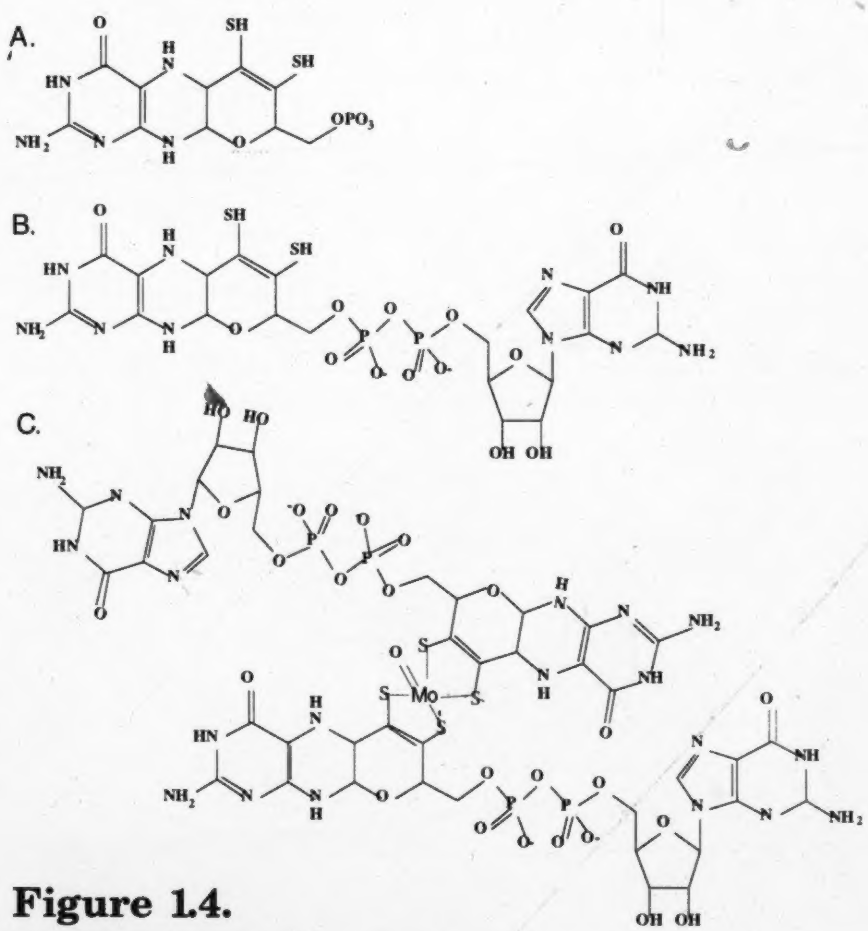

Figure 1.4.

Structures of Moco Derivatives

A. Molybdopterin (MPT)
B. Molybdopterin guanine dinucleotide (MGD)
C. Bis-molybdopterin guanine dinucleotide - ligating Mo (bis-MGD)

The thiol groups from structures A., B., and C., can ligate either a Mo or W. Additional ligands will be present to complete the coordination sphere of the Mo. The designation moco refers to all moco derivatives (A-C). A. MPT refers to moco with no appended nucleotide. This was the original structure determined for moco. B. Molybdopterin dinucleotide refers to any dinucleotide derivative. MGD is one such derivative, although the nucleotide appended can also be AMP, inosine monophosphate, or cytidine monophosphate. C. The prefix bis is appended to designate that two moco's are ligated together. The example depicted here shows two MGD ligated together. Additional ligands will be present to complete the coordination sphere of the Mo.

original structure for moco - molybdopterin (MPT) (1.4. A.), a nucleotide (guanosine monophosphate (GMP), cytidine monophosphate (CMP), AMP, or inosine monophosphate (IMP)) was sometimes appended in a pyrophosphate linkage to MPT, resulting in a variety of moco dinucleotide derivatives (Figure 1.4. B.) [41, 117, 122]. The function of the nucleotide portion of the moco is at present a mystery.

Recently the crystallization of several molybdoenzymes has confirmed the structure of MPT and dinucleotide derivatives of moco, but also revealed one additional level of complexity. The Mo (or W) can be coordinated by two MPT's or MPT dinucleotide derivatives, resulting in bis-moco (Figure 1.4. C.) [43, 55, 203, 220, 223].

The *E. coli* gene loci *moa-moe* are involved in the biosynthetic pathway of moco (Figure 1.5.) [197]. The pathway begins with an unknown derivative of guanosine being converted to the sulfur free precursor Z. This involves MoaA, MoaB and MoaC [282]. Precursor Z is then converted to MPT involving converting factor containing bound sulfur (MoaD, MoaE) [188-190]. MoeB is responsible for reactivation by resulfuration of the small subunit of the converting factor [294]. In the last step, MPT is converted into molybdopterin guanine dinucleotide (MGD) by MobA and MobB [76, 119]. Mo is transported into the cell by modA-D [116, 199], and is processed and inserted into moco by mogA. [130].

1.3.4. Translocation of Respiratory Enzymes Across the Cytoplasmic Membrane

A number proteins in the electron transport chain have periplasmic subunits. As a result, they possess an N-terminal leader responsible for their translocation [72, 254]. Leader sequences are 18-26 amino acids long, and have amino acid biases, but share no homology or conserved motifs [24]. They are characterized by a positively charged N-terminus, followed by a hydrophobic core, and a hydrophilic carboxy-terminal cleavage site possessing small amino acids at the $^{-}1$ and $^{-}3$ positions to the site of cleavage (C). The leader sequence is generally

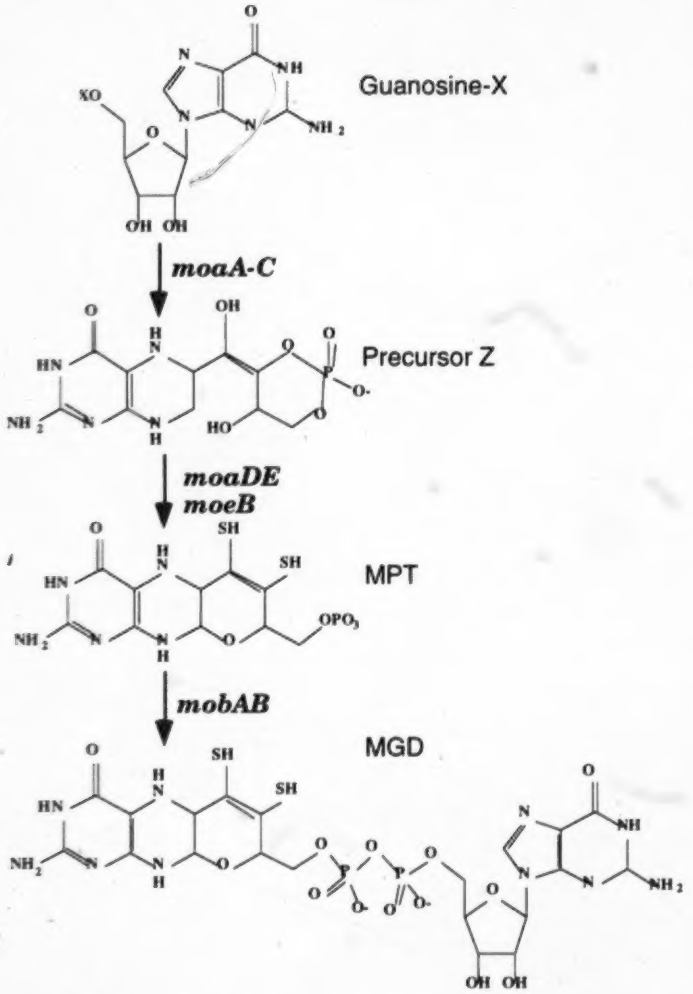
Guanosine-X
XO
moaA-C
Precursor Z
moaDE
moeB
MPT
mobAB
MGD

Figure 1.5.

Biosynthetic Pathway for Moco in *E. coli*

The genes responsible for each step in the biosynthetic pathway are indicated beside the arrows, and the name of each structure is indicated to it's right. In addition to the pathway indicated above, *modA-D* and *mogA*, are responsible for Mo processing and Mo insertion into moco, respectively.

cleaved in the periplasm by leader peptidase I [63, 182, 262].

Sequence analysis of periplasmic proteins binding a subset of redox cofactors, including flavin, moco, Fe-S clusters, Ni-Fe complexes, and tryptophan tryptophylquinone, revealed these proteins have long (~58) amino acid leaders. In addition, these leaders have the consensus motif (S/T)-R-R-X-F-L-K. Berks hypothesized that proteins with this "double-arginine" leader assemble in the cytoplasm, and the fully folded cofactor-containing proteins are translocated to the periplasm through an export apparatus distinct from the Sec-system [24]. Evidence suggests at least two double-arginine containing proteins bind cofactor prior to translocation of the fully folded protein [201, 217], and translocation appears to be dependent on the pmf but not on Sec-proteins [217]. In addition, components of the translocation apparatus appear to have been identified [267]. Thus, some periplasmic respiratory subunits are translocated by the Sec-system, while those binding a subset of redox cofactors are translocated by this novel system.

1.3.5. Transport of Substrates to the Cytoplasm

Transmembrane carriers are required for the transport of substrates that are oxidized or reduced in the cytoplasm. Expression of these carriers varies, depending on the growth conditions and availability of substrate [255]. Examples of these transporters include PutP, an sodium proline symporter, and GlpF involved in glycerol uptake [70, 166].

1.3.6. Electron Transport Chain Components

1.3.6.1. Q

E. coli synthesize three different membrane localized Q's that mediate electron and proton transfer between the primary dehydrogenases and terminal reductases [81, 247]. UQ is a benzene derivative, while menaquinone (MQ) and demethylmenaquinone (DMQ) are naphthalene derivatives (Figure 1.6.) [175]. UQ, DMQ, and MQ, show decreasing redox potentials of $^{+}113$, $^{+}36$ and $^{-}74$ mV, respectively (Table 1.1) [81, 277]. *E. coli* Q's generally possess a side chain with eight prenyl units, although minor amounts of Q's with other numbers of prenyl units do exist [175].

UQ is at least four times more abundant than MQ plus DMQ in aerobically grown cells, whereas UQ is one third or less as abundant as MQ and DMQ in anaerobically grown cells [192, 263, 278]. The variation in Q ratio's observed with changes in O_2 tension is not mediated by FNR or ArcAB [224, 254]. Q ratios also vary depending on the growth conditions (i.e. presence of specific oxidant and reductant) [254]. Dehydrogenases and terminal reductases generally select Q with the best suited redox potential. As a result, UQ is generally employed for O_2 respiration, UQ and MQ for nitrate respiration, while MQ and DMQ are utilized for electron acceptors other than nitrate [81].

1.3.6.2. Primary Dehydrogenases Using Various Substrates

1.3.6.2.1. Proline

Proline dehydrogenase (PutA) catalyzes the oxidation of proline or pyrroline-5-carboxylic acid without production of a pmf. It is a homodimer with each subunit possessing a non-covalently bound FAD [47]. PutA is membrane bound only when proline concentrations are high, or membrane components are reduced [279]. Binding to the membrane is concomitant with reduction of bound FAD, and a conformational change in PutA [48]. In addition, PutA acts as a DNA binding protein to repress its own expression [47].

1.3.6.2.2. Pyruvate

Pyruvate oxidase (PoxB) is responsible for the oxidation of pyruvate to acetate and carbon dioxide, and is not coupled to production of a pmf. It contains non-covalently bound FAD and thiamine pyrophosphate as cofactors [81]. PoxB is purified as a soluble protein.

A. Ubiquinone-8

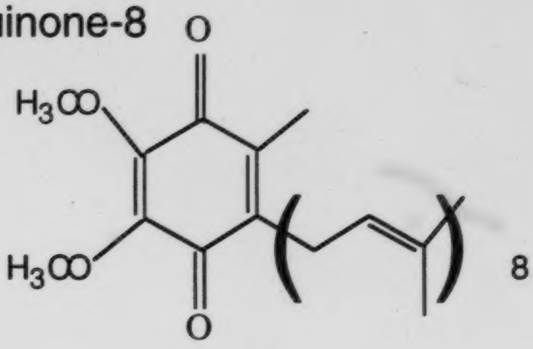
O
H3CO
H3CO
O
8

B. Demethylmenaquinone-8

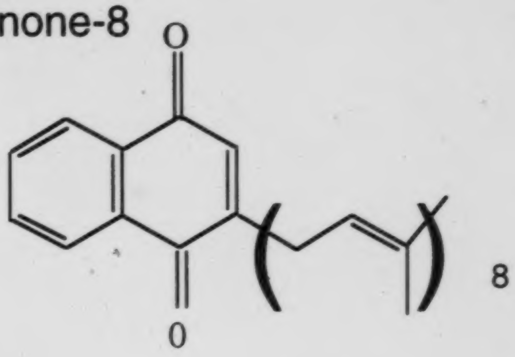

C. Menaquinone-8

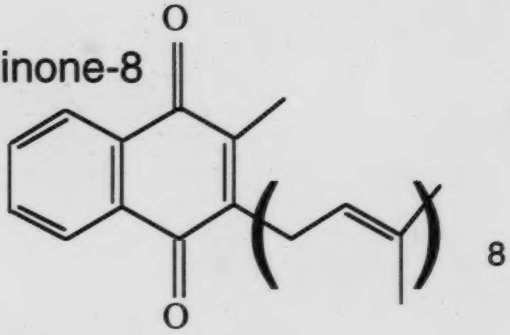

Figure 1.6.

Structures of the Oxidized forms of UQ, DMQ and MQ

However, PoxB will bind to membranes with the addition of cofactor and substrate, allowing it to interact with the Q pool. Substrate and cofactor are believed to induce a conformational change in PoxB exposing an amphipathic helix [84, 85].

1.3.6.2.3. D- and L-Lactate

D-lactate dehydrogenase (Dld) with non-covalently bound FAD, and L-lactate dehydrogenase (Lld) with bound FMN, oxidize D- and L-lactate to pyruvate, respectively. Dld and Lld are both monomeric and membrane bound, but contain no apparent membrane spanning segments [81]. These enzymes are apparently not coupled to production of a pmf [81, 168].

1.3.6.2.4. Glucose

Glucose dehydrogenase (Gcd) is a monomer with five transmembrane-spanning segments. It oxidizes glucose to gluconate on the periplasmic side of the membrane, and this reaction is apparently not coupled to synthesis of a pmf [81]. It uses the cofactor PQQ not synthesized by *E. coli*. As a result, Gcd activity requires externally provided PQQ [81, 258].

1.3.6.2.5. Gly-3-P

There are two gly-3-P dehydrogenases that oxidize gly-3-P to dihydroxyacetone phosphate. The aerobically expressed enzyme (GlpD) is a monomer with non-covalently bound FAD [81]. It does not appear to possess any transmembrane segments [13]. The anaerobic enzyme (GlpACB) is a heterotrimer. The GlpAC catalytic dimer has been purified from the soluble fraction of the cell, and appears to non-covalently bind FAD and FMN, by GlpA and GlpC, respectively [59, 139]. GlpB may possess two Fe-S clusters, and although tightly associated with the membrane, does not appear to possess any transmembrane spanning segments [59, 260]. GlpAC may associate with GlpB transiently or may fall off the membrane once the cells are broken [259].

1.3.6.2.6. Succinate

Succinate dehydrogenase (SdhABCD) oxidizes succinate to fumarate without generation of a pmf [81, 255]. It belongs to a family of related proteins that includes *E. coli* fumarate reductase (FrdABCD). SdhA binds FAD covalently, and is the site of succinate oxidation. SdhB is the electron transfer subunit with [2Fe-2S], [3Fe-4S], and [4Fe-4S] clusters. SdhC and SdhD are membrane anchor subunits that share heme b_{556} and are responsible for Q reduction [81].

1.3.6.2.7. Formate

Formate is oxidized to carbon dioxide by two homologous formate dehydrogenases [81]. FdhGHI is expressed under anaerobic conditions in the presence of nitrate [23, 155]. In contrast, FdoGHI is expressed constitutively at low levels [194]. The physiological role of FdoGHI is not known. It is postulated that FdhGH and FdoGH face the periplasm where they produce a pmf by chemical production of scalar protons [81]. The formate oxidizing subunits FdhG and FdoG contain moco [81], with one of the Mo ligands possibly being seleno-Cys (Se-Cys) encoded by an opal codon [81, 83]. The electron transfer subunits FdhH and FdoH bind four [4Fe-4S] clusters, while the membrane anchor subunits FdhI and FdoI bind heme *b* [22, 81].

The formate hydrogenlyase complex is responsible for coupling formate oxidation with H_2 production without the use of Q as a mediator [255]. The formate dehydrogenase subunit (FdhF) that composes part of the formate hydrogenlyase complex has been crystallized [43]. The crystal structure confirms FdhF uses Se-Cys as a Mo ligand, and binds a [4Fe-4S] cluster via Cys residues in the N-terminus [14, 83, 293]. The FdnG and FdoG sequences are homologous to FdhF, and share the opal codon and Cys residues responsible for incorporation of Se-Cys and Fe-S cluster ligation, respectively. This suggests they are structurally and functionally similar to FdhF [22, 81, 246]

1.3.6.2.8. H_2

Hydrogenases 1 (HyaABC) and 2 (HybABC) both oxidize H_2 to protons under anaerobic conditions in the absence of nitrate. Generation of a pmf is likely due to the production of two periplasmic chemical protons. Two cytoplasmic protons are used in Q reduction [81, 126]. The HyaB and HybC subunits bind a Ni-M cluster, the likely site of H_2 oxidation. While, the electron transfer subunits, HyaA and HybA, contain two and four [4Fe-4S] clusters, respectively. The electrons may then be transferred to the putative third heme *b* binding subunits HyaC and HybB, and then to the Q pool [81, 261].

1.3.6.2.9. NADH

E. coli expresses two distinct NADH dehydrogenases (NDH-I and NDH-II). NDH-I is composed of 14 subunits containing FMN and 5-8 Fe-S clusters [38, 153, 230, 264]. It is a homologue of mitochondrial complex I [264]. NDH-I generates a pmf by pumping protons across the membrane, although the process by which this occurs is at present unknown [81, 168]. In contrast, NDH-II is composed of one subunit with no transmembrane segments, containing FAD as its only cofactor [115, 288]. It is not coupled to proton translocation [81]. Both NDH-I and NDH-II are expressed aerobically. In addition, NDH-I is expressed anaerobically, and expression increases in the presence of nitrate [40, 86].

1.3.6.3. Terminal Reductases Using Various Substrates

1.3.6.3.1. O_2

E. coli expresses three oxidases (CyoABCD, CydAB, and CyxAB) that reduce O_2 to water [81]. CyoABCD is structurally distinct from the other two oxidases, and predominates when *E. coli* is grown at high O_2 tension [9, 61, 145, 200]. Q is oxidized by CyoA [273], and the electrons are passed from Q to heme b_{562}, and subsequently to the binuclear center (heme o_3 and Cu), where O_2 binds and is reduced. All three prosthetic groups are found in CyoB. In addition to the two scalar protons released on the periplasm on Q oxidation, two protons are pumped across the membrane by the integral membrane subunit CyoB. Helix VIII in CyoB is amphipathic, and polar residues may form a proton conducting channel from the cytoplasm to the periplasm [78, 81]. The functions of CyoC and CyoD are not known [81].

The integral membrane protein CydAB has a low K_m for O_2, and predominates under low O_2 tension [61, 81]. Q oxidation appears to occur at the periplasmic face of the membrane by CydA, resulting in release of two protons to the periplasm. The Q electrons are transferred to heme b_{558} in CydA [81, 158, 177, 286], and then to heme b_{595} and heme *d* where O_2 is reduced. Heme b_{595} and heme *d* are bound by both CydA and CydB [81].

An additional oxidase may be expressed from *cyxAB* under low O_2 tension. These genes are homologous to *cydAB*. At present, the importance of CyxAB is not known [81].

1.3.6.3.2. Nitrite

E. coli synthesizes a periplasmic nitrite reductase (NrfABCD) binding both heme *c* and Fe-S clusters. It conserves the energy of nitrite reduction in the presence of the electron donor formate [3, 65, 104]. Since reduction of nitrite in the periplasm results in consumption of periplasmic protons, translocation of protons to the periplasm must occur concomitantly to explain respiratory growth on nitrite [255]. NrfABCD is induced by anaerobiosis and nitrite, mediated by FNR and NarP [65, 251].

1.3.6.3.3. Fumarate

FrdABCD is homologous to SdhABCD although it preferentially mediates fumarate reduction [54, 81]. Although electron transfer to fumarate generates a pmf with the electron donors H_2, NADH, gly-3-P and formate [92, 93, 95], FrdABCD does not appear to be a coupled enzyme [80, 243, 255]. The catalytic subunit FrdA contains covalently bound FAD [269], the electron transfer subunit FrdB contains three Fe-S clusters ([2Fe-2S], [3Fe-4S], and [4Fe-4S]) [167], while FrdC and FrdD are the anchor subunits essential for binding of FrdA and FrdB to the membrane, and for electron transfer from MQ [54, 60, 154]. FrdABCD is expressed in response to anaerobiosis, but is repressed by nitrate [111, 124, 125].

1.3.6.3.4. Nitrate

E. coli express three nitrate reductases. Nitrate reductase-A (NarGHI) and -Z (NarZYV) are membrane bound, with their catalytic subunits facing the cytoplasm [33, 105, 108, 127], while the seven subunit Nap is found in the periplasm [88]. Formate, gly-3-P, H_2, NADH, lactate, succinate, and malate are all effective electron donors for nitrate respiration [109, 237]. Generation of a pmf is observed on reduction of nitrate, and is likely via scalar reactions [79, 128, 179].

NarGHI and Nap are induced by anaerobiosis and nitrate [88, 236], and Nap is additionally induced by nitrite [88]. In contrast, NarZYX is expressed at low levels under aerobic conditions, and there is no change in expression in the presence of nitrate or nitrite [105, 108]. The unusual regulation of NarZYV suggests it may be responsible for a low level of nitrate respiration during transition from aerobiosis to anaerobiosis prior to synthesis of NarGHI [81].

Of the homologous enzymes NarGHI and NarZYV, the former has been studied in much more detail [33, 34]. However, they both appear to possess catalytic subunits binding moco (NarG, NarZ), electron transfer subunits with Fe-S clusters (one [3Fe-4S] and two [4Fe-4S]) (NarH and NarY), and membrane anchors binding two hemes (b_{556}) (NarI and NarV) [4, 34, 90]. Studies suggest the low- and high-potential hemes are near the periplasmic and cytoplasmic surface of the membrane, respectively [163]. In addition, stoichiometric amounts of MQ have been found attached to purified NarGH, suggesting MQ may be an additional prosthetic group involved in electron transfer in NarG or NarH [45]. The third gene in the NarGHJI and NarZYWV operons coding for NarGHI and NarZYV encodes a fourth polypeptide, NarJ and NarW, respectively. These polypeptides are important for assembly of active enzyme [36, 73]. They are suggested to be system-specific chaperones that maintain NarG and NarZ in appropriate conformations to bind moco [32, 156]. Subunits from NarGHI and NarZYV are interchangeable, and can be used to compose heterologous nitrate reductases, although the heterologous nitrate reductases are less stable and have lower activity [35, 36].

Nap is believed to be composed of seven subunits, including one moco containing (NapA), two c-type cytochromes, and three Fe-S containing subunits. The function of this reductase, as well as sequence of electron transfer through these subunits is at present speculative [88]. The periplasmic nitrate reductase of *Thiosphaera pantotropha* has been suggested to be involved in disposing of excess reducing equivalents. However, in contrast to nap, this enzyme is expressed under aerobic conditions [20].

1.3.6.3.5. S- and N-oxides

There are three enzymes responsible for growth on S- and N-oxides in the presence of a non-fermentable carbon source - adenosine N-oxide (ANO) reductase, TMAO reductase (TorA) and DmsABC. ANO reductase is distinct from DmsABC and TorA, and conserves the energy of ANO reduction [216]. The identity of this enzyme, and whether it binds moco is not known.

TorA is encoded by the *torCAD* operon [176], and is purified from the periplasm as a moco containing enzyme able to reduce TMAO and other N-oxides [64, 228, 284]. TorC is a periplasmic penta-heme *c* binding protein attached to the membrane by an amino terminal anchor, while TorD is an integral membrane protein with unknown function

[176]. A model of electron transfer has been proposed whereby the TorC heme *c* domain located closest to the membrane would accept electrons from MQ [174, 176]. Subsequently the second heme domain of TorC would transfer electrons to TorA [176]. However, this model does not account for the function of TorD. *In vivo* reduction of TMAO is known to be coupled to production of a pmf. However, it is not known whether TorCAD is a coupled enzyme [81]. Since reduction of TMAO in the periplasm consumes two periplasmic protons, translocation of protons to the periplasm, must occur concomitantly to explain respiratory growth on TMAO.

torCAD expression is induced by a variety of S- and N-oxides [107, 185, 228]. Induction appears to be mediated by the non-essential TorT - a periplasmic inducer-binding protein, TorS - a membrane localized sensor/transmitter, and TorR - a positive regulator [131, 132, 186]. *torCAD* expression is not repressed by nitrate [185, 227], and its anaerobic induction is not mediated by FNR [185, 232]. As a result no NarL or FNR boxes are found in the 5' untranslated sequence of *torCAD* [176].

1.4. Bacterial Utilization of S- and N-oxides

1.4.1. Ecology of Substrates

DmsABC can reduce a variety of S- and N-oxides [270], including the naturally occurring pyridine N-oxide (PNO), DMSO, and TMAO. Substituted PNO's are found as soil contaminants. They are constituents of crude petroleum and coal tar, and are used as organic solvents and drugs [226].

DMSO and dimethylsulfide (DMS) are important components of the global sulfur cycle, and are involved in the transfer of sulfur from the sea through the air to land surfaces. DMS is believed to be the major source of reduced sulfur, and is important in global climate regulation [134, 137, 159]. DMS is produced by planktonic algae and zooplankton [8, 82], bacterial decomposition of animal manure, sewage, and plant material [15], and degradation of sulfur-containing pesticides [271]. DMS is volatile and escapes from oceans and soil surfaces, into the atmosphere, where it can be oxidized to DMSO [8, 16, 135, 137, 159]. DMSO is hygroscopic and is scrubbed from the atmosphere [8, 16, 135, 137, 159]. It is found at nM concentrations in bodies of water and rain [7, 8, 16, 135, 137, 159] Accumulation of DMSO is also the result of bacterial degradation of dimethylsulfonioproprionate excreted by planktonic algae and zooplankton [8], bacterial oxidation of DMS [94, 289], and manmade processes through its use as a solvent, and as effluent from wood pulp mills [280].

TMAO may be produced by bacterial oxidation of trimethylamine (TMA) [202]. In addition, TMAO is found at high concentrations (mM) in marine fish and invertebrates [87, 183], while lower concentrations are found in fresh water animals (μM) [87]. TMAO appears to be used as an osmostabilizer [183], as it has been shown to counteract the effects of urea and inorganic ions [42, 231]. When a marine fish or invertebrate dies, bacteria reduce TMAO, producing the volatile and odorous TMA, resulting in the characteristic smell of rotting fish [18]. In fact, TMA concentration can be used as a measure of bacterial fish decomposition [18].

The widespread occurrence of DMSO and TMAO, suggests these compounds serve as true physiological substrates for reductases [8, 16, 135, 137]. Characterization of the process of bacterial reduction of DMSO and TMAO, may aid in our understanding of the global sulfur cycle, and fish spoilage, respectively.

1.4.2. Bacterial DMSO/TMAO Reduction

Widespread microbial reduction of DMSO and TMAO has been observed [10, 16, 29, 56, 67, 74, 75, 129, 150, 184, 212, 220, 221, 223, 228, 235, 239, 241, 256]. Many of these reductases have been purified [10, 56, 149, 150, 172, 173, 219, 225, 227, 270, 284], their nucleotide sequences determined [27, 100, 142, 157, 176], been shown to possess moco [10, 56, 172, 219, 270, 284], broad substrate specificity [10, 56, 161, 212, 219, 228, 270], and couple reduction of DMSO and TMAO to extrusion of protons [235, 241]. Depending on the bacterial species, TMAO and DMSO reductases show diversity in prosthetic groups, subunit composition, and cellular location [10, 171].

1.4.3. *Rhodobacter sphaeroides* DMSO Reductase

The periplasmic DMSO reductase from *Rhodobacter* (*R.*) *sphaeroides* (DMSOR) is the best characterized anaerobic respiratory S- or N-oxide reductase [5]. It is encoded within an operon downstream from genes coding for a pentaheme cytochrome, and transmembrane protein. The proteins within this operon share sequence similarity with, TorC, TorD, and TorA of 40%, 26%, 48% [252]. DMSOR also shares 54% similarity, and 32% identity with DmsABC [245]. The operon is induced by the divergently transcribed activator DmsR in the presence of DMSO or TMAO [149, 253]. DMSOR has been kinetically characterized to some extent, and has been shown to reduce TMAO as well as a variety of S-oxides [1, 2, 219]. DMSOR has a sixty-six and three fold lower K_m and k_{cat}, respectively, for DMSO than TMAO [219]. In addition, DMSOR has been shown to be enantioselective, and reduces S-oxides in the S configuration when the two carbons adjacent to the sulfoxide are distinct (aromatic versus non-aromatic) [1, 2].

DMSOR is a soluble protein [287], and as such, efforts to crystallize it were successful [220]. The DMSOR protein structure can be divided into four domains that surround the buried moco. These domains are not formed by continuous stretches of polypeptide, and residues that contact the moco are scattered throughout the sequence. While the rest of the bis-MGD is buried, the Mo is exposed at the bottom of a 35 Å funnel. In the oxidized form, Mo(VI) is ligated by four dithiolene sulfurs, S147 and an oxo-ligand. The dithiolene sulfurs are asymmetrically coordinated to the Mo. This may be aided by distinct differences in the conformations of the P and Q pterins. In the reduced state only three dithiolenes coordinate the Mo(IV), in addition to S147. Although there are no major conformational changes to the protein on reduction of the Mo, loss of one of the dithiolenes may be facilitated by a conformational change of the Q pterin [220].

Four other Mo or W-moco containing enzymes have also been crystallized. They are the aldehyde oxidoreductases from *Pyrococcus furiosus* and *Desulfovibrio gigas* [55, 203], FdhF [43], and *R. capsulatus* DMSO reductase [141, 170, 223]. The enzymes listed above do not all share sequence homology, but rather fall into different moco containing oxido-reductase enzyme families. They bind different forms of moco, and some have additional prosthetic groups. Nonetheless, they share the buried moco accessible at the bottom of what has been described as a funnel, tunnel, or channel. It leads from the surface of the protein to the Mo atom of the moco, located approximately in the center of the protein [55, 203, 220, 223].

Examination of the oxidized and reduced forms of the DMSOR crystal structure have allowed generation of a plausible mechanism of DMSO reduction as shown in Figure 1.7. Binding of DMSO to Mo(IV) through its oxygen (1) would weaken the S=0 bond (2). Subsequent transfer of electrons to DMSO would result in release of DMS, possibly aided by a conformational change of the Q pterin (3). The oxygen from DMSO would be left as an oxo ligand. Reduction of Mo(VI) in two one proton one electron steps, would regenerate the reduced enzyme, and result in release of water (4,5) [220]. Examination of *R. capsulatus* DMSO reductase in complex with DMSO confirms binding of DMSO to Mo(IV) weakens the sulfur oxygen double bond [169].

1.4.4. S- and N-oxide Reduction in *E. coli*

In addition to the three terminal reductases DmsABC, TorA and ANO reductase, there are three additional soluble monomeric S-oxide reductases. The two biotin sulfoxide reductases (BisC and BisZ) [68, 69, 187] and methionine sulfoxide peptide reductase (MsrA) [46, 195] are not involved in respiration. They are responsible for reducing oxidized

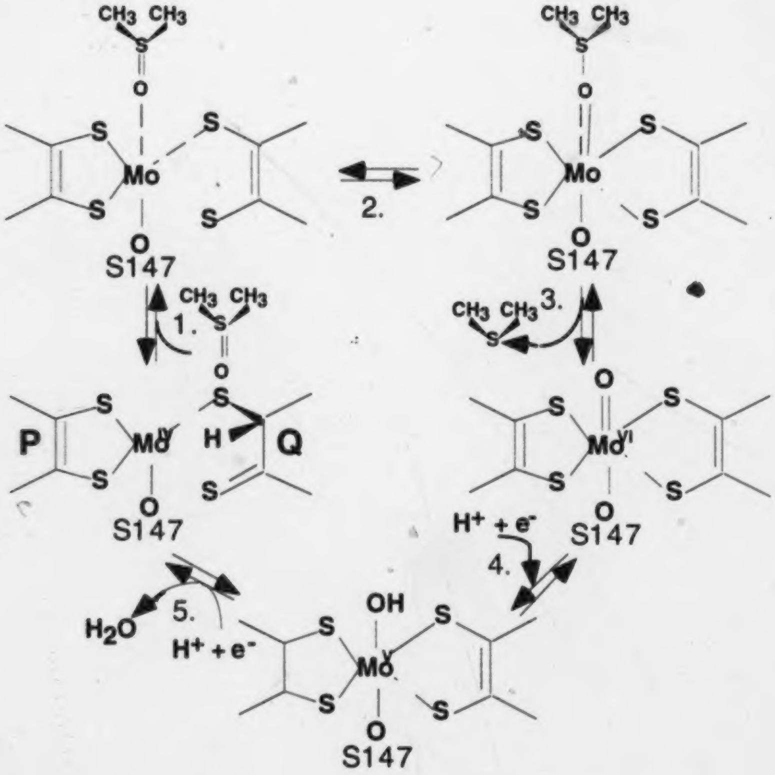
CH3 CH3
S
O
S
Mo
S
S
S
O
S147
2.
1.
3.
P
Q
H
Mo^VI
Mo^IV
H+ + e-
4.
5.
H2O
OH
Mo^V
S147

Figure 1.7.

Proposed Reaction Mechanism for DMSOR

S147 indicates the Mo ligand. P and Q refer to the two pterins [220].

biotin and Met, respectively, in a repair or scavenging mechanism [187, 195]. BisC and BisZ are homologous to DmsABC and are molybdoenzymes [68, 193], while MsrA is not [46].

1.5. DmsABC

1.5.1. Bioenergetics of Growth on DMSO

1.5.1.1. *In vivo* Electron Donors and Acceptors

E. coli can grow by respiration in the presence of a variety of S- and N-oxides and a non-fermentable carbon source [29, 215]. DmsABC is solely responsible for growth on DMSO and methionine sulfoxide, while both TorA and DmsABC are responsible for growth on TMAO and PNO [216]. Glycerol, H_2, and formate have been shown to be suitable electron donors for DMSO reduction [29, 30, 216, 277], while lactate was not [30, 292].

Using MQ and UQ mutants, it has been shown that DmsABC utilizes MQ, and DMQ to a lesser extent, but not UQ [174, 277, 278]. A comparison of the redox potentials for Q's (MQ $^{-}$74, DMQ $^{+}$36, UQ $^{+}$113) and substrates (TMAO $^{+}$130 mV, DMSO $^{+}$160 mV) (Table 1.1) [277] reveals the redox potential for UQ may be too high for reduction of S- and N-oxides.

There is no evidence of cytochrome involvement in DMSO reduction [271] even though DMSO and TMAO induce synthesis of *b*- and *c*-type cytochromes [106, 213, 283]. The cytochrome inhibitors azide and cyanide [30], and mutations in heme or siroheme biosynthesis do not affect DMSO reduction [265].

1.5.1.2. H^+/e^- Ratio and Model for the Generation of a Proton Gradient

E. coli can acidify the medium with the addition of DMSO or TMAO to energized cells [30, 242]. An apparent 2.8-2.9 $H^+/2e^-$ ratio was obtained for DMSO reduction with energized cells [30, 38]. This compares with a value of 3.3 $H^+/2e^-$ for nitrate respiration [30].

The simplest model to explain this $H^+/2e^-$ would suggest two protons are the result of scalar reactions involving Q, while an additional proton is pumped across the membrane either by dehydrogenase or DmsABC. However, a 0.4 $H^+/2e^-$ ratio was observed for DMSO reduction when NDH-I was inhibited with capsaicin, or when using NDH-I mutants. This suggests DmsABC is minimally involved in generation of a pmf [38]. In addition, it has been demonstrated that the growth rate of a NDH-I mutant is half that of a wild-type strain when grown anaerobically by respiration on DMSO. This indicates the importance of NDH-I for respiratory growth on DMSO [243]. The involvement of DmsABC in generation of a proton gradient by scalar or vectorial reactions must be determined experimentally to answer this question.

1.5.2. Molecular Genetics of the *dms* Operon

1.5.2.1. Structure and Organization of the *dms* Operon

The *dmsABC* operon is located at 20.0 minutes on the *E. coli* chromosome. The operon codes for three proteins with molecular weights of 82 350 Da (DmsA), 23 070 Da (DmsB), and 30 789 Da (DmsC) [27]. The type and location of proteins within the *dmsABC* operon parallels that of *E. coli* nitrate reductase-A [33], and -Z [34], and formate dehydrogenase H [39], O [191], and N [22]. The 5' proximal gene in these operons codes for a moco containing catalytic subunit (DmsA), followed by an Fe-S cluster containing electron transfer protein (DmsB), and terminated by a hydrophobic anchor (DmsC).

Ribosome binding sites are found upstream of the putative initiating codons for DmsA, DmsB and DmsC. The latter two ribosome binding sites overlap sequence coding for DmsA and DmsB, respectively [27].

The transcription initiation start site falls 218 nucleotides upstream of the putative initiating codon of DmsA. This results in an unusually long 5' untranslated sequence [77]. This may be due to selection of an incorrect initiating Met [24]. Use of an upstream Met would shorten the 5' untranslated sequence to a more reasonable length. The transcriptional start site is preceded by a reasonable $^{-}$10, but poor $^{-}$35 sequence. This latter feature is characteristic of positively regulated genes [77].

An FNR binding site is centered fifty nucleotides upstream of the transcriptional start site, characteristic of genes positively regulated by FNR [77]. In addition three NarL binding sites have been identified at positions $^{-}$39, $^{-}$19, and $^{+}$3, relative to the translational start site [77, 250]. Speculation would suggest binding of NarL to the NarL binding sites, would impede transcription by RNA polymerase. The spacing of the NarL binding sites suggests NarP may not bind to these sequences [66].

The *dmsABC* transcript is likely terminated by a classical rho-independent terminator downstream of *dmsC* [27].

1.5.2.2. Other Genes Required for DmsABC

FNR, moco (*moa, mob, moe, and mog*), and MQ biosynthetic pathway mutants, are deficient for respiratory growth on DMSO [29, 265]. In addition, mutation of NDH-I results a drop in respiratory growth on DMSO [243]. These results suggest FNR positively regulates *dmsABC* expression, and DmsABC binds moco and oxidizes MQ. In addition, NDH-1 is important for anaerobic growth with DMSO as terminal electron acceptor.

1.5.3. Expression of DmsABC

1.5.3.1. Expression of Wild-type Chromosomal DmsABC

Expression of DmsABC varies depending on the presence of O_2, nitrate, and carbon source. A change in growth conditions from aerobic to anaerobic results in a sixty-five fold increase in expression, and this increase was abolished in an FNR mutant. Mo was required for both complete induction by anaerobiosis and complete repression by aerobiosis. Addition of nitrate to anaerobically growing cells resulted in a twelve fold decrease in expression that dropped to 1.4 and 1.6 fold, in NarL and NarX mutants, respectively [62]. Whether NarX/NarQ or NarL/NarP mutants would relieve residual nitrate repression has not been determined [238]. DmsABC expression was the highest for anaerobic growth on sorbitol and glycerol. The effect of carbon source on expression was not a result of catabolite repression [62].

1.5.3.2. Mutant Chromosomal and Plasmid Encoded DmsABC Expression

Truncation or deletion of each of the three subunits in the *dmsABC* operon separately, indicates expression of all three subunits is necessary for anaerobic respiratory growth on DMSO. If *dmsA* is deleted, or *dmsB* is truncated, both DmsA and DmsB are absent, as indicated by immunoblot analysis. This suggests the stability of DmsA and DmsB depends on the presence of the other subunit. Growth of *dmsABC* mutants deleted for any of the chromosomally encoded subunits can be restored if wild-type copies of the missing subunits are plasmid expressed. This suggests post-translational protein assembly of DmsABC [214].

1.5.4. Enzymology of DMSO reductase

DmsABC has been purified to homogeneity from the membrane fraction, and has been demonstrated to possess a broad substrate specificity reducing a number of compounds including DMSO, TMAO, PNO, and chlorate. DmsABC has a lower K_m and k_{cat} for DMSO than TMAO [270]. As a result, whole cells challenged with DMSO and TMAO reduce DMSO preferentially [28].

DmsABC will accept electrons *in vitro* from reduced benzyl viologen ($BVH^{\cdot +}$), methyl viologen ($MVH^{\cdot +}$), flavin mononucleotide ($FMNH_2$), flavin adenine dinucleotide ($FADH_2$) and the MQ analogues 2,3-dimethyl-1,4-napthoquinol ($DMNH_2$), and 2-hydroxy-3-(3-methyl-2-butenyl)-1,4-napthoquinone (lapachol) [29, 204, 214]. Interestingly, electron transfer from BVH$\cdot^+$ is not dependent on wild-type DmsABC capable of electron transfer from the MQ pool [208, 214]. Electron transfer from BVH$\cdot^+$ appears to bypass one or all of the Fe-S clusters [208]. A similar result has also been found for NarGH, where the Fe-S centers do not appear necessary for nitrate dependent BVH$\cdot^+$ oxidation [50]. However, electron transfer from $DMNH_2$ and lapachol requires DmsA, DmsB, and DmsC, and this is inhibited by the quinone analogue 2-n-heptyl-4-hydroxyquinoline-N-oxide (HOQNO) [204, 205, 214].

1.5.5. Topological Organization of DmsABC

1.5.5.1. Topological Organization of DmsABC With Respect to the Membrane

Approximately 56-77% of DMSO reductase activity is found in the membrane fraction due to DmsABC. In addition, the soluble dimer (DmsAB) accumulates in the soluble fraction, and accounts for 23-44% of DMSO reductase activity [29, 214]. DmsABC was not released from the membrane by washing with low or high ionic strength buffer. However, a variety of detergents solubilized DmsABC, suggesting it is localized to the membrane by a membrane intrinsic subunit [270].

A mutant was isolated that was unable to target DmsA to the membrane, or NapA and TorA to the periplasm. Complementing DNA has been sequenced, and has been suggested to compose membrane targeting and translocation (MTT) machinery [267]. The structure and function of this machinery has not yet been determined.

The amino terminal sequence of purified DmsA as determined by Edman degradation, aligns downstream from the putative translational start site. This suggested the nascent polypeptide was proteolytically cleaved [27]. This sixteen residue peptide cleaved from DmsA shares properties characteristic of signal sequences [63], and initially suggested DmsA may be localized to the periplasm.

Studies carried out to determine the cellular localization of DmsA and DmsB using a variety of biochemical, immunological, and electron microscopic techniques, indicated DmsAB was located on the cytoplasmic face of the membrane [214], while DmsC provided anchoring for the dimer to the membrane [216]. The results were the following : Chloroform and osmotic wash techniques revealed no DmsA or DmsB in the periplasm, and DMSO reductase activity in whole cells was stimulated by the addition of detergent for a membrane impermeable electron donor. DmsAB was susceptible to proteases, lactoperoxidase iodination, and DmsAB-antibody agglutination, only in inverted vesicles. In addition, electron microscopic observation of thin sections showed labeling of DmsA and DmsB on the cytoplasmic surface of the inner membrane [214]. Independent studies using dysprosium-ethylenediaminetetraacetic acid (DyEDTA) and electron paramagnetic resonance (EPR), and examination of β-lactamase fusions in DmsA and DmsB, also confirmed their cytoplasmic orientation. DyEDTA alters EPR features of Fe-S centers, and as a result, addition of DyEDTA to whole cells or inside-out vesicles allows the distance between DyEDTA and Fe-S clusters to be determined. Dy-EDTA was found to be closer to the DmsB Fe-S clusters in inverted vesicles [209]. All β-lactamase fusions in DmsA and DmsB were sensitive to ampicillin, indicating the DmsA and DmsB β-lactamase fusions were found in the cytoplasm. In addition, fusion of alkaline-phosphatase (PhoA) within the terminating codon of DmsC resulted in assembly of functional DmsABC. This indicates the fused periplasmic PhoA does not interfere with binding of DmsAB to DmsC [272]. It has also been shown that in the absence of DmsC, DmsA and DmsB are localized to the periplasm, suggesting DmsC acts as a stop transfer signal [267].

Due to these overwhelming results, it was postulated the DmsA "leader" was an evolutionary vestige [27], since other related soluble S- and N-oxide reductases are known to be periplasmically localized [56, 75, 220, 223]. Cleavage of the sixteen residue leader may have resulted from proteolysis during cell lysis or purification [27]. Only recently have inhibitors for leader peptidase I been found [63], thus at the time it was not possible to use protease inhibitors during cell lysis to prevent cleavage of the leader from DmsA.

Recent sequence analysis has suggested DmsA may initiate at a Met twenty-nine residues upstream from the originally proposed Met. If correct, DmsA would possess a double-arginine leader, postulated to be responsible for translocating fully folded proteins to the periplasm [24]. This observation suggests DmsA should be localized to the periplasm. However, as indicated above, there is overwhelming evidence that DmsAB is located on the cytoplasmic face of the membrane [209, 214]. Experiments will be needed to determine the correct initiating Met, and if necessary the importance of the double-arginine leader in production of functional DmsABC.

1.5.5.2. Topological Organization of DmsA, DmsB, and DmsC with Respect to Each Other

Both anti-DmsA and anti-DmsB antibodies label inverted vesicles, and both DmsA and DmsB are protease sensitive when attached to the membrane, indicating both DmsA and DmsB are accessible to the cytoplasm [214]. This is in contrast to FrdABCD, where FrdA is thought to umbrella FrdB, protecting FrdB from proteolysis and iodination [58, 154].

1.5.6. DmsC

Although there is substantial sequence similarity between DmsA and DmsB, and other moco and Fe-S cluster containing proteins, respectively, there is little sequence conservation between DmsC and other anchor subunits for respiratory enzymes. Unlike DmsA and DmsB, DmsC is not antigenic and is not visualized on Coomassie blue polyacrylamide stained gels [249].

1.5.6.1. Topology of DmsC

Hydropathy analysis predicts DmsC contains eight transmembrane helices [27]. The use of β-lactamase and PhoA gene fusions within DmsC revealed the amino and carboxyl termini are exposed to the periplasm, and the polypeptide threads though the membrane as predicted [272].

1.5.6.2. DmsC Anchors DmsAB to the Membrane

Unlike FrdABCD and SdhABCD where the membrane anchors are composed of two small subunits [54, 58, 60], the large single subunit DmsC is responsible for anchoring DmsA and DmsB to the membrane. This interaction is stabilized by substrate [214]. The entire DmsC appears to be necessary for this function, as gene fusions that truncate DmsC resulted in accumulation of DmsAB in the soluble fraction [272].

1.5.6.3. DmsAB is More Stable in the Presence of DmsC

Like FrdCD [58], DmsC stabilizes the catalytic dimer. While membrane bound or purified DmsABC is stable to freezing in liquid N_2 and thawing, incubation at 4°C for four hours, or 30°C for 45 minutes, the DmsAB dimer is not, with only 30%, 40%, and 12% activity left, respectively [216].

1.5.6.4 DmsC is Responsible for MQ Binding

DmsABC catalyzes the oxidation of $DMNH_2$ and lapachol in the presence of S- or N-oxide, but DmsAB cannot. This suggests DmsC retains the MQ binding site [205, 214]. H65 in DmsC is suggested to compose part of this binding site, as $DmsABC^{H65R}$ is unable to oxidize reduced MQ (MQH_2) *in vivo*, and HOQNO no longer effects the lineshape of DmsB cluster 1 altered from a [4Fe-4S] to [3Fe-4S] cluster [210]. More recently, 1:1 HOQNO binding to DmsC has been demonstrated, and is abolished in the H65 mutant [290]. Sequence comparisons suggest H65 is equivalent to H82 in FrdC. Mutation of this residue in FrdC also blocks *in vivo* MQH_2 and *in vitro* $DMNH_2$ oxidation by FrdABCD, as well as HOQNO effects on Fe-S cluster 3 of FrdB are similar [211, 268].

FrdABCD, NarGHI, and CyoABCD have been suggested to possess two Q binding sites. MQH_2 is suggested to bind to FrdABCD at Q_B (low affinity/dissociable - Q_L) site. It is released once oxidized, after its electrons have been transferred to non-dissociable Q at the Q_A (high affinity/non-dissociable - Q_H) site [275, 276]. NarI and CyoO are also suggested to possess Q_L and Q_H binding sites [164, 165, 218]. For NarI, Q is suggested to bind to Q_L site and electrons are subsequently transferred through the low and high potential hemes and Q_H before being transferred to NarH [164, 165]. Analysis using HOQNO has demonstrated there is one dissociable Q site in DmsC [290]. The possibility of an additional high affinity site has not been explored. However, two Q binding sites would be difficult to reconcile with existing data. If DmsC had two Q binding sites, HOQNO would bind at the Q_L site, and there would be an additional Q bound at the Q_H site between HOQNO and the Fe-S clusters. This would make interaction between HOQNO and the Fe-S clusters improbable. However, HOQNO has been observed to alter the lineshape of DmsB Fe-S cluster 1 when altered from a [4Fe-4S] cluster to a [3Fe-4S], indicating their close proximity and lack of intermediate redox centers [210].

1.5.6.5 The Role of DmsC in Electron and Proton Transfer

In contrast to DmsC, the membrane anchor subunits of NarGHI [163], NarZYV, FdhGHI [25], FdoGHI, and HyaABC, are suggested to bind two heme *b*'s [81], while SdhABCD binds only one [140]. It is likely these hemes facilitate electron transfer between the Q pool, and electron transfer subunits. In addition, the cytochrome oxidases each bind one heme *b* involved in electron transfer from the Q pool to the site of O_2 reduction [81]. NrfABCD, TorCAD, and Nap are anaerobic periplasmic respiratory enzymes that all appear to use multiple heme *c*'s in electron transfer from the Q pool [88, 104, 176]. Since DmsC is missing these extra prosthetic groups, electron transfer through DmsC must occur by an alternate mechanism.

The MQ binding site in DmsC may either be near the periplasmic or cytoplasmic surface of the membrane and this results in different consequences for proton and electron transfer within DmsC. With DmsAB on the cytoplasmic face of the membrane [209, 214, 267], and the MQ binding site near the periplasmic surface, a pmf would be generated by scalar reactions, but a mechanism would be needed for the translocation of electrons to the Fe-S clusters (Figure 1.8. A1.). If the MQ binding site is near the cytoplasmic surface, there is no difficulty in electron transfer to the Fe-S clusters. However, this would require a mechanism for proton translocation if DmsABC were found to generate a pmf (Figure 1.8. C.).

DmsC residue H65 has been demonstrated to be part of the MQH_2 binding site [210, 290], and topological analysis suggests H65 is near the periplasmic surface of the membrane [272]. With DmsAB on the cytoplasmic face of the membrane [209, 214, 267] these observations support a model for the scalar generation of a proton gradient by DmsABC involving MQH_2 binding to DmsC near the periplasmic surface of the membrane. To explain electron transfer from the periplasmic half of DmsC to the DmsB Fe-S clusters, DmsB may protrude into DmsC to make the distance between the MQH_2 binding site and the Fe-S clusters shorter (Figure 1.8. B.), and/or residues in DmsC may aid in movement of electrons to the Fe-S clusters. The first hypothesis is consistent with the observation that HOQNO affects the lineshape of Fe-S cluster 1 altered from a [4Fe-4S] to a [3Fe-4S] cluster. In addition, DmsB mutants altered in cluster 1 were unable to oxidize the Q pool, but maintained the ability to reduce the Q pool. This suggests mutation of cluster 1 in DmsB results in decreased binding of MQH_2 to DmsC, but MQ binding remains unchanged [210]. Together these results suggest the MQH_2 binding site and Fe-S cluster 1 are in close proximity [210]. DyEDTA/EPR analysis suggests cluster 1 is close to the interface between DmsB and DmsC [209]. However, the method is not accurate enough to differentiate between DmsB residing on the top of DmsC, or slight penetration of DmsB into DmsC. However, an alternate explanation for the interaction of HOQNO with cluster 1

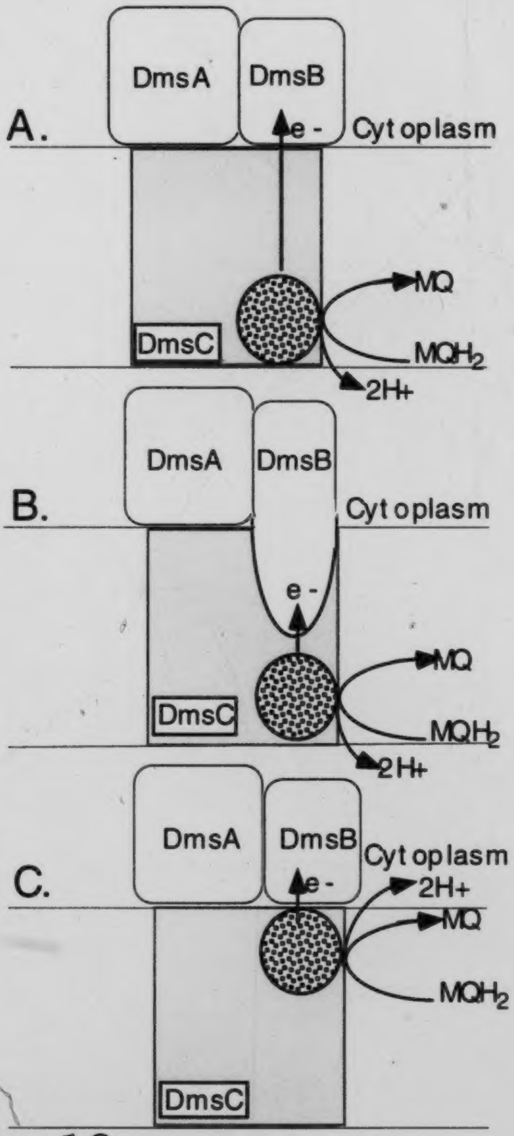
A.
DmsA
DmsB
e -
Cytoplasm
MQ
DmsC
MQH_2
2H+
B.
DmsA
DmsB
Cytoplasm
e -
MQ
DmsC
MQH_2
2H+
C.
DmsA
DmsB
Cytoplasm
e -
2H+
MQ
MQH_2
DmsC

Figure 18.

Schematic of MQH_2 Binding to DmsC and Electron Transfer to DmsB

Scenarios of MQH_2 binding are shown, with the MQH_2 binding site shown on DmsC as a square patched circle. The location of the binding site has ramifications for generation of a pmf by DmsABC, and electron transfer to DmsB. In B. DmsB is shown to protrude into DmsC.

would suggest the MQH_2 binding site is closer to the cytoplasmic surface of the membrane due to a shift in DmsC helix II (Figure 1.8.C.). This would abolish production of a pmf by DmsABC via scalar reactions. If DmsABC were proven to generate a pmf, this could still be explained by DmsC translocating protons to the periplasm by a proton wire. This hypothesis is consistent with the following result. Over-expression of DmsC in *E. coli,* in the absence of DmsAB is lethal. However, lethality can be overcome by expression in a F_0F_1 ATPase mutant, or in eukaryotic cells. This suggests lethality by DmsC may be the result of uncoupling of the cells to protons by forming a proton wire or channel, and F_0F_1 ATPase depleting cellular ATP in an effort to maintain the pmf [249].

1.5.7. DmsB

The ultraviolet (UV) absorption spectra of DmsABC between 325 and 450 nm is rather non-descript, but is somewhat characteristic of Fe-S containing proteins [270].

1.5.7.1. DmsB is an Fe-S Protein

DmsB has sixteen Cys residues arranged in four groups (numbered I-IV starting at the amino terminus), and the spacing between the Cys's is characteristic of enzymes binding [4Fe-4S] clusters (Figure 1.9.) [27]. Beginning at the amino terminus, the four Cys's in each of the groups are labeled C_A, C_B, C_C, and C_D. The first three Cys's of a group (C_A-I, C_B-I, C_C-I) ligate one cluster, as well as a fourth (C_D-x) distant Cys from another group [53]. Four [4Fe-4S] cluster binding motifs exist consisting of four Cys's with specific spacing, and in some cases an additional conserved Lys or Pro. DmsB possesses one of each of the four [4Fe-4S] cluster binding motifs. Group I is motif I, group II is motif II, group III is motif III, and group IV is motif IV [81].

The Fe-S clusters in DmsB are visible by EPR spectroscopy, and the intensity of the Fe-S clusters corresponds to 3.82 spins per DmsABC. The EPR spectra could be best fitted by four [4Fe-4S]

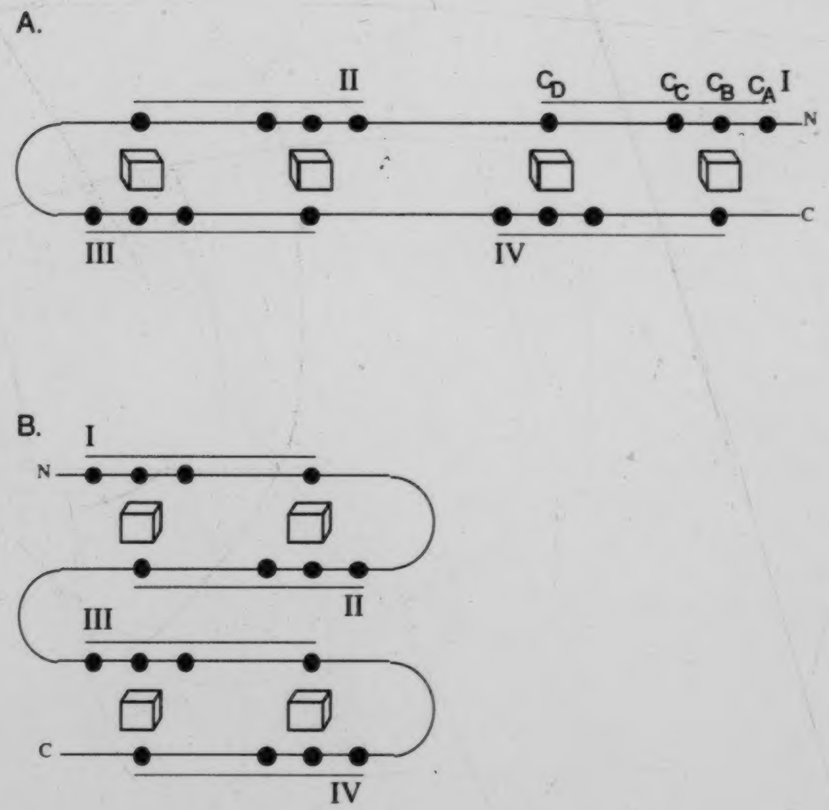

Figure 1.9.

Gene Insertion and Gene Duplication Models for Fe-S Cluster Binding in DmsB

The predicted group ligation is indicated for the gene insertion (A.) and gene duplication (B.) models for formation of DmsB from two bacterial two [4Fe-4S] ferredoxin progenitors. The polypeptide is schematically indicated, and the amino (N) and carboxy (C) termini are indicated. The Cys's are indicated by filled circles, and the Fe-S clusters are depicted by boxes. Cys groups I-IV and labelled, and the Cys residues belonging to them are underlined. The Cys's C_A, C_B, C_C, and C_D, are labelled for Cys group I in the gene insertion model, but the labels apply for all groups. In A. groups I and IV are paired, while in B. groups I and II are paired.

clusters with midpoint potentials at pH 7.0 ($E_{m,7}$) of $^{-}50/^{-}60$, $^{-}120/^{-}122$, $^{-}240$, and $^{-}330$ mV, referred to as clusters 1-4, in order of decreasing potential. (The two values for $E_{m,7}$ for cluster 1 and 2 are for alternate determinations [53, 210]). The reduced EPR signal is quite complex. This is due to magnetic interactions between the reduced Fe-S clusters. As a result, specific features of the reduced EPR signal cannot be assigned to particular Fe-S clusters. There appears to be a strong magnetic interaction between Fe-S clusters 1 and 2 (the $^{-}50$ and $^{-}120$ mV clusters). However, due to the overall complexity of the EPR signal, once clusters 1 and 2 are reduced, it is not possible to determine whether clusters 3 and 4 interact (the $^{-}240$ and $^{-}330$ mV clusters). However, the EPR spectrum can generally be interpreted as two pairs of interacting [4Fe-4S] clusters, with each pair sharing spectroscopic similarities with the bacterial [4Fe-4S] ferredoxins [210].

1.5.7.2. Mutagenesis of DmsB Cys Residues to Define the Cys Groups (I-IV) that Ligate Each of the Four Fe-S Clusters (1-4)

In an effort to identify the Cys groups (I-IV) that ligate each of the four Fe-S clusters in DmsB (1-4), site-directed mutagenesis was employed to alter the Fe-S cluster composition of DmsB. This was attempted by mutation of C_B from each group [208]. Similar efforts have been made for respiratory enzymes with Fe-S clusters including NarGHI [11, 12, 91], and FrdABCD [167, 274], by mutating numerous Cys residues believed to ligate the Fe-S clusters.

Mutation of C102, C_B in group III, to Trp, Ser, Tyr, and Phe, resulted in loss of the $^{-}50$ mV [4Fe-4S] cluster, and appearance of a new $^{+}220$ or $^{+}260$ mV [3Fe-4S] cluster for the Trp and Ser mutants, respectively [208, 210]. Alteration of cluster 1 results in loss of growth on glycerol/DMSO minimal media (Gly/DMSO), indicating the importance of cluster 1 in DmsABC function, and indicating C_B in group III ligates cluster I [208].

Unfortunately, mutation of Cys C_B from groups II and IV, resulted in an inability of DmsAB to assemble onto the membrane, suggesting structural alteration of the mutated enzymes. Mutation of Cys C_B from group I resulted in poor accumulation of DmsB on the membrane, and as a result, mutants were difficult to characterize by EPR spectroscopy [205].

Models for ferredoxins with two [4Fe-4S] clusters suggest C_A, C_B,and C_C, ligate the first cluster, and C_D ligates the paramagnetically interacting cluster and vice versa [271]. If DmsB is composed of two ferredoxin motifs (two [4Fe-4S] clusters) [271], this could either be the result of a gene duplication, or gene insertion event (Figure 1.9.). Group III has been demonstrated to ligate the $^{-}$50 mV cluster (see above) [210]. Since the $^{-}$50 mV and $^{-}$120 mV clusters are known to interact [208], the gene insertion (Figure 1.9. A.) and gene duplication models (Figure 1.9. B.) predict group II and IV ligate the $^{-}$120 mV cluster, respectively. In addition, the gene insertion and gene duplication models predict group I and II, and group I and III, respectively, share more sequence similarity. Sequence analysis suggests clusters I and II, and III and IV, are most similar supporting the gene insertion model [205]. Determination of the Cys groups responsible for ligating the clusters 1-4 in NarH also support the gene insertion model for evolution from two [4Fe-4S] ferridoxin progenitors [91]. Mutation of additional Cys residues will be required to unequivocally identify the clusters (1-4) that are ligated by each of the Cys groups (I-IV).

1.5.7.3. Electron Flow Through DmsB

Reduction of DMSO requires two electrons. However, there are four Fe-S clusters, each that could carry one electron. This indicates all the Fe-S clusters may not be needed for electron transfer to the Mo [271]. With the redox potentials of MQ and DMSO being $^{-}$80 and $^{+}$160 mV, respectively, it appears only clusters 1 and 2 ($^{-}$50 and $^{-}$120 mV, respectively) have reasonable midpoint potentials to mediate electron transfer. Clusters 3 and 4 ($^{-}$220 and $^{-}$330 mV, respectively) appear to have potentials that are too low to mediate electron transfer for the reaction. [53]. A similar situation is observed in FrdABCD [143], and NarGHI [25]. However, since the low potential Fe-S clusters are found along an electron pathway, their low potential may not exclude them from electron transfer. For example, lowering the midpoint potential of the $^{-}330$ mV cluster of FrdB even further impaired function, suggesting this low potential cluster may be used for electron transfer [143]. Alternatively, the low potential clusters may play a structural role. Mutagenesis studies on DmsB, NarH, and FrdB, have indicated disruption of Fe-S clusters often leads to defects in enzyme assembly [11, 143, 167, 205]. Finally, it has been suggested that low potential clusters may play a role in regulating the activity of the enzyme. In the case of NarH, exposure to low redox potentials has been observed to activate the enzyme. This has been suggested to be mediated by reduction of the low potential clusters, and would occur *in vivo* under anaerobic conditions [21].

Cluster 1 ($^{-}50$ mV) appears to be the entry point for electrons into DmsB, since alteration of this cluster affects electron transfer from the MQH$_2$ pool, but does not affect the ability of the rest of the clusters to be oxidized by DMSO [210]. This is consistent with results indicating cluster 1 is near the MQ binding site, as addition of HOQNO results in lineshape changes to cluster 1 when altered from a [4Fe-4S] cluster to a [3Fe-4S] cluster [210]. In addition, DyEDTA/EPR analysis suggests cluster 1 is close to the interface between DmsB and DmsC [209]. HOQNO has no effect on the lineshape of clusters 2, 3, and 4, indicating they are more distant from the MQH$_2$ binding site [210]. Although these results suggest electron transfer from MQH$_2$ to cluster 1, the pathway of electrons from cluster 1 to DmsA is at present unknown. However, the Mo and Fe-S clusters appear to be in close proximity, between 8 and 12 Å, as suggested by their EPR spin-spin interactions [53].

1.5.8. DmsA

1.5.8.1. DmsABC is a Molybdoenzyme

Tungstate inhibits growth of *E. coli* on Gly/DMSO [207], as does mutation at the *moa, mob,* and *moe* loci (Figure 1.5.) [29]. This suggests one of the enzymes necessary for growth on Gly/DMSO is a molybdoenzyme with a dinucleotide form of the cofactor [89, 119, 120].

Membrane bound DmsABC binds stoichiometric amounts of Mo, as indicated by mass spectrometry, and EPR spin quantitations of the Mo in comparison to the DmsB Fe-S signals [205]. Only 0.34 moles of Mo were found per mole of purified DmsABC, indicating Mo loss during purification [270]. This is in contrast to DMSOR where 0.93 moles of Mo were found per mol of purified enzyme [99]. The redox poised EPR spectra of DmsABC demonstrates the presence of Mo(V). The Mo has $E_{m,7}$'s of $^-90/^-175$ and $-75/^-15$ mV for the IV/V and V/VI couples, respectively. (The two values are for alternate determinations [53, 245]). The Mo EPR lineshape suggests DmsABC and NarGHI have similar binding geometries. However, they possess different Mo $E_{m,7}$'s (NarGHI : $^+180$ and $^+220$ mV for the IV/V and V/VI couples, respectively) that fit well with their alternate substrates (Table 1.1) [271].

The UV absorption spectra for purified DmsABC has a peak at 290 nm, presumably from bound moco [270]. The presence of moco in DmsABC has been shown unequivocally by conversion of released cofactor to the fluorescent derivative FormA, and reconstitution of moco deficient *Neurosporra crassa* NADH-phosphate (NADPH) nitrate reductase with denatured extract from DmsABC [270].

The pathway of moco insertion into DmsABC has been studied using cells grown on Gly/DMSO in the presence of tungstate, or with a *mob* mutation. Growth in the presence of tungstate inhibits insertion of moco into DmsABC, as does a *mob* mutation. These results indicate nucleotide and Mo addition to MPT precedes cofactor insertion into

DmsABC [207]. A similar study has recently been performed on NarGHI, with similar results obtained, confirming the pathway of moco insertion as suggested from results with DmsABC [206]. Molybdoenzyme crystal structures reveal the moco is buried within the protein, suggesting cofactor addition should precede the final folding of the polypeptide [43, 55, 203, 220, 223].

1.5.8.2. DmsA Binds Moco

Preparations enriched in DmsA indicate strong Mo EPR signals, but weak Fe-S signals, indicating the Mo is ligated by DmsA [53].

Multiple sequence alignments of moco containing subunits from prokaryotic enzymes reveal blocks of sequence homology separated by sequence that differs in length and composition (Figure 1.10.) [25, 271, 281]. The alignments suggest the enzymes share a similar polypeptide fold and active site [220, 223, 281]. This has been confirmed by analysis of the crystal structures of DMSOR, FdhF, and *R. capsulatus* DMSO reductase [43, 220, 223]. Sequence comparisons confirm DmsA binds moco, and is the site of DMSO reduction [27, 244, 271].

Molybdoenzymes in the family that do not possess an additional Fe-S cluster containing subunit (BisC, BisZ, and TorA), are missing the first homologous sequence block [176]. As a result, it has been suggested to be important in electron transfer between the moco and Fe-S binding subunits [244].

DmsA is found on the surface of the cytoplasmic membrane [214, 272], and is the site of DMSO reduction [27, 244, 271]. This has implications for S- and N-oxide accessibility to the active site. Although no transporter has been implicated in the transfer of S- and N-oxides across the membrane, whole cells are capable of using S- and N-oxides, indicating they are able to reach the cytoplasmic compartment (chapter 6 and [229]).

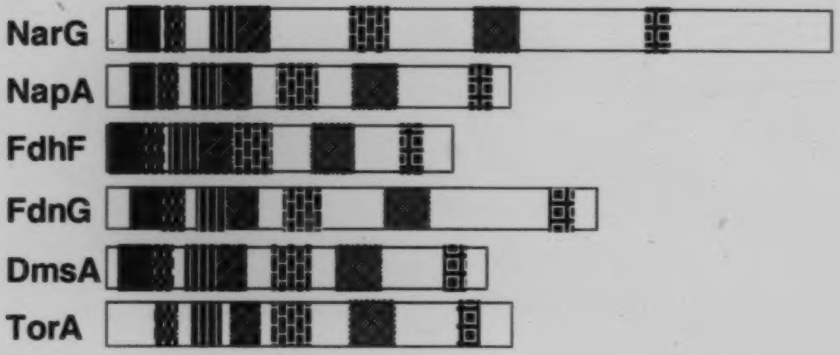

Figure 1.10.

Blocks of Sequence Homology are Shared Between Prokaryotic Moco Containing Enzymes

Selected *E. coli* molybdoenzymes are shown. The polypeptides and their blocks of homology are represented as rectangular units, and different patterned blocks, respectively. Molybdoenzymes in the family that do not possess an additional Fe-S cluster containing subunit (BisC, BisZ, and TorA), are missing the first homologous sequence block [176]. A portion of the second homologous sequence block has been demonstrated to compose a large portion of the active site funnel [169, 220, 223], and possess the Mo ligand [169, 220, 223, 245].

1.5.8.3. Engineering a Novel Fe-S Cluster into DmsA

There are a number of conserved Cys residues within the first homologous sequence block in prokaryotic molybdoenzymes with Fe-S cluster containing subunits. For some of the proteins in the family, including NapA, FdhG, FdoG, and FdhF, the Cys spacing resembles an Fe-S cluster binding motif [244]. In fact, FdhF and the periplasmic *Thiosphaera pantotropha* nitrate reductase have been shown to ligate a [4Fe-4S] cluster [43, 44]. These Fe-S clusters are likely involved in electron transfer between subunits [43]. However, for other proteins in this family, including DmsA, NarG, and NarZ, the spacing is incorrect for ligation of an Fe-S cluster. Three residues are found between the first His/Cys and the second Cys of the motif, rather than correct spacing of two residues [244].

Site-directed mutagenesis of DmsA was used to remove the second Cys of the motif (creating DmsA mutants C38S and C38A), and correct the spacing between the first two Cys residues (creating DmsA mutant N37C,C38S). The C38S, C38A, and N37C,C38S mutants, were each observed to have incorporated a novel [3Fe-4S] cluster, with $E_{m,7}$'s of $^{+}75/^{+}140$, $^{+}165/^{+}200$, and $^{+}40/^{+}200$ mV, respectively. The large range in $E_{m,7}$ for each of the novel Fe-S cluster's is likely a result of Fe-S cluster instability. These results confirmed wild-type DmsA does not ligate a Fe-S cluster [246] as suggested for those prokaryotic molybdoenzymes with the correct Cys spacing in the first homologous sequence block [81]. However, alteration of the sequence will allow an Fe-S cluster to be ligated. The ability of DmsA to ligate a Fe-S cluster at its N-terminus may have been lost during evolution [246].

A similar study performed on NarGHI confirms the observation above. Mutation of the first conserved residue (His-50) suggested to be involved in Fe-S cluster ligation resulted in no alteration in the number or redox potential of Fe-S clusters in NarGHI. This indicates both the conserved residues in DmsA, and NarG, are not involved in the ligation of an Fe-S cluster [162].

1.5.8.4. Electron Transfer Through DmsA

The first block of sequence homology found in prokaryotic molybdoenzymes with Fe-S cluster containing subunits have five conserved residues (K28, C38, C42, C75, and R77). These residues were mutated in DmsA, and their function was examined by the ability of DmsABC to support growth on Gly/DMSO, reduce DMSO using $BVH^{\cdot +}$ and $DMNH_2$, and accept electrons from the Q pool. Two of these residues (K28 and C75) showed no measurable effect on any of the parameters tested, while C38, C42, and R77, had variable effects on the parameters measured. This suggests electrons from the various electron donors follow different paths to reach the Mo. All three residues were necessary for electron flow to and from the Q pool, and growth on Gly/DMSO. R77 was essential for $DMNH_2$ oxidase activity, while mutation of C38 and C42 showed lowered activity with this substrate. Only C42 was found to be important for $BVH^{\cdot +}$ oxidase activity [244]. Although the N-terminal portion of DmsA does not ligate an Fe-S cluster (see above section 1.5.8.3.) as has been demonstrated for some other prokaryotic molybdoenzymes [43, 44, 246], some of the conserved residues still appear important for electron transfer to the Mo [246]. The crystal structure of FdhF implicates K44 in electron transfer from the pterin ring of the moco to the [4Fe-4S] cluster [43]. K44 in FdhF is equivalent to R77 in DmsA [25], confirming a role for R77 in electron transfer from DmsB to the moco in DmsA.

1.5.8.5. The Protein Ligand of Mo

The DMSOR and FdhF crystal structures reveal a single protein ligand to the Mo, a Ser and Seleno-Cys (Se-Cys), respectively [43, 220]. Alignment of prokaryotic moco containing enzymes reveals the protein ligand in DMSOR and FdhF is a conserved residue, being either a Ser (DmsA, BisC, BisZ, and TorA), Cys (NarG, NarZ, and NapA), or seleno-Cys (FdhF, FdoG, and FdnG) [25, 245]. Mutation of this residue in DmsA (S176) to Ala, Cys, or His, resulted in an inability to grow on Gly/DMSO, or reduce DMSO in the presence of $BVH^{\cdot +}$. In addition, the mutated enzymes showed altered Mo redox potentials and EPR lineshapes, consistent with S176's role as a Mo ligand. The S176A mutant was trapped in the Mo(V) state, while the Mo(V) state was completely inaccessible in the S176H mutant. In addition, Mo(V) in the S176C mutant appeared to interact with the $^{-}240$ mV cluster [245].

1.6. Thesis Objectives

The objectives of this thesis were :

1. Examination of the Soluble Subunits (DmsAB) of DMSO Reductase (DmsABC)
2. Structural Identification and Quantitation of the Molybdenum Cofactor in DmsABC
3. Determination of the Initiating Met for DmsA and Importance of the DmsA Leader Sequence
4. Assay Examination and Development for DmsABC
5. Examination of the Substrate Specificity of DmsABC and TMAO Reductase (TorA)
6. Modulation of the Substrate Specificity of DmsABC
7. Elucidation and Characterization of Pyridine N-oxide Reductase

This thesis focuses on DmsABC (Chapters 2, 3, 4, 5, 6, and 7). However, our research led us to discover a previously uncharacterized S- and N-oxide reductase (Chapter 8), and our collaboration with Dr. Giordano led to our involvement in the kinetic characterization of TorA (Chapter 9). The research performed in this thesis was also influenced by various interests in the lab (Chapters 2, 5, and 6), and by developments in our field of research : observation of a nucleotide appended to MPT in DMSOR [119] (Chapter 3), sequence analysis of redox cofactor containing enzymes [24] (Chapter 4), and the DMSOR crystal structure [220] (Chapter 7).

Due to the potential usefulness of soluble DMSO reductase for X-ray crystallographic studies or cyclic voltametry, we examined the properties of soluble DmsAB lacking the DmsC anchor subunit (Chapter 2). This included reconstitution of moco into apo-DmsA. We outlined a preliminary purification scheme for DmsAB, and characterized some salient features of DmsABC structure and function.

The structure of the moco in DmsA was addressed (Chapter 3). Studies indicated the locus responsible for addition of nucleotide to MPT [119] was required for DmsABC function [29]. To determine whether nucleotide was appended to MPT in DmsA, and the identity of the nucleotide, DmsABC was purified, and moco from DmsABC was characterized by fluorescence and absorption spectroscopy.

Sequence analysis of redox cofactor-containing proteins [24] suggested the proposed initiating Met for DmsA was incorrect. In addition, this analysis suggested the DmsA N-terminal leader contained a novel double-arginine consensus, important for the translocation of a subset of redox cofactor containing proteins across the membrane. W determined the correct initiating Met for DmsA, and the importance of the DmsA leader and double-arginine consensus for production of functional DmsABC (Chapter 4). This was achieved by creating a number of site-directed mutants, and using polymerase chain reaction (PCR) and cloning to create a number of *tac* promoter constructs. These DmsABC mutants and constructs were examined for growth on Gly/DMSO, accumulation, and expression.

Chapter 5 presents the results of a kinetic characterization of DmsABC, and further results are presented in Chapters 6 and 7. In an effort to understand assay parameters influencing DmsABC activity, we examined two commonly employed assays (Chapter 5). We also examined the usefulness of nuclear magnetic resonance (NMR) spectroscopy for kinetic analysis of DmsABC. In addition, the kinetic constants for the electron donor part of the reaction were determined.

The substrate specificity of DmsABC [270] was examined in detail (Chapter 6), in order to gain an understanding of the parameters affecting substrate binding and turnover. The kinetic constants for more than fifty S- and N-oxides and miscellaneous compounds were determined. The ability of these substrates to serve as anaerobic terminal electron acceptor in wild-type *E. coli* was monitored.

Key residues potentially influencing substrate specificity were identified by examination of the DMSOR crystal structure [220], and comparison of DmsA and DMSOR sequences (Chapter 7). Site-directed mutagenesis was employed to alter active site residues in DmsA. Seventeen DmsA mutants were created, and their growth, accumulation, and kinetic parameters were examined.

An effort was made to determine the role of DmsABC and TorA in respiratory growth (Chapter 8). As a result, we identified an additional anaerobically expressed energy conserving terminal reductase, that allows anaerobic growth on substituted PNO's in the presence of glycerol. This enzyme, PNO reductase (PNOR), was characterized for activity, accumulation, localization, and was partially purified. We also isolated a mutant with increased PNOR activity. The identity of this newly identified terminal reductase is proposed.

With a desire to compare the substrate specificities of DmsABC and TorA, we performed a kinetic analysis of TorA (Chapter 9). It was similar to that performed on DmsABC (Chapter 6).

The work reported herein has broadened our understanding of the structure and function of DmsABC, TorA and PNOR. The data obtained allows us to pursue previously unavailable avenues of research for proteins involved in electron transport.

1.7. References

1. Abo, M., Tachibana, M., Okubo, A. and Yamazaki, S. (1994) Enantioselective reduction of the sulfoxide to sulfide in methyl phenyl sulfoxide by dimethyl sulfoxide reductase from *Rhodobacter sphaeroides* f. s. *denitrificans*. Biosci. Biotech. Biochem. 58, 596-597.

2. Abo, M., Tachibana, M., Okubo, A. and Yamazaki, S. (1995) Enantioselective deoxygenation of alkyl aryl sulfoxides by DMSO reductase from *Rhodobacter sphaeroides* f.s. *denitrificans*. Bioorg. Med. Chem. 3, 109-112.

3. Abou-Jaoude, A., Chippaux, M. and Pascal, M.-C. (1979) Formate-nitrite reduction in *Escherichia coli* K-12. 1. Physiological study of the system. Eur. J. Biochem. 95, 309-314.

4. Adams, M.W.W. and Mortenson, L.E. (1982) The effect of cyanide and ferricyanide on the activity of the dissimilatory nitrate reductase of *Escherichia coli*. J. Biol. Chem. 257, 1791-1799.

5. Alef, K. (1987) The interaction between dimethylsulfoxide and nitrate reducing pathways in *Rhodobacter capsulatus*. FEMS Microbiol. Lett. 48, 11-14.

6. Allen, J.F. (1993) Redox control of transcription: sensors, response regulators, activators and repressors. FEBS Lett. 3, 203-207.

7. Andreae, M.O. (1980) Dimethylsulfoxide in marine and freshwaters. Limnol. Oceonogr. 25, 1054-1063.

8. Andreae, M.O. and Crutzen, P.J. (1997) Atmospheric aerosols: biogeochemical sources and role in atmospheric chemistry. Science 276, 1052-1057.

9. Anraku, Y. and Gennis, R.B. (1987) The aerobic respiratory chain of *Escherichia coli*. Trends Biochem. Sci. 12, 262-266.

10. Arata, H., Shimiza, M. and Takimiya, K.-I. (1992) Purification and properties of trimethylamine N-oxide reductase from aerobic photosynthetic bacterium *Roseobacter denitrificans*. J. Biochem. 112, 470-475.

11. Augier, V., Asso, M., Guigliarelli, B., More, C., Bertrand, P., Santini, C.-L., Blasco, F., Chippaux, M. and Giordano, G. (1993) Removal of the high-potential [4Fe-4S] center of the β-subunit

from *Escherichia coli* nitrate reductase. Physiological, biochemical, and EPR characterization of site-directed mutated enzymes. Biochem. 32, 5099-5108.

12. Augier, V., Guigliarelli, B., Asso, M., Bertrand, P., Frixon, C., Giordano, G., Chippaux, M. and Blasco, F. (1993) Site directed mutagenesis of conserved cysteine residues within the β-subunit of *Escherichia coli* nitrate reductase. Physiological, biochemical, and EPR characterization of site-directed mutated enzymes. Biochem. 32, 2013-2023.

13. Austin, D. and Larson, T.J. (1991) Nucleotide sequence of the *glpD* gene encoding aerobic *sn*-glycerol 3-phosphate dehydrogenase of *Escherichia coli* K-12. J. Bact. 173, 101-107.

14. Axley, M.J., Grahame, D.A. and Stadtman, T.C. (1990) *Escherichia coli* formate-hydrogen lyase. Purification and properties of the selenium-dependent formate dehydrogenase component. J. Biol. Chem. 265, 18213-18218.

15. Banwart, W.L. and Bremner, J.M. (1976) Evolution of volatile sulfur compounds from soils treated with sulfur-containing organic compounds. Soil Biol. Biochem. 8, 439-443.

16. Barrett, E.L. and Kwan, H.S. (1985) Bacterial reduction of trimethylamine oxide. Ann. Rev. Microbiol. 39, 131-49.

17. Bauder, R., Tshisuaka, B. and Lingens, F. (1990) Microbial metabolism of quinoline and related compounds. VII. Quinoline oxidoreductase from *Pseudomonas putida* a molybdenum-containing enzyme. Biol. Chem. Hoppe-Seyler 371, 1137-1144.

18. Beatty, S.A. and Gibbons, N.E. (1937) The measurement of spoilage in fish. J. Biol. Bd. Can. 3, 77-91.

19. Beinert, H. (1990) Recent developments in the field of iron-sulfur proteins. FASEB 4, 2483-2491.

20. Bell, L.C., Page, M.D., Berks, B.C., Richardson, D.J. and Ferguson, S.J. (1993) Insertion of transposon Tn5 into a structural gene of the membrane-bound nitrate reductase of *Thiosphaera pantotropha* results in anaerobic overexpression of periplasmic nitrate reductase activity. J. Gen Micro. 139, 3205-3214.

21. Bennett, B. and Bray, R.C. (1994) Further studies on redox-related activation and deactivation of *E. coli* nitrate reductase: a

possible physiologically relevant role for the low potential [4Fe-4S] centers. Biochem. Soc. Trans. 22, 283S.

22. Berg, B.L., Li, J., Heider, J. and Stewart, V. (1991) Nitrate-inducible formate dehydrogenase in *Escherichia coli* K-12. I. Nucleotide sequence of the *fdhGHI* operon and evidence that opal (UGA) encodes selenocysteine. J. Biol. Chem. 266, 22380-22385.

23. Berg, B.L. and Stewart, V. (1990) Structural genes for nitrate-inducible formate dehydrogenase in *Escherichia coli* K-12. Genet. 125, 691-702.

24. Berks, B.C. (1996) A complex export pathway for proteins binding complex redox cofactors? Mol. Micro. 22, 393-404.

25. Berks, B.C., Page, D., Richardson, D.J., Reilly, A., Cavill, A., Outen, F. and Ferguson, S.J. (1995) Sequence analysis of subunits of the membrane-bound nitrate reductase from a denitrifying bacterium: the integral membrane subunit provides a prototype for the dihaem electron-carrying arm of a redox loop. Mol. Micro. 15, 319-331.

26. Bertram, P.A., Schmitz, R.A., Linder, D. and Thauer, R.T. (1994) Tungstate can substitute for molybdate in sustaining growth of *Methanobacterium thermoautotrophicum.* Identification and characterization of a tungsten isoenzyme of formylmethanofuran dehydrogenase. Arch. Microbiol. 161, 220-228.

27. Bilous, P.T., Cole, S.T., Anderson, W.F. and Weiner, J.H. (1988) Nucleotide sequence of the *dmsABC* operon encoding the anaerobic dimethylsulphoxide reductase of *Escherichia coli.* Mol. Micro. 2, 785-795.

28. Bilous, P.T. and Weiner, J.H. Unpublished results.

29. Bilous, P.T. and Weiner, J.H. (1985) Dimethyl sulfoxide reductase activity by anaerobically grown *Escherichia coli*. J. Bacteriol. 162, 1151-1155.

30. Bilous, P.T. and Weiner, J.H. (1985) Proton translocation coupled to dimethyl sulfoxide reduction in anaerobically grown *Escherichia coli* HB101. J. Bacteriol. 163, 369-375.

31. Bilous, P.T. and Weiner, J.H. (1988) Molecular cloning and expression of the *Escherichia coli* dimethyl sulfoxide reductase operon. J. Bacteriol. 170, 1511-1518.

32. Blasco, F., Dos-Santos, J.-P., Magalon, A., Frixon, C., Guigliarelli, B., Santini, C.-L. and Giordano, G. (1998) NarJ is a specific chaperone required for molybdenum cofactor assembly in nitrate reductase A of *Escherichia coli*. Mol. Microbiol. In press.

33. Blasco, F., Iobbi, C., Giordano, G., Chippaux, M. and Bonnefoy, V. (1989) Nitrate reductase of *Escherichia coli:* completion of the nucleotide sequence of the *nar* operon and reassessment of the role of the α and β subunits in iron binding and electron transfer. Mol. Gen. Genet. 218, 249-256.

34. Blasco, F., Iobbi, C., Ratouchniak, J., Bonnefoy, V. and Chippaux, M. (1990) Nitrate reductases of *Escherichia coli*: sequence of the second nitrate reductase and comparison with that encoded by the *narGHJI* operon. Mol. Gen. Genet. 222, 104-111.

35. Blasco, F., Nunzi, F., Pommier, J., Brasseur, R., Chippaux, M. and Giordano, G. (1992) Formation of active heterologous nitrate reductases between nitrate reductases A and Z of *Escherichia coli*. Mol. Micro. 6, 209-219.

36. Blasco, F., Pommier, J., Augier, V., Chippaux, M. and Giordano, G. (1992) Involvement of the *narJ* or *narW* gene product in the formation of active nitrate reductase in *Escherichia coli*. Mol. Micro. 6, 221-230.

37. Bogachev, A.V., Murtazina, R.A. and Skulachev, V.P. (1993) Cytochrome *d* induction in *Escherichia coli* growing under unfavorable conditions. FEBS Lett. 336, 75-78.

38. Bogachev, A.V., Murtazina, R.A. and Skulachev, V.P. (1996) H+/e- stoichiometry for NADH dehydrogenase I and dimethyl sulfoxide reductase in anaerobically grown *Escherichia coli* cells. J. Bact. 178, 6233-6237.

39. Bohm, R., Sauter, M. and Bock, A. (1990) Nucleotide sequence and expression of an operon in *Escherichia coli* coding for formate hydrogenlyase components. Mol. Micro. 4, 231-243.

40. Bongaerts, J., Zoske, S., Weidner, U. and Unden, G. (1995) Transcriptional regulation of the proton-translocating NADH dehydrogenase genes (*nuoA-N*) of *Escherichia coli* by electron acceptors, electron donors and gene regulators. Mol. Micro. 16 521-534.

41. Borner, G., Karrasch, M. and Thauer, R.K. (1991) Molybdopterin adenine dinucleotide and molybdopterin hypoxanthine dinucleotide in formylmethanofuran dehydrogenase from

Methanobacterium thermoautotrophicum (Marbug). FEBS Lett. 290, 31-34.

42. Bowlus, R.D. and Somero, G.N. (1979) Solute compatibility with enzyme function and structure: rationales for the selection of osmotic agents and end-products of anaerobic metabolism in marine invertebrates. J. Exp. Zool. 208, 137-152.

43. Boyington, J.C., Gladyshev, V.N., Khangulov, S.V., Stadtman, T.C. and Sun, P.D. (1997) Crystal structure of formate dehydrogenase H: catalysis involving Mo, molybdopterin, selenocysteine, and an Fe_4S_4 cluster. Science 275, 1305-1308.

44. Breton, J., Berks, B.C., Reilly, A., Thomson, A.J., Ferguson, S.J. and Richardson, D.J. (1994) Characterization of the paramagnetic iron-containing redox centers of *Thiosphaera pantotropha* periplasmic nitrate reductase. FEBS Lett. 345, 76-80.

45. Brito, F., DeMoss, J.A. and Dubourdier, M. (1995) Isolation and identification of menaquinone-9 from purified nitrate reductase of *Escherichia coli.* J. Bact. 177, 3728-3735.

46. Brot, N., Rahman, M.A., Moskovitz, J. and Weissbach, H. (1995) *Escherichia coli* peptide methionine sulfoxide reductase cloning, high expression, and purification. Meth. Enzymol. 251, 462-470.

47. Brown, E.D. and Wood, J.M. (1992) Redesigned purification yields a fully functional PutA protein dimer from *Escherichia coli.* J. Biol. Chem. 267, 13086-13092.

48. Brown, E.D. and Wood, J.M. (1993) Conformational change and membrane association of the PutA protein are coincident with reduction of its FAD cofactor by proline. J. Biol. Chem. 268, 8972-8979.

49. Bruschi, M. and Guerlesquin, F. (1988) Structure, function and evolution of bacterial ferredoxins. FEMS Microbiol. Rev. 54, 155-176.

50. Buc, J., Santini, C.-L., Blasco, G., Giordani, R., Cardenas, M.L., Chippaux, M., Cornish-Bowden, A. and Giordano, G. (1995) Kinetic studies of a soluble $\alpha\beta$ complex of nitrate reductase α from *Escherichia coli.* Use of various $\alpha\beta$ mutants with altered β subunits. Eur. J. Biochem. 234, 766-772.

51. Burgess, B.K. and Lowe, D.J. (1996) Mechanism of molybdenum nitrogenase. Chem. Rev. 96, 2983-3011.

52. Burgmayer, S.J.N. and Stiefel, E.I. (1985) Molybdenum enzymes, cofactors, and model systems. The chemical uniqueness of molybdenum. J. Chem. Ed. 62, 943-953.

53. Cammack, R. and Weiner, J.H. (1990) Electron paramagnetic resonance spectroscopic characterization of dimethyl sulfoxide reductase of *Escherichia coli*. Biochemistry 29, 8410-8416.

54. Cecchini, G., Ackrell, B.A.C., Deshler, J.O. and Gunsalus, R.P. (1986) Reconstitution of quinone reduction and characterization of *Escherichia coli* fumarate reductase activity. J. Biol. Chem. 261, 1808-1814.

55. Chan, M.K., Mukund, S., Kletzin, A., Adams, M.W.W. and Rees, D.C. (1995) Structure of a hyperthermophilic tungstopterin enzyme, aldehyde ferredoxin oxidoreductase. Science 267, 1463-1469.

56. Clarke, G.J. and Ward, F.B. (1988) Purification and properties of trimethylamine N-oxide reductase from *Shewanella* sp. NCMB 400. J. Gen. Microbiol. 133, 379-386.

57. Cole, J. (1996) Nitrate reduction to ammonia by enteric bacteria: redundancy, or a strategy for survival during oxygen starvation. FEMS Microbiol. Lett. 136, 1-11.

58. Cole, S.T., Condon, C., Lemire, B.D. and Weiner, J.H. (1985) Molecular biology, biochemistry, and bioenergetics of fumarate reductase, a complex membrane-bound iron-sulfur flavoenzyme of *Escherichia coli*. Biochim. Biophys. Acta 811, 381-403.

59. Cole, S.T., Eiglmeier, K., Ahmed, S., Honore, N., Elmes, L., Anderson, W.F. and Weiner, J.H. (1988) Nucleotide sequence and gene-polypeptide relationships of the *glpABC* operon encoding the anaerobic *sn*-glycerol-3-phosphate dehydrogenase of *Escherichia coli* K-12. J. Bact. 170, 2448-2456.

60. Condon, C. and Weiner, J.H. (1988) Fumarate reductase of *Escherichia coli*: an investigation of function and assembly using *in vivo* complementation. Mol. Micro. 2, 43-52.

61. Cotter, P.A., Chepuri, V., Gennis, R.B. and Gunsalus, R.P. (1990) Cytochrome o (*cyoABCD*) and *d* (*cydAB*) oxidase gene expression in *Escherichia coli* is regulated by oxygen, pH, and the *fnr* gene product. J. Bact. 172, 6333-6338.

62. Cotter, P.A. and Gunsalus, R.P. (1989) Oxygen, nitrate, and molybdenum regulation of *dmsABC* gene expression in *Escherichia coli*. J. Bact. 171, 3817-3823.

63. Dalbey, R.E., Lively, M.O., Bron, S. and VanDijh, J.M. (1997) The chemistry and enzymology of the type I signal peptidases. Prot. Sci. 6, 1129-1138.

64. Darwala, R. and Meganathan, R. (1991) Dimethyl sulfoxide reductase is not required for trimethylamine N-oxide reduction in *Escherichia coli*. FEMS Microbiol. Lett. 83, 255-260.

65. Darwin, A., Jussain, J., Griffiths, L., Grove, J., Sambongi, Y., Busby, S. and Cole, J. (1993) Regulation and sequence of the structural gene for cytochrome *c*552 from *Escherichia coli*, not a hexaheme but a 50 kDa tetrahaem nitrite reductase. Mol. Micro. 9, 1255-1265.

66. Darwin, A.J., Tyson, K.L., Busby, S.J.W. and Stewart, V. (1997) Differential regulation by the homologous response regulators NarL and NarP of *Escherichia coli* K-12 depends on DNA binding site arrangement. Mol. Micro. 25, 583-595.

67. DeBont, J.A.M., VanDijken, J.P. and Harder, W. (1981) Dimethyl sulphoxide and dimethyl sulfide as carbon, sulfur and energy source for growth of *Hyphomicrobium* S. J. Gen. Micro. 127, 315-323.

68. delCampillo-Campbell, A. and Campbell, A. (1996) Alternative gene for biotin sulfoxide reduction in *Escherichia coli* K-12. J. Mol. Evol. 42, 85-90.

69. delCampillo-Campbell, A., Dykhuizen, D. and Cleary, P. (1979) Enzymic reduction of d-biotin d-sulfoxide to d-biotin. Meth. Enzymol. 62, 379-385.

70. DeMoss, J.A. and Hsu, P.Y. (1991) NarK enhances nitrate uptake and nitrite excretion in *Escherichia coli*. J. Bact. 173, 3303-3310.

71. Demple, B. (1997) Study of redox-regulated transcription factors in prokaryotes. Methods 11, 267-278.

72. denBlaausen and Driessen, A.J.M. (1996) Sec-dependent preprotein translocation in bacteria. Arch. Microbiol. 165, 1-8.

73. Dubourdieu, M. and DeMoss, J.A. (1992) The *narJ* gene product is required for biogenesis of respiratory nitrate reductase in *Escherichia coli*. J. Bact. 174, 867-872.

74. Easter, M.C., Gibson, D.M. and Ward, F.B. (1982) A conductance method for the assay and study of bacterial trimethylamine oxide reduction. J. Appl. Bact. 52, 357-365.

75. Easter, M.C., Gibson, D.M. and Ward, F.B. (1983) The induction and location of trimethylamine-N-oxide reductase in *Alteromonas* sp. NCMB 400. J. Gen. Microbiol. 129, 3689-3696.

76. Eaves, D.J., Palmer, T. and Boxer, D.H. (1997) The product of the molybdenum cofactor gene *mobB* of *Escherichia coli* is a GTP binding protein. Eur. J. Biochem. 246, 690-697.

77. Eigimeier, K., Honore, N., Iuchi, S., Lin, E.C.C. and Cole, S.T. (1989) Molecular genetic analysis of FNR-dependent promoters. Mol. Micro. 3, 869-878.

78. Garcia-Horsman, J.A., Puustinen, A., Gennis, R.B. and Wilstrom, M. (1995) Proton transfer in cytochrome *bo3* ubiquinol oxidase of *Escherichia coli*: Second-site mutations in subunit I that restore proton pumping in the mutant Asp135-Asn. Biochem. 34, 4428-4433.

79. Garland, P.B., Downie, A. and Haddock, B.A. (1975) Proton translocation and the respiratory nitrate reductase of *Escherichia coli*. Biochem. J. 152, 547-559.

80. Geisler, V., Ullmann, R. and Kroger, A. (1994) The direction of the proton exchange associated with the redox reactions of menaquinone during electron transport in *Wolinella succinogenes*. Biochim. Biophys. Acta 1184, 219-226.

81. Gennis, R. and Stewart, V. (1996) Respiration, in *Escherichia coli* and *Salmonella* cellular and molecular biology. (Neidhardt, F.C., ed.), Vol. 1, p. 217-261, ASM Press, Washington.

82. Gibson, J.A.E., Garrick, R.C., Burton, H.R. and McTaggart, A.R. (1990) Dimethylsulfide and the algae *Phaeocyctis pouchetii*. Mar. Biol. 104, 339-346.

83. Gladyshev, V.N., Khangulov, S.V., Axley, M.J. and Stadtman, T.C. (1994) Coordination of selenium to molybdenum in formate dehydrogenase H from *Escherichia coli*. Proc. Natl. Acad. Sci. 91, 7709-7711.

84. Grabau, C., Chang, Y. and J. E. Cronan, J. (1989) Lipid binding by *Escherichia coli* pyruvate oxidase is disrupted by small alterations of the carboxy-terminal region. J. Biol. Chem. 264, 12510-12519.

85. Grabau, C. and Cronan, J.E. (1986) *In vivo* function of *Escherichia coli* pyruvate oxidase specifically requires a functional lipid binding site. Biochem. 25, 3748-3751.

86. Green, J. and Guest, J.R. (1994) Regulation of transcription at the *ndh* promoter of *Escherichia coli* by FNR and novel factors. Mol. Micro. 12, 433-444.

87. Groninger, H.S. (1959) The occurrence and significance of trimethylamine oxide in marine animals. U. S. Fish and Wildlife Service Sp. Sci. Report No. 333, 1-17.

88. Grove, J., Tanapongpipat, S., Thomas, G., Griffiths, L., Crooke, H. and Cole, J. (1996) *Escherichia coli* K-12 genes essential for the synthesis of *c*-type cytochromes and a third nitrate reductase located in the cytoplasm. Mol. Micro. 19, 467-481.

89. Guerrero, M.G. and Vega, J.M. (1975) Molybdenum and iron as functional constituents of the enzymes of the nitrate-reducing system of *Azotobacter chroococcum.* Arch. Mircobiol. 102, 91-94.

90. Guigliarelli, B., Asso, M., More, C., Augier, V., Blasco, F., Pommier, J., Giordano, G. and Bertrand, P. (1992) EPR and redox characterization of iron-sulfur centers in nitrate reductases A and Z from *Escherichia coli*. Evidence for a high-potential and a low-potential class and their relevance in the electron-transfer mechanism. Eur. J. Biochem. 207, 61-68.

91. Guigliarelli, B., Magalon, A., Asso, M., Bertrand, P., Frixon, C., Giordano, G. and Blasco, F. (1996) Complete coordination of the four Fe-S centers of the β-subunit from *Escherichia coli* nitrate reductase. Physiological, biochemical, and EPR characterization of site-directed mutants lacking the highest or lowest potential [4Fe-4S] clusters. Biochem. 35, 4828-4836.

92. Haddock, B.A. and Kendall-Tobias, M.W. (1975) Functional anaerobic electron transport linked to the reduction of nitrate and fumarate in membranes from *Escherichia coli* as demonstrate by quenching of atebrin fluorescence. Biochem. J. 152, 655-659.

93. Haddock, B.A. and Schairer, H.U. (1973) Electron-transport chains of *Escherichia coli.* Eur. J. Biochem. 35, 34-45.

94. Hanlon, S.P., Toh, T.-H., Solomon, P.S., Holt, R.A. and McEwan, A.G. (1996) Dimethylsulfide:acceptor oxidoreductase from *Rhodobacter sulfidophilus*. The purified enzyme contains *b*-type haem and a pterin molybdenum cofactor. Eur. J. Biochem. 239, 391-396.

95. Hellingwerf, K.J., Bolscher, J.G.M. and Konigs, W.N. (1981) The electrochemical proton gradient generated by the fumarate-reductase system in *Escherichia coli* and its bioenergetic implications. Eur. J. Biochem. 113, 369-374.

96. Hensgens, C.M.H., Hagen, W.R. and Hansen, T.A. (1995) Purification and characterization of a benzylviologen-linked, tungsten-containing aldehyde oxidoreductase from *Desulfovibrio gigas*. J. Bact. 177, 6195-6200.

97. Hille, R. (1996) The mononuclear molybdenum enzymes. Chem. Rev. 96, 2757-2816.

98. Hille, R. and Sprecher, H. (1987) On the mechanism of action of xanthine oxidase. Evidence in support of an oxo transfer mechanism in the molybdenum-containing hydroxylases. J. Biol. Chem. 262, 10914-10917.

99. Hilton, J.C. and Rajagopalan, K.V. (1996) Identification of the molybdenum cofactor of dimethyl sulfoxide reductase from *Rhodobacter sphaeroides* f. sp. *denitrificans* as bis(molybdopterin guanine dinucleotide)molybdenum. Arch. Biochem. Biophys. 325, 139-143.

100. Hilton, J.C. and Rajagopalan, K.V. (1996) Molecular cloning of dimethyl sulfoxide reductase from *Rhodobacter sphaeroides*. Biochim. Biophys. Acta 1294, 111-114.

101. Howard, J.B. and Rees, D.C. (1996) Structural basis of biological nitrogen fixation. Chem. Rev. 96, 2965-2982.

102. Huber, C., Caldeira, J., Jongejan, J.A. and Simon, H. (1994) Further characterization of two different reversible aldehyde oxidoreductases from *Clostridium formicoaceticum*, one containing tungsten and the other molybdenum. Arch. Microbiol. 162, 303-309.

103. Huber, C., Skopan, H., Feicht, R., White, H. and Simon, H. (1995) Pterin cofactor, substrate specificity, and observations on the kinetics of the reversible tungsten-containing aldehyde oxidoreductase from *Clostridium thermoaceticum*. Arch. Microbiol. 164, 110-118.

104. Hussain, H., Grove, J., Griffiths, L., Busby, S. and Cole, J. (1994) A seven-gene operon essential for formate-dependent nitrite reduction to ammonia by enteric bacteria. Mol. Micro. 12, 153-163.

105. Iobbi, C., Santini, C.-L., Bonnefoy, V. and Giordano, G. (1987) Biochemical and immunological evidence for a second nitrate reductase in *Escherichia coli* K-12. Eur. J. Biochem. 168, 451-459.

106. Iobbi-Nivol, C., Crooke, H., Griffiths, L., Grove, J., Hussain, H., Pommier, J., Mejean, V. and Coli, J.A. (1994) A reassessment of the range of *c*-type cytochromes synthesized by *Escherichia coli* K-12. FEMS Microbiol. Lett. 119, 84-94.

107. Iobbi-Nivol, C., Pommier, J., Simala-Grant, J.L., Mejean, V. and Giordano, G. (1996) High substrate specificity and induction characteristics of trimethylamine N-oxide reductase of *Escherichia coli*. Biochim. Biophys. Acta 1294, 77-82.

108. Iobbi-Nivol, C., Santini, C.-L., Blasco, F. and Giordano, G. (1990) Purification and further characterization of the second nitrate reductase of *Escherichia coli* K12. Eur. J. Biochem. 188, 679-687.

109. Iuchi, S., Aristarkhov, A., Dong, J.M., Taylor, J.S. and Lin, E.C.C. (1994) Effects of nitrate respiration on expression of the Arc-controlled operons encoding succinate dehydrogenase and flavin-linked L-lactate dehydrogenase. J. Bact. 176, 1695-1701.

110. Iuchi, S., Chepuri, V., Fu, H.-A., Gennis, R.B. and Lin, E.C.C. (1990) Requirement for terminal cytochromes in generation of the aerobic signal for the *arc* regulatory system in *Escherichia coli*: Study utilization deletions and *lac* fusions of *cyo* and *cyd*. J. Bact. 172, 6020-6025.

111. Iuchi, S. and Lin, E.C.C. (1987) The *narL* gene product activates the nitrate reductase operon and represses the fumarate reductase and trimethylamine-oxide reductase operons in *Escherichia coli*. Proc. Natl. Acad. Sci. 84, 3901-3905.

112. Iuchi, S. and Lin, E.C.C. (1993) Adaptation of *Escherichia coli* to redox environments by gene expression. Mol. Microbiol. 9, 9-15.

113. Iuchi, S., Matsuda, Z., Fujiwara, T. and Lin, E.C.C. (1990) The *arcB* gene of *Escherichia coli* encodes a sensor-regulator protein for anaerobic repression of the *arc* modulon. Mol. Micro. 4, 715-727.

114. Iuchi, S. and Weiner, L. (1996) Cellular and molecular physiology of *Escherichia coli* in the adaptation to aerobic environments. J. Biochem. 120, 1055-1063.

115. Jawarowski, A., Mayo, G., Shaw, D.C. and Campbell, H.D. (1981) Characterization of the respiratory NADH dehydrogenase of *Escherichia coli* and reconstitution of NADH oxidase in *ndh* mutant membrane vesicles. Biochem. 20, 3621-3628.

116. Johann, S. and Hinton, S.M. (1987) Cloning and nucleotide sequence of the *chlD* locus. J. Bact. 169, 1911-1916.

117. Johnson, J.L., Bastian, N.R. and Rajagopalan, K.V. (1990) Molybdopterin guanine dinucleotide: A modified form of molybdopterin identified in the molybdopterin cofactor of dimethyl sulfoxide reductase from *Rhodobacter sphaeroides* forma specialis *denitrificans*. Proc. Natl. Acad. Sci. 87, 3190-3194.

118. Johnson, J.L., Hainline, B.E., Rajagopalan, K.V. and Arison, B.H. (1984) The pterin component of the molybdenum cofactor. Structural characterization of two fluorescent derivatives. J. Biol. Chem. 259, 5414-5422.

119. Johnson, J.L., Indermaur, L.W. and Rajagopalan, K.V. (1991) Molybdenum cofactor biosynthesis in *Escherichia coli*. Requirement of the *chlB* gene product for the formation of molybdopterin guanine dinucleotide. J. Biol. Chem. 266, 12140-12145.

120. Johnson, J.L. and Rajagopalan, K.V. (1976) Electron paramagnetic resonance of the tungsten derivative of rat liver sulfite oxidase. J. Biol. Chem. 251, 5505-5511.

121. Johnson, J.L. and Rajagopalan, K.V. (1982) Structural and metabolic relationship between the molybdenum cofactor and urothione. Proc. Natl. Acad. Sci. USA 79, 6856-6860.

122. Johnson, J.L., Rajagopalan, K.V. and Meyer, O. (1990) Isolation and characterization of a second molybdopterin dinucleotide molybdopterin cytosine dinucleotide. Arch. Biochem. Biophys. 283, 542-545.

123. Johnson, J.L., Rajagopalan, K.V., Mukund, S. and Adams, M.W.W. (1993) Identification of molybdopterin as the organic component of the tungsten cofactor in four enzymes from hyperthermophilic archaea. J. Biol. Sci. 268, 4848-4852.

124. Jones, H.M. and Gunsalus, R.P. (1985) Transcription of the *Escherichia coli* fumarate reductase genes (*frdABCD*) and their coordinate regulation by oxygen, nitrate, and fumarate. J. Bact. 164, 1100-1109.

125. Jones, H.M. and Gunsalus, R.P. (1987) Regulation of *Escherichia coli* fumarate reductase (*frdABCD*) operon expression by respiratory electron acceptors and the *fnr* gene product. J. Bact. 169, 3340-3349.

126. Jones, R.W. (1980) The role of the membrane-bound hydrogenase in the energy-conserving oxidation of molecular hydrogen by *Escherichia coli*. Biochem. J. 188, 345-350.

127. Jones, R.W. and Garland, P.B. (1977) Sites and specificity of the reaction of bipyridylium compounds with anaerobic respiratory enzymes of *Escherichia coli*. Biochem. J. 164, 199-211.

128. Jones, R.W., Lamont, A. and Garland, P.B. (1980) The mechanism of proton translocation driven by the respiratory nitrate reductase complex of *Escherichia coli*. Biochem. J. 190, 79-94.

129. Jonkers, H.M., vanderMaarel, M.J.E.C. and vanGemerden, H. (1996) Dimethylsulfoxide reduction by marine sulfate-reducing bacteria. FEMS Microbiol. Lett. 136, 283-287.

130. Joshi, M.S., Johnson, J.L. and Rajagopalan, K.V. (1996) Molybdenum cofactor biosynthesis in *Escherichia coli mod* and *mog* mutants. J. Bact. 178, 4310-4312.

131. Jourlin, C., Bengrine, A., Chippaux, M. and Mejean, V. (1996) An unorthodox sensor protein (TorS) mediates the induction of the *tor* structural genes in response to trimethylamine N-oxide in *Escherichia coli*. Mol. Micro. 20, 1297-1306.

132. Jourlin, C., Simon, G., Pommier, J., Chippaux, M. and Mejean, V. (1996) The periplasmic TorT protein is required for trimethylamine N-oxide reductase gene induction in *Escherichia coli*. J. Bact. 178, 1219-1223.

133. Karrasch, M., Borner, G., Enssle, M. and Thauer, R.K. (1990) The molybdoenzyme formylmethanofuran dehydrogenase from *Methanosarcina barkeri* contains a pterin cofactor. Eur. J. Biochem. 194, 367-372.

134. Kellogg, W.W., Cadle, R.D., Allen, E.R., Lazrus, A.L. and Martell, E.A. (1972) The sulfur cycle. Man's contributions are compared

to natural sources of sulfur compounds in the atmosphere and oceans. Science 175, 587-596.

135. Kelly, D.J., Richardson, D.J., Ferguson, S.J. and Jackson, J.B. (1988) Isolation of transposon Tn5 insertion mutants of *Rhodobacter capsulatus* unable to reduce trimethylamine-N-oxide and dimethylsulphoxide. Arch. Microbiol. 150, 138-144.

136. Khoroshilova, N., Popescu, C., Munck, E., Beinert, H. and Kiley, P.J. (1997) Iron-sulfur cluster disassembly in the FNR protein of *Escherichia coli* by O_2: [4Fe-4S] to [2Fe-2S] conversion with loss of biological activity. Proc. Natl. Acad. Sci. 94, 6087-6092.

137. Kiene, R.P. and Bates, T.S. (1990) Biological removal of dimethylsulphide from sea water. Nature 345, 702-705.

138. Kim, J. and Rees, D.C. (1992) Crystallographic structure and functional implications of the nitrogenase molybdenum-iron protein from *Azotobacter vinelandii*. Nature 360, 553-560.

139. Kistler, W.S. and Lin, E.C.C. (1972) Purification and properties of the flavine-stimulated anaerobic L-α-glycerophosphate dehydrogenase of *Escherichia coli*. J. Bact. 12, 539-547.

140. Kita, K., Vibat, C.R.T., Meinahardt, S., Guest, J.R. and Gennis, R.B. (1989) One step purification from *Escherichia coli* of complex II (succinate:ubiquione oxidoreductase) associated with succinate reducible cytochrome *b*556. J. Biol. Chem. 264, 2672-2677.

141. Knablein, J., Dobbek, H., Ehlert, S. and Schneider, F. (1997) Isolation, cloning, sequence analysis and X-ray structure of dimethyl sulfoxide/trimethylamine N-oxide reductase from *Rhodobacter sphaeroides*. Biol. Chem. 378, 293-302.

142. Knablein, J., Mann, K., Ehlert, S., Fonstein, M., Huber, R. and Schneider, F. (1996) Isolation, cloning, sequence analysis and localization of the operon encoding dimethyl sulfoxide/trimethylamine N-oxide reductase from *Rhodobacter capsulatus*. J. Mol. Biol. 263, 40-52.

143. Kowal, A.T., Werth, M.T., Manadori, A., Cecchini, G., Schroder, I., Gunsalus, R.P. and Johnson, M.J. (1995) Effect of cysteine to serine mutations on the properties of the [4Fe-4S] center in *Escherichia coli* fumarate reductase. Biochem. 34, 12284-12293.

144. Kramer, S.P., Johnson, J.L., Ribeiro, A.A., Millington, D.S. and Rajagopalan, K.V. (1987) The structure of the molybdenum cofactor. Characterization of di-(carboxyamidomethyl)molybdopterin from sulfite oxidase and xanthine oxidase. J. Biol. Chem. 262, 16357-16363.

145. Kranz, R.G. and Gennis, R.B. (1983) Immunological characterization of the cytochrome *o* terminal oxidase from *E. coli*. J. Biol. Chem. 258, 10614-10621.

146. Kruger, B. and Meyer, O. (1986) The pterin (bactopterin) of carbon monoxide dehydrogenase from *Pseudomonas carboxydoflava*. Eur. J. Biochem. 157, 121-128.

147. Kruger, B. and Meyer, O. (1987) Structural elements of bactopterin from *Pseudomonas carboxydoflava* carbon monoxide dehydrogenase. Biochim. Biophys. Acta 912, 357-364.

148. Kruger, B., Meyer, O., Nagel, M., Andreesen, J.R., Meincke, M., Bock, E., Blumle, S. and Zumft, W.G. (1987) Evidence for the presence of bactopterin in eubacterial molybdoenzymes nicotinic acid dehydrogenase, nitrite oxidoreductase, and respiratory nitrate reductase. FEMS Microbiol. Lett. 48, 225-227.

149. Kurihara, F.N. and Satoh, T. (1988) A single enzyme is responsible for both dimethylsulfoxide and trimethylamine-N-oxide respirations as the terminal reductase in a photodenitrifier *Rhodobacter sphaeroides* f.s. *denitrificans*. Plant. Cell. Physiol. 29, 377-379.

150. Kwan, H.S. and Barrett, E.L. (1983) Purification and properties of trimethylamine oxide reductase from *Salmonella typhimurium*. J. Bact. 155, 1455-1458.

151. Langen, R., Jensen, G.M., Jacob, U., Stephens, R.J. and Warshel, A. (1992) Protein control of iron-sulfur cluster redox potentials. J. Biol. Chem. 267, 25635-25627.

152. Lazazzera, B.A., Beinert, H., Khoroshilova, N., Kennedy, M.C. and Kiley, P.J. (1996) DNA binding and dimerization of the Fe-S containing FNR protein from *Escherichia coli* are regulated by oxygen. J. Biol. Chem. 271, 2762-2768.

153. Leif, H., Sled, V.D., Ohnishi, T., Weiss, H. and Friedrich, T. (1995) Isolation and characterization of the proton-translocating NADH:ubiquinone oxidoreductase from *Escherichia coli*. Eur. J. Biochem. 230, 538-548.

154. Lemire, B.D., Robinson, J.J., Bradley, R.D., Scraba, D.G. and Weiner, J.H. (1983) Structure of fumarate reductase on the cytoplasmic membrane of *Escherichia coli.* J. Bact. 155, 391-397.

155. Li, J. and Stewart, V. (1992) Localization of upstream sequence elements required for nitrate and anaerobic induction of *fdn* (formate dehydrogenase N) operon expression in *Escherichia coli.* J. Bact. 174, 4935-3942.

156. Liu, X. and DeMoss, J.A. (1997) Characterization of NarJ, a system-specific chaperone required for nitrate reductase biogenesis in *Escherichia coli.* J. Biol. Chem. 272, 24266-24271.

157. Loosemore, S.M., Shortreed, J.M., Coleman, D.C., England, D.M. and Klein, M.H. (1996) Sequences of the genes encoding the A, B and C subunits of the *Haemophilus influenza* dimethylsulfoxide reductase complex. Gene 169, 137-138.

158. Lorence, R.M., Carter, K., Gennis, R.B., Matsushita, K. and Kaback, H.R. (1988) Trypsin proteolysis of the cytochrome *d* complex of *Escherichia coli* selectively inhibits ubiquinol oxidase activity while not affecting N,N,N',N'-tetramethyl-p-phenylenediamine oxidase activity. J. Biol. Chem. 263, 5271-5276.

159. Lovelock, J.E., Maggs, R.J. and Rasmussen, R.A. (1972) Atmospheric dimethyl sulfide and the natural sulphur cycle. Nature 237.

160. Lynch, A.S. and Lin, E.C.C. (1996) Responses to molecular oxygen, in *Escherichia coli* and *Salmonella* cellular and molecular biology. (Neidhardt, F.C., ed.), Vol. 1, p. 1526-1538, ASM Press, Washington.

161. MacEwan, A.G., Wetstein, H.G., Meyer, O., Jackson, J.B. and Ferguson, S.J. (1987) The periplasmic nitrate reductase of *Rhodobacter capsulatus*; purification, characterisation and distinction from a single reductase for trimethylamine-N-oxide dimethylsulphoxide and chlorate. Arch. Microbiol. 147, 340-345.

162. Magalon, A., Asso, M., Guigliarelli, B., Rothery, R.A., Bertrand, P., Giordano, G. and Blasco, F. (1998) Molybdenum cofactor properties and [Fe-S] cluster coordination in *Escherichia coli* nitrate reductase A : Investigation by site-directed mutagenesis of the conserved His-50 residue in the NarG subunit. Manuscript in preparation.

163. Magalon, A., Lemesle-Meunier, D., Rothery, R.A., Frixon, C., Weiner, J.H. and Blasco, F. (1997) Heme axial ligation by the highly conserved his residues in helix II of cytochrome *b* (NarI) of *Escherichia coli* nitrate reductase A (NarGHI). J. Biol. Chem. 272, 25652-25658.

164. Magalon, A., Rothery, R.A., Giordano, G., Blasco, F. and Weiner, J.H. (1997) Characterization by electron paramagnetic resonance of the role of the *Escherichia coli* nitrate reductase (NarGHI) iron-sulfur clusters in electron transfer to nitrate and identification of a semiquinone radical intermediate. J. Bact. 179, 5037-5045.

165. Magalon, A., Rothery, R.A., Lemesle-Meunier, D., Frixon, C., Weiner, J.H. and Blasco, F. (1998) Inhibitor-binding within the NarI subunit (cytochromeb_{nr}) of *Escherichia coli* nitrate reductase A. J. Biol. Chem. Submitted.

166. Maloney, P.C. and Wilson, T.H. (1996) Ion-coupled transport and transporters, in *Escherichia coli* and *Salmonella* cellular and molecular biology. (Neidhardt, F.C., ed.), Vol. 1, p. 1130-1148, ASM Press, Washington.

167. Manodori, A., Cecchini, G., Schroder, I., Gunsalus, R.P., Werth, M.T. and Johnson, M.K. (1992) [3Fe-4S] to [4Fe-S] cluster conversion in *Escherichia coli* fumarate reductase by site-directed mutagenesis. Biochemistry 31, 2703-2712.

168. Matsushita, K. and Kaback, H.R. (1986) D-lactate oxidation and generation of the proton electrochemical gradient in membrane vesicles from *Escherichia coli* GR19N and in proteoliposomes reconstituted with purified D-lactate dehydrogenase and cytochrome *o* oxidase. Biochem. 25, 2321-2327.

169. McAlpine, A.S., McEwan, A.G. and Bailey, S. (1998) The high resolution crystal structure of DMSO reductase in complex with DMSO. J. Mol. Biol. In press.

170. McAlpine, A.S., McEwan, A.G., Shaw, A.L. and Bailey, S. (1998) Molybdenum active center of DMSO reductase from *Rhodobacter capsulatus* : crystal structure of the oxidised enzyme at 1.82Å resolution and the dithionite-reduced enzyme at 2.8Å resolution. J. Biol. Inorg. Chem. In press.

171. McEwan, A.G., Benson, N., Bonnett, T.C., Hanlon, S.P., Ferguson, S.J., Richardson, D.J. and Jackson, J.B. (1991) Bacterial dimethyl sulphoxide reductases and nitrate reductases. Biochem. Soc. Trans 19, 605-608.

172. McEwan, A.G., Ferguson, S.J. and Jackson, J.B. (1991) Purification and properties of dimethyl sulphoxide reductase from *Rhodobacter capsulatus.* A periplasmic molybdoenzyme. Biochem. J. 274, 305-307.

173. McEwan, A.G., Wetzstein, H.G., Meyer, O., Jackson, J.B. and Ferguson, S.J. (1987) The periplasmic nitrate reductase of *Rhodobacter capsulatus*; purification characterisation and distinction from a single reductase for trimethylamine N-oxide, dimethylsulphoxide and chlorate. Arch. Microbiol. 147, 340-345.

174. Meganathan, R. (1984) Inability of *men* mutants of *Escherichia coli* to use trimethylamine-N-oxide as an electron acceptor. FEMS Microbiol. Lett. 24, 57-62.

175. Meganathan, R. (1996) Biosynthesis of the isoprenoid quinones menaquinone (vitamin K2) and ubiquinone (coenzyme Q), in *Escherichia coli* and *Salmonella* cellular and molecular biology. (Neidhardt, F.C., ed.), Vol. 1, p. 642-656, ASM Press, Washington.

176. Mejean, V., Iobbi-Nivol, C., Lepelletier, M., Giordano, G., Chippaux, M. and Pascal, M.-C. (1994) Trimethylamine N-oxide anaerobic respiration in *Escherichia coli* : involvement of the *tor* operon. Mol. Microbiol. 11, 1169-1179.

177. Miller, M.J. and Gennis, R.B. (1985) The cytochrome *d* complex is the coupling site in the aerobic respiratory chain of *Escherichia coli.* J. Biol. Chem. 260, 14003-14008.

178. Mitchell, P. (1967) Proton-translocation phosphorylation in mitochondria, chloroplasts and bacteria: natural fuel cells and solar cells. Fed. Proc. 26, 1370-1379.

179. Morpeth, F.F. and Boxer, D.H. (1985) Kinetic analysis of respiratory nitrate reductase from *Escherichia coli* K12. Biochem. 24, 40-46.

180. Mukund, S. and Adams, M.W.W. (1991) The novel tungsten-iron-sulfur protein of the hyperthermophilic archaebacterium, *Pyrococcus furiosus*, is an aldehyde ferredoxin oxidoreductase. Evidence for its participation in a unique glycolytic pathway. J. Biol. Chem. 266, 14208-14216.

181. Nagel, M., Koenig, K. and Andreesen, J.R. (1989) Bactopterin as component of eubacterial dehydrogenases involved in hydroxylation reactions initiating the degradation of nicotine, nicotinate, and 2-furancarboxylate. FEMS Microbiol. Lett. 60, 323-326.

182. Nielsen, H., Engelbrecht, J., Brunak, S. and vonHeijne, G. (1997) Identification of prokaryotic and eukaryotic signal peptides and prediction of their cleavage sites. Prot. Eng. 10, 1-6.

183. Norris, E.R. and Benoit, G.J. (1944) Studies on trimethylamine oxide. I. Occurrence of trimethylamine oxide in marine organisms. J. Biol. Chem. 158, 433-438.

184. Oren, A. and Truper, H.G. (1990) Anaerobic growth of halophilic archaebacteria by reduction of dimethylsulfoxide and trimethylamine N-oxide. FEMS Microbiol. Lett. 70, 33-36.

185. Pascal, M.-C., Burini, J.-F. and Chippaux, M. (1984) Regulation of the trimethylamine N-oxide (TMAO) reductase in *Escherichia coli* : Analysis of *tor*:Mud1 operon fusion. Mol. Gen. Genet. 195, 351-355.

186. Pascal, M.-C., Lepelletier, M., Giordano, G. and Chippaux, M. (1991) A regulatory mutant of the trimethylamine N-oxide reductase of *Escherichia coli* K12. FEMS Microbiol. Lett. 78, 297-300.

187. Pierson, D.E. and Campbell, A. (1990) Cloning and nucleotide sequence of *bisC*, the structural gene for biotin sulfoxide reductase in *Escherichia coli.* J. Bact. 172, 2194-2198.

188. Pitterle, D.M., Johnson, J.L. and Rajagopalan, K.V. (1993) *In vitro* synthesis of molybdopterin from precursor Z using purified converting factor. Role of protein-bound sulfur in formation of the dithiolene. J. Biol. Chem. 268, 13506-13509.

189. Pitterle, D.M. and Rajagopalan, K.V. (1989) Two proteins encoded at the *chlA* locus constitute the converting factor of *Escherichia coli chlA1.* J. Bact. 171, 3373-3378.

190. Pitterle, D.M. and Rajagopalan, K.V. (1993) The biosynthesis of molybdopterin in *Escherichia coli.* Purification and characterization of the converting factor. J. Biol. Chem. 268, 13499-13505.

191. Plunkett, G., Burland, V., Daniels, D.L. and Blattner, F.R. (1993) Analysis of the *Escherichia coli* genome. III. DNA sequence of the region from 87.2 to 89.2 minutes. Nuc. Acids Res. 21, 3391-3398.

192. Polglase, W.J., Pun, W.T. and Withaar, J. (1966) Lipoquinones of *Escherichia coli.* Biochim. Biophys. Acta 118, 425-426.

193. Pollock, V.V. and Barber, M.J. (1995) Molecular cloning and expression of biotin sulfoxide reductase from *Rhodobacter sphaeroides* forma sp. *denitrificans.* Arch. Biochem. Biophys. 318, 322-332.

194. Pommier, J., Mandrand, M.A., Holt, S.E., Boxer, D.H. and Giordano, G. (1992) A second phenazine methosuphate-linked formate dehydrogenase isoenzyme in *Escherichia coli.* Biochim. Biophys. Acta 1107, 305-313.

195. Rahman, M.A., Nelson, H., Weissbach, H. and Brot, N. (1992) Cloning, sequencing, and expression of the *Escherichia coli* peptide methionine sulfoxide reductase gene. J. Biol. Chem. 267, 15549-15551.

196. Rajagopalan, K.V. (1991) Novel aspects of the biochemistry of the molybdenum cofactor. Adv. Enz. Rel. Areas Mol. Biol. 64, 215-289.

197. Rajagopalan, K.V. (1996) Biosynthesis of the molybdenum cofactor, in *Escherichia coli* and *Salmonella* cellular and molecular biology. (Neidhardt, F.C., ed.), Vol. 1, p. 674-679, ASM Press, Washington.

198. Reams, S.G. and Clark, D.P. (1988) Glucose repression of anaerobic genes of *Escherichia coli* is independent of cyclic AMP. FEMS Microbiol. Lett. 56, 231-236.

199. Rech, S., Wolin, C. and Gunsalus, R.P. (1996) Properties of the periplasmic ModA molybdate-binding protein of *Escherichia coli.* J. Biol. Chem. 271, 2557-2562.

200. Rice, C.W. and Hempfling, W.P. (1978) Oxygen-limited continuous culture and respiratory energy conservation in *Escherichia coli.* J. Bact. 134, 115-124.

201. Rodrique, A., Boxer, D.J., Mandrand-Berthelot, M.A. and Wu, L.-F. (1996) Requirement for nickel of the transmembrane translocation of NiFe-hydrogenase 2 in *Escherichia coli.* FEBS Lett. 392, 81-86.

202. Rohlfs, R.J. and Hille, R. (1991) Intramolecular electron transfer in trimethylamine dehydrogenase from bacterium W3A1. J. Biol. Chem. 266, 15244-15252.

203. Romao, M.J., Chan, M.K., Mukund, S., Kletzin, A., Adams, M.W.W. and Rees, D.C. (1995) Crystal structure of the xanthine

oxidase-related aldehyde oxido-reductase from *D. gigas*. Science 270, 1170-1176.

204. Rothery, R., Chatterjee, I., Kiema, G., McDermott, M.T. and Wiener, J.H. (1998) Hydroxylated napthoquinones as substrates for *Escherichia coli* anaerobic reductases. Submitted. Biochem. J.

205. Rothery, R. and Weiner, J.H. Unpublished results.

206. Rothery, R.A., Magalon, A., Giordano, G., Guigliarelli, B., Blasco, F. and Weiner, J.H. (1998) The molybdenum cofactor of *Escherichia coli* nitrate reductase A (NarGHI) effect of a *mobAB* mutation and interactions with [Fe-S] clusters. J. Biol. Chem. In press.

207. Rothery, R.A., Simala-Grant, J.L., Johnson, J.L., Rajagopalan, K.V. and Weiner, J.H. (1995) Association of molybdopterin guanine dinucleotide with *Escherichia coli* dimethylsulfoxide reductase : Effect of tungstate and a *mob* mutant. J. Bacteriol. 177, 2057-2063.

208. Rothery, R.A. and Weiner, J.H. (1991) Alteration of the iron-sulfur cluster composition of *Escherichia coli* dimethyl sulfoxide reductase by site-specific mutagenesis. Biochemistry 30, 8296-8305.

209. Rothery, R.A. and Weiner, J.H. (1993) Topological characterization of *Escherichia coli* DMSO reductase by electron paramagnetic spectroscopy of an engineered [3Fe-4S] cluster. Biochem. 32, 5855-5861.

210. Rothery, R.A. and Weiner, J.H. (1996) Interaction of an engineered [3Fe-4S] cluster with a menaquinol binding site of *Escherichia coli* DMSO reductase. Biochem. 35, 3247-3257.

211. Rothery, R.A. and Weiner, J.H. (1998) Interaction of a menaquinol binding site with the [3Fe-4S] cluster of *Escherichia coli* fumarate reductase. Manuscript in preparation.

212. Sajitz, P., Klemme, J.-H., Koch, H.-G. and Molitor, M. (1993) Isolation and properties of trimethylamine N-oxide/dimethylsulfoxide reductase from the purple bacterium *Rhodospirillum rubrum*. Z. Naturforsch. 48c, 812-814.

213. Sakaguchi, M. and Kawai, A. (1978) Presence of *b*- and *c*-type cytochromes in the membrane of *Escherichia coli* induced by trimethylamine N-oxide. Bull. Jap. Soc. Sci. Fish. 44, 999-1002.

214. Sambasivarao, D., Scraba, D.G., Trieber, C. and Weiner, J.H. (1990) Organization of dimethyl sulfoxide reductase in the plasma membrane of *Escherichia coli.* J. Bacteriol 172, 5938-5948.

215. Sambasivarao, D. and Weiner, J.H. (1991) Differentiation of the multiple S- and N-oxide reducing activities of *Escherichia coli.* Curr. Microbiol. 23, 105-110.

216. Sambasivarao, D. and Weiner, J.H. (1991) Dimethylsulfoxide reductase of *Escherichia coli* : an investigation of function and assembly by use of *in vivo* complementation. J. Bacteriol. 173, 5935-5943.

217. Santini, C.-L., Ize, B., Chantal, A., Muller, M., Giordano, G. and Wu, L.-F. (1998) A novel Sec-independent periplasmic protein translocation pathway in *Escherichia coli.* EMBO J. 17, 101-112.

218. Sato-Watanabe, M., Mogi, T., Ogura, T., Kitagawa, T., Miyoshi, H., Iwamura, H. and Anraku, Y. (1994) Identification of a novel quinone-binding site in the cytochrome *bo* complex from *Escherichia coli.* J. Biol. Chem. 46, 28908-28912.

219. Satoh, T. and Kurihara, F.N. (1987) Purification and properties of dimethylsulfoxide reductase containing a molybdenum cofactor from a photodenitrifier, *Rhodopseudomonas sphaeroides* f.s. *denitrificans.* J. Biochem 102, 191-197.

220. Schindelin, H., Kisher, C., Hilton, J., Rajagopalan, K.V. and Rees, D.C. (1996) Crystal structure of DMSO reductase: Redox-linked changes in molybdopterin coordination. Science 272, 1615-1621.

221. Schinschel, C. and Simon, H. (1993) Effect of carbon sources and electron acceptors in the growth medium of *Proteus* spp. on the formation of (R)-2-hydroxycarboxylate viologen oxidoreductase and dimethylsulphoxide reductase. Appl. Microbiol. Biotechnol. 38, 531-536.

222. Schmitz, R.A., Albracht, S.P.J. and Thauer, R.K. (1992) A molybdenum and a tungsten isoenzyme of formylmethanofuran dehydrogenase in a thermophilic archaeon *Methanobacterium thermoautotrophicum.* Eur. J. Biochem. 209, 1013-1018.

223. Schneider, F., Lowe, J., Huber, R., Schindelin, H., Kisker, C. and Knablein, J. (1996) Crystal structure of dimethyl sulfoxide reductase from *Rhodobacter capsulatus* at 1.88 A resolution. J. Mol. Biol. 263, 53-69.

224. Shestopalov, A.I., Bogachev, A.V., Murtazina, R.A., Viryasov, M.B. and Skulachev, V.P. (1997) Aeration dependent changes in composition of the quinone pool in *Escherichia coli*. FEBS Lett. 404, 272-274.

225. Shimokowa, O. and Ishimoto, M. (1979) Purification and some properties of the inducible tertiary amine N-oxide reductase from *Escherichia coli*. J. Biochem. 86, 1709-1717.

226. Shukla, O.P. (1984) Microbial transformation of pyridine derivatives. J. Sci. Ind. Res. 43, 98-116.

227. Silvestro, A., Pommier, J. and Giordano, G. (1988) The inducible trimethylamine *N*-oxide reductase of *Escherichia coli* K12 : biochemical and immunological studies. Biochim. Biophys. Acta. 954, 1-13.

228. Silvestro, A., Pommier, J., Pascal, M.-C. and Giordano, G. (1989) The inducible trimethylamine N-oxide reductase of *Escherichia coli* K12: its localization and inducers. Biochim. Biophys. Acta 999, 208-216.

229. Simala-Grant, J.L. and Weiner, J.H. Unpublished results.

230. Sled, V.D., Friedrich, T., Leid, H., Weiss, H., Meinhardt, S.M., Fukumori, Y., Calhoun, M.W., Gennis, R.B. and Ohnishi, T. (1993) Bacterial NADH-quinone oxidoreductase: iron-sulfur clusters and related problems. J. Bioenerg. Biomemb. 25, 347-356.

231. Somero, G.M. (1983) Environmental adaptation of proteins: strategies for the conservation of critical functional and structural traits. Comp. Biochem. Physiol. 76A, 621-633.

232. Spiro, S. and Guest, J.R. (1990) FNR and its role in oxygen-regulated gene expression in *Escherichia coli*. FEMS Microbiol. Rev. 75, 399-428.

233. Spiro, S. and Guest, J.R. (1991) Adaptive responses to oxygen limitation in *Escherichia coli*. TIBS 16, 310-314.

234. Spiro, S., Roberts, R.E. and Guest, J.R. (1989) FNR-dependent repression of the *ndh* gene of *Escherichia coli* and metal ion requirement for FNR-regulated gene expression. Mol. Micro. 3, 601-608.

235. Stenberg, E., Styrvold, O.B. and Strom, A. (1982) Trimethylamine oxide respiration in *Proteus* sp. strain NTHC153:

electron transfer-dependent phosphorylation and L-serine transport. J. Bact. 149, 22-28.

236. Stewart, V. (1982) Requirement of FNR and NarL functions for nitrate reductase expression in *Escherichia coli* K-12. J. Bact. 151, 1320-1325.

237. Stewart, V. (1988) Nitrate respiration in relation to facultative metabolism in enterobacteria. Microbiol. Rev. 52, 190-232.

238. Stewart, V. and Rabin, R.S. (1995) Dual sensors and dual response regulators interacts to control nitrate- and nitrite-responsive gene expression in *Escherichia coli,* in Two-component signal transduction (Hoch, J.A. and Silhavy, T.J., eds.), Vol. 1, 1st ed., p. 233-252, ASM Press, Washington.

239. Strom, A.R., Olafson, J.A. and Larsen, H. (1979) Trimethylamine oxide: A terminal electron acceptor in anaerobic respiration of bacteria. J. Gen. Micro. 112, 315-320.

240. Stryer, L. (1988) Biochemistry. Vol. 1, 3rd ed., p. 144,W. H. Freeman and Company, New York.

241. Styvold, O.B. and Stom, A. (1984) Dimethylsulphoxide and trimethylamine oxide respiration of *Proteus vulgaris.* Evidence for a common terminal reductase system. Arch. Microbiol. 140, 74-78.

242. Takagi, H., Tsuchiya, T. and Ishimoto, M. (1981) Proton translocation coupled to trimethylamine N-oxide reduction in anaerobically grown *Escherichia coli*. J. Bacteriol. 148, 762-768.

243. Tran, Q.H., Bongaerts, J., Vlad, D. and Unden, G. (1997) Requirement for the proton-pumping NADH dehydrogenase I of *Escherichia coli* in respiration of NADH to fumarate and its bioenergetic implications. Eur. J. Biochem. 244, 155-160.

244. Trieber, C.A., Rothery, R.A. and Weiner, J.H. (1994) Multiple pathways of electron transfer in dimethyl sulfoxide reductase of *Escherichia coli.* J. Biol. Chem. 269, 7103-7109.

245. Trieber, C.A., Rothery, R.A. and Weiner, J.H. (1996) Consequences of removal of a molybdenum ligand (DmsA-Ser176) of *Escherichia coli* dimethyl sulfoxide reductase. J. Biol. Chem. 271, 27339-27345.

246. Trieber, C.A., Rothery, R.A. and Weiner, J.H. (1996) Engineering a novel iron-sulfur cluster into the catalytic subunit

of *Escherichia coli* dimethyl-sulfoxide reductase. J. Biol. Chem. 271, 4620-4626.

247. Trumpower, B.L. (1981) New concepts on the role of ubiquinone in the mitochondrial respiratory chain. J. Bioenerg. Biomemb. 13, 1-24.

248. Trumpower, B.L. and Gennis, R.B. (1994) Energy transduction by cytochrome complexes in mitochondrial and bacterial respiration : the enzymology coupling electron transfer reactions to proton translocation. Annu. Rev. Biochem. 63, 675-716.

249. Turner, R.J., Busaan, J.L., Lee, J.H., Michalak, M. and Weiner, J.H. (1997) Expression and epitope tagging of the membrane anchor subunit (DmsC) of *Escherichia coli* dimethyl sulfoxide reductase. Prot. Eng. 10, 285-290.

250. Tyson, K.L., Bell, A.I., Cole, J.A. and Busby, S.J.W. (1993) Definition of nitrite and nitrate response elements at the anaerobically inducible *Escherichia coli nirB* promoter: interactions between FNR and NarL. Mol. Micro. 7, 151-157.

251. Tyson, K.L., Cole, J.A. and Busby, S.W.J. (1994) Nitrite and nitrate regulation at the promoters of two *Escherichia coli* operons encoding nitrite reductase. Mol. Micro. 13, 1045-1055.

252. Ujiiye, T., Yamamoto, I., Nakama, H., Okubo, A. and Yamazaki, S. (1996) Nucleotide sequence of the genes, encoding the pentaheme cytochrome (*dmsC*) and the transmembrane protein (*dmsB*) involved in dimethylsulfoxide respiration from *Rhodobacter sphaeroides* f. sp. *denitrificans*. Biochim. Biophys. Acta 1277, 1-5.

253. Ujiiye, T., Yamamoto, I. and Satoh, T. (1997) The *dmsR* gene encoding a dimethyl sulfoxide-responsive regulator for expression of *dmsCBA* (dimethyl sulfoxide respiratory genes) in *Rhodobacter sphaeroides* f. sp. *denitrificans*. Biochim. Biophys. Acta. 1353, 84-92.

254. Unden, G. (1988) Differential roles for menaquinone and demethylmenaquinone in anaerobic electron transport of *E. coli* and their *fnr*-independent expression. Arch. Microbiol. 150, 499-503.

255. Unden, G. and Bongaerts, J. (1997) Alternative respiratory pathways of *Escherichia coli*: energetics and transcriptional regulation in response to electron acceptors. Biochim. Biophys. Acta 1320, 217-234.

256. Unemoto, T., Hayashi, M., Miyaki, K. and Hayashi, M. (1965) Intracellular localization and properties of trimethylamine-N-oxide reductase in *Vibrio parahaemolyticus.* Biochim. Biophys. Acta 110, 319-328.

257. VanHellemond, J.J. and Tielens, A.G.M. (1994) Expression and functional properties of fumarate reductase. Biochem. J. 304, 321-331.

258. vanSchie, B.J., Hellingwerf, K.J., vanDijken, J.P., Elferink, M.G.L., vanDijl, J.M., Kuenen, J.G. and Konigs, W.N. (1985) Energy transduction by electron transfer via pyrrolo-quinone-dependent glucose dehydrogenase in *Escherichia coli*, *Pseudomonas aeroginosa*, and *Acinetobacter calcoaceticus* (var. *lwoffi*). J. Bact. 163, 493-499.

259. Varga, M.E.R. and Weiner, J.H. Unpublished results.

260. Varga, M.E.R. and Weiner, J.H. (1995) Physiological role of GlpB of anaerobic glycerol-3-phosphate dehydrogenase of *Escherichia coli.* Biochem. Cell Biol. 73, 147-153.

261. Volbeda, A., Charon, M.-H., Piras, C., Hatchikian, E.C., Frey, M. and Fontecilla-Camps, J.C. (1995) Crystal structure of the nickel-iron hydrogenase from *Desulfovibrio gigas.* Nature 373, 580-587.

262. vonHeijne, G. (1985) Signal sequences the limits of variation. J. Mol. Biol. 184, 99-105.

263. Wallace, B.J. and Young, I.G. (1977) Role of quinones in electron transport to oxygen and nitrate in *Escherichia coli.* Biochim. Biophys. Acta 461, 84-100.

264. Weidner, U., Geier, S., Ptock, A., Friedrich, T., Leif, H. and Weiss, H. (1993) The gene locus of the proton-translocating NADH:ubiquinone oxidoreductase in *Escherichia coli.* J. Mol. Biol. 233, 109-122.

265. Weiner, J.H. Unpublished results.

266. Weiner, J.H. (1992) The fumarate and dimethylsulphoxide reductases of anaerobic electron transport in *Escherichia coli*: current status and future perspectives. World J. Microbiol. Biotechnol. 8, 102-106.

267. Weiner, J.H., Bilous, P.T., Shaw, G., Lubitz, S.P., Thomas, G.H., Cole, J.A. and Turner, R.J. (1998) Novel and ubiquitous system

for the membrane targeting and translocation of proteins containing a double arginine leader. In press. Cell.

268. Weiner, J.H., Cammack, R., Cole, S.T., Condon, C., Honore, N., Lemire, B.D. and Shaw, G. (1986) A mutant of *Escherichia coli* fumarate reductase decoupled from electron transport. Proc. Natl. Acad. Sci. 83, 2056-2060.

269. Weiner, J.H. and Dickie, P. (1979) Fumarate reductase of *Escherichia coli*: elucidation of the covalent-flavin unit. J. Biol. Chem. 254, 8590-8593.

270. Weiner, J.H., MacIsacc, D.P., Bishop, R.E. and Bilous, P.T. (1988) Purification and properties of *Escherichia coli* dimethyl sulfoxide reductase, an iron-sulfur molybdoenzyme with broad substrate specificity. J. Bacteriol. 170, 1505-1510.

271. Weiner, J.H., Rothery, R.A., Sambasivarao, D. and Trieber, C.A. (1992) Molecular analysis of dimethylsulfoxide reductase : a complex iron-sulfur molybdoenzyme of *Escherichia coli*. Biochim. Biophys. Acta 1102, 1-18.

272. Weiner, J.H., Shaw, G., Turner, R.J. and Trieber, C.A. (1993) The topology of the anchor subunit of dimethyl sulfoxide reductase of *Escherichia coli*. J. Biol. Chem. 268, 3238-3244.

273. Welter, R., Gu, L.-Q., Y, C.-A., Rumblay, J. and Gennis, R. (1994) Identification of the ubiquinol-binding site in the cytochrome *bo*3-ubiquinol oxidase of *Escherichia coli*. J. Biol. Chem. 269, 28834-28838.

274. Werth, M.T., Cecchini, G., Schoroder, I., Lasage, S., Gunsalus, R.P. and Johnson, K. (1992) Site-directed mutagenesis of conserved cysteine residues in *Escherichia coli* fumarate reductase : Modification of the spectroscopic and electrochemical properties of the [2Fe-2S] cluster. Proc. Natl. Acad. Sci. 87, 8965-8969.

275. Westenberg, D.J., Gunsalus, R.P., Ackrell, B.A.C. and Cecchini, G. (1990) Electron transfer from menaquinol to fumarate. Fumarate reductase anchor polypeptide mutants of *Escherichia coli*. J. Biol. Chem. 265, 19560-19567.

276. Westenberg, D.J., Gunsalus, R.P., Ackrell, B.A.C., Sices, H. and Cecchini, G. (1993) *Escherichia coli* fumarate reductase *frdC* and *frdD* mutants. Identification of amino acid residues involved in catalytic activity with quinones. J. Biol. Chem. 268, 815-822.

277. Wissenbach, U., Kroger, A. and Unden, G. (1990) The specific functions of menaquinone and demethylquinone in anaerobic respiration with fumarate, dimethylsulfoxide, trimethylamine N-oxide and nitrate by *Escherichia coli*. Arch. Microbiol. 154, 60-66.

278. Wissenbach, U., Ternes, D. and Unden, G. (1992) An *Escherichia coli* mutant containing only demethylmenaquinone, but no menaquinone: effects on fumarate, dimethylsulfoxide, trimethylamine N-oxide and nitrate respiration. Arch. Microbiol. 158, 68-73.

279. Wood, J.M. (1987) Membrane association of proline dehydrogenase in *Escherichia coli* is redox dependent. Proc. Natl. Acad. Sci 84, 373-377.

280. Wood, P.M. (1981) The redox potential for dimethyl sulphoxide reduction to dimethyl sulphide. FEBS Lett. 124, 11-14.

281. Wootton, J.C., Nicolson, R.E., Cock, J.M., Walters, D.E., Burke, J.F., Doyle, W.A. and Bray, R.C. (1991) Enzymes depending on the pterin molybdenum cofactor : sequence families, spectroscopic properties of molybdenum and possible cofactor-binding domains. Biochim. Biophys. Acta 1057, 157-185.

282. Wuebbens, M.M. and Rajagopalan, K.V. (1995) Investigation of the early steps of molybdopterin biosynthesis in *Escherichia coli* through the use of *in vivo* labeling studies. J. Biol. Chem. 270, 1082-1087.

283. Yamamoto, I., Hinakura, M., Seki, S., Seki, Y. and Kondo, H. (1990) Anaerobic induction of trimethylamine N-oxide reductase and cytochromes by dimethyl sulfoxide in *Escherichia coli*. Curr. Microbiol. 20, 245-249.

284. Yamamoto, I., Okubo, M. and Ishimoto, M. (1986) Further characterization of trimethylamine N-oxide reductase from *Escherichia coli* a molybdoprotein. J. Biochem. 99, 1773-1779.

285. Yamamoto, I., Saiki, T., Lie, S.-M. and Ljungdahl, L.G. (1983) Purification and properties of NADP-dependent formate dehydrogenase from *Clostridium thermoaceticum,* a tungsten-selenium-iron protein. J. Biol. Chem. 258, 1826-1832.

286. Yang, F.-D., Yu, L., Yu, C.-A., Lorence, R.M. and Gennis, R.B. (1986) Use of an azido-ubiquinone derivative to identify subunit I as the ubiquinol binding site of the cytochrome *d* terminal oxidase complex of *Escherichia coli*. J. Biol. Chem. 14987-14990.

287. Yoshida, Y., Takai, M., Satoh, T. and Takami, S. (1991) Molybdenum requirement for translocation of dimethylsulfoxide reductase to the periplasmic space in a photodenitrifier, *Rhodobacter sphaeroides* f. s. *denitrificans.* J. Bact. 173, 3277-3281.

288. Young, I.G., Rogers, B.L., Campbell, H.D., Jaworowski, A. and Shaw, D.C. (1981) Nucleotide sequence coding for the respiratory NADH dehydrogenase of *Escherichia coli.* Eur. J. Biochem. 116, 165-170.

289. Zeyer, J., Eicher, P., Wakeham, S.G. and Schwarzenbach, R.P. (1987) Oxidation of dimethyl sulfide to dimethyl sulfoxide by phototrophic purple bacteria. Appl. Environ. Micro. 53, 2026-2032.

290. Zhao, Z. and Weiner, J.H. (1998) Interaction of HOQNO with dimethylsulfoxide reductase of *Escherichia coli.* J. Biol Chem. Submitted.

291. Ziegelhoffer, E.C. and Kiley, P.J. (1995) *In vitro* analysis of a constitutively active mutant form of the *Escherichia coli* global transcription factor FNR. J. Mol. Biol. 245, 351-361.

292. Zinder, S.H. and Brock, T.D. (1978) Dimethyl sulphoxide reduction by micro-organisms. J. Gen. Microbiol. 105, 335-342.

293. Zinoni, F., Birkmann, A., Stadtman, T.C. and Bock, A. (1986) Nucleotide sequence and expression of the selenocysteine-containing polypeptide formate dehydrogenase (formate-hydrogen-lyase-linked) from *Escherichia coli.* Proc. Natl. Acad. Sci. 83, 4650-4654.

294. Zurick, T.R., Pitterle, D.M. and Rajagopalan, K.V. (1991) Molybdopterin biosynthesis role of the *chlN* gene product. FASEB J. 5, A470.

Chapter 2 : Characterization of DmsAB

2.1. Introduction

DmsABC and TorA are reductases with overlapping substrate specificities. However, TorA does not interfere with the analysis of DmsABC in cell extracts, since TorA is only expressed when induced [17]. In contrast, DmsABC is expressed constitutively under anaerobiosis [11].

DmsABC is a membrane protein composed of three subunits [6]. DmsC is responsible for anchoring DmsA and DmsB to the membrane [29], and is the site of MQH_2 oxidation [26, 40]. Although DmsABC is a membrane protein, 23-46% of DMSO reductase activity is found in the cell supernatant fraction [5, 27] mediated by DmsAB [27]. DMSO reductase activity in the membrane in mediated by DmsABC [29]. The presence of DmsAB in the cytoplasm is not specific to plasmid overexpression, but is also observed when DmsABC is expressed solely from the chromosome [6, 29].

DmsABC is a membrane protein, and Triton X-100 is used for its purification. This detergent is fluorescent, and interferes with fluorescence studies, including those to determine the structure of moco in DmsABC. In contrast, no detergent would be needed for purification of DmsAB making it useful for numerous studies. For example, crystallization of the dimer would likely be easier than that of DmsABC/Triton X-100 micelles [18].

DmsA belongs to a family prokaryotic molybdoenzymes [4, 39, 41]. Pleiotropic loss of molybdoenzyme activity is observed when a mutation occurs in any of the genes necessary for moco biosynthesis [35]. It is possible to reconstitute molybdoenzyme activity by mixing the soluble fractions from two moco deficient strains with mutations at different loci [3]. Biochemical complementation results, as mixing of the two soluble fractions results in a full complement of proteins necessary for the biosynthesis of moco. Since reconstitution uses only the soluble fractions from moco biosynthetic mutants, in our case, reconstitution experiments would involve DmsAB.

Due to the potential usefulness of DmsAB in the absence of the membrane anchor subunit, we have characterized and confirmed salient features of DmsAB structure and function. First, DmsAB/DmsABC stability was assessed over time in the presence of various compounds. Second, reconstitution of moco into apo-DmsAB was attempted. The data obtained highlights one aspect of DmsC function in the holoenzyme, underlines the different processes of activity loss for DmsAB and DmsABC, and outlines avenues to pursue for any future purification of DmsAB.

2.2. Materials and Methods

2.2.1. Materials

All materials were reagent grade, and were purchased from commercial sources.

2.2.2. Strains and Plasmids

E. coli strains HB101, DSS301, DSS401, RK5208 and AP15, and plasmids pDMS159, pDMS160, and pDMSC59X used in this study, are described in Table 2.1. Plasmids pDMS159 and pDMS160 are identical with respect to the *dmsABC* operon, however, pDMS160 is missing 1.66 kilobase pairs (kbp) 3' to *dmsC*. Strains were transformed with pDMS159 or pDMS160, for overexpression of DmsABC. pDMSC59X carries wild-type DmsA and DmsB, while DmsC is truncated at L76 by a PhoA fusion. All manipulations of plasmids and strains were carried out essentially as described by Sambrook [30].

Table 2.1.

E. coli Strains and Plasmids Used in this Study

Strain or Plasmid	Description	Source
Strain		
HB101	*supE*44 *hsdS*20($r_B^-m_B^-$) *recA*13 *ara*-14 *procA*2 *lacY*1	[8]
DSS301	*supE*44 *hsdS*20($r_B^-m_B^-$) *recA*13 *ara*-14 *proA*2 *lacY*1 *gal*K2 *rpsL*20*xyl*-5 *mtl*-1 Δ*dmsABC*	[29]
DSS401	*ara*D139 (*lac*IPOZYA-*arg*F)U169 *rps*L *thi* Δ*dmsABC* Kan^R	[28]
RK5208	F- *ara*D139 *lac*U169 *gyr*A *thi rps*L *mob*207::Mu *cys*	[36]
AP15	F-*thr leu his pro arg thi ade gal lac*Y *mal*E *xyl ara mtl str* T1^R γ^R *chl*A	[3]
Plasmid		
pBR322	Tet^R Amp^R	Pharmacia
pDMS159	pBR322 Amp^R (*dmsABC*)$^+$	[6]
pDMS160	pBR322 Amp^R (*dmsABC*)$^+$	[25]
pDMSC59X	pBR322 Amp^R (*dmsAB*)$^+$(*C'phoA*)	[29]

2.2.3. Media and Growth Conditions

Strains were grown aerobically in Luria-Bertani medium (LB) or Terrific Broth [30] overnight, and these cultures were used as 1% inocula for anaerobic growth on glycerol minimal media [5] or LB. As necessary, 50-100 μg/mL ampicillin, or 40 μg/mL kanamycin, was included in the growth medium.

For reconstitution experiments, cells were grown on LB anaerobically for 24 hours at 30°C.

In all other instances, bacteria were grown anaerobically on glycerol fumarate minimal media (Gly/Fum) for 48 hours, at 30°C or 37°C as indicated previously [5], with the following exceptions. 0.16% peptone was substituted for casamino acids, and streptomycin sulfate was not included in the growth medium. Proline, leucine and vitamin B1, were included at a final concentration of 0.005%.

2.2.4. Preparation of Membrane and Supernatant Fractions

Large cell volumes were harvested using a Pellicon membrane system equipped with a Millipore polysulfone PTNK filter. Bacterial cells were pelleted by centrifugation at 9,500 x g for 10 minutes. Cell pellets were resuspended in buffer (50 mM 3-[*N*-morpholino]propane sulfonic acid (MOPS) pH 7.0, 5 mM ethylenediaminetetraacetic acid (EDTA), and 70 mM TMAO) [25]), and broken by French pressure lysis. As necessary membrane and supernatant fractions were separated by centrifugation [5].

2.2.5. Enzyme Assays

The 50 mM MOPS used in these assays was degassed and bubbled with N_2. Either 70 mM TMAO, or 10 mM nitrate, was used for all assays. TMAO was used to assay DmsAB/DmsABC on a routine basis, since TMAO has a higher k_{cat} than DMSO (Chapter 6).

Substrate-dependent oxidation of $BVH^{\cdot+}$ was monitored at 570 nm, using a Gilford 250 spectrophotometer at 37°C. The order of addition to the cuvette was : oxidized benzyl viologen (BV^{2+}), substrate, dithionite, and enzyme. For open cuvette (non-stoppered) assays, benzyl viologen (BV) was used at a final concentration of 0.2 mM (ε $BVH^{\cdot+}$ = 7.8×10^3L mol^{-1} cm^{-1}), and sodium dithionite (dithionite) at a concentration of 0.33 mM. Closed cuvette assays (stoppered) were performed by transferring buffer to a cuvette, that was subsequently stoppered, excluding air. Hamilton syringes were used for the ordered addition as above. A stable baseline was confirmed prior to addition of enzyme. For closed cuvette assays, BV was used at final concentration of 0.2 mM, and dithionite was added to approximately 0.1 mM, to give an absorbance of about 1.0 optical density unit (OD). Several assays were performed for each of the conditions examined. The values used were the means. In all cases, the standard deviation of the means was less than 10% unless otherwise indicated in the Figure or Table legends. One unit of enzyme activity corresponds to 2 µmol of $BVH^{\cdot+}$ oxidized per minute, or 1 µmol N-oxide or nitrate reduced per minute.

2.2.6. Separation of Low and High Molecular Weight Fractions

Supernatant from HB101/pDMS160, and a solution containing blue dextran, were passed separately down a 3 mL Sephadex-G25 column. Fractions were collected, and visualized by eye for color, to identify fractions containing overexpressed DmsAB (brown), and blue dextran. Each of the fractions collected were also tested for reductase activity.

2.2.7. Purification of DmsAB

HB101/pDMS160 supernatant was used for all purification procedures.

2.2.7.1. Ammonium Sulfate Precipitation

For the ammonium sulfate backwash technique, supernatant was brought to 50% ammonium sulfate saturation. After incubation for 30 minutes on ice with occasional mixing, protein was pelleted by centrifugation at 9,500 g for 10 minutes. The drained and dried pellet was resuspended with decreasing concentrations of saturated ammonium sulfate (45%, 40%, 35%, and 30%), and the above procedure was repeated. Pellets were resuspended in 50 mM MOPS. Each fraction was assayed for reductase activity and protein concentration.

Also, supernatant with column buffer (50 mM N-[2-hydroxyethyl]piperazine-N'[3-propanesulfonic acid] (EPPS) pH 8.35, 5 mM phenylmethyl sulfonyl fluoride (PMSF), and 40% glycerol), and either 25% or 40% glycerol, was used for ammonium sulfate precipitation. Precipitation was performed as indicated above except the saturation of ammonium sulfate was increased in 10% increments.

2.2.7.2. Heat Purification of DmsAB

Supernatant was incubated at 52°C or 62°C. Samples were taken at various times, incubated on ice for 10 minutes, and centrifuged at 9,500 x g for 10 minutes, to separate coagulated protein from protein of interest. Samples were assayed for reductase activity and protein concentration.

2.2.7.3. Whatman DE-52 Column

One mL supernatant was added to a 10 mL Whatman DE-52 column. The column was washed with six volumes of column buffer. Bound protein was eluted with a ten column volume gradient of column buffer, with 0-250 mM KCl. Six mL and 1 mL fractions were collected prior to, and after loading, respectively. Fractions were analyzed for reductase activity, OD at 280 nm, and protein concentration.

2.2.8. Stability/Stabilization of DmsAB/DmsABC

Aliquots of HB101/pDMS160 supernatant or membranes, were precipitated with 2 or 3 volumes saturated ammonium sulfate, respectively, by incubating for 15 minutes on ice with occasional mixing, and subsequent centrifugation at 15,000 x g for 10 minutes. The pellets were drained, dried of excess liquid, and resuspended in water and reagent as indicated in Tables 2.3. and 2.4. Samples were left at 0°C, and reductase activity was measured after the time indicated in the Figure and Table legends.

When protease inhibitor cocktail was added to membranes, the final concentrations of protease inhibitor in µg/mL are : aprotinin, 0.1; phosphoramidon, 0.1; L-1-chloro-3-[4-tosylamido]-7-amino-2-heptanone-HCl (TLCK-HCl), 0.1; L-1-chloro-3-[4-tosylamido]-4-phenyl-2-butanone (TPCK), 0.2; (4-amidino-phenyl)methane-sulfonyl fluoride (APMSF), 0.1; E-64, 0.1; leupeptin, 0.05; pepstatin 0.01.

2.2.9. Reconstitution of DmsAB and NarGH from *moa* and *mob* Mutants

Supernatants from the moco-deficient strains RK5208/pDMS159 and AP15 were mixed, flushed with N_2, and incubated at 37°C for the times indicated in Table 2.5. The reconstituted samples were analyzed for reductase activity and protein concentration. The small amount of endogenous activity found in the RK5208/pDMS159 and AP15 supernatants, were subtracted from the reconstituted activities.

2.2.10. Analytical Techniques

Protein concentrations were determined as published previously [21]. Polyacrylamide gel electrophoresis (PAGE) was performed using the BioRad mini-gel system, with a discontinuous sodium dodecyl sulfate (SDS) buffer system [19]. Gels were stained with Coomassie blue, and destained [20]. Confirmation of bands on the polyacrylamide gel corresponding to DmsA and DmsB, was determined by Western blotting [27]. DmsA and DmsB antibody were used separately. ECL Western blotting detection reagents from Amersham Life Sciences were used for blot development. No antibody has been successfully raised against DmsC.

2.3. Results

2.3.1. Localization of DmsAB in Supernatant and Membrane Fractions

HB101/pDMS160 grown on Gly/Fum shows TMAO reductase activity in both supernatant and membrane fractions, while DSS401, a strain bearing a deletion of the *dmsABC* operon does not (Table 2.2.). This indicates DmsAB/DmsABC is responsible for TMAO reductase activity under these growth conditions. TorA can also reduce TMAO, however its expression is not induced under these conditions [17].

DSS301/pDMSC59X lacks functional DmsC, and essentially all reductase activity is found in the supernatant fraction (Table 2.2). The small amount of activity found in the membrane fraction is likely the result of small amounts of supernatant remaining with the membrane fraction since the membranes were not washed.

Localization of DmsA and B subunits in HB101/pDMS160 and DSS301/pDMSC59X was confirmed by Western blotting, and showed a similar profile to that expected from the activity numbers (data not shown). This confirms DmsC is responsible for the localization of DmsAB to the membrane. Since much of the DmsAB is found in the supernatant even when DmsC is present, as in HB101/pDMS160 (Table 2.2.), it is possible that either some DmsAB falls off the membrane on cell breakage, or DmsAB present in the supernatant has not yet been localized to the membrane.

Table 2.2.

TMAO Reductase Activity in Various Strains and Fractions From Cells Grown Anaerobically on Gly/Fum

Sample	Sp. Act. Membrane (u/mg)	% Total Act. (Membranes)	Sp. Act. Supernatant (u/mg)	% Total Act. (Supernatant)
HB101/pDMS160	30.7	25	16.1	75
DSS301/pDMSC59X	6	5	23	95
DSS401	0	-	0	-

Abbreviations are : Sp. Act. (specific activity), and Total Act. (total activity). One unit (u) equals 1μmole TMAO reduced per minute. Reductase activity was determined with 70 mM TMAO using the open cuvette assay. HB101 is wild-type, while DSS301 and DSS401 are both deleted for DmsABC.

2.3.2. TMAO Reductase Activity is Found in the High Molecular Weight Fraction

HB101/pDMS160 supernatant and blue dextran were each passed down a Sephadex-G25 column, to separate the low and high molecular weight fractions. TMAO reductase activity and brown color, characteristic of overexpressed DmsAB/DmsABC, were found to elute in the same fraction as blue dextran. This confirms the high TMAO reductase activity observed in the supernatant fraction was protein mediated, and not merely an artifact.

2.3.3. Preliminary Purification of DmsAB

Due to our interest in obtaining soluble DmsAB, we made preliminary attempts at its purification. We found these attempts resulted in more than desirable losses in activity, with minimal if any increase in specific activity.

Using the ammonium sulfate backwash technique on HB101/pDMS160 supernatant, only 54% of DmsAB activity was recovered, and it was spread across all backwash fractions. Specific activity dropped from 36.4 u/mg to 30.7 u/mg.

Heat purification of DmsAB from HB101/pDMS160 supernatant was attempted at both 52°C and 62°C. At both temperatures, no fold purification was achieved. Specific activity was between 35 and 40 u/mg. 75% and 60% activity remained at 5 minutes, when incubated at 52°C and 62°C, respectively (Figure 2.1.). Activity loss seemed to plateau around 60% for incubation at 52°C. This may suggest there are two forms of the enzyme, although we have no other data to support this.

DmsABC has been purified previously [9, 39], and is not particularly unstable, although it has been shown that moco is lost during purification (Chapter 3 and [39]). The lack of fold purification by these steps, confirms DmsAB is more unstable than DmsABC.

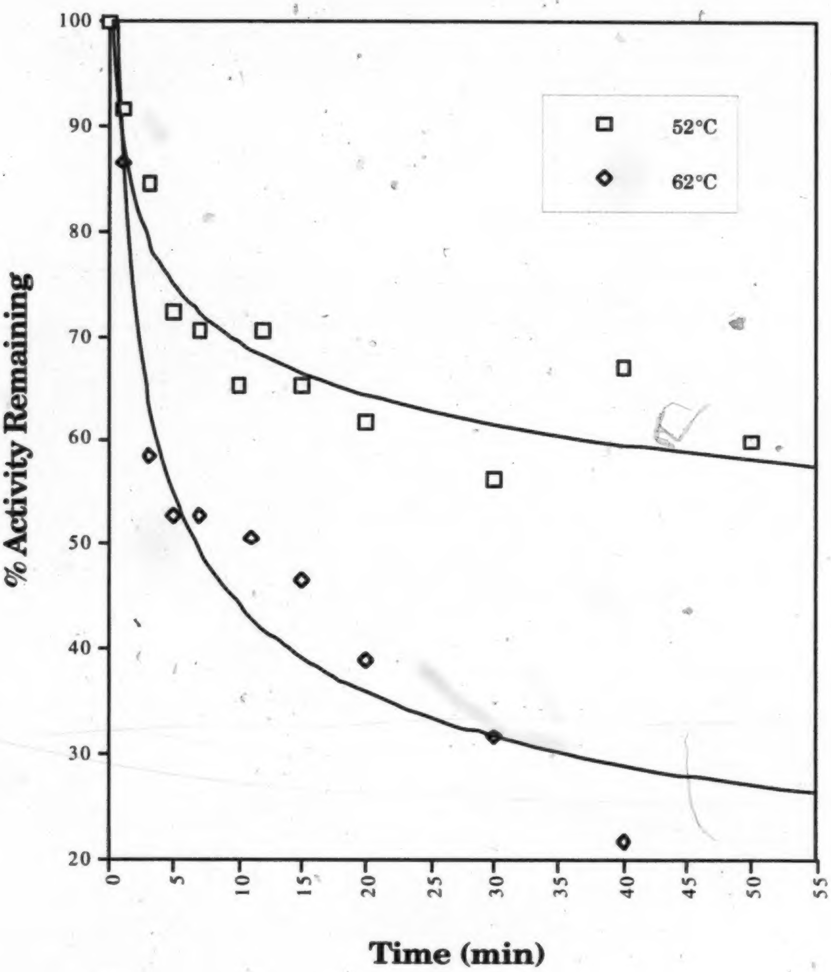

Figure 2.1.

Loss of DmsAB Activity in HB101/pDMS160 Supernatant Over Time at 52 and 62°C

Reductase activity was measured with TMAO using the open cuvette assay. HB101/pDMS160 supernatant contained 50 mM MOPS (pH 7.0), 5 mM EDTA, and 70 mM TMAO.

2.3.4. Stability and Stabilization of DmsAB/DmsABC

The stability of DmsAB was examined at 4°C, $^{-}$70°C, and 21°C.

Various batches of supernatant from HB101/pDMS160, were incubated at 4°C and assayed for DmsAB activity over time. Approximately 50% of the activity was lost after 2 days. Contrary to previously published results, no DmsAB activity was lost after one freeze/thaw cycle ($^{-}$70°C) [28].

Only 50% of DmsAB activity remained if HB101/pDMS160 supernatant was incubated at 21°C for 4 hours. after 18 hours, only 20% of DmsAB activity remained.

These results demonstrate the instability of DmsAB activity at 4°C and 21°C. As a result, compounds were added to supernatant in an attempt to maintain DmsAB activity over time.

Buffers, reducing and oxidizing agents, substrates, and a variety of other compounds were added to an ammonium sulfate precipitate of HB101/pDMS160 supernatant, in an attempt to stabilize DmsAB activity (Table 2.3.).

HB101/pDMS160 supernatant was incubated with "Good" buffers at their pka's. "Good" buffers were chosen, as they are known to be relatively free of non-specific buffer effects [37]. Little if any stabilization of DmsAB activity was observed with the chosen buffers. Figure 2.2. shows the activity remaining drops slightly as the buffer is poised at more alkaline pH values.

Ferricyanide and BV^{2+} are the only compounds that appeared to destabilize DmsAB activity further. Interestingly, both may oxidize DmsAB if any reducing equivalents are present in the enzyme. This suggests DmsAB is more stable under reducing conditions. Except for 20% glycerol, most of the compounds tested had no major effect on

Table 2.3.

Stabilization of DmsAB in HB101/pDMS160 Supernatant

Compound(s) added				**% Activity Remaining After 48 hours at 4°C +/- Standard Deviation**
no addition				62 +/- 2.7
Various Buffers				
50 mM MES	pH 6.15	2[N-morpholino]ethanesulfonic acid	pKa 6.1	59 +/- 4.0
50 mM MOPS	pH 7.20	3-[N-morpholino]propane sulfonic acid	pKa 7.2	66 +/- 3.2
50 mM BICINE	pH 8.35	N,N-bis[2hydroxyethyl]glycine	pKa 8.35	63 +/- 6.7
50 mM CHES	pH 9.30	2-[N-cyclohexylamino]ethane-sulfonic acid	pKa 9.3	59 +/- 7.3
50 mM CAPS	pH 10.4	3-[cyclohexylamino]propane-sulfonic acid	pKa 10.4	50 +/- 7.1
Compare the following to 50 mM MOPS for background 50 mM MOPS pH 7.2				66 +/- 3.2
Substrates				
50 mM MOPS + 100 mM TMAO				66 +/- 6.5
50 mM MOPS + 30 mM DMSO				67 +/- 11
50 mM MOPS + 0.1 mM BV^{2+}				51 +/- 7.9
Reducing Agents				
50 mM MOPS + 5 mM Glutathione				64 +/- 5.1
50 mM MOPS + 5 mM β-Mercaptoethanol				61 +/- 12.2
50 mM MOPS + 5 mM β-Mercaptoamine				59 +/- 1.2
50 mM MOPS + 5 mM Dithiothreitol (DTT)				69 +/- 3.6
Miscellaneous Compounds				
50 mM MOPS + 1 mM EDTA				58 +/- 2.0
50 mM MOPS + 20% Glycerol				95 +/- 8.0
Compare the following to "His buffer" for background 20 mM Histidine pH 6.8, 10% glycerol, 0.5 mM EDTA, and 0.5 mM DTT				74 +/- 17
Oxidizing Agents				
His buffer + 20 mM Ascorbic Acid				70 +/- 5.2
His buffer + 10 mM Ferricyanide				22 +/- 5.7
Protease Inhibitor				
His buffer + 10 mM PMSF				80 +/- 4.2
Metal Ion				
His buffer + 1 µM Ferric Chloride				63 +/- 5.2

Ammonium sulfate pellets of HB101/pDMS160 supernatant were resuspended in the presence of the compounds listed above. Reductase activity was measured using TMAO and the open cuvette assay.

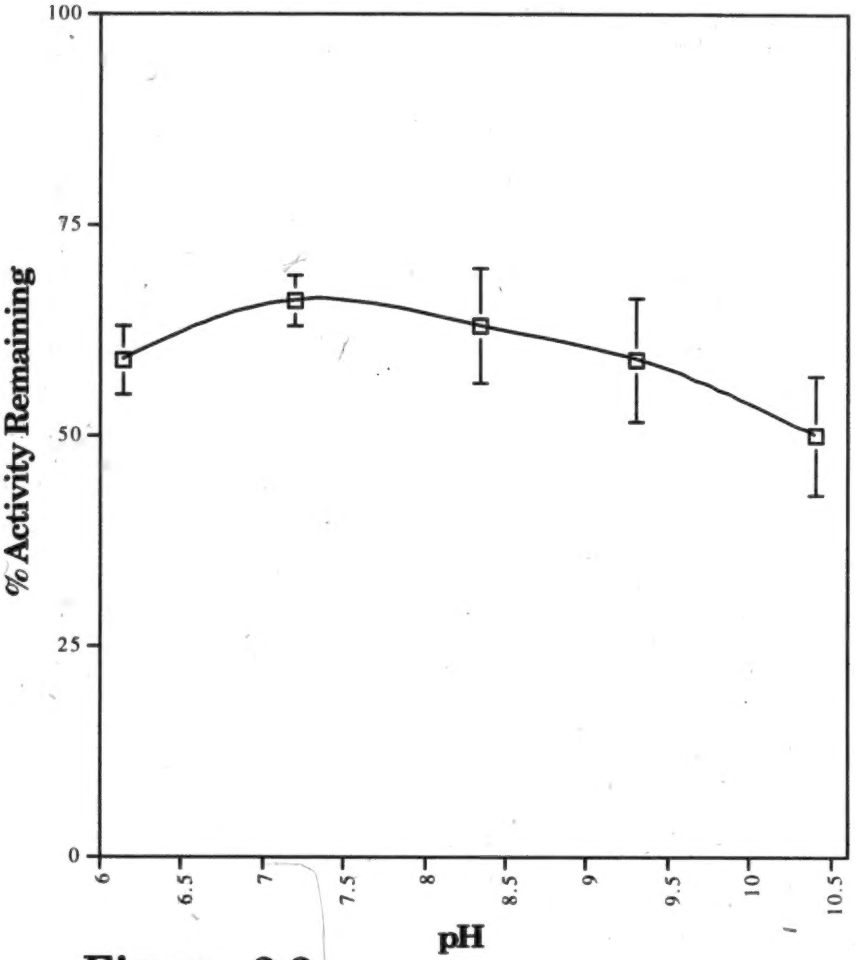

Figure 2.2.

pH Stability Profile for DmsAB in HB101/pDMS160 Supernatant

Ammonium sulfate precipitate of HB101/pDMS160 supernatant was resuspended in various "Good" buffers (50 mM) : MES, pH 6.15; MOPS, pH 7.2; BICINE, pH 8.35; CHES, pH 9.3; CAPS, pH 10.4. % Activity remaining was measured after 48 hours at 4°C, using TMAO as substrate, and the open cuvette assay. Deviation from the average is from muliple determinations of a single sample.

DmsAB stability. 10% glycerol appears to stabilize DmsAB to a lesser extent than 20% glycerol, as DmsAB activity was lower in His buffer, which contains 10% glycerol, than in MOPS plus 20% glycerol.

DmsAB activity could also be stabilized by resuspending ammonium sulfate pellets of HB101/pDMS160 supernatant in 20% and 40% ethylene glycol. Seventy-eight% and 82% activity remained after 26 hours at 4°C compared with 56% for the water/5 mM PMSF control. However, ethylene glycol did not stabilize DmsAB as well as 20% glycerol.

There was a large difference between the stability of DmsAB in supernatant (Table 2.3.) and DmsABC in membranes (Table 2.4.). It takes approximately 5.5 times as long to lose the same amount of DmsABC activity, as is lost for DmsAB. While addition of protease inhibitors and glycerol resulted in modest increases in stability, TMAO shows a marked ability to stabilize DmsABC. This is in contrast to observations with DmsAB where addition of TMAO resulted in no increase in stability (Table 2.3.).

2.3.5. Attempted Purification of DmsAB

Using the information obtained regarding DmsAB stability, purification was attempted using ion-exchange and ammonium sulfate precipitation.

Using a Whatman DE-52 column and column buffer composed of 50 mM EPPS pH 8.35, 5 mM PMSF, and 40% glycerol, DmsAB was purified from HB101/pDMS160 supernatant (Figure 2.3.). Unfortunately on our best attempt, only 66% of the activity was recovered, with a 1 fold drop in specific activity.

Inclusion of 40% glycerol in the HB101/pDMS160 supernatant resulted in an inability to precipitate DmsAB using ammonium sulfate. Decreasing glycerol concentration to 25% resulted in 85% of DmsAB precipitating between 40% and 95% ammonium sulfate saturation. No

Table 2.4.

Stabilization of DmsABC

Compound(s) added	% Activity Remaining after 11 days at 4°C
Water	57
50 mM EPPS	67
50 mM EPPS + 5 mM DTT	70
50 mM EPPS + 1 mM PMSF	79
50 mM EPPS + protease inhibitor cocktail	85
50 mM EPPS + 35% glycerol	83
50 mM EPPS + 70 mM TMAO	100

Ammonium sulfate pellets of HB101/pDMS160 membranes were resuspended in the presence of the compounds listed above. DmsABC activity was measured using TMAO and the open cuvette assay. When protease inhibitor cocktail was used, the final concentrations of protease inhibitors in µg/mL are : aprotinin, 0.1; phosphoramidon, 0.1; TLCK-HCl, 0.1; TPCK, 0.2; APMSF, 0.1; E-64, 0.1; leupeptin, 0.05; pepstatin 0.01. EPPS is N-[2-hydroxyethyl] piperazine-N'[3-propanesulfonic acid].

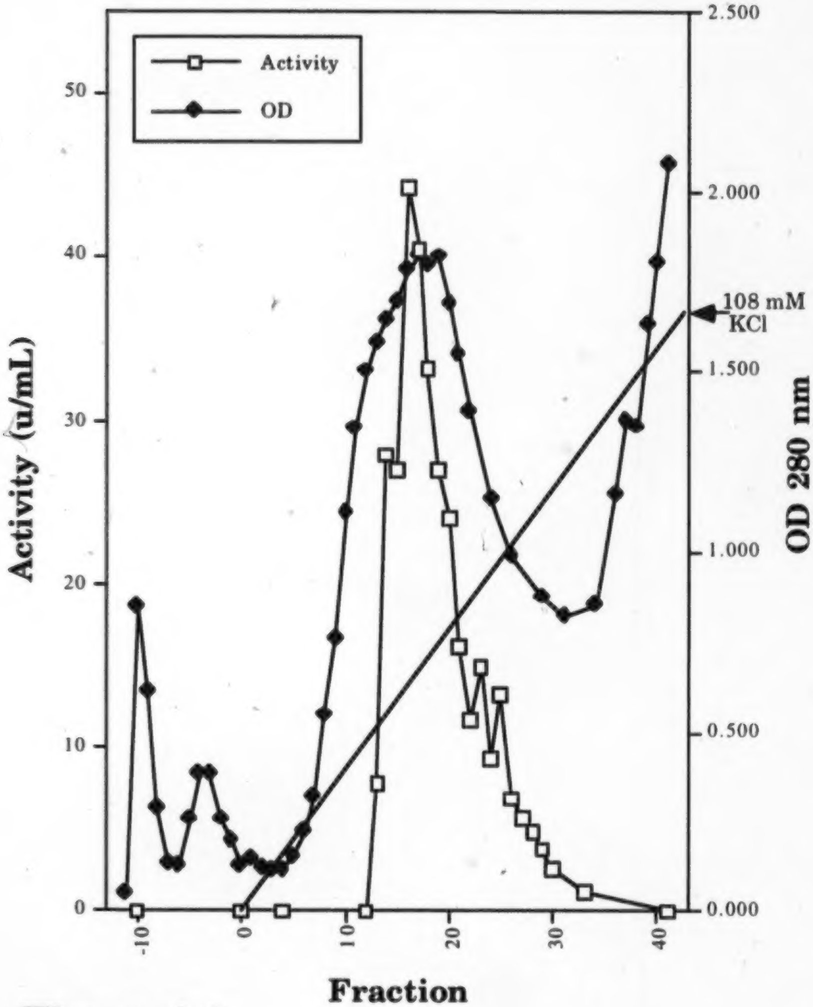

Figure 2.3.

Purification of DmsAB using a Whatman DE-52 Column

Activity was measured with TMAO using the open cuvette assay. A unit (u) equals 1μmole TMAO reduced per minute. HB101/pDMS160 supernatant was loaded onto the column at fraction -11, and the elution gradient was started at fraction 0. The KCl gradient is shown with a straight line. The arrow indicates the KCl concentration at fraction 43.

increase in specific activity was observed due to precipitation of DmsAB over a broad range of percent ammonium sulfate saturation.

2.3.6. Reconstitution of DmsAB

Mutants in the biosynthetic pathway of moco demonstrate pleiotropic loss of all molybdoenzymes [35]. It is possible to reconstituteenzyme activity by mixing the supernatants from two strains bearing different genetic lesions in the moco biosynthetic pathway. RK5208 and AP15, possess mutations at the *mob* [36] and *moa* [3] loci, respectively. Figure 2.4. depicts a schematic of reconstitution of DmsAB from AP15 and RK5208. When using *moa*$^-$ and *mob*$^-$ supernatants for reconstitution, *mob*$^-$ (RK5208) provides MPT, and FA from *moa*$^-$ (AP15) converts it to MGD [7, 13].

The soluble dimer (NarGH) of NarGHI is routinely reconstituted [14-16, 24], and was used as a control to ensure the correct conditions for reconstitution were being employed.

Supernatants from RK5208/pDMS160 and AP15 were incubated together for reconstitution of molybdoenzymes. The substrates TMAO and nitrate, were used to examine reconstitution of DmsAB and NarGH, respectively. Table 2.5. shows reconstitution of NarGH was 4.6 to 46 fold better than DmsAB, and increases with time of reconstitution. Reconstitution of DmsAB did not increase over time.

2.4. Discussion

The results reported herein confirmed DmsC is responsible for anchoring DmsAB to the membrane. These data also confirmed the apparent instability of DmsAB, compared to DmsABC, suggesting a role for DmsC in the stabilization of DmsABC. Different compounds stabilized DmsAB and DmsABC, and this suggested different pathways/processes lead to loss of activity for DmsAB and DmsABC.

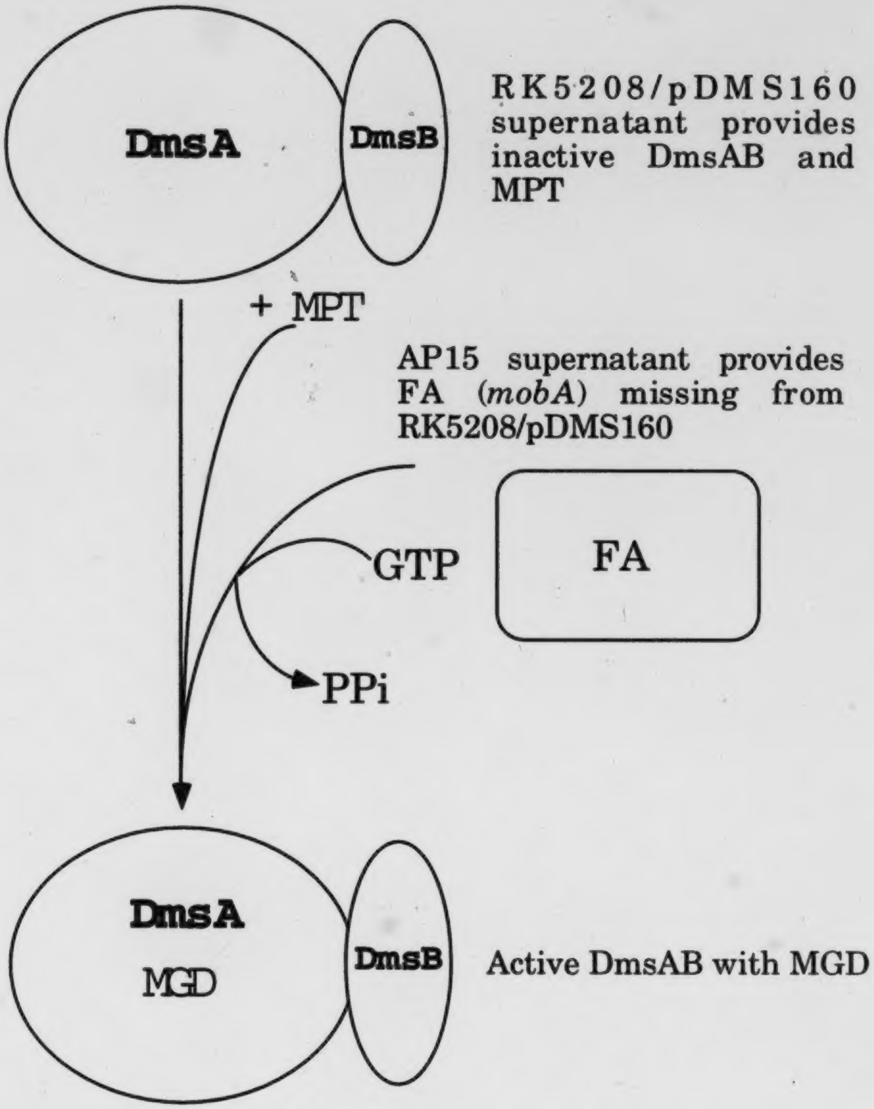
DmsA
DmsB
RK5208/pDMS160 supernatant provides inactive DmsAB and MPT
+ MPT
AP15 supernatant provides FA (*mobA*) missing from RK5208/pDMS160
GTP
FA
PPi
DmsA
MGD
DmsB
Active DmsAB with MGD

Figure 2.4.

Schematic of DmsAB Reconstitution Using RK5208/pDMS160 and AP15 Supernatants
GTP stands for guanosine triphosphate, and PPi for pyrophosphate [14, 24, 31].

Table 2.5.

Reconstitution of DmsAB and NarGH Using *moa*$^-$ (AP15) and *mob*$^-$ (RK5208/pDMS160) Supernatants

		Specific Activity u/mg	
Substrate	**Incubation Time : 37°C (minutes)**	**30**	**60**
Nitrate		0.17	1.7
TMAO		0.0037	0.0037
Fold Difference in Reconstitution for NarGH/DmsAB		46	460

Reductase activity was measured using the closed cuvette assay, and either 70 mM TMAO or 10 mM nitrate, for DmsAB and NarGH reconstitution, respectively. One unit (u) equals 1μmole TMAO or nitrate reduced per minute. The small amount of endogenous activity found in the RK5208/pDMS159 and AP15 supernatants, were subtracted from the reconstituted activities.

The results in sections 2.3.1. and 2.3.2. demonstrated all TMAO reductase activity was the result of DmsAB/DmsABC under the growth conditions employed, and DmsAB was present in the supernatant fraction. Since NarGH is easily purified [1, 2], purification of DmsAB from the supernatant appeared a reasonable goal. However, preliminary purification (section 2.3.3) suggested unlike NarGH [1, 2], DmsAB activity was unstable, and activity was lost readily during manipulations.

Stabilization studies (section 2.3.4.) demonstrated glycerol was able to maintain DmsAB activity. Glycerol has been characterized as a good protein stabilizing agent, although how it stabilizes is not completely understood [23]. It has been suggested to encourage protein-protein interactions [12], and mimics conditions of relatively low water activity, making it more difficult for protein to denature, as a structured glycerol-solvent is formed [33]. DmsAB may have evolved to be stable when bound to the membrane anchor DmsC, involving more protein-protein interactions, and less mobile water interactions.

The stability patterns of DmsAB and DmsABC were compared. TMAO stabilizes DmsABC activity, while glycerol stabilizes DmsAB activity, and the reverse was not observed. Loss of DmsAB activity is likely due to denaturation, while loss of DmsABC activity may be via active site instability. It is known that DmsABC loses cofactor during purification (Chapter 3), and TMAO may slow this process. The crystal structures of DMSOR and *R. capsulatus* DMSO reductase indicate a twelve residue peptide appears to form a lid blocking the active site tunnel when substrate is bound. Since DmsA and the aforemetioned DMSO reductases are believed to share a similar polypeptide fold [22, 32], binding of TMAO to DmsA may cause blockage of the active-site tunnel when the analogous peptide in DmsA prevents the loss of moco. Alternatively, binding of substrate (TMAO) may stabilize DmsABC from proteolytic digestion, as addition of protease inhibitors was observed to increase DmsABC stability.

Our initial attempts at purification (section 2.3.3.) employed a heat step. This relies on denaturation of contaminating proteins before the protein of interest. Since DmsAB appears to be highly susceptible to denaturation, this was likely a poor choice. In addition, the ammonium sulfate backwash technique resulted in poor yield and fold purification possibly due to denaturation of protein during repeated resuspension of the pellet, although care was taken to minimize frothing.

The inclusion of high concentrations of glycerol in the buffers to stabilize DmsAB, would decrease the efficiency of purification techniques based on hydrogen bonding or hydrophobic interactions [33]. However, ion exchange, hydroxylapatite, and gel filtration, would be reasonable techniques to pursue. Since ion exchange and hydroxylapatite require binding of protein to matrix, denaturation may occur at this step. This may explain the poor recovery achieved using the former technique (section 2.3.5.). Use of gel filtration or preparative polyacrylamide gels looks very promising, as no binding step is required, but dilution of protein as a result of either of these two techniques could result in protein instability. However, preliminary experiments suggest this will not be the case. Techniques necessitating changes in temperature should probably be avoided, unless DmsAB is stabilized in the presence of glycerol to such an extent that increased temperature no longer affects enzyme stability.

Reconstitution of DmsAB from moco deficient strains was poor. Inactivation of DmsAB during incubation at 37°C likely competes with reconstitution of activity. After 30 minutes of reconstitution, NarGH reconstituted 46 fold better than DmsAB. This occurred although NarGH consisted of a smaller fraction of protein than DmsAB under these growth conditions. DmsAB was overexpressed from a plasmid, and NarGH was not induced, but was only found at basal anaerobic levels. Previous inability to obtain reconstituted DmsAB [34] was likely due to the low level of reconstitution.

DmsC is known to be important in the membrane anchoring of DmsAB, and Q binding [27]. These studies have confirmed an additional role for DmsC, in stabilizing the DmsAB dimer. This is similar to FrdABCD, where the anchor subunits FrdCD stabilize FrdAB [10]. DmsAB activity is easily lost, although it can be maintained in the presence of glycerol. These studies pave the way for any future purification of DmsAB. This has been the first successful attempt at reconstitution of DmsAB from moco deficient strains.

2.5. References

1. Augier, V., Asso, M., Guigliarelli, B., More, C., Bertrand, P., Santini, C.-L., Blasco, F., Chippaux, M. and Giordano, G. (1993) Removal of the high-potential [4Fe-4S] center of the β-subunit from *Escherichia coli* nitrate reductase. Physiological, biochemical, and EPR characterization of site-directed mutated enzymes. Biochem. 32, 5099-5108.

2. Augier, V., Guigliarelli, B., Asso, M., Bertrand, P., Frixon, C., Giordano, G., Chippaux, M. and Blasco, F. (1993) Site directed mutagenesis of conserved cysteine residues within the β-subunit of *Escherichia coli* nitrate reductase. Physiological, biochemical, and EPR characterization of site-directed mutated enzymes. Biochem. 32, 2013-2023.

3. Azoulay, E. and Puig, J. (1969) Reconstitution of enzymatically active particles from inactive soluble elements in *Escherichia coli* K-12. Biochem. Biophys. Res. Comm. 33, 1019-1024.

4. Berks, B.C., Page, D., Richardson, D.J., Reilly, A., Cavill, A., Outen, F. and Ferguson, S.J. (1995) Sequence analysis of subunits of the membrane-bound nitrate reductase from a denitrifying bacterium: the integral membrane subunit provides a prototype for the dihaem electron-carrying arm of a redox loop. Mol. Micro. 15, 319-331.

5. Bilous, P.T. and Weiner, J.H. (1985) Dimethyl sulfoxide reductase activity by anaerobically grown *Escherichia coli*. J. Bacteriol. 162, 1151-1155.

6. Bilous, P.T. and Weiner, J.H. (1988) Molecular cloning and expression of the *Escherichia coli* dimethyl sulfoxide reductase operon. J. Bacteriol. 170, 1511-1518.

7. Boxer, D.H., Low, D.C., Pommier, J. and Giordano, G. (1987) Involvement of a low-molecular-weight substance in *in vitro* activation of the molybdoenzyme respiratory nitrate reductase from a *chl*B mutant of *Escherichia coli*. J. Bact. 169, 4678-4685.

8. Boyer, H.W. and Roulland-Dussoix, D. (1969) A complementary analysis of the restriction and modification of DNA in *Escherichia coli*. J. Mol. Biol. 41, 459.

9. Cammack, R. and Weiner, J.H. (1990) Electron paramagnetic resonance spectroscopic characterization of dimethyl sulfoxide reductase of *Escherichia coli*. Biochemistry 29, 8410-8416.

10. Cole, S.T., Condon, C., Lemire, B.D. and Weiner, J.H. (1985) Molecular biology, biochemistry, and bioenergetics of fumarate reductase, a complex membrane-bound iron-sulfur flavoenzyme of *Escherichia coli*. Biochim. Biophys. Acta 811, 381-403.

11. Cotter, P.A. and Gunsalus, R.P. (1989) Oxygen, nitrate, and molybdenum regulation of *dmsABC* gene expression in *Escherichia coli*. J. Bact. 171, 3817-3823.

12. Dignam, J.D. (1990) Preparation of extracts from higher eukaryotes, in Guide to protein purification. (Deutscher, M.P., ed.), Vol. 182, p. 197, Academic Press, Inc., Toronto.

13. Giordano. G. Personal communication.

14. Giordano, G., Boxer, D.H. and Pommier, J. (1990) Molybdenum cofactor requirement for *in vitro* activation of apo-molybdoenzymes of *Escherichia coli*. Mol. Micro. 4, 645-650.

15. Giordano, G., Medani, C.-L., Boxer, D.H. and Azoulay, E. (1982) Effects of tungstate and molybdate on the *in vitro* reconstitution of nitrate reductase in *Escherichia coli* K-12. FEMS Microbiol. Lett. 13, 317-323.

16. Giordano, G., Saracino, L. and Grillet, L. (1985) Identification in various chlorate-resistance mutants of a protein involved in the activation of nitrate reductase in the soluble fraction of *chlA* mutant of *Escherichia coli* K-12. Biochim. Biophys. Acta 839, 181-190.

17. Iobbi-Nivol, C., Pommier, J., Simala-Grant, J.L., Mejean, V. and Giordano, G. (1996) High substrate specificity and induction characteristics of trimethylamine N-oxide reductase of *Escherichia coli*. Biochim. Biophys. Acta 1294, 77-82.

18. Kadner, R.J. (1996) Cytoplasmic membrane. in *Escherichia coli* and *Salmonella* cellular and molecular biology. (Neidhardt, F.C., ed.), Vol. 1, p. 58-87, ASM Press, Washington.

19. Laemmli, U.K. (1970) Cleavage of structural proteins during the assembly of the head of bacteriophage T4. Nature 227, 680-685.

20. Lemire, B.D., Robinson, J.J. and Weiner, J.H. (1982) Identification of membrane anchor polypeptides of *Escherichia coli* fumarate reductase. J. Bacteriol. 152, 1126-1131.

21. Markwell, M.A.D., Haas, S.M., Bieber, L.L. and Tolbert, N.E. (1978) A modification of the Lowry procedure to simplify protein determination in membrane and lipoprotein samples. Anal. Biochem. 87, 206-210.

22. McAlpine, A.S., McEwan, A.G. and Bailey, S. (1998) The high resolution crystal structure of DMSO reductase in complex with DMSO. J. Mol. Biol. In press.

23. Neugebauer, J.M. (1990) Detergents : An overview, in Guide to protein purification. Methods in Enzymology, (Deutscher, M.P., ed.), Vol. 182, First ed., p. 258, Academic Press, Inc., Toronto.

24. Palmer, T., Santini, C.-L., Iobbi-Nivol, C., Eaves, D., Boxer, D.H. and Giordano, G. (1996) Involvement of the *narJ* and *mob* gene products in distinct steps in the biosynthesis of the molybdoenzyme nitrate reductase in *Escherichia coli*. Mol. Micro. 20, 875-884.

25. Rothery, R.A. and Weiner, J.H. (1991) Alteration of the iron-sulfur cluster composition of *Escherichia coli* dimethyl sulfoxide reductase by site-specific mutagenesis. Biochemistry 30, 8296-8305.

26. Rothery, R.A. and Weiner, J.H. (1996) Interaction of an engineered [3Fe-4S] cluster with a menaquinol binding site of *Escherichia coli*. Biochem. 35, 3247-3257.

27. Sambasivarao, D., Scraba, D.G., Trieber, C. and Weiner, J.H. (1990) Organization of dimethyl sulfoxide reductase in the plasma membrane of *Escherichia coli*. J. Bacteriol 172, 5938-5948.

28. Sambasivarao, D. and Weiner, J.H. (1991) Differentiation of the multiple S- and N-oxide reducing activities of *Escherichia coli*. Curr. Microbiol. 23, 105-110.

29. Sambasivarao, D. and Weiner, J.H. (1991) Dimethylsulfoxide reductase of *Escherichia coli* : an investigation of function and assembly by use of *in vivo* complementation. J. Bacteriol. 173, 5935-5943.

30. Sambrook, J., Fritsch, E.F. and Maniatis, T. (1989) Molecular cloning : A laboratory manual. Cold Spring Harbor Laboratory Press, Cold Spring Harbor, N.Y.

31. Santini, C.-L., Iobbi-Nivol, C., Romane, C., Boxer, D.H. and Giordano, G. (1992) Molybdoenzyme biosynthesis in *Escherichia coli*: *In vitro* activation of purified nitrate reductase from a *chlB* mutant. J. Bact. 174, 7934-7940.

32. Schindelin, H., Kisher, C., Hilton, J., Rajagopalan, K.V. and Rees, D.C. (1996) Crystal structure of DMSO reductase: Redox-linked changes in molybdopterin coordination. Science 272, 1615-1621.

33. Scopes, R.K. (1987) Maintenance of active enzymes, in Protein purification principles and practice. (Cantor, C.R., ed.), Vol. 1, 2nd ed., p. 251-252, Springer-Verlag, New York.

34. Silvestro, A., Pommier, J. and Giordano, G. (1986) Molybdenum cofactor: a component in the *in vitro* activation of both nitrate reductase and trimethylamine-N-oxide reductase activities in *Escherichia coli* K12. Biochim. Biophys. Acta 872, 243-252.

35. Stewart, V. (1988) Nitrate respiration in relation to facultative metabolism in enterobacteria. Microbiol. Rev. 52, 190-232.

36. Stewart, V. and MacGregor. (1982) Nitrate reductase in *Escherichia coli* K-12: Involvement of *chl*C, *chl*E, and *chl*G loci. J. Bacteriol. 151, 788-799.

37. Stoll, J.S. and Blanchard, J.S. (1990) Buffers : principles and practice, in Guide to protein purification. (Deutscher, M.P., ed.), Vol. 182, p. 26, Academic Press, Inc., Toronto.

38. Trieber, C.A., Rothery, R.A. and Weiner, J.H. (1994) Multiple pathways of electron transfer in dimethyl sulfoxide reductase of *Escherichia coli*. J. Biol. Chem. 269, 7103-7109.

39. Weiner, J.H., MacIsacc, D.P., Bishop, R.E. and Bilous, P.T. (1988) Purification and properties of *Escherichia coli* dimethyl

sulfoxide reductase, an iron-sulfur molybdoenzyme with broad substrate specificity. J. Bacteriol. 170, 1505-1510.

40. Weiner, J.H., Rothery, R.A., Sambasivarao, D. and Trieber, C.A. (1992) Molecular analysis of dimethylsulfoxide reductase : a complex iron-sulfur molybdoenzyme of *Escherichia coli*. Biochim. Biophys. Acta 1102, 1-18.

41. Wootton, J.C., Nicolson, R.E., Cock, J.M., Walters, D.E., Burke, J.F., Doyle, W.A. and Bray, R.C. (1991) Enzymes depending on the pterin molybdenum cofactor : sequence families, spectroscopic properties of molybdenum and possible cofactor-binding domains. Biochim. Biophys. Acta 1057, 157-185.

Chapter 3 : Structural Characterization and Quantitation of the Moco in Purified DmsA*

3.1. Introduction

Mo has been selected by nature for use in two cofactors [7, 12]. The first, the multinuclear M center, contains both Fe and Mo, and catalyzes the conversion of N_2 to ammonia by nitrogenase [6, 14]. The second Mo containing cofactor is the pterin containing moco utilized by all other molybdoenzymes [20, 34] (Figure 1.4.).

Moco is highly O_2 labile, and as a result its structure was originally extrapolated from the structural characterization of a number of stable oxidized derivatives [15, 16, 18, 21].

It was thought the structure of moco was identical for all moco containing enzymes (Figure 1.4. A.). However, it became apparent that moco from some prokaryotic enzymes had a higher molecular weight than expected [22-24]. Eventually, it was demonstrated that in addition to the original structure for moco - MPT, a nucleotide (GMP, CMP, AMP, IMP) was sometimes appended in a pyrophosphate linkage to MPT, resulting in a variety of moco derivatives (Figure 1.4. B.) [3, 15,

---

* A version of this chapter has been published. Rothery, R. A., Simala-Grant, J. L., Johnson, J. L., Rajagopalan, K. V., and Weiner, J. H. (1995) Association of molybdopterin guanine dinucleotide with *Escherichia coli* dimethyl sulfoxide reductase: Effect of tungstate and a *mob* mutation. J. Bact. 177, 2057-2063. This chapter includes Figure 1 from this paper (now Figure 3.3.), as well as other previously unpublished data. Results from this paper obtained by Richard Rothery, and discussion relating to this data, is not included in this chapter. DMSOR used for the control was supplied by Drs. Johnson and Rajagopalan.

19]. It is not known whether all enzymes within an organism possess the same moco derivative.

Recently the crystallization of several molybdoenzymes has confirmed a variety of moco structures, revealing one more level of complexity. The Mo can be coordinated by two MPT's or MPT dinucleotide derivatives - bis-moco (Figure 1.4. C.) [5, 9, 27, 31, 32].

In 1991, it was shown that the final step in moco biosynthesis in *E. coli,* was the addition of GMP to MPT, to form MGD (Figure 1.5.) [17]. Earlier studies indicated that the locus responsible for this reaction was required for DmsABC function, suggesting MGD was the form of moco present in this enzyme [2].

The form of moco in DmsABC was determined using purified enzyme. Moco from DmsABC was converted to two stable oxidized derivatives, and these derivatives were analyzed by absorption and fluorescence spectroscopy. The amount of moco in purified DmsABC, was quantitated to determine whether purified DmsABC contained stoichiometric amounts of moco.

3.2. Materials and Methods

3.2.1. Materials

All materials were of reagent grade and were purchased from commercial sources.

3.2.2. Strains and Plasmids

E. coli strains HB101 (*supE*44 *hsdS*20($r_B^- m_B^-$) *recA*13 *ara*-14 *procA*2 *lacY*1 [4]) and RK5208 (F- *ara*D139 *lac*U169 *gyr*A *thi* *rps*L *mob*207::Mu *cys* [35]), and plasmid pDMS160 (pBR322 Amp^R (*dmsABC*)$^+$ [29]) were used in this study. Strains were transformed with pDMS160, for overexpression of DmsABC. RK5208 bears a mutation in the biosynthetic pathway for moco and so can be used as a negative control. All manipulations of plasmids and strains were carried out essentially as described by Sambrook *et al.* [30].

3.2.3. Media and Growth Conditions

Strains were grown aerobically in LB or Terrific Broth [30] overnight, and these cultures were used as 1% inocula for Gly/Fum minimal media [2]. Bacteria were grown anaerobically on minimal media for 48 hours at 37°C for HB101, and 30°C for RK5208 as indicated previously [2], with the following exceptions. 0.16% peptone was substituted for casamino acids, and streptomycin sulfate was not included in the growth medium. Proline, leucine and vitamin B1, were included at a final concentration of 0.005%. 50-100 μg/mL ampicillin was included in the growth medium.

3.2.4. Purification of DmsABC

HB101/pDMS160 was grown at 37°C, for 48 hours, in 19 L carboys, on Gly/Fum medium. Cells were harvested using a Pellicon membrane system equipped with a Millipore polysulfone PTNK filter. The concentrated cell mixture was then centrifuged at 9,500 x g for 10 minutes, and subsequently resuspended in buffer [29]. Everted vesicles were prepared [2], and membrane fractions were extracted twice with C12E8 [8]. DmsABC was purified from solubilized membrane proteins on a DEAE-cellulose (Whatman DE-52) column as indicated previously [36]. Purified DmsABC was desalted on a G-25 Sephadex column.

3.2.5. Purification of DMSOR

DMSOR was purified using a published procedure [1]. Briefly, DMSO reductase in the supernatant fraction, from broken cells, was purified by ammonium sulfate precipitation, and on DEAE-Sepharose CL-4B fast flow, Superose-12 fast protein liquid chromatography (FPLC), and hydroxylapatite columns.

3.2.6. Identification of Moco Structure

Moco from HB101 and RK5208 membranes overexpressed for DmsABC, were converted to FormA derivative to confirm moco content [16].

Moco from purified DmsABC was oxidized to carboxyamidomethyl (cam) and gentle-FormA derivatives, and analyzed as indicated previously [15, 17]. Fluorescence and absorption spectra were compared to standard spectra of cam-MPT-GMP, FormA-GMP, cam-MPT, Form A, and GMP [15].

3.2.7. Quantitation of MPT in DmsABC

Moco, from equivalent amounts of DmsABC and DMSOR, was converted to FormA derivative and quantitated by fluorescence [16].

3.2.8. Analytical Techniques

Protein concentrations were determined by the method of Markwell et al. [25].

3.3. Results

3.3.1. Identification of Moco Structure in DmsABC

HB101/pDMS160 membranes overexpressed for DmsABC were shown to possess moco by conversion to the fluorescent FormA derivative (Figure 3.1.). Membranes from RK5208/pDMS160, a strain blocked at the last step of moco biosynthesis, showed no FormA (Figure 3.1.).

DmsABC was purified from HB101/pDMS160 using the non-fluorescent detergent C12E8 to facilitate analysis. Since moco is highly O_2 labile, moco from purified DmsABC was oxidized to two stable oxidized derivatives- gentle-FormA and cam. The gentle-FormA and

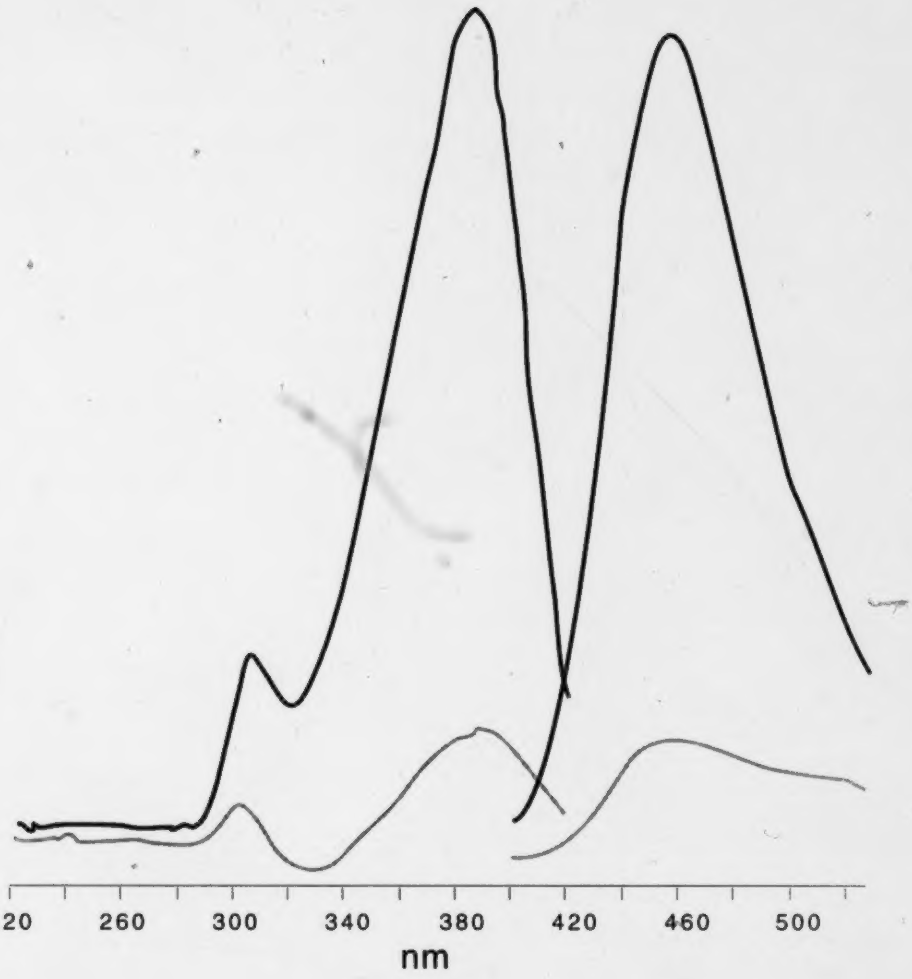

Figure 3.1.

Fluorescence Excitation and Emission Spectra of FormA from HB101/pDMS160 (top) and RK5208/pDMS160 (bottom) Membranes

Fluoresence was measured in 1 M NaOH. RK5208 is a mutant in the biosynthetic pathway of moco.

cam oxidations [15, 17] avoid the boiling step employed in the FormA assay [16], allowing the pyrophosphate bond to remain intact.

Oxidized dinucleotide moco derivatives showed lower than expected fluorescence, since the appended nucleotide quenches the pterin fluorescence [17]. The gentle-FormA derivative from DmsABC showed a 10-fold increase in fluorescence (excitation 380 nm emission 450 nm),after treatment with nucleotide pyrophosphatase to cleave appended nucleotide from pterin [17]. This indicates MPT is linked in a pyrophosphate linkage to a nucleotide in DmsABC.

To determine the identity of the nucleotide attached to MPT in DmsABC, optical spectroscopy was performed on the two stable oxidized derivatives of moco. The cam derivative showed UV absorption maxima of 250, 277, and 370 nm (Figure 3.2.), and the gentle-FormA derivative showed absorption maxima of 255, 295, and 370 nm (Figure 3.3.). The absorption maximum at 250-255 nm is characteristic of GMP attached to MPT [15]. The absorption spectra of the cam and gentle FormA derivatives matched standards for cam-MPT-GMP, and FormA-GMP.

The cam and gentle-FormA derivatives were subsequently cleaved with nucleotide pyrophosphatase. Cam-MPT and FormA could be separated from GMP by HPLC, and characterized by absorption spectroscopy. The cam derivative showed maxima at 245, 290 and 370 nm, while the FormA derivative showed absorption maxima at 305 and 360. GMP showed an absorption maxima 255 nm. The spectra all overlapped well with standard library spectra for cam-MPT, FormA, and GMP respectively (data not shown).

These data all indicated DmsABC possesses moco with GMP appended to MPT (MGD).

3.3.2 Quantitation of MPT in DmsABC

The amount of MGD per mole of DmsA was quantitated by extracting FormA from equivalent amounts of DmsABC and DMSOR.

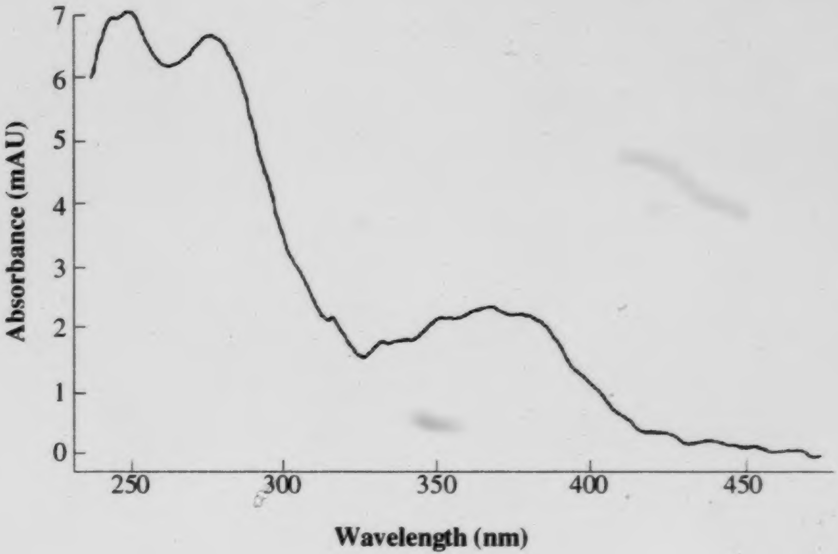

Figure 3.2.

Absorption Spectra of Oxidized Cam Derivative Prepared from Purified DmsABC in 50 mM Ammonium Acetate (pH 6.8)

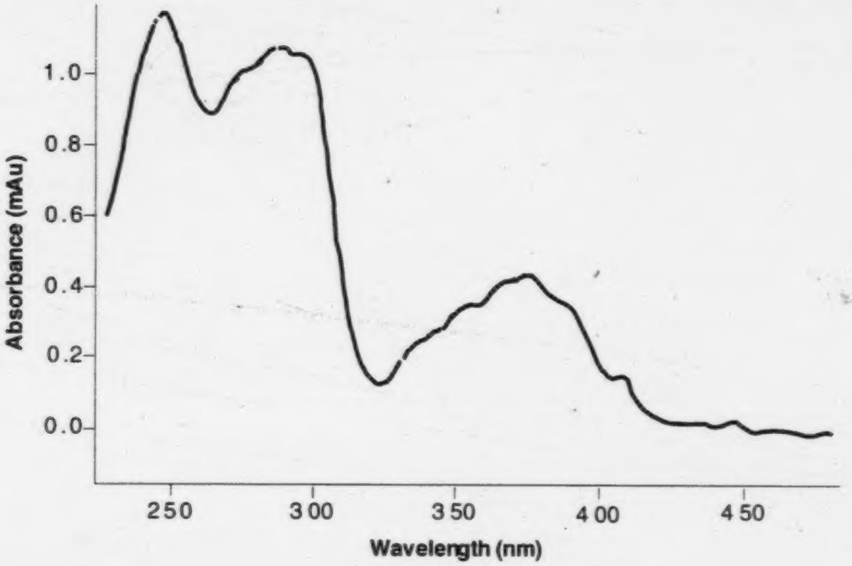

Figure 3.3.

Absorption Spectra of Gentle-FormA Derivative from Purified DmsABC in 50 mM Ammonium Acetate (pH 6.8)

On a molar basis, purified DmsABC contained only 22% of MGD found in purified DMSOR (Table 3.1.).

3.4. Discussion

We have shown MGD is the moco derivative found in DmsABC. This is in agreement with earlier results showing DmsABC is not functional in a strain deficient in the attachment of GMP to MPT [2]. MGD is also found in the soluble, periplasmic DMSOR [15]. Our results, as well as unpublished results [26] indicating NarGHI binds MGD, suggests all *E. coli* enzymes may utilize the same moco derivative.

Purified DMSO reductase from *R. capsulatus* has 80% occupancy by MGD [33] while in DMSOR, 0.93 moles of Mo were found per mol of purified enzyme [13]. Purified DmsABC contains approximately 22% of the MGD found in DMSOR. Taking into consideration the MGD content in DMSOR, occupancy in DmsA increases slightly to 23.5%. This quantitation of MGD compares fairly well with atomic emission spectrometry measurements of the concentration of Mo present in purified preparations (0.34 moles of Mo per mole of DmsABC) [36]. It appears that a major proportion of moco may either be dissociating, or being oxidatively destroyed during DmsABC purification.

DMSOR has two MGD's per Mo (bis-MGD) [31]. The similar quantitation of Mo as determined by atomic emission spectrometry, and moco in DmsABC as determined by a comparison with the MGD content in DMSOR was observed. This suggests DmsA also binds bis-MGD. This could be unequivocally determined by quantitation of phosphate and GMP in comparison to Mo [33]. However, as indicated above, since MGD is lost during purification, quantitation experiments would be better performed after development of a new purification scheme that maintained stoichiometric amounts of cofactor.

Table 3.1.

FormA Fluorescence from Equivalent Amounts of DmsABC and DMSOR

	Arbitrary Fluorescence Units			
Sample	**Emission Max 450 nm pH 6.9**	**%**	**Emission Max 456 nm pH 10.0**	**%**
DmsABC	4.3	21.4	7.8	22.0
DMSOR	20.1	100	35.4	100

An excitation wavelength of 380 nm was used to measure FormA fluorescence in 1 M NaOH. % is of arbitrary fluorescence units for DMSOR.

Mass spectroscopy and EPR demonstrate the Mo concentration in membranes from cells overexpressing DmsABC, is stoichiometric with the concentration of enzyme [28]. This indicates the biosynthetic pathway for moco is able to handle overexpression of DmsABC, membrane bound DmsA is fully occupied with MGD, and DmsA loses moco during purification.

Two uncertainties remain in the structure of moco in DmsA : Mo ligation, and pterin redox state. In the absence of an X-ray crystal structure, extended-xray-absorption-fine-structure [11], and reduction of electron acceptors by moco [10, 33] could be performed, to answer these questions. Our results suggest DmsABC binds MGD, which is likely the case for all *E. coli* enzymes.

3.5. References

1. Bastian, N.R., Kay, C.J., Barber, M.J. and Rajagopalan, K.V. (1991) Spectroscopic studies of the molybdenum-containing dimethyl sulfoxide reductase from *Rhodobacter sphaeroides*. J. Biol. Chem. 266, 45-51.

2. Bilous, P.T. and Weiner, J.H. (1985) Dimethyl sulfoxide reductase activity by anaerobically grown *Escherichia coli*. J. Bacteriol. 162, 1151-1155.

3. Borner, G., Karrasch, M. and Thauer, R.K. (1991) Molybdopterin adenine dinucleotide and molybdopterin hypoxanthine dinucleotide in formylmethanofuran dehydrogenase from *Methanobacterium thermoautotrophicum* (Marbug). FEBS 290, 31-34.

4. Boyer, H.W. and Roulland-Dussoix, D. (1969) A complementary analysis of the restriction and modification of DNA in *Escherichia coli*. J. Mol. Biol. 41, 459.

5. Boyington, J.C., Gladyshev, V.N., Khangulov, S.V., Stadtman, T.C. and Sun, P.D. (1997) Crystal structure of formate

dehydrogenase H: catalysis involving Mo, molybdopterin, selenocysteine, and Fe_4S_4 cluster. Science 275, 1305-1308.

6. Burgess, B.K. and Lowe, D.J. (1996) Mechanism of molybdenum nitrogenase. Chem. Rev. 96, 2983-3011.

7. Burgmayer, S.J.N. and Stiefel, E.I. (1985) Molybdenum enzymes, cofactors, and model systems. The chemical uniqueness of molybdenum. J. Chem. Ed. 62, 943-953.

8. Cammack, R. and Weiner, J.H. (1990) Electron paramagnetic resonance spectroscopic characterization of dimethyl sulfoxide reductase of *Escherichia coli*. Biochemistry 29, 8410-8416.

9. Chan, M.K., Mukund, S., Kletzin, A., Adams, M.W.W. and Rees, D.C. (1995) Structure of a hyperthermophilic tungstopterin enzyme, aldehyde ferredoxin oxidoreductase. Science 267, 1463-1469.

10. Gardlik, S. and Rajagopalan, K.V. (1991) Oxidation of molybdopterin in sulfite oxidase by ferricyanide. J. Biol. Chem. 266, 4889-4895.

11. George, G.N., Hilton, J. and Rajagopalan, K.V. (1996) X-ray absorption spectroscopy of dimethyl sulfoxide reductase from *Rhodobacter sphaeroides*. J. Am. Chem. Soc. 118, 1113-1117.

12. Hille, R. (1996) The mononuclear molybdenum enzymes. Chem. Rev. 96, 2757-2816.

13. Hilton, J.C. and Rajagopalan, K.V. (1996) Identification of the molybdenum cofactor of dimethyl sulfoxide reductase from *Rhodobacter sphaeroides* f. sp. *denitrificans* as bis(molybdopterin guanine dinucleotide)molybdenum. Arch. Biochem. Biophys. 325, 139-143.

14. Howard, J.B. and Rees, D.C. (1996) Structural basis of biological nitrogen fixation. Chem. Rev. 96, 2965-2982.

15. Johnson, J.L., Bastian, N.R. and Rajagopalan, K.V. (1990) Molybdopterin guanine dinucleotide: A modified form of molybdopterin identified in the molybdopterin cofactor of dimethyl sulfoxide reductase from *Rhodobacter sphaeroides* forma specialis *denitrificans*. Proc. Natl. Acad. Sci. 87, 3190-3194.

16. Johnson, J.L., Hainline, B.E., Rajagopalan, K.V. and Arison, B.H. (1984) The pterin component of the molybdenum cofactor.

Structural characterization of two fluorescent derivatives. J. Biol. Chem. 259, 5414-5422.

17. Johnson, J.L., Indermaur, L.W. and Rajagopalan, K.V. (1991) Molybdenum cofactor biosynthesis in *Escherichia coli*. Requirement of the *chlB* gene product for the formation of molybdopterin guanine dinucleotide. J. Biol. Chem. 266, 12140-12145.

18. Johnson, J.L. and Rajagopalan, K.V. (1982) Structural and metabolic relationship between the molybdenum cofactor and urothione. Proc. Natl. Acad. Sci. USA , 6856-6860.

19. Johnson, J.L., Rajagopalan, K.V. and Meyer, O. (1990) Isolation and characterization of a second molybdopterin dinucleotide molybdopterin cytosine dinucleotide. Arch. Biochem. Biophys. 283, 542-545.

20. Kim, J. and Rees, D.C. (1992) Crystallographic structure and functional implications of the nitrogenase molybdenum-iron protein from *Azotobacter vinelandii*. Nature 360, 553-560.

21. Kramer, S.P., Johnson, J.L., Ribeiro, A.A., Millington, D.S. and Rajagopalan, K.V. (1987) The structure of the molybdenum cofactor. Characterization of di-(carboxamidomethyl)molybdopterin from sulfite oxidase and xanthine oxidase. J. Biol. Chem. 262, 16357-16363.

22. Kruger, B. and Meyer, O. (1986) The pterin (bactopterin) of carbon monoxide dehydrogenase from *Pseudomonas carboxydoflava*. Eur. J. Biochem. 157, 121-128.

23. Kruger, B. and Meyer, O. (1987) Structural elements of bactopterin from *Pseudomonas carboxydoflava* carbon monoxide dehydrogenase. Biochim. Biophys. Acta 912, 357-364.

24. Kruger, B., Meyer, O., Nagel, M., Andreesen, J.R., Meincke, M., Bock, E., Blumle, S. and Zumft, W.G. (1987) Evidence for the presence of bactopterin in eubacterial molybdoenzymes nicotinic acid dehydrogenase, nitrite oxidoreductase, and respiratory nitrate reductase. FEMS Microbiol. Lett. 48, 225-227.

25. Markwell, M.A.D., Haas, S.M., Bieber, L.L. and Tolbert, N.E. (1978) A modification of the Lowry procedure to simplify protein determination in membrane and lipoprotein samples. Anal. Biochem. 87, 206-210.

26. Rajagopalan, K.V. and Johnson, J.L. (1992) The pterin molybdenum cofactors. J. Biol. Chem. 267, 10199-10202.

27. Romao, M.J., Chan, M.K., Mukund, S., Kletzin, A., Adams, M.W.W. and Rees, D.C. (1995) Crystal structure of the xanthine oxidase-related aldehyde oxido-reductase from *D. gigas*. Science 270, 1170-1176.

28. Rothery, R.A. and Weiner, J.A. Unpublished results.

29. Rothery, R.A. and Weiner, J.H. (1991) Alteration of the iron-sulfur cluster composition of *Escherichia coli* dimethyl sulfoxide reductase by site-specific mutagenesis. Biochemistry 30, 8296-8305.

30. Sambrook, J., Fritsch, E.F. and Maniatis, T. (1989) Molecular cloning : A laboratory manual. Cold Spring Harbor Laboratory Press, Cold Spring Harbor, N.Y.

31. Schindelin, H., Kisher, C., Hilton, J., Rajagopalan, K.V. and Rees, D.C. (1996) Crystal structure of DMSO reductase: Redox-linked changes in molybdopterin coordination. Science 272, 1615-1621.

32. Schneider, F., Lowe, J., Huber, R., Schindelin, H., Kisker, C. and Knablein, J. (1996) Crystal structure of dimethyl sulfoxide reductase from *Rhodobacter capsulatus* at 1.88 A resolution. J. Mol. Biol. 263, 53-69.

33. Solomon, P.S., Lane, I., Hanson, G. and McEwan, A.G. (1997) Characterisation of the pterin molybdenum cofactor in dimethylsulfoxide reductase of *Rhodobacter capsulatus*. Eur. J. Biochem. 246, 200-203.

34. Stewart, V. (1988) Nitrate respiration in relation to facultative metabolism in enterobacteria. Microbiol. Rev. 52, 190-232.

35. Stewart, V. and MacGregor. (1982) Nitrate reductase in *Escherichia coli* K-12: Involvement of *chl*C, *chl*E, and *chl*G loci. J. Bacteriol. 151, 788-799.

36. Weiner, J.H., MacIsacc, D.P., Bishop, R.E. and Bilous, P.T. (1988) Purification and properties of *Escherichia coli* dimethyl sulfoxide reductase, an iron-sulfur molybdoenzyme with broad substrate specificity. J. Bacteriol. 170, 1505-1510.

Chapter 4 : Mutation of the DmsA Leader Sequence and Analysis by Growth, Accumulation, and Expression Studies*

4.1. Introduction

Proteins destined to the periplasm in Gram negative bacteria possess an N-terminal leader sequence that directs translocation via the Sec-system [17]. Leader sequences are 18-26 amino acids long, and have amino acid biases, but no homology or conserved motifs [2]. Rather, they are characterized by a positively charged N-terminus (N), followed by a hydrophobic core (H), and hydrophilic carboxy-terminal cleavage site possessing small amino acids at the $^-1$ and $^-3$ positions to the site of cleavage (C). The leader sequence is generally cleaved in the periplasm by leader peptidase I [7, 18, 42].

The amino terminal sequence of purified DmsA, as determined by Edman degradation, begins with the sequence Val, Asp, Ser. These amino acids align downstream from a potential translational start site sixteen residues upstream. This suggests the nascent polypeptide is proteolytically cleaved [3]. This sixteen-residue peptide shares properties characteristic of leader sequences [7, 18, 42], and initially suggested DmsA may be localized to the periplasm.

---

* Site-directed mutagenesis, quantitative growth experiments, and Western blots of constructs using the native promoter were performed by Joanne Simala-Grant. Some subcloning was performed by Gillian Shaw. Raymond Turner also performed subcloning, qualitative growth experiments, and expression studies using the T7 and *tac* promoters.

A version of this chapter is being prepared for submission. Simala-Grant, J. L., Turner, R. J., and J. H. Weiner Analysis of the leader sequence of DmsA *E. coli* dimethyl sulfoxide reductase.

Many studies were carried out to determine the intracellular localization of DmsA and DmsB using a variety of biochemical, immunological, and electron microscopic techniques [27]. The sum of the evidence indicated DmsAB was located on the cytoplasmic face of the membrane [27], while DmsC provides anchoring of the dimer to the membrane (Chapter 2, [29]). Independent studies using DyEDTA and EPR [24], and examination of β-lactamase fusions in DmsA and DmsB [45], also confirmed their cytoplasmic orientation.

Based on the above studies, it was postulated that the DmsA "leader" was an evolutionary vestige [3], since other related and soluble S- and N-oxide reductases are known to be periplasmically localized [6, 9, 32, 33]. Cleavage of the sixteen residue leader may have resulted from proteolysis during cell lysis or purification [3]. Only recently have inhibitors for leader peptidase I been found [7], thus it was not possible to use protease inhibitors during cell lysis to prevent cleavage of the leader from DmsA.

Many periplasmic proteins participate in oxidative-reduction reactions and require electron transfer cofactors such as flavin, moco, Fe-S clusters, Ni-Fe complexes, and tryptophan tryptophylquinone. Recently Berks found that most of these redox proteins have long (~58) amino acid leaders. These leaders have the consensus motif (S/T)-R-R-X-F-L-K [2]. It was hypothesized that proteins with this "double-arginine" leader assemble in the cytoplasm, and then the fully folded cofactor containing proteins are translocated to the periplasm through an export mechanism distinct from the Sec-system [2]. Evidence suggests at least two double-arginine containing proteins bind cofactor prior to translocation of the fully folded protein [21, 31], and translocation appears to be dependent on the pmf but not on Sec-proteins [31].

Interestingly it was found that DmsA has a double-arginine leader if translation began at a Met residue located 29 amino acids upstream ($M^{-}29$) from the originally proposed initiating residue (M1) (Figure 4.1.). It is worth noting that the membrane topology of many proteins with double-arginine leaders, including several membrane-bound proteins including FdoGHI [1] and *Wolinella succinogenes* polysulfide reductase, has not been experimentally demonstrated [2]. As a result, like DmsAB, they may also face the cytoplasm.

In this chapter the two potential initiating Met's were examined and translation was demonstrated to begin at $M^{-}29$. The leader, and specifically the double-arginine consensus, were observed to be essential for production of functional DmsABC under anaerobic conditions. The growth properties, accumulation, and expression of several site-directed mutants, as well as constructs allowing translation initiation at alternate Met's are described. A model, including ideas originally proposed by Berks [2], is given to explain the role of the double-arginine leader in membrane targeting and translocation.

4.2. Materials and Methods

4.2.1. Materials

Oligonucleotides were purchased from the Biochemistry DNA Core facility at the University of Alberta. Restriction endonucleases and modifying enzymes were obtained from Life Technologies Inc., and the Sculptor™ *in vitro* mutagenesis kit was obtained from Amersham Corp. All other materials were reagent grade, and were obtained from commercial sources.

4.2.2. Strains and Plasmids

E. coli strains and plasmids used in this study, are described in Tables 4.1. and 4.2. TG1 was used for routine DNA manipulation and

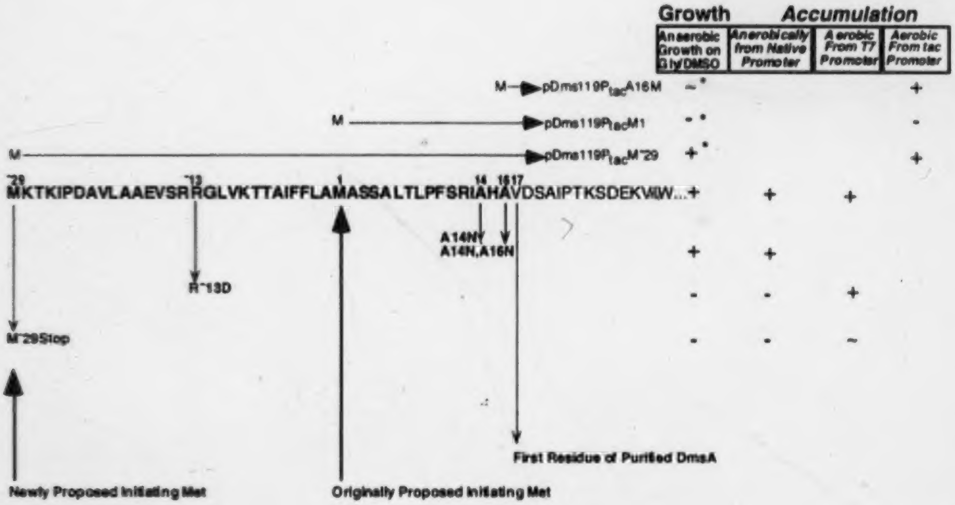
Growth
Accumulation
Anaerobic Growth on Gly/DMSO
Anerobically from Native Promoter
Aerobic From T7 Promoter
Aerobic From tac Promoter
M
pDms119P$_{tac}$A16M
~*
+
M
pDms119P$_{tac}$M1
-*
-
M
pDms119P$_{tac}$M^{-}29
+*
+
$^{-}$29
$^{-}$13
1
14
16
17
MKTKIPDAVLAAEVSRRGLVKTTAIFFLAMASSALTLPFSRIAHAVDSAIPTKSDEKVIW...
+
+
+
A14N
A14N,A16N
+
+
R^{-}13D
-
-
+
M^{-}29Stop
-
-
~
First Residue of Purified DmsA
Newly Proposed Initiating Met
Originally Proposed Initiating Met

Figure 4.1.

Schematic of the DmsA Leader Sequence

Growth and Accumulation Data for Leader Sequence Mutants and *tac* Constructs

Numbering of the DmsA leader is as previously published [3, 44]. Important residues are numbered, and indicated with an arrow. The originally proposed translational start site (M1) [3] and newly proposed translational start site (M^{-}29) are indicated [2], as well as the N-terminal amino acid (V17) from purified DmsABC as determined by Edman degradation [3].

Four leader sequence mutants were created, M^{-}29Stop, R^{-}13D, A14N, and A14N,A16N. Additionally, three DmsABC constructs were made that allow expression from the *tac* promoter from three alternate Met's, M^{-}29, M1 and M16. M16 was inserted prior to V17 for this construct.

Anaerobic growth and anaerobic accumulation experiments were performed in DSS301 a strain bearing a deletion for the *dmsABC* operon. The * indicates isopropyl β-D-thiogalactopyranoside (IPTG) was added to the media to induce expression from the *tac* promoter. Aerobic accumulation of DmsA and DmsB was determined under anaerobic conditions from the natural promoter, aerobically from the T7 promoter by heat induction, and the *tac* promoter by IPTG induction. Aerobic expression from the T7 and *tac* promoters was done in K38 and HB101, respectively. - indicates no growth, accumulation, or expression, + indicates growth, accumulation or expression, and the ~ indicates trace growth, or poor expression and subsequent degradation.

Table 4.1.

E. coli Strains Used in this Study

Strains	**Description**	**Source**
Strains		
TG1	*supE*44 *hsdS*20($r_B^-m_B^-$) *recA*13 *ara*-14 *proA*2 *lacY*1 *gal*K2 *rpsL*20*xyl*-5 *mtl*-1	Amersham
HB101	*supE*44 *hsdS*20($r_B^-m_B^-$) *recA*13 *ara*-14 *procA*2 *lacY*1	[5]
DSS301	TG1 *ΔdmsABC*	[28]
K38	HfrC *pho*A4 *pit*-10 *ton*A22 *omp*F267 *rel*A1	[26]

Table 4.2.

Plasmids and Phage Used in this Study

Plasmids or Phage	Description	Source
Plasmids		
pTZ18R	Amp^R *lacZ'*	Pharmacia
pBR322	Tet ^{R} Amp^R	Pharmacia
pGP1-2	Kan^R cI$_{857}$ T7 RNA polymerase under λP2	S. Tabor
pDMS223	pTZ18R Amp^R *lacZ'* (*dmsABC*)$^+$	[23]
pDMS223M$^-$29Stop	pTZ18R Amp^R (*dmsA*M$^-$29→Stop) (*dmsBC*)$^+$	This study.
pDMS223R$^-$13D	pTZ18R Amp^R (*dmsA*R$^-$13→D) (*dmsBC*)$^+$	This study.
pDMS223M$^-$29	pTZ18R Amp^R Δpromoter (M$^-$29*dmsA*) (*dmsBC*) $^+$	This study.
pDMS223M1	pTZ18R Amp^R Δpromoter (*dmsA*ΔM$^-$29→A$^-$1) (*dmsBC*)$^+$	This study.
pDMS223A16M	pTZ18R Amp^R) Δpromoter (*dmsA*A16→M) (*dmsBC*)$^+$	This study.
pDMS160	pBR322 Amp^R (*dmsABC*)$^+$	[23]
pDMS170	pBR322 Amp^R (*dmsABC*)$^+$	[34]
pDMS160A14N	pBR322 Amp^R (*dmsA*A14→N) (*dmsBC*)$^+$	This study.
pDMS160A14N,A16N	pBR322 Amp^R (*dmsA*A14→N,A16→N) (*dmsBC*)$^+$	This study.
pDMS160M$^-$29Stop	pBR322 Amp^R (*dmsA*M$^-$29→Stop) (*dmsBC*)$^+$	This study.
pDMS160R$^-$13D	pBR322 Amp^R (*dmsA*R$^-$13→D) (*dmsBC*)$^+$	This study.
pMS119EH	lacI$_Q$ P$_{tac}$ Amp^R	[35]
pDMS119P$_{tac}$M$^-$29	pMS119EH Amp^R P$_{tac}$M-29 (*dmsABC*)$^+$	This study.
pDMS119P$_{tac}$M1	pMS119EH Amp^R P$_{tac}$ M1 (*dmsA*ΔM$^-$29→A$^-$1) (*dmsBC*)$^+$	This study.
pDMS119P$_{tac}$A16M	pMS119EH Amp^R P$_{tac}$A16 (*dmsA*ΔM$^-$29→A16 A16→M) (*dmsBC*)$^+$	This study.
Phage		
M13K07	Kan^R	Pharmacia

growth inhibition studies, DSS301 for plasmid overexpression of wild-type and mutant DmsABC in a *ΔdmsABC* background, K38 for T7 expression, and DSS301 and HB101 for *tac* expression studies. pDMS160 and pDMS170 are equivalent plasmids used for overexpression of DmsABC.

4.2.3. Analysis of the DmsA Upstream Region for Leader Peptidase I Cleavage Sites

The upstream translated region of DmsA with altered residues, was submitted for analysis of potential leader peptidase I cleavage sites at the Center for Biological Analysis home page (http://www.cbs.dtu.dk/) [18]

4.2.4. Site-directed Mutagenesis of the DmsA Leader Sequence

All manipulations of plasmids and strains were carried out essentially as described by Sambrook *et al.* [30]. The mutants were generated by site-directed mutagenesis of single stranded pDMS223 [23], using the Sculptor^{TM} kit (Amersham), and mutagenic primers. The following primers were used for site-directed mutagenesis to generate the following mutants : 5'GTGAGCCATTTAAAAAACGAAAATCC3', M^{-}29Stop; 5'GGTGAGTCGCGATGGTTTGGTAAAAAC3', R^{-}13D and 5'TTAGTCGGATTAATCACAATGTCGATAGCG3', A14N and the double mutant A14N,A16N. Mutant DNA was subcloned into pDMS160 using *Bgl*II and *Eco*RI, and resequenced to confirm the mutation.

4.2.5. PCR of DmsA and Subsequent Cloning into pMS119EH

PCR using Taq polymerase was performed using template of wild-type *dmsABC* operon from plasmids pDMS223 or pDMS160. Three alternate PCR products were amplified using the 5' primers 5'ATATGAATTCTCGATGTATACAAGCC3', 5'ATATGAATTCATGGCCAGCAGCGCATTAAC3', and 5'ATATGAATTCATGGTCGATAGCGCCATTCC3', and the identical 3' primer 5'GCCGTCATTTCCGGGCCACG3'. These primers resulted in amplification of DmsA starting from $M^{-}29$, M1, and M16 mutated from A16, respectively (Figure 4.1.), to nucleotide 2040 in DmsA [3]. All three 5' primers contained an *Eco*RI restriction enzyme site to allow cloning of the PCR product into pDMS223 using *Eco*R1 and *Eco*RV. The *Eco*RV restriction enzyme site falls within the PCR product located at nucleotide 1465 in DmsA [3]. *Eco*RI/*Sal*I fragments from pDMS223M^{-}29, pDMS223M1, and pDMS223A16M, were moved into pMS119EH to create pDMS119P_{tac} plasmids (pDMS119$P_{tac}M^{-}$29, pDMS119P_{tac}M1, and pDMS119P_{tac}A16M. At least two different PCR clones were utilized in subsequent expression experiments. pDMS223M1 was sequenced to confirm the construct.

4.2.6. Media and Growth Conditions

Cells were grown aerobically in LB or Terrific Broth [30] overnight, and these cultures were used as 1% inocula unless otherwise indicated. Antibiotics were included as necessary.

Glycerol minimal media was as indicated previously [4], with the following exceptions. 0.16% peptone was substituted for casamino acids, and streptomycin sulfate was not included in the growth medium. Vitamin B1, proline, and leucine, were included at final concentrations of 0.005%.

4.2.7. Quantitative and Qualitative Anaerobic Growth Experiments

Transformed DSS301 or TG1, were grown overnight, and used as inocula for glycerol minimal media. Quantitative growth experiments were performed on DSS301 or TG1 recombinants in Klett flasks, using either fumarate (positive control) (Gly/Fum) or DMSO (Gly/DMSO) as electron acceptor [28]. Klett units were measured with a Klettmeter using a #66 filter at various times up to 48 hours. Qualitative growth experiments were performed on DSS301 constructs in 11 mL screw-capped and parafilm sealed tubes filled with Gly/DMSO. Isopropyl β-D-thiogalactopyranoside (IPTG) was added to final concentrations of 0, 0.01, 0.1, or 1 mM. Growth was assessed by eye at 24 and 36 hours.

4.2.8. Aerobic Expression of DmsABC from the T7 Promoter

K38 with pGP1-2 and pTZ18R or pDMS223 plasmids, was grown overnight at 30°C. The cultures were diluted 1/10 into LB, and grown with shaking at 30°C for about 3 hours, to an OD between 0.5 and 0.7. An equal volume of LB plus antibiotics heated to 55°C was added to the cultures, and they were incubated at 42°C with shaking for 15 minutes. Rifampicin was then added to a final concentration of 200 μg/mL. The cells were incubated at 42°C for an additional 15 minutes, and transferred to 37°C. Samples were removed just before heat induction (time 0), and at 0.5, 1, 2, and 21 hours.

4.2.9. Aerobic Expression of DmsABC from the *tac* Promoter

Overnight cultures of HB101 with DmsABC cloned into the pMS119 expression vector, were used as 2% inocula for 250 mL LB. The cultures were grown for 2 hours, and IPTG added to 0.2 mM. The cultures were transferred to 30°C and incubated with gentle shaking for an additional 18 hours.

4.2.10. Preparation of Membrane and Supernatant Fractions

Cells were pelleted by centrifugation at 9,500 g for 10 minutes, resuspended [23], and everted envelopes were prepared by French Press lysis [4]. The supernatant and membrane fractions were separated by differential centrifugation [23]. Membranes were washed twice with 50 mM MOPS pH 7.0, prior to use.

4.2.11. Analytical Techniques

DNA sequencing was carried out using an Applied Biosystems model 373A DNA sequencer in the Department of Biochemistry DNA Core facility at the University of Alberta.

PAGE was performed using the BioRad mini-gel, or Protean IIxi 20 cm slab gel system, with a discontinuous SDS buffer system [14]. Gels were stained with Coomassie blue, and destained [15].

Western blotting was performed using affinity purified polyclonal DmsA and DmsB antibody separately, or together, as indicated in the text [28]. ECL western blotting detection reagents from Amersham Life Sciences were used for blot development. No antibody has been successfully raised against DmsC [39].

4.3. Results

4.3.1. Site-directed Mutagenesis of the Newly Proposed Initiating Met ($M^{-}29$) for DmsA

The N-terminal amino acid sequence of DmsA is shown in Figure 4.1. The originally proposed (M1) [3] and newly proposed ($M^{-}29$) [2] translational start sites are indicated, as well as the first residue of purified DmsA determined by Edman degradation [3]. The numbering of amino acids follows that proposed by Bilous et al., with M1 located sixteen residues upstream of V17, the N-terminal amino acid of purified DmsA [3]. Residues preceding M1 are given negative numbers.

To determine the correct initiating Met for DmsA, the Met start codon proposed by Berks [2], $M^{-}29$, was mutated to a stop codon, creating mutant $M^{-}29$Stop. If translation initiates at the originally proposed Met (M1), this mutation should have no effect on production of functional DmsABC.

4.3.2. Anaerobic Growth of $M^{-}29$Stop on Gly/DMSO

DmsABC is the only enzyme able to conserve the redox energy of DMSO reduction. As a result, DSS301, a strain deleted for the *dmsABC* operon, grows anaerobically on Gly/DMSO only in the presence of a complementing plasmid encoding functional DmsABC.

Plasmid pDMS170 supported growth of DSS301 on Gly/DMSO, while pBR322 and pDMS160M^{-}29Stop did not (Figure 4.1.). This indicates mutant M^{-}29Stop does not accumulate functional DmsABC, and suggests the correct initiating Met is M^{-}29. The inability of pDMS160M-29Stop to allow growth of DSS301 on Gly/DMSO may be the result of either lack of expression, rapid degradation, or accumulation of non-functional DmsABC in the M^{-}29Stop mutant

4.3.3. Anaerobic Accumulation of M^{-}29Stop DmsABC

DmsABC overexpressed from a plasmid competes for membrane assembly with chromosomally-encoded DmsABC [38]. As a result, if the plasmid encodes accumulating non-functional DmsABC, decreased DMSO dependent growth will be observed, due to the assembly of non-functional enzyme overwhelming the chromosomally encoded subunits. If the non-functional subunits are rapidly degraded, or do not accumulate, they will not overwhelm the wild-type copy and growth will be maintained.

To determine whether M^{-}29Stop accumulates non-functional DmsABC, an *E. coli* strain possessing a functional chromosomal copy of *dmsABC*, TG1 was transformed with pDMS160M^{-}29Stop. TG1/pDMS160M^{-}29Stop showed an equivalent doubling time on Gly/DMSO to untransformed TG1. The absence of growth of DSS301/pDMS160M^{-}29Stop was thus due to an inability to accumulate protein. These results suggested DmsA does not accumulate if translation initiates from M1.

Accumulation of DmsAB can also be monitored by Western blotting of DSS301 (*ΔdmsABC*) expressing wild-type and mutant DmsABC from plasmid. Anaerobically grown DSS301/pDMS170 accumulated both DmsA and DmsB, while DSS301/pBR322, and DSS301/pDMS160M^{-}29Stop essentially did not (Figure 4.1 and 4.2.). There was a very small amount of DmsB in one of the M^{-}29Stop mutant samples, but this was almost negligible compared to the pDMS170 sample. This confirms DmsA does not accumulate in the M^{-}29Stop

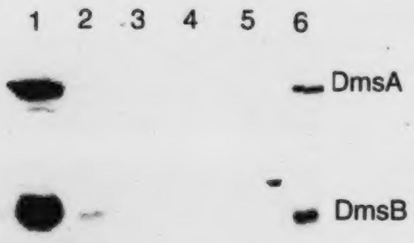

Figure 4.2.

Western Blot Analysis for DmsA and DmsB Expressed Anaerobically from Their Natural Promoter for Wild-Type, M^{-}29Stop, and R^{-}13D Mutants

DSS301 with pBR322, pDMS170, pDMS160M^{-}29Stop, or pDMS160R^{-}13D, were grown anaerobically for 48 hours on Gly/Fum and harvested. 10 μg DSS301 were run on a 12.5% SDS-polyacrylamide gel, along with 30 μg purified DmsABC. Proteins were transferred to nitrocellulose, and a Western blot was performed using DmsA and DmsB polyclonal antibodies separately as indicated in the top and bottom panels, respetively. 1. DSS301/pDMS170, 2. DSS301/pDMS160M^{-}29Stop, 3. DSS301/pBR322, 4. DSS301/pDMS160M^{-}29Stop, 5. DSS301/pDMS160R^{-}13D, 6. purified DmsABC.

mutant under anaerobic growth conditions, and DmsB accumulates to very low levels. This also suggests DmsB is not synthesized, or is degraded in the absence of DmsA.

4.3.4. Aerobic T7 Promoter Driven Expression of M^{-}29Stop DmsA and DmsB

We attempted to differentiate lack of accumulation due to lack of synthesis, or synthesis followed by rapid degradation using a T7 promoter driven system.

Expression from the T7 promoter was examined under aerobic conditions at 0, 0.5, 1, 2, and 21 hours after heat induction. Samples were analyzed on a SDS-polyacrylamide gel, and DmsA and DmsB were visualized by Western blotting using DmsA and DmsB antibodies in tandem (Figure 4.3.).

As expected, K38/pTZ18R lacked DmsA and DmsB. K38/pDMS223 expressed large and constant quantities of DmsA and DmsB, appearing after 30 minutes of induction. As observed previously, DmsB electrophoresed as a smear [29]. Mutant M^{-}29Stop showed an initial burst of DmsA and DmsB after 30 minutes. By 2.0 hours DmsA began to disappear, and after 21 hours no DmsA was observed. DmsB remained relatively constant during this time period. The intensity of M-29Stop-DmsA was approximately 10-fold less than wild-type DmsA. These data indicate aerobic expression of DmsA M^{-}29Stop is limited and unstable. Translation initiation is likely from M1 under aerobic conditions from the T7 promoter. However, expression from M1 was very poor compared to wild-type expression.

4.3.5. PCR Mutagenesis and Cloning of DmsABC to Generate DmsA Expressed from the *tac* Promoter Initiating at M^{-}29 or M1

PCR and cloning were used to create two constructs of *dmsABC* in pMS119EH, allowing *dmsABC* to be expressed from the *tac* promoter

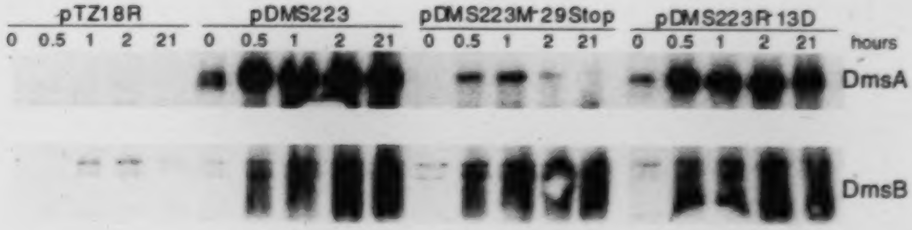
pTZ18R
pDMS223
pDMS223M-29Stop
pDMS223R-13D
0 0.5 1 2 21
0 0.5 1 2 21
0 0.5 1 2 21
0 0.5 1 2 21
hours
DmsA
DmsB

Figure 4.3.
Western Analysis of DmsA and DmsB Expressed Aerobically from the T7 Promoter for Wild-type, M^{-}29Stop and R^{-}13D Mutants

K38/pGP1-2 with pTZ18R, pDMS223, pDMS223M^{-}29Stop, or pDMS223R^{-}13D were induced for expression by incubation at 42°C for 30 minutes. Aliquots were taken at various times as indicated in hours, before and after heat induction. 35 µg of protein was run in each lane on a 12.5% SDS-polyacrylamide gel. Proteins were transferred to nitrocellulose, and a Western blot was performed using DmsA and DmsB antibodies in tandem. The bands corresponding to DmsA and DmsB are shown in the top and bottom panels, respectively.

using either M^{-}29 or M1 as the initiating codon for DmsA. In these constructs, the *tac* promoter was followed immediately by M^{-}29, or M1. No native 5' promoter sequence is present. The Shine-Dalgarno sequence for each Met was provided by the expression vector.

4.3.6. Qualitative Anaerobic Growth on Gly/DMSO for DSS301 with pDMSP$_{tac}$M^{-}29 and pDMSP$_{tac}$M1

Anaerobic growth of DSS301 (Δ*dmsABC*) on Gly/DMSO transformed with pMS119EH, pDMS119P$_{tac}$M^{-}29, or pDMS119P$_{tac}$M1, was assessed visually. IPTG was included at 0, 0.01, 0.1, and 1 mM, to induce expression from the *tac* promoter.

The plasmid pDMS119P$_{tac}$M^{-}29 was only able to support growth on Gly/DMSO when IPTG was present below 0.1 mM. IPTG exceeding 0.1 mM prevented growth (Table 4.3.). This indicates DmsA expression can initiate at M^{-}29 when expressed from the tac promoter, and that higher levels of overexpression resulted in loss of DmsABC function. This may be the result of overexpression non-function.

The plasmid pDMS119P$_{tac}$M1 could not support anaerobic growth of DSS301 on Gly/DMSO at any level of IPTG, indicating the importance of residues $^{-}$29 to $^{-}$1 for production of functional DmsABC. This agrees with the observed lack of anaerobic growth on Gly/DMSO for M^{-}29Stop, and confirmed that M^{-}29 is the correct initiating residue.

4.3.7. Aerobic Expression of DmsA and DmsB from the *tac* Promoter in pDMS119P$_{tac}$M^{-}29 and pDMS119P$_{tac}$M1

The qualitative anaerobic Gly/DMSO growth experiments of DSS301 with pDMS119P$_{tac}$M^{-}29 and pDMS119P$_{tac}$M1, indicated functional DmsABC was produced only by pDMS119P$_{tac}$M^{-}29. To examine aerobic expression of DmsA and DmsB, the constructs were transformed into HB101, grown aerobically, and induced with 0.2 mM IPTG. NarGHI is synthesized, and is functional using this procedure

Table 4.3.

Qualitative Anaerobic Growth on Gly/DMSO of DSS301 Transformed with *tac* Constructs

DSS301	**IPTG mM**			
with Plasmid	**0**	**0.01**	**0.1**	**1**
pDMS119P$_{tac}$M^{-}29	+	+++	+	-
pDMS119P$_{tac}$M1	-	-	-	-
pDMS119P$_{tac}$A16M	~	-	-	-
pMS119EH	-	-	-	-

DSS301 with pMS119EH and pDMS119 plasmids were grown anaerobically on Gly/DMSO in sealed screw-capped tubes, and were examined visually at 24 and 36 hours for growth. Maximal growth is indicated by +++, minimal growth by +, trace growth by ~, and no growth by -. The pDMS119 plasmids have *dmsABC* directly behind the *tac* promoter starting at M^{-}29, M1 or M16 (mutated from an A), with no native upstream untranslated or translated sequence. (See Figure 4.1 for a schematic). DmsABC was expressed from the *tac* promoter with IPTG.

[12]. The membrane and soluble fractions of lysed cells were electrophoresed on a SDS-polyacrylamide gel, followed by Western blot analysis with DmsA and DmsB antibodies.

DSS301/pDMS119$P_{tac}$$M^{-}$29 run on an SDS-polyacrylamide gel showed DmsA and DmsB in the membrane and supernatant fractions, while DSS301/pDMS119P_{tac}M1 did not (Figure 4.4). This indicated aerobic expression can occur from M^{-}29 but not M1. This confirms previous observations indicating M^{-}29 is the correct initiating Met.

The DmsA results were more easily visualized by Western analysis of membrane and supernatant fractions in Figure 4.5. A 20 cm SDS-polyacrylamide gel was run, rather than mini-gels, and the lower molecular weight proteins were run off the gel to better separate the various forms of DmsA. This gave at least 15 cm of resolution for DmsA compared to the mini-gels with only 1-2 cm of resolution. Western blot analysis of the gel was performed using DmsA antibody.

The membrane fraction of HB101/pDMS119$P_{tac}$$M^{-}$29 showed three forms of DmsA, while HB101/pDMS119P_{tac}M1 showed a complete absence of DmsA. This confirms DmsA is not expressed from M1, and that M^{-}29 is the correct initiating codon. (The three DmsA bands in HB101/pDMS119$P_{tac}$$M^{-}$29 will be discussed in results section 4.3.10.)

4.3.8. PCR Mutagenesis and Cloning of DmsABC to Generate a Construct Where DmsA is Missing its Leader Sequence

To determine the necessity of the leader (residues $^{-}$29 to 16) for production of functional DmsABC, a construct was created placing *dmsABC* behind the *tac* promoter, initiating from a Met inserted prior to the amino terminal amino acid (V17) of purified DmsA. This construct (pDMS119P_{tac}A16M), missing *dmsABC* coding sequence 5' to A17, is similar to that described in results section 4.3.5.

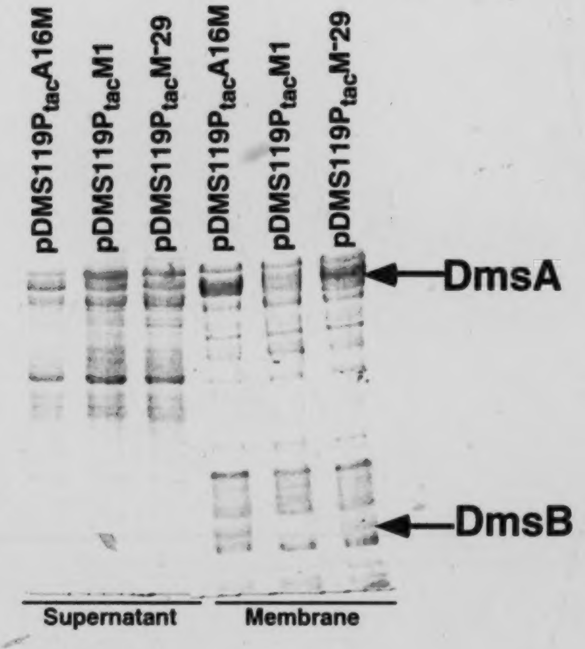
pDMS119PtacA16M
pDMS119PtacM1
pDMS119PtacM-29
pDMS119PtacA16M
pDMS119PtacM1
pDMS119PtacM-29
DmsA
DmsB
Supernatant
Membrane

Figure 4.4.

Coomassie Blue Stained SDS-polyacrylamide Gel of Aerobically Expressed DmsABC from *tac* Promoter Constructs

HB101 transformed with *tac* promoter constructs (see Figure 4.1.) were grown aerobically. Expression from the *tac* promoter was induced by 0.2 mM IPTG. 50 µg of membrane and supernatent fractions were loaded on a 12.5% gel.

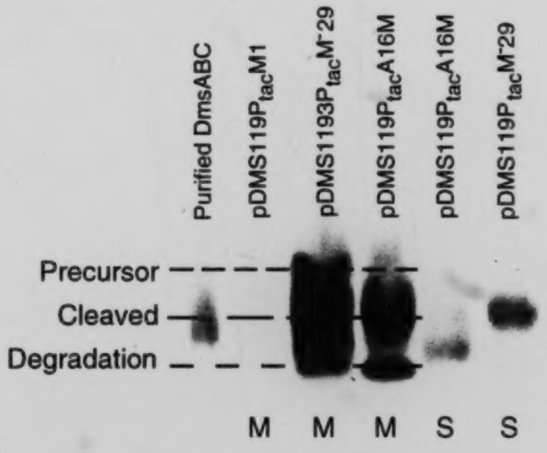
Purified DmsABC
pDMS119P_{tac}M1
pDMS1193P_{tac}M^{-}29
pDMS119P_{tac}A16M
pDMS119P_{tac}A16M
pDMS119P_{tac}M^{-}29
Precursor
Cleaved
Degradation
M
M
M
S
S

Figure 4.5.

Western Analysis of Aerobically Expressed DmsABC from *tac* Promoter Constructs Probed with DmsA Antibody

HB101 with the three *tac* promoter constructs (see Figure 4.1.) were grown aerobically in the presence of IPTG. Membrane (M) and supernatent (S) fractions were obtained from the harvested cells. Fifty μg of protein was subjected to a 15 cm separation on a 20 cm 12.5% SDS-polyacrylamide gel. Thus, the lower molecular weight proteins were run off to get maximal separation of the various forms of DmsA. Proteins were transferred to nitrocellulose, and probed with DmsA antibody.

4.3.9. Qualitative Anaerobic Growth of DSS301/pDMS119 P_{tac}-A16M on Gly/DMSO

Anaerobic growth of DSS301 (Δ*dmsABC*) on Gly/DMSO transformed with pDMS119P_{tac}A16M was assessed visually as in results section 4.3.6. The plasmid pDMS119P_{tac}A16M supported only trace levels of anaerobic growth of DSS301 on Gly/DMSO at any level of IPTG (Table 4.3.), indicating the importance of the DmsA leader for production of functional DmsABC. This result did not differentiate between the inability to initiate at M16, initiation and rapid degradation, or accumulation of non-functional protein.

4.3.10. Aerobic Expression of DmsA and DmsB from the *tac* Promoter in pDMS119P_{tac}A16M

The qualitative anaerobic Gly/DMSO growth of DSS301/pDMS119P_{tac}A16M indicates functional DmsABC is not produced. To differentiate between an inability to initiate at M16, initiation and rapid degradation, or accumulation of non-functional protein, aerobic expression of DmsA and DmsB was examined as in results section 4.3.7.

Cell lysates run on an SDS-polyacrylamide gel, of DSS301/pDMS119P_{tac}A16M grown aerobically, and induced for expression from the *tac* promoter, showed DmsA and DmsB in the membrane and supernatant fractions (Figure 4.4.). This indicated translation can initiate from M16. Since DmsAB was found in the membrane, DmsAB can localize to the membrane in the absence of the leader ($M^{-}29$ to A16). Since DSS301/pDMS119P_{tac}A16M did not grow anaerobically on Gly/DMSO (results section 4.3.9), this suggests the membrane-bound DmsABC is not functional.

The DmsA results are more easily visualized by Western blot analysis of membrane and supernatant fractions in Figure 4.5. It is not possible to unequivocally assign the identity of each of the DmsA bands, however, we can suggest their identity.

We would suggest the intermediate and darkest band in pDMS119P_{tac}A16M membranes, the construct lacking the leader, is the clipped form of DmsA. It was also found in pDMS119P_{tac}M^{-}29 membranes and purified DmsABC. Note that the darkest band in pDMS119P_{tac}A16M supernatant ran lower than in the membrane fraction of the same construct. This band must also be DmsA missing residues M^{-}29 to A16, although it appeared the supernatant and membrane forms of DmsA from the same construct run slightly differently. We would suggest the lowest band, found in pDMS119P_{tac}A16M and pDMS119P_{tac}M^{-}29 membrane samples, was a degradation product. It was missing most importantly from the purified sample, as well as the supernatant samples. Lastly, we would postulate the highest band observed only in pDMS119P_{tac}M^{-}29 membranes, was the unclipped form of DmsA, and was equivalent to the band observed in pDMS119P_{tac}M^{-}29 supernatant, although it ran lower in the supernatant sample.

These results confirm although the leader was necessary for production of functional DmsABC (results section 4.3.9.), DmsABC can localize to the membrane in the absence of leader.

4.3.11. Site-directed Mutagenesis of the Double-Arginine Consensus in DmsA

Results section 4.3.9. showed the leader was necessary for production of functional DmsABC. Since the correct initiating Met is $^{-}$29, DmsA is observed to possess a double-arginine leader. Comparison of double-arginine leaders reveals the two Arg residues are invariant (Figure 4.1.), and the frequency of the other amino acids in the motif is greater than 50% [2]. To determine the importance of the double-arginine consensus for production of functional DmsABC, the second Arg of the motif was mutated to an Asp, to create mutant R^{-}13D.

4.3.12. Anaerobic Growth of DSS301/pDMS160R13D On Gly/DMSO

As in results section 4.3.2., growth of DSS301/pDMS160R^{-}13D was examined to determine whether functional DmsABC is produced. Plasmid pDMS160R^{-}13D was unable to support growth of DSS301 on Gly/DMSO (Figure 4.1.). This indicates mutant R^{-}13D does not encode functional DmsABC, and suggests the double-arginine consensus plays an essential role for production of functional DmsABC. These results do not differentiate between lack of expression, rapid degradation, or accumulation of non-functional DmsABC in the R^{-}13D mutant.

4.3.13. Anaerobic Accumulation of R^{-}13D DmsABC

To determine whether R^{-}13D accumulated non-functional DmsABC, TG1 was transformed with pDMS160R^{-}13D, and anaerobic growth was examined as in results section 4.3.3. DSS301/pDMS160R^{-}13D showed an equivalent doubling time on Gly/DMSO as untransformed TG1. This indicates DmsABC does not accumulate in the R^{-}13D mutant. Thus, absence of anaerobic growth of DSS301/pDMS160R^{-}13D (results section 4.3.12) on Gly/DMSO is due to inability to accumulate protein. Mutation of the double-arginine consensus prevents accumulation, indicating the importance of this motif in expression and/or stabilization of DmsABC.

To confirm the above result, a Western blot of a SDS-polyacrylamide gel of anaerobically grown DSS301/pDMS160R-13D was performed, as in results section 4.3.3. (Figure 4.1 and 4.2.). No DmsA or DmsB was observed in DSS301/pDMS160R^{-}13D. This confirms DmsA does not accumulate in the R^{-}13D mutant, and suggests DmsB is degraded, or is not synthesized, in the absence of DmsA.

4.3.14. Aerobic T7 Promoter Driven Expression of R^{-}13D DmsA and DmsB

To determine whether DmsA and DmsB can be synthesized aerobically in the R^{-}13D mutant, we examined T7 promoter driven expression as in results section 4.3.4 (Figure 4.3.). DmsA and DmsB appeared after 30 minutes of induction, and remained constant in the R^{-}13D mutant. The intensity is approximately half of that observed for wild-type DmsABC. These results indicate DmsA and DmsB can be expressed aerobically when the second Arg of the double-arginine consensus is mutated, although R^{-}13D does not accumulate anaerobically (results section 4.3.13.).

4.3.15. Analysis of Potential DmsA Leader Sequences

Potential DmsA leader sequences were examined utilizing software available at the Center for Biological Analysis web site [18]. This was done to determine the most appropriate amino acid mutations to make in DmsA in order to create a mutant that leader peptidase I would not cleave. This analysis suggested mutation of both A14 and A16 was necessary to inhibit cleavage. An additional secondary cleavage site with low probability was identified between T7 and L8, for mutation of residues 14 and 16 to Asp, Arg, Asn, or Thr.

The double mutant A14N,A16N was selected for mutation (Figure 4.1.), as leader peptidase I would have a low probability of cleavage between A16 and V17. Additionally, the mutation A14N,A16N introduced an additional *Asn*I restriction site into the coding sequence, allowing mutated DNA to be identified by restriction enzyme digestion.

4.3.16. Creation of Cleavage Site Mutants

The DmsA leader sequence cleavage site was mutated in an attempt to generate a stable pre-DmsA polypeptide, to assess the necessity of leader sequence cleavage for production of functional

DmsABC. Two leader sequence cleavage mutants were obtained, A14N and A14N,A16N.

4.3.17. Anaerobic Growth of Cleavage Site Mutants on Gly/DMSO

As in results section 4.3.2., the ability of cleavage site mutants to complement DSS301 (*ΔdmsABC*) for anaerobic growth on Gly/DMSO was examined. Plasmids pDMS170, pDMS160A14N and pDMS160A14N,A16N complemented anaerobic growth of DSS301 on Gly/DMSO (Figure 4.1). DSS301/pDMS170, DSS301/pDMS160A14N, and DSS301/pDMS160A14N,A16N, showed equivalent doubling times (data not shown) (approximately 5 hours). This indicates wild-type plasmid, as well as DmsA mutants A14N and A14N,A16N encode functional DmsABC. From these results we cannot conclude whether the leader sequence is cleaved (unlikely as suggested by cleavage site analysis), not cleaved, or cleaved at the low probability secondary site. (Further experiments are underway to answer this question.)

4.4. Discussion

The results reported herein indicate the correct initiating Met for DmsA is 29 residues upstream of the initially proposed Met (Figure 4.1.). The entire leader sequence was shown to be necessary for production of functional DmsA, with the double-arginine consensus being of particular importance.

M1 was originally selected as the initiating codon, as it is the first Met upstream of the N-terminal amino acid of purified DmsA, and it possesses a good 5' Shine-Dalgarno sequence [3]. However, the sequence 5' to $M^{-}29$ does not show an apparent ribosome binding site (GAGTGA) [36]. Nonetheless, M-29 is the actual initiating codon as shown by non-functional DmsABC in the $M^{-}29$Stop mutant and pDMS119P_{tac}M1 construct.

Alignment of recently available DMSO reductase sequences from *Haemophilus* (*H.*) *influenza*, and *E. coli* (1996 *H. influenza*, 1997*E. coli*), demonstrate M1 is not conserved (Figure 4.6.), while the upstream double-arginine consensus is. This provides additional support that $M^{-}29$ is the correct initiating amino acid.

The mRNA encoding *dmsABC* showed an unusually long 5' untranslated region of 218 nucleotides [10]. However, translation initiation at $M^{-}29$ shortens the 5' untranslated region to a more reasonable 131 nucleotides.

The pDMS119P_{tac}A16M construct resulted in production of non-functional DmsABC, as did mutant $R^{-}13D$. This indicated the leader sequence was important, and in particular, $R^{-}13$ played an important role in the function of the leader sequence. The observation that mutation of an amino acid within a leader sequence alters function, was in marked contrast to that generally observed for leader peptides [2]. The $R^{-}13D$ mutation altered the N-terminal leader sequence charge from $^{+}3$ to $^{+}2$. Nonetheless, studies have shown that the number of positive charges in a leader sequence was unimportant, as long as the global charge of the amino terminal region remained positive [13, 20, 41]. Leader sequence mutations that have been shown to impair leader function, were the mutation of a hydrophobic residue within the H-region, to a hydrophilic one [11]. $R^{-}13$ is found 5' to the hydrophobic portion of the leader, thus mutant $R^{-}13D$ was not a similar type of mutation.

Two similar mutagenesis studies on the double-arginine consensus have been performed. These have examined the double-arginine leader from *Desulfovibrio vulgaris* [Ni-Fe] hydrogenase [19], and *Pseudomonas stutzeri* nitrous oxide reductase [8]. Mutation of the first Arg of the double-arginine consensus was demonstrated to inhibit translocation of β-lactamase when fused to the leader peptide from the hydrogenase [19], and resulted in non-translocated cytoplasmic apo-

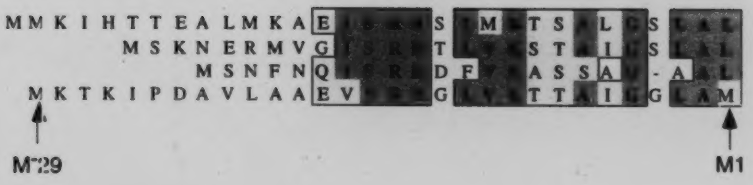

Figure 4.6.

Alignment of Amino Acid Sequences of DMSO Reductases from *E. coli* and *H. influenza*

Sequences (*E. coli* K-12) were aligned using MacVector 6.0.1. (Oxford Molecular Group PLC). Homologous residues and those with conservative substitutions are boxed. Dark shaded residues are conserved, and light shaded residues indicate conservative substitutions. The N-terminal amino acid sequences from top to bottom are : *E. coli* potential DMSO reductase-A, *E. coli* potential DMSO reductase-B, *H. influenza* DMSO reductase, DmsABC. M1 indicates the originally proposed Met for DmsABC, and M^{-}29 the newly proposed Met.

nitrous oxide reductase [8]. Results from these two studies, and this chapter, indicate mutation of the invariant Arg residues in the double-arginine consensus abolishes leader sequence function. Additionally, since hydrogenase [19] and nitrous oxide reductase [8] mutants were not translocated, this indicates the mutated double-arginine leader sequences were not recognized by the Sec-system.

The double-arginine leader has been suggested to be important for translocation of periplasmic proteins binding a subset of redox cofactors [2]. DmsA possesses a double-arginine leader, although it is not a periplasmic protein [24, 27, 45]. Minor modifications to Berks translocation model [2] would allow reconciliation with observed experimental results. Thus, we propose a revised model that defines the role of the double-arginine leader for membrane targeting and translocation of cytoplasmic and periplasmic proteins.

The model initiates with ribosome synthesizing protein (Figure 4.7.). In accordance with the model proposed by Berks [2], protein folds (1a) within the cytoplasm, and if appropriate binds additional soluble subunits lacking a leader sequence (2a). The double-arginine leader is recognized by subunits that are part of a membrane targeting and translocation (MTT) complex (2a) [43]. Translocation of protein is then initiated, and the leader is cleaved by leader peptidase I. Protein that interacts with membrane intrinsic subunits at the cytoplasmic surface (3a), will remain in the cytoplasm, with the membrane intrinsic subunits acting as "stop transfer" signals. The protein will be functional, and localized to the cytoplasmic surface of the membrane. Proteins that do not bind membrane intrinsic subunits, or those that interact with membrane intrinsic subunits on the periplasmic face of the membrane, will be translocated along with bound subunits lacking leader sequence (3b), since there are no interactions preventing their

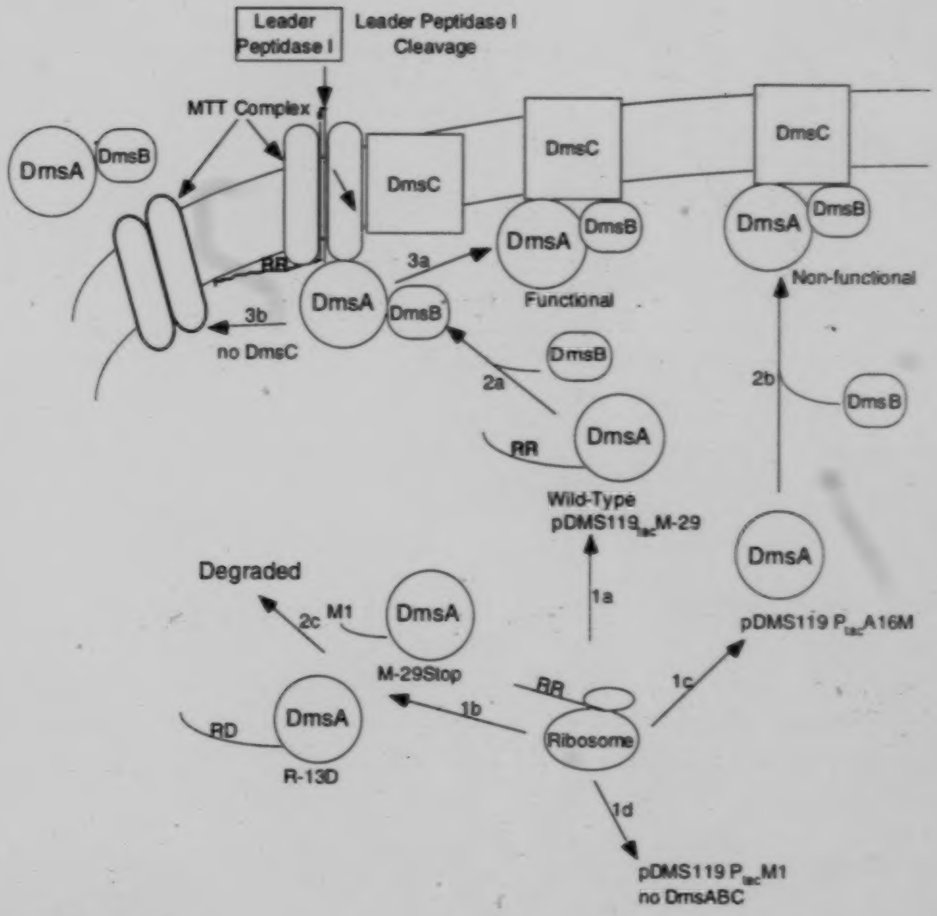
Leader Peptidase I
Leader Peptidase I Cleavage
MTT Complex
DmsA
DmsB
DmsC
DmsC
DmsC
RR
3a
3b
no DmsC
DmsA
DmsB
Functional
DmsA
DmsB
Non-functional
DmsB
2a
RR
DmsA
2b
DmsB
Wild-Type
pDMS119 P lac M-29
DmsA
1a
Degraded
2c
M1
DmsA
M-29Stop
pDMS119 P lac A16M
RR
1c
RD
DmsA
1b
Ribosome
R-13D
1d
pDMS119 P lac M1
no DmsABC

Figure 4.7.

Double-Arginine Leader Dependent Membrane Targeting and Translocation Model for Cytoplasmic and Periplasmic Proteins

The plasmids/constructs that follow each of the pathways are indicated by the construct name, listed directly after the arrow initiating that pathway. Additionally, the results with hydrogenase and nitrous oxide reductase, indicate protein with altered double-arginine leader follows pathway 1b [8, 19]. Results suggest double-arginine containing protein is folded prior to translocation (HybABC) [21] and the folded protein has bound cofactor (HybABC and TorA) [21, 31]. Suggestion that soluble subunits lacking a leader can be translocated concurrently with double-arginine leader containing protein (2a), is supported by experiments on hydrogenase [16, 40] and aldehyde dehydrogenase [37]. The results reported within reference [43], support pathway 3a and 3b, and are the origin of the name "membrane targeting and translocation" (MTT). In addition, translocation of TorA appears to be independent of the Sec-system, and dependent on the pmf [31].

transfer. This will result in functional periplasmic protein. (Pathways 3a and 3b are supported by the following observations. DmsAB is found in the cytoplasm, or on the cytoplasmic surface of the membrane in wild-type cells. However, in the absence of DmsC, the majority of DmsAB is found in the periplasm. [43].) Alternatively, protein synthesized with no leader sequence (1c), that interacts with membrane intrinsic subunits on the cytoplasmic surface, will localize to the membrane (2b). Since the double-arginine leader protein was not targeted by the MTT complex, it will be non-functional. In the event that the double-arginine leader is altered, soluble proteins will accumulate in the cytoplasm (1b), or will be degraded (2c). They will not be translocated by the Sec-system.

A mutant has been obtained that shows pleiotropic loss of activity of double-arginine leader containing proteins [43], distinguishing this MTT system from the Sec-system. Nonetheless, it would be interesting to see if double-arginine leader possessing proteins were functional and targeted correctly if their double-arginine leaders were exchanges for Sec leaders. This model would predict the double-arginine leader proteins would not be targeted correctly or functional, or if targeted would be non-functional.

Berks suggests the double-arginine leader pathway is involved in translocation of folded proteins [2]. Addition of cofactor to HybC has been demonstrated to occur in the cytoplasm, and is concomitant with conversion to a protease stable form of the protein [21]. However, it could be argued that the protein may be unfolded prior to, or concomitant with translocation. β-galactosidase with fused Sec-leader is not translocated by the Sec-system due to its rapid folding in the cytoplasm. Examining translocation of β-galactosidase engineered with a double-arginine leader would test this hypothesis. Observation that β-galactosidase with fused double-arginine leader is translocated to the periplasm would confirm translocation of fully folded protein.

It was observed that apo-nitrous oxide reductase accumulated in the cytoplasm when its double-arginine leader was altered [8]. This suggests the double-arginine leader is important for cofactor insertion. Since M^{-}29Stop and R^{-}13D mutants do not accumulate under anaerobic conditions, these DmsABC mutants cannot be tested for moco insertion. Additionally, moco appears limiting under aerobic conditions, resulting in non-stoichiometric quantities of moco in aerobically expressed wild-type DmsABC [22]. However, experiments are underway to determine whether DmsABC expressed anaerobically from pDMS119P$_{tac}$M^{-}29 and pDMS119P$_{tac}$A16M constructs contain moco. These results may provide evidence that the double-arginine leader is important for cofactor insertion.

Why some moco containing enzymes require a double-arginine leader, while others do not, may depend on their affinity for moco. NarGHI does not possess a double-arginine leader, while DmsABC does. It has been observed that NarGHI has a tighter affinity for moco. When moco is limiting, as in a *moeB* mutant, or in aerobically grown cells, NarGHI is fully functional, while DmsABC is not [22, 46]. Alternatively, the double-arginine leader could be an evolutionary vestige for the cytoplasmic membrane-bound proteins with periplasmic homologues, at present acting to aid in cofactor insertion and/or membrane targeting.

Although the results indicate the leader sequence is necessary, our data does not indicate whether leader sequence cleavage is necessary for production of functional DmsABC. Studies are underway to determine whether mutants A14N and A14N,A16N are cleaved correctly, uncleaved, or cleaved at the low probability secondary site. Our preliminary results suggest A14N and A14N,A16N mutants are cleaved at the low probability secondary site.

The results reported herein also provide additional evidence that DmsAB is localized to the cytoplasmic face of the membrane. Proteins that localize to the membrane by binding to membrane intrinsic subunits would be expected to only bind to one surface of the membrane, depending on the productive interactions between the soluble and membrane intrinsic subunits. DmsAB from pDMS119P$_{tac}$A16M can localize to the membrane although DmsA in this construct is lacking a leader. Since DmsA from pDMS119P$_{tac}$A16M cannot be translocated across the membrane by any translocation system, pDMS119P$_{tac}$A16M-DmsA must be cytoplasmic. This indicates DmsA and DmsB bind to the cytoplasmic face of DmsC.

Previously other lines of evidence have been used to suggest DmsAB are localized to the periplasm. It has been incorrectly referenced [2] that a β-lactamase fusion to the periplasmic tail of the eight-transmembrane-helix DmsC, prevents binding of the DmsAB pair [45]. Additionally, it has been suggested that DmsAB is periplasmic, since it has been observed that one of the Fe-S clusters interacts with DmsC residue H65, believed to be close to the periplasmic side of the membrane [25]. Rather than discarding all biochemical, biophysical and immunological data supporting a cytoplasmic location for DmsAB (this chapter and [24, 27, 45]), we propose that either DmsB (and possibly DmsA) protrudes slightly into the membrane, decreasing the distance between the Fe-S clusters and H65, or that DmsC helix II is shifted slightly such that H65 is closer to the cytoplasmic surface (see Figure 1.8.).

The double-arginine translocation model proposed by Berks [2], and modified herein for reconciliation with experimental data, is provocative and still quite hypothetical. Further evidence is needed to define the boundaries of this novel targeting and translocation system.

4.5. References

1. Benoit, S., Abaibou, H. and Mandrand-Berthelot, M.A. (1997) Membrane topology of the aerobic formate dehydrogenase of *Escherichia coli.* Anaerobic Metabolism Electron Transfer Systems and Regulation. Marsaille-Carry-Le-Rouet, Abstract 4.

2. Berks, B.C. (1996) A complex export pathway for proteins binding complex redox cofactors? Mol. Micro. 22, 393-404.

3. Bilous, P.T., Cole, S.T., Anderson, W.F. and Weiner, J.H. (1988) Nucleotide sequence of the *dmsABC* operon encoding the anaerobic dimethylsulphoxide reductase of *Escherichia coli.* Mol. Micro. 2, 785-795.

4. Bilous, P.T. and Weiner, J.H. (1985) Dimethyl sulfoxide reductase activity by anaerobically grown *Escherichia coli.* J. Bacteriol. 162, 1151-1155.

5. Boyer, H.W. and Roulland-Dussoix, D. (1969) A complementary analysis of the restriction and modification of DNA in *Escherichia coli.* J. Mol. Biol. 41, 459.

6. Clarke, G.J. and Ward, F.B. (1988) Purification and properties of trimethylamine N-oxide reductase from *Shewanella* sp. NCMB 400. J. Gen. Microbiol. 133, 379-386.

7. Dalbey, R.E., Lively, M.O., Bron, S. and VanDijh, J.M. (1997) The chemistry and enzymology of the type I signal peptidases. Prot. Sci. 6, 1129-1138.

8. Dreusch, A., Burgissser, D.M., Heizmann, C.W. and Zumft, W.G. (1997) Lack of copper insertion into unprocessed cytoplasmic nitrous oxide reductase generated by an R20D substitution in the arginine consensus motif of the signal peptide. Biochim. Biophys. Acta 1319, 311-318.

9. Easter, M.C., Gibson, D.M. and Ward, F.B. (1983) The induction and location of trimethylamine-N-oxide reductase in *Alteromonas* sp. NCMB 400. J. Gen. Microbiol. 129, 3689-3696.

10. Eigimeier, K., Honore, N., Iuchi, S., Lin, E.C.C. and Cole, S.T. (1989) Molecular genetic analysis of FNR-dependent promoters. Mol. Micro. 3, 869-878.

11. Gennity, J., Goldstein, J. and Inouye, M. (1990) Signal peptide mutants of *Escherichia coli.* J. Bioenerg. Biomemb. 22, 233-269.

12. Guigliarelli, B., Magalon, A., Asso, M., Bertrand, P., Frixon, C., Giordano, G. and Blasco, F. (1996) Complete coordination of the four Fe-S centers of the β-subunit from *Escherichia coli* nitrate reductase. Physiological, biochemical, and EPR characterization of site-directed mutants lacking the highest or lowest potential [4Fe-4S] clusters. Biochem. 35, 4828-4836.

13. Kadonaga, J.T., Pluckthum, A. and Knowles, J.R. (1985) Signal sequence of β-lactamase. J. Biol. Chem. 260, 16192-16199.

14. Laemmli, U.K. (1970) Cleavage of structural proteins during the assembly of the head of bacteriophage T4. Nature 227, 680-685.

15. Lemire, B.D., Robinson, J.J. and Weiner, J.H. (1982) Identification of membrane anchor polypeptides of *Escherichia coli* fumarate reductase. J. Bacteriol. 152, 1126-1131.

16. Menon, N.K., Robbins, J., Wendt, J.C., Shanmugam, K.T. and Przybyla, A.E. (1991) Mutational analysis and characterization of the *Escherichia coli hya* operon, which encodes [NiFe] hydrogenase I. J. Bact. 173, 4851-4861.

17. Murphy, C.K. and Beckwith, J. (1996) Export of proteins to the cell envelope in *Escherichia coli,* in *Escherichia coli* and *Salmonella* cellular and molecular biology. (Neidhardt, F.C., ed.), Vol. 1, p. 967-978, ASM Press, Washington.

18. Nielsen, H., Engelbrecht, J., Brunak, S. and vonHeijne, G. (1997) Identification of prokaryotic and eukaryotic signal peptides and prediction of their cleavage sites. Prot. Eng. 10, 1-6.

19. Niviere, V., Wong, S.-L. and Voordouw, G. (1992) Site-directed mutagenesis of the hydrogenase signal peptide consensus box prevents export of a β-lactamase fusion protein. J. Gen. Microbiol. 138, 2173-2183.

20. Puziss, J.W., Fikes, J.D. and Bassford, P.J. (1989) Analysis of mutational alterations in the hydrophilic segment of the maltose-binding protein signal peptide. J. Bact. 171, 2303-2311.

21. Rodrique, A., Boxer, D.J., Mandrand-Berthelot, M.A. and Wu, L.-F. (1996) Requirement for nickel of the transmembrane translocation of NiFe-hydrogenase 2 in *Escherichia coli.* FEBS Lett. 392, 81-86.

22. Rothery, R. and Weiner, J.H. Unpublished results.

23. Rothery, R.A. and Weiner, J.H. (1991) Alteration of the iron-sulfur cluster composition of *Escherichia coli* dimethyl sulfoxide reductase by site-specific mutagenesis. Biochemistry 30, 8296-8305.

24. Rothery, R.A. and Weiner, J.H. (1993) Topological characterization of *Escherichia coli* DMSO reductase by electron paramagnetic spectroscopy of an engineered [3Fe-4S] cluster. Biochem. 32, 5855-5861.

25. Rothery, R.A. and Weiner, J.H. (1996) Interaction of an engineered [3Fe-4S] cluster with a menaquinol binding site of *Escherichia coli*. Biochem. 35, 3247-3257.

26. Russel, M. and Model, P. (1984) Replacement of the fip gene of *Escherichia coli* by an inactive gene cloned on a plasmid. J. Bact. 159, 1034-1039.

27. Sambasivarao, D., Scraba, D.G., Trieber, C. and Weiner, J.H. (1990) Organization of dimethyl sulfoxide reductase in the plasma membrane of *Escherichia coli*. J. Bacteriol 172, 5938-5948.

28. Sambasivarao, D. and Weiner, J.H. (1991) Differentiation of the multiple S- and N-oxide reducing activities of *Escherichia coli*. Curr. Microbiol. 23, 105-110.

29. Sambasivarao, D. and Weiner, J.H. (1991) Dimethylsulfoxide reductase of *Escherichia coli* : an investigation of function and assembly by use of *in vivo* complementation. J. Bacteriol. 173, 5935-5943.

30. Sambrook, J., Fritsch, E.F. and Maniatis, T. (1989) Molecular cloning : A laboratory manual. Cold Spring Harbor Laboratory Press, Cold Spring Harbor, N.Y.

31. Santini, C.-L., Ize, B., Chantal, A., Muller, M., Giordano, G. and Wu, L.-F. (1998) A novel Sec-independent periplasmic protein translocation pathway in *Escherichia coli*. EMBO J. 17, 101-112.

32. Schindelin, H., Kisher, C., Hilton, J., Rajagopalan, K.V. and Rees, D.C. (1996) Crystal structure of DMSO reductase: Redox-linked changes in molybdopterin coordination. Science 272, 1615-1621.

33. Schneider, F., Lowe, J., Huber, R., Schindelin, H., Kisker, C. and Knablein, J. (1996) Crystal structure of dimethyl sulfoxide reductase from *Rhodobacter capsulatus* at 1.88 A resolution. J. Mol. Biol. 263, 53-69.

34. Simala-Grant, J.L. and Weiner, J.H. (1998) Modulation of the substrate specificity of dimethylsulfoxide reductase of *Escherichia coli*. Eur. J. Biochem. 251, 510-515.

35. Strack, B., Lessel, M., Calendar, R. and Lanka, E. (1992) A common sequence motif -E-G-Y-A-T-A-, identified within the primase domains of plasmid-encoded I- and P-type DNA primases and the α protein of the *Escherichia coli* satellite phage P4. J. Biol. Chem. 267, 13062-13072.

36. Stryer, L. (1988) Biochemistry. Vol. 1, 3rd ed., p. 753, W. H. Freeman and Company, New York.

37. Tamaki, T., Horinouchi, S., Fukaya, M., Okumura, H., Kawamura, Y. and Beppu, T. (1989) Nucleotide sequence of the membrane-bound aldehyde dehydrogenase gene from *Acetobacter polyoxogenes.* J. Biochem. 106, 541-544.

38. Trieber, C.A., Rothery, R.A. and Weiner, J.H. (1996) Consequences of removal of a molybdenum ligand (DmsA-Ser176) of *Escherichia coli* dimethyl sulfoxide reductase. J. Biol. Chem. 271, 27339-27345.

39. Turner, R.J., Busaan, J.L., Lee, J.H., Michalak, M. and Weiner, J.H. (1997) Expression and epitope tagging of the membrane anchor subunit (DmsC) of *Escherichia coli* dimethyl sulfoxide reductase. Prot. Eng. 10, 285-290.

40. vanDongen, W., Hagen, W., vandenBerg, W. and Veeger, C. (1988) Evidence for an unusual mechanism of membrane translocation of the periplasmic hydrogenase of *Desulfovibrio vulgaris* (Hidenborough), as derived from expression in *Escherichia coli.* FEMS Microbiol. Lett. 50, 5-9.

41. Vlasuk, G.P., Inouye, S., Ito, H., Itakura, K. and Inouye, M. (1983) Effects of the complete removal of basic amino acid residues from the signal peptide on secretion of lipoprotein in *Escherichia coli.* J. Biol. Chem. 258, 7141-7148.

42. vonHeijne, G. (1985) Signal sequences the limits of variation. J. Mol. Biol. 184, 99-105.

43. Weiner, J.H., Bilous, P.T., Shaw, G., Lubitz, S.P., Thomas, G.H., Cole, J.A. and Turner, R.J. (1998) Novel and ubiquitous system for the membrane targeting and translocation of proteins containing a double arginine leader. Cell, In press.

44. Weiner, J.H., Rothery, R.A., Sambasivarao, D. and Trieber, C.A. (1992) Molecular analysis of dimethylsulfoxide reductase : a complex iron-sulfur molybdoenzyme of *Escherichia coli.* Biochim. Biophys. Acta 1102, 1-18.

45. Weiner, J.H., Shaw, G., Turner, R.J. and Trieber, C.A. (1993) The topology of the anchor subunit of dimethyl sulfoxide reductase of *Escherichia coli.* J. Biol. Chem. 268, 3238-3244.

46. Weiner, J.H., Turner, R.J., Bilous, P., Rothery, R., Sambasivarao, D, and Shaw, G. (1998) Characterization of a novel *moeB*

mutant unable to assemble molybdopterin cofactor into dimethylsulfoxide reductase. Manuscript in preparation.

Chapter 5 : DmsABC Assay Characterization and Development*

5.1. Introduction

Several assays have been developed to monitor the activity of terminal reductases. The most widely used is a spectrophotometric assay, measuring the substrate-dependent oxidation of reduced viologen. Both open cuvette [40, 46, 54] and closed cuvette versions [9, 38] of this assay have been developed. Open cuvette assays leave the assay constituents exposed to air/O_2, while for the closed cuvette assay, O_2 is excluded by stoppering the cuvette, and by using degassed and N_2 bubbled buffer. Although viologens are not Q analogues, and electrons bypass normal flow through the enzyme [24, 50, 51], the popularity of viologen assays results from assay simplicity, and ease of obtaining substrate.

Spectroscopic assays using a variety of Q analogues have also been developed. Once again, open cuvette [46, 55], and closed cuvette versions have been developed [27, 35, 43, 51]. These assays are slightly more complicated due to severe O_2 sensitivity [11, 43], poorer solubility of Q [25] as compared with viologens, overlapping wavelengths of oxidized and reduced Q [32], difficulty in obtaining substrate, and difficulty in determining the actual concentration of Q in the membrane bilayer [13].

These optical spectroscopy assays can be used to measure DMSO reduction by DmsABC. However, they measure either oxidation of reducing agent, or electron donor, rather than formation of reduced product, and are limited by the extinction coefficient of the compound followed.

---

* A version of this chapter has been published. Simala-Grant, J. L. and Weiner, J. H. (1996) Kinetic analysis and substrate specificity of *Escherichia coli* dimethylsulfoxide reductase. Microbiol. 142, 3231-3239. This chapter includes Figure 2 from this paper (now Figure 5.1.), as well as other previously unpublished data.

Since DMSO and DMS are compounds important in the global sulfur cycle [2], and TMAO and TMA are found in high concentrations in marine fish and invertebrates [39], techniques have been developed to determine their concentrations in air, water, and marine organisms, and these techniques could be used for kinetic analysis. These techniques include analysis by gas chromatography (DMSO/DMS/TMA) [1, 20, 42], mass spectroscopy (DMSO) [4], titration with picrate salt (TMA) [36], TMA specific electrode [10], and conductance changes (TMA) [12, 41]. However, none of these techniques are as convenient as the spectroscopic assays listed above.

In addition to the techniques listed above that measure product formation, two others have also been developed. Micellar electrokinetic chromatography (MEKC) [48], and NMR spectroscopy [26], have been used to measure DMS, and DMS/TMA formation, respectively. These techniques are more time consuming than the spectroscopic techniques, but may prove useful for those with the equipment necessary to carry out this type of analysis.

Our lab has historically used the open cuvette assay due to its ease, generally using $BVH^{\cdot +}$ or as necessary $DMNH_2$, as electron donor. Our collaboration with Dr. Giordano of the CNRS in Marseille France, led to our introduction to the closed cuvette assay.

We have characterized parameters influencing DmsABC activity in the open and closed cuvette assays, and determined kinetic constants for the electron donor portion of the reaction, using $BVH^{\cdot +}$ and $DMNH_2$. We have also examined the usefulness of NMR spectroscopy for kinetic analysis of DmsABC.

5.2. Methods and Materials

5.2.1. Materials

S- and N-oxides were purchased from Sigma or Aldrich. 2,3 dimethyl-1,4-napthoquinone (DMN) was a gift from A. Kroger, J. W. Goethe University, Frankfurt, Germany. All other materials were reagent grade, and were purchased from commercial sources.

5.2.2. Strains and Plasmids

E. coli strain HB101 (*supE*44 *hsdS*20($r_B^-m_B^-$) *recA*13 *ara*-14 *procA*2 *lacY*1 [6]) and plasmid pDMS160 (pBR322 Amp^R $(dmsABC)^+$ [45]), were used in this study. HB101 was transformed with pDMS160, for overexpression of DmsABC. All manipulations of plasmids and strains were carried out essentially as described by Sambrook *et al.* [47].

5.2.3. Media and Growth Conditions

HB101/pDMS160 was grown aerobically in LB or Terrific Broth [47] overnight, and these cultures were used as 1% inocula for Gly/Fum, as indicated previously [5], with the following exceptions. 0.16% peptone was substituted for casamino acids, and streptomycin sulfate was not included in the growth medium. Vitamin B1, proline and leucine were included at a final concentration of 0.005%. 50-100 μg/mL ampicillin was included in the growth medium.

5.2.4. Purification of DmsABC

HB101/pDMS160 grown anaerobically on Gly/Fum, in 19 L carboys, for 48 hours, at 37°C, was harvested using a Pellicon membrane system equipped with a Millipore polysulfone PTNK filter. The concentrated cell mixture was then centrifuged at 9,500 x g for 10 minutes, and subsequently resuspended in buffer [45]. Everted envelopes were prepared by French pressure lysis and centrifugation [5]. As necessary, membrane fractions were extracted with Triton X-100 [8]. DmsABC was purified from solubilized membrane proteins on either a DEAE-cellulose (Whatman DE-52) column as indicated previously [52], except that a 0-0.2 M KCl gradient was used, equivalent to ten column volumes, or on a DEAE-Sepharose CL-6B column with a 50-300 mM NaCl gradient, equivalent to two column volumes.

5.2.5. Kinetic Assays

Degassed and N_2 bubbled 50 mM MOPS, pH 7.0, was used as the buffer for all assays. Electron donor and acceptor were varied as necessary while maintaining a constant final assay volume. Assay temperature is indicated in the Table notes. Enzyme was stored at -70°C prior to use. When diluted, it was stored on ice during the day, to obtain reproducible results.

A Gilford 250 spectrophotometer was used for BV and DMN assays.

S- and N-oxide dependent oxidation of $BVH^{\cdot+}$, was monitored at 570 nm. The order of addition was : BV^{2+}, S- or N-oxide, dithionite, and enzyme unless otherwise indicated. For open cuvette (non-stoppered) assays, BV was used at a final concentration of 0.2 mM unless otherwise indicated ($\varepsilon\ BVH^{\cdot+} = 7.8\times10^{3}$ L mol^{-1} cm^{-1}), and sodium dithionite (dithionite) at a concentration of 0.33 mM. Closed cuvette assays (stoppered) were performed by transferring buffer to a cuvette, that was subsequently stoppered, excluding air. Hamilton syringes were used for the ordered addition as above. A stable baseline was confirmed prior to addition of enzyme. For closed cuvette assays, BV was used at final concentration of 0.2 mM, and dithionite was added to approximately 0.1 mM, to give an absorbance of about 1.0 OD, unless otherwise indicated in the text. One unit of enzyme activity corresponds to 2 µmol of $BVH^{\cdot+}$ oxidized per minute, or 1 µmole of S- or N-oxide reduced per minute.

$$1.\ S_2O_4 + 2H_20 + O_2 \longrightarrow 4HSO_3$$

$$2.\ S_2O_4 + 2H_20 + 2BV^{2+} \longrightarrow 2HSO_3 + 2BVH^{\cdot+}$$

Dithionite serves to reduce BV^{2+} (equation 2) However in the closed cuvette assay dithionite will also react with the oxygen dissolved in solution.

DMNH$_2$ oxidation was followed by monitoring the S- or N-oxide dependent decrease in dithionite absorbance at 317 nm (ε dithionite = 8.0 mM^{-1} cm^{-1}) [55]. A 1 x 1 cm cuvette was used, and a 9 x 9 mm quartz spacer was inserted into the cuvette to employ a light path of 1 mm. Dithionite, TMAO and DMSO, were used at the following final concentrations in mM : 1.8, 379, and 7.5, respectively, unless otherwise indicated. 1 unit of enzyme activity corresponds to 1 μmol of dithionite or DMNH$_2$ oxidized, or S- or N-oxide reduced per minute.

For assays utilizing NMR spectroscopy, buffer was transferred to a 0.5 mL NMR tube being bubbled with N_2. Hamilton syringes were used for the ordered addition of : BV (0.2 mM), TMAO (70 mM) / DMSO (0.9 mM), enzyme, and dithionite (0.2 mM). A Varian Unity 300 NMR spectrometer was used to collect ^{1}H-NMR spectra at 300 MHz. The spectra in each set were acquired with a 60 degree pulse over a sweep width of 4000 Hz, and with a total recycle time of 23.90 s. The data was collected in 32 K data points, zero filled to 64 K, and transformed with a linebroadening of 1.0 Hz. Each spectrum was individually drift corrected to allow accurate measurement of peak heights and integrals.

For determination of kinetic constants, between 3 and 9 assays were performed at each substrate concentration, and 5-8 different substrate concentrations were examined to determine each K_m. The values used were the means. In all cases, the standard deviation of the means was less than 10%. A range of substrate concentrations was chosen that varied from at least two times less than the K_m to five times greater than the K_m. We ensured only a small fraction of substrate was utilized during the experiment. K_m and V_{max} values were determined from Eadie-Hofstee plots [14]. The kinetic values obtained are apparent values, with either saturating electron donor or acceptor. As necessary,

k_{cat} values were determined by estimating enzyme purity from PAGE analysis, as indicated in analytical techniques.

5.2.6. Analytical Techniques

Protein concentrations were determined [33], prior to performing PAGE using the BioRad mini-gel system, with a discontinuous SDS buffer system [28]. Gels were stained with Coomassie blue, destained [30], and scanned with a Joyce-Loebel Chromoscan 3 densitometer, to determine DmsABC purity. Confirmation of bands on the polyacrylamide gel corresponding to DmsA and B, was determined by Western blotting [46]. DmsA and B polyclonal antibodies were used separately. ECL western blotting detection reagents from Amersham Life Sciences were used for blot development. No antibody has been successfully raised against DmsC. This subunit's position was estimated from its known molecular weight, and migration as compared with previously purified DmsABC.

5.3. Results

5.3.1. Dithionite Inhibits DmsABC

We examined the kinetic parameters of DmsABC, with the substrate TMAO, using both open and closed cuvette assays (Table 5.1.). The open cuvette assay has been traditionally used by our lab, however the closed cuvette assay was introduced to our lab by Dr. Gerard Giordano. With membrane-bound DmsABC, the K_m values determined using either assay type were similar. However, when assays were carried out with purified DmsABC, we noted at least a four-fold higher apparent K_m value for TMAO under open cuvette conditions compared with closed cuvette conditions. The closed cuvette K_m for purified DmsABC was close to the value for membrane-bound DmsABC. k_{cat} values were depressed about 15%, when using open cuvette conditions.

Table 5.1.

TMAO K_m Values for DmsABC, Using Open and Closed Cuvette Assays

	TMAO K_m	
Enzyme	**Open Cuvette Assay**	**Closed Cuvette Assay**
Membrane Bound	32	25
Detergent Solubilized	42	ND
Purified	72	18

K_m values are reported in mM. Assays were performed at 21°C. ND indicates not determined. Detergent solubilized DmsABC was used immediately after extraction.

When the assays were performed with detergent-solubilized DmsABC, used immediately after extraction, an intermediate K_m for TMAO was obtained utilizing the open cuvette assay, potentially resulting from enzyme showing intermediate inhibition (see below).

Further investigation of the two assays indicated the apparent K_m differences resulted from the dithionite used to produce $BVH^{\cdot+}$. The open cuvette assay requires an excess of dithionite to BV. This results in a lag phase before consumption of $BVH^{\cdot+}$ is observed, during which time the excess dithionite is being consumed. In contrast closed cuvette assay excludes O_2, (using a stoppered cuvette filled with degassed and N_2-bubbled buffer), and uses only enough dithionite to reduce a portion of the BV^{2+}. Figure 5.1. illustrates the K_m values obtained when increasing concentrations of dithionite were used in the closed cuvette assay, in essence mimicking the conditions of the open cuvette assay, with excess dithionite, but no airspace at the top of the cuvette. Purified enzyme was used, with TMAO as substrate. If you extrapolate the line in Figure 5.1., it suggests the K_m for TMAO using 0 mM dithionite would be essentially equivalent to that of the closed cuvette assay. Dithionite appears to approximate a competitive inhibitor, as apparent K_m increases with increasing dithionite concentration in the assay. Increasing concentrations of dithionite had less effect on V_{max} (Figure 5.1.). This effect is observed although all of the dithonite was consumed prior to measurment in the open and closed cuvette assay. It was not possible to quantitate this inhibition accurately, because of assay constraints, as dithionite was used in both assays to reduce BV^{2+}.

We found the product of dithionite oxidation, sodium bisulfite, was also an inhibitor of DmsABC. (See reaction 2 page 163.) Breakdown of all dithionite in the cuvette, would result in a maximum total bisulfite concentration of 0.66 or 0.2 mM, in the open and closed cuvette assays, respectively. 0.66 mM bisulfite has no effect on the apparent K_m for TMAO. The half maximal inhibition of velocity for bisulfite occurred at 25 mM. This indicates that although bisulfite was

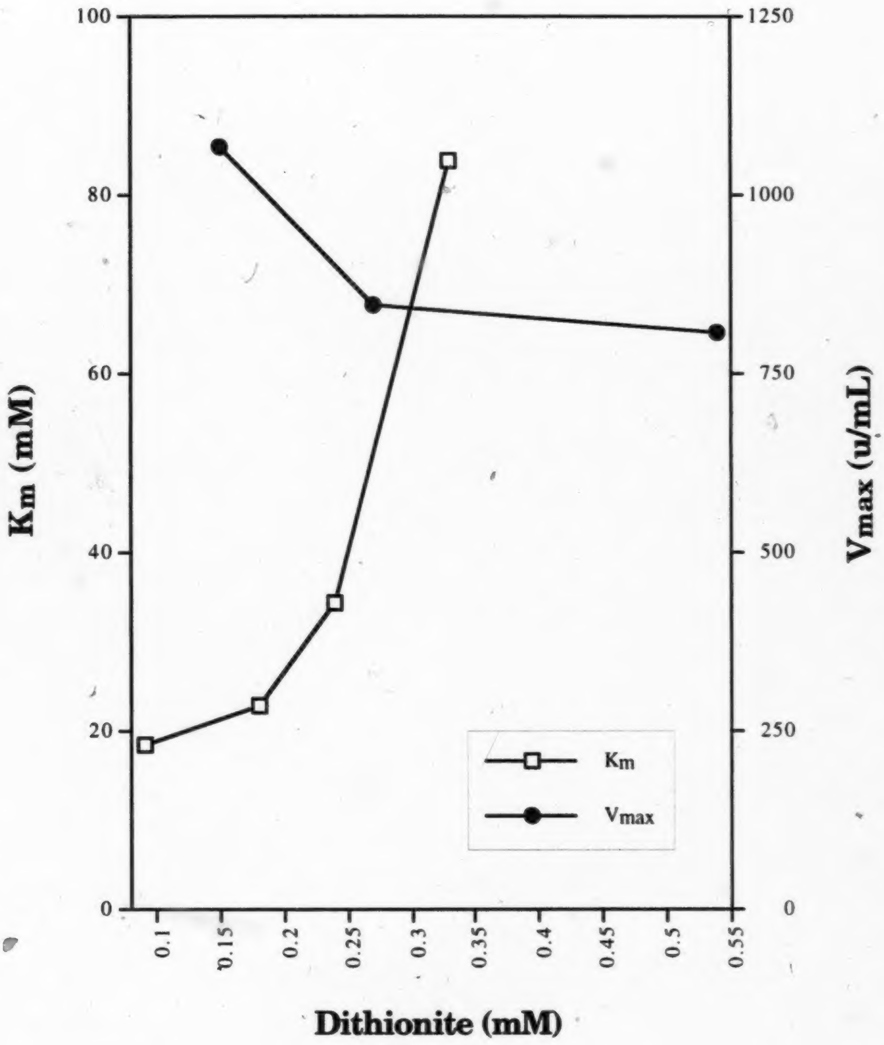

Figure 5.1.

TMAO K_m and V_{max} Values for Purified DmsABC, Using the Closed Cuvette Assay with Increasing Concentrations of Dithionite

Assays were performed at 21°C.

an inhibitor of velocity at high concentrations, the inhibition we have documented as occurring during the open cuvette assay was due to excess dithionite, and not bisulfite produced during the assay.

Order of addition effects are also observed. If dithionite is incubated with DmsABC prior to the addition of substrate, k_{cat} values drop to approximately 50% of their normal value. (K_m values were not determined under these conditions.) This inactivation occurs within 45 seconds. Concentrations of PNO, DMSO, and TMAO, 5 times above their K_m, were not able to reverse dithionite inactivation if DmsABC came into contact with dithionite before substrate.

5.3.2. Glycerol Depresses Apparent K_m and V_{max} Values

The open cuvette assay was used to determine the K_m for TMAO in the presence of increasing concentrations of glycerol. (Since glycerol is known to be a good protein stabilizing agent [37], we thought glycerol might stabilize purified enzyme, such that it would behave like membrane bound enzyme in Table 5.1.). As the amount of glycerol in the buffer increased, K_m and V_{max} values decreased, both at approximately the same rate (Figure 5.2. and Table 5.2.). The effects observed with increasing amounts of glycerol in the buffer suggests glycerol is approximating an uncompetitive inhibitor, binding strictly to the ES complex. Since enzyme stored in the presence of glycerol and then diluted for use in assays (See Table 2.4.) does not show the extreme drop in velocity as observed here, this confirms inhibition is reversible. As a result, the use of glycerol in buffers does not appear to be a concern.

5.3.3. Apparent K_m and k_{cat} Values for $BVH^{\cdot+}$ and $DMNH_2$

Apparent K_m and k_{cat} values for the artificial electron donors $BVH^{\cdot+}$ and $DMNH_2$, were determined using saturating concentrations of TMAO and DMSO.

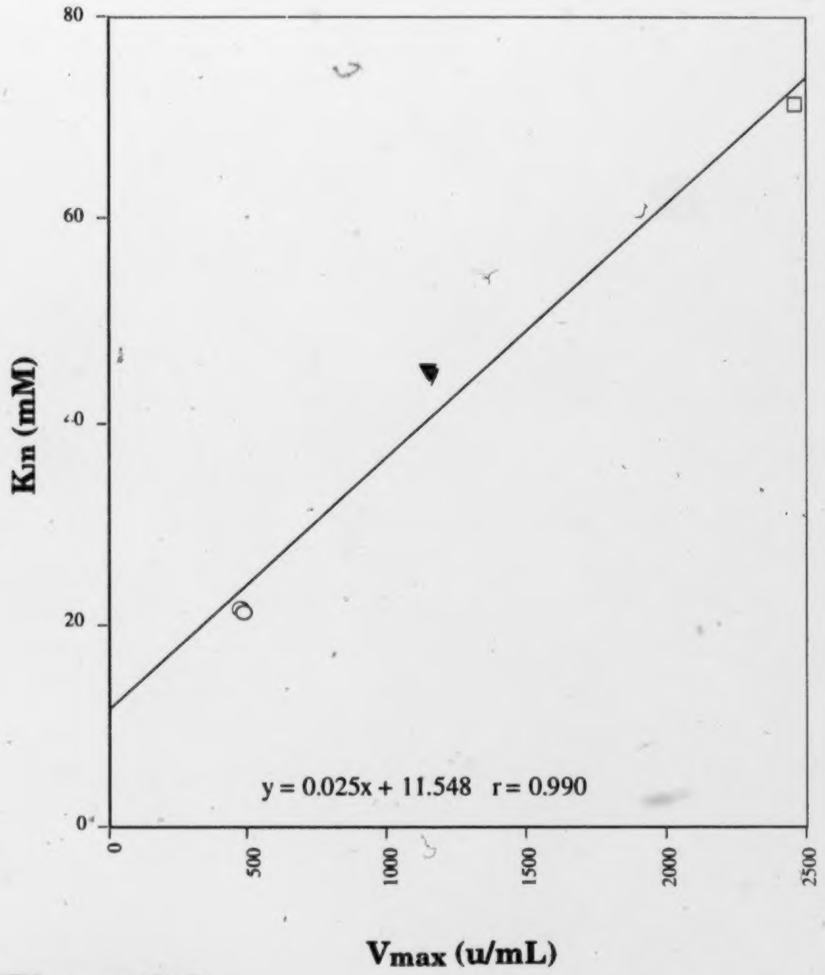

Figure 5.2.

TMAO K_m versus V_{max} for Purified DmsABC, with Increasing Concentrations of Glycerol in the Assay Buffer

Open cuvette assays were performed at 21°C. ☐ no glycerol : K_m 72, V_{max} 2460; ▼ 20% glycerol K_m 32, V_{max} 1160; O 40% glycerol K_m 21, V_{max} 494. One u (unit) of enzyme activity corresponds to 1 μmol of dithonite oxidized or S- or N- oxide reduced per minute.

Table 5.2.

TMAO K_m and V_{max} for Purified DmsABC, Using Increasing Concentrations of Glycerol in the Open Cuvette Assay

% Glycerol	K_m	Relative K_m	V_{max}	Relative V_{max}
0	72	100	2460	100
20	32	63	1160	47.3
40	21	30	494	20.1

Assays were performed at 21°C. K_m's are reported in mM, V_{max}'s in u/mL. Relative K_m and V_{max} values are expressed as a % of K_m or V_{max} using no glycerol in the assay buffer. One u (unit) of enzyme activity corresponds to 1 μmol of dithonite oxidized or S- or N- oxide reduced per minute.

The DMN open cuvette assay requires excess dithionite to DMN. As a result, DmsABC, overexpressed in membranes, is the desired form of the enzyme for use in these assays, since dithionite does not competitively inhibit this form of the enzyme (Table 5.1.).

Membrane samples contain endogenous MQ that could interfere with $DMNH_2$ kinetics, if reduced by dithionite. Endogenous reduced MQH_2, and $DMNH_2$, could compete for binding to DmsABC. We examined whether endogenous MQ was reduced by dithionite, and subsequently used by DmsABC. Membranes enriched in DmsABC were incubated with DMSO and dithionite. Little dithionite was consumed, indicating reduction of endogenous MQ by dithionite and utilization of reduced MQH_2 by DmsABC is minimal during the course of the experiment.

Table 5.3. shows the K_m and k_{cat} values for $DMNH_2$ and $BVH^{\cdot +}$, using either saturating TMAO or DMSO

Unfortunately, the $BVH^{\cdot +}$ K_m's are too low to be determined by this technique. The K_m's for $DMNH_2$ are 0.028 and 0.23, for DMSO and TMAO, respectively (Table 5.3.).

The BV k_{cat}'s are highly influenced by electron acceptor while the k_{cat}'s for DMN are not. This suggests the kinetic mechanisms for BV and DMN differ.

(Chapter 6 addresses the kinetic parameters for the electron acceptor side of the reaction.)

5.3.4. DmsABC Kinetic Assay Using NMR Spectroscopy

NMR spectroscopy is more sensitive than optical spectroscopy, in that NMR has a detection limit of 10 nmoles of TMA, while optical spectroscopy has a detection limit of 100 nmoles of product formed. With NMR spectroscopy it is possible to alter BV concentration outside

Table 5.3.

Electron Donor K_m and V_{max} for DmsABC, with Saturating Electron Acceptor

Electron Donor	Electron Acceptor	K_m (mM)	V_{max} (u/mg)
$DMNH_2$	TMAO	0.225	196
$DMNH_2$	DMSO	0.028	140
$BVH^{\cdot+}$	TMAO	<0.02	601
$BVH^{\cdot+}$	DMSO	<0.02	40.0

The DMN open cuvette assay, or BV closed cuvette assay, was performed at 30°C, using washed membranes. spectra not shown). One u (unit) of enzyme activity corresponds to 1 μmol of dithonite or $DMNH_2$ oxidized, or S- or N- oxide reduced per minute.

the optically measurable range. As a result, this technique may allow determination of the K_m for $BVH^{\cdot +}$. NMR spectroscopy has been used previously to examine DmsABC turnover, but only in whole cells [26].

NMR spectroscopy was examined as a method of measuring the kinetics of product formation (DMS and TMA) using detergent solubilized DmsABC. Under the conditions employed, all peaks could be assigned as follows in ppm : MOPS = 2.05, 2.95, and 3.85; BV^{2+} = 5.9, 7.5, 8.5, 9.1; $BVH^{\cdot +}$ = 7.5; TMAO = 3.24; TMA = 2.875; and DMS = 2.058. Figure 5.3. shows conversion of TMAO to TMA by DmsABC (full spectra not shown). It is also possible to follow the conversion of DMSO to DMS by DmsABC; however, it is slightly more difficult under the conditions employed, as the DMS peak falls under the MOPS 2.05 ppm peak (Figure 5.4.). Use of an alternative buffer, that does not possess a 2.05 ppm peak, would be preferred to perform accurate and quantitative kinetics using DMSO as substrate.

TMA production was followed by obtaining spectra every 23.9 s, and TMA peaks were integrated from each spectra (Figure 5.5.). A plot of TMA peak integral height versus spectra number demonstrates product formation is linear over time (Figure 5.6.). Various concentrations of enzyme could be used in the assay, demonstrating product formation was also linear with respect to enzyme concentration (Figure 5.6).

For the determination of kinetic constants, measurements would be taken before substantial amounts of product had formed. However, Figure 5.6. shows that when 10% of TMAO was converted to TMA, no product inhibition was observed.

The conditions chosen for NMR kinetics closely parallel those of the closed cuvette assay, the differences being the NMR tube, method of measurement, and enzyme is added before dithionite. The k_{cat}

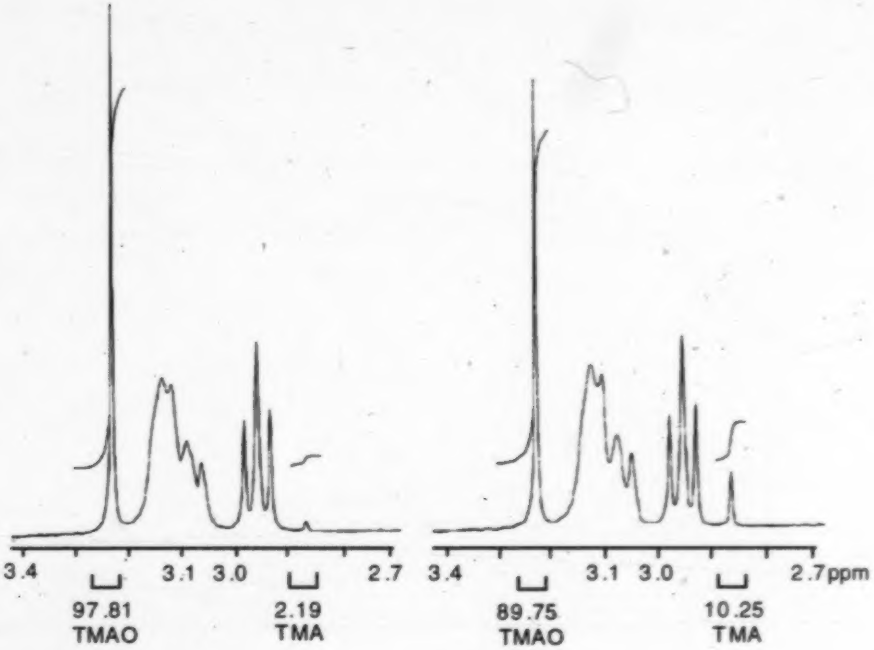

Figure 5.3.

DmsABC Kinetic NMR Spectra with TMAO as Substrate

Left spectra time = 0. Right spectra time = 12 minutes. TMAO and TMA peaks are labelled and integrated. The % area of integration of TMAO and TMA, is indicated with respect to the sum of these peaks. Twenty uL detergent solubilized DmsABC was used, and the assay was performed as indicated in Materials and Methods.

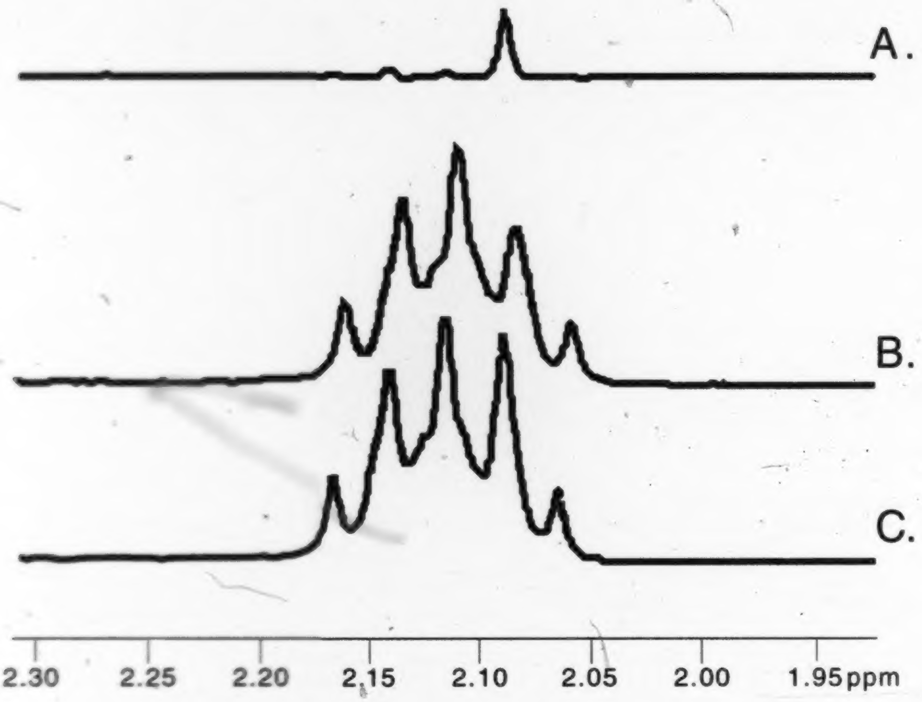

Figure 5.4.

DmsABC Kinetic NMR Spectra Using DMSO as Substrate

Twenty uL detergent solubilized DmsABC was used for the assay as indicated in Material and Methods. A. Difference spectra, B. Spectra at Time 0, C. Spectra at 30 minutes.

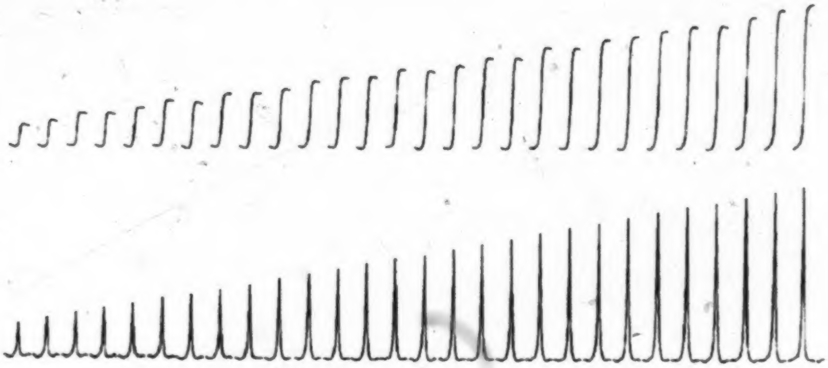

Figure 5.5.

TMA Peaks and Corresponding Integrals Over Time

Twenty uL detergent solubilized DmsABC was used for the assay, as indicated in Materials and Methods. Spectra were obtained every 23.9 seconds. The TMA peak from each spectra, and its corresponding integral, are plotted above.

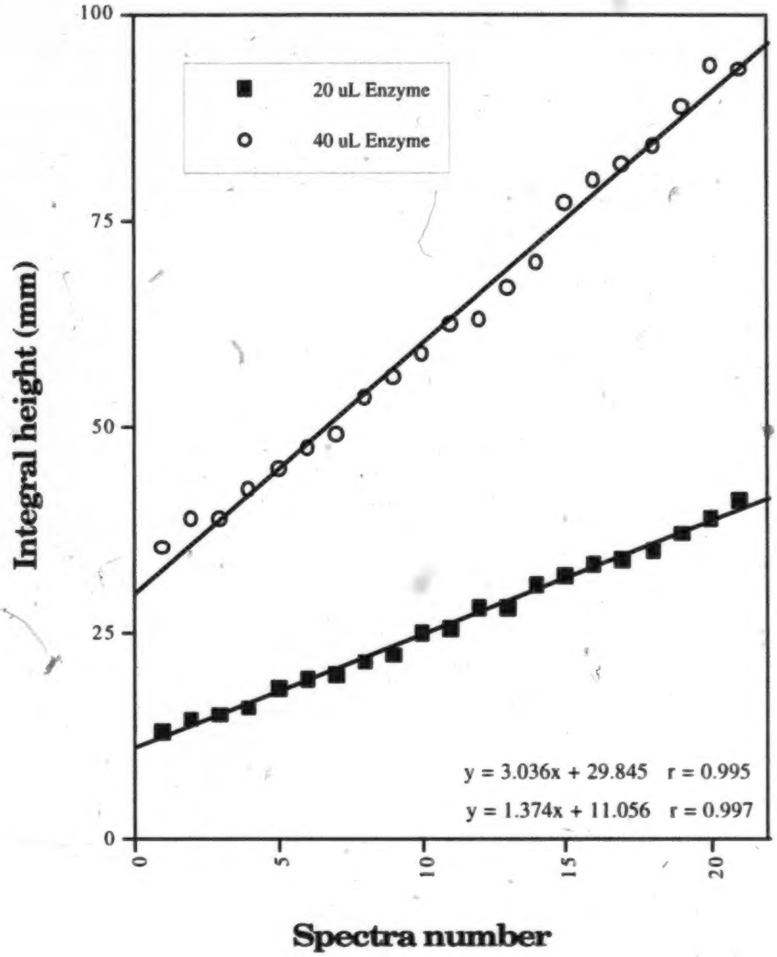

Figure 5.6.

TMA Integral Height is Linear with Time, and Two Concentrations of DmsABC

The TMA peaks from each spectra, obtained as indicated in Materials and Methods, were integrated, and integral height measured.

determined by NMR spectroscopy, using saturating BV and TMAO, was 1/3 that determined optically using the closed cuvette assay. To try and identify the source of this discrepancy, optical assays were performed using shortened NMR tubes, and modified cuvette holder. DmsABC activity as calculated by optical spectroscopy or by NMR, using an NMR tube, gave the same low results. The decreased k_{cat} values could be the result of increased surface area of the NMR tube as compared with the cuvette, or slow mixing due to narrow NMR tube width. The large surface area of the NMR tube may cause some inactivation due to denaturation, as the enzyme passes down the side of the tube. However, this is not likely, as NMR tubes of different lengths showed the same low k_{cat}. Slow mixing as a result of narrow tube width, could result in DmsABC contacting dithionite prior to substrate, resulting in partial inactivation. To rectify this, we tried using a large diameter NMR tube.However, O_2 interference resulted due to a large increase in the total volume of gas above the sample. On mixing, the dithionite was immediately oxidized.

5.4. Discussion

The results reported herein suggest caution when using enzyme assays. Compounds or conditions necessary for assay function, may inhibit the enzyme of interest. We have shown excess dithionite to approximate a competitove inhibitor, and glycerol to be an uncompetitive inhibitor of DmsABC. Conditions inherent to the NMR spectroscopy assay appear to inhibit DmsABC velocity. Nevertheless, kinetic parameters can be obtained using these assays, and do yield useful information regarding enzyme function.

Only 0.26 moles of MGD are found per mole of purified DmsABC [44]. A major proportion of cofactor appears to either dissociate, or is oxidatively destroyed during enzyme purification. This observation suggests DmsABC tertiary structure may change during, and subsequent to extraction from the membrane. This change in tertiary structure not only allows moco to dissociate or be oxidatively destroyed, but correlates with the ability of dithionite to act as a competitive inhibitor. We observed dithionite approximates a competitive inhibitor of purified, but not membrane bound DmsABC. Freshly solubilized DmsABC was inhibited to an intermediate extent. This suggests structural changes occur on extraction from the membrane, and become more severe after purification.

Various anions have been observed to ligate to Mo(V) in molybdoenzymes [7, 16, 17, 19, 29]. It has been postulated that dithionite may also be able to ligate Mo(V) [3]. Dithionite may competitively inhibit DmsABC through its ligation to the Mo, interfering with enzyme activity. We would suggest this can only occur once tertiary structure is perturbed, as in purified enzyme, or less so in detergent solubilized enzyme.

Another feature of dithionite inhibition involves the order of addition effects observed. A similar observation has been characterized for NDH-I. Incubation of electron donor with enzyme, prior to addition of electron acceptor, resulted in increased K_m and decreased k_{cat} [21, 34]. Inhibition of NDH-I is suggested to be irreversible. Our results also suggest enzyme reduction by dithionite under non-turnover conditions, may damage DmsABC thereby decreasing its velocity. Further analysis could characterize the site of inhibition, and whether this inhibition is reversible.

Since excess dithionite inhibits DmsABC, future assay characterization could involve the use of viologens reduced in an electrochemical cell [23, 49], or MQ analogues reduced separate from the assay mixture, using sodium borohydride [35], acidified zinc, or NADH dehydrogenase [31]. These procedures solve two problems : they eliminate the use of dithionite, and result in minimal or no transfer of excess reducing equivalents to the assay.

Glycerol has been observed to bind to Mo(V) of DMSOR, locking it in this redox state, under non-turnover conditions [15, 18]. Glycerol appears to act as an uncompetitive inhibitor of DmsABC, as increasing concentrations in the assay result in a decrease in K_m and V_{max} values for electron acceptor. Since we observed this inhibition under turnover conditions, it is not likely glycerol is inhibiting the enzyme in the same manner as was observed for DMSOR [15, 18]. One would likely predict competitive inhibition from their observations. Reduction of DMSO involves two protons, and increasing concentrations of glycerol could result in a solvent effect, such that glycerol interferes with the donation of protons from water to an active site residue.

Control experiments suggested endogenous MQ did not interfere with DMN kinetics. MQ was not reduced and oxidized in the presence of dithionite and DMSO. However, future kinetic studies could employ the use of mutants deficient in MQ synthesis [53]. This would ensure no interference by endogenous MQ reduced by $DMNH_2$.

Since this work was performed two MQ analogues have been tested as substrates of DmsABC. Lapachol was found to be a substrate with a k_{cat} and K_m of 191 s^{-1} and 0.24 mM, respectively [43]. These values are within 95% of those obtained for $DMNH_2$ in this chapter. In contrast, 5-hydroxy-2-methyl-1,4-napthoquinone (plumbagin), was not observed to be a substrate for DmsABC. This may be due to the absence of a methyl group in the 3' position, its additional hydroxy group, or less likely due to its increased redox potential [43]. To examine the structure of the MQH_2 binding site in DmsABC, this study could be extended by using additional MQ analogues. Alternatively, natural Q's could be used by fusing Q containing liposomes with membranes deficient in Q [53]. Since the Q binding site exists within the membrane bilayer, Q K_m's include their partition coefficient, eliminating a direct K_m comparison. However, methods have been developed to overcome this difficulty [13].

Our preliminary results, suggests BV and DMN utilize different kinetic mechanisms. This is not surprising since the same has been found for NarGHI, when using BV, methyl viologen (MV), duroquinol, and ubiquinol-1 [35]. Trieber et al. have shown electrons from different sources follow differing paths through DmsABC [50], and it is widely accepted that Q analogues and viologens bind to different sites on terminal reductases [11, 51]. These observations support the potential for different kinetic mechanisms when using Q analogues and viologens with DmsABC.

The NMR spectroscopy assay was examined further, using detergent solubilized DmsABC. Unfortunately, some condition related most likely to the NMR tube itself, resulted in a lowered k_{cat} for BVH$\cdot^{+}$/TMAO. Although requiring more time, this assay requires the same amount of enzyme as optical assays. It is particularly suitable for following TMA production, which cannot be done using an optical assay. Changing the buffer system, and possibly incorporating a small percentage of methanol or ethanol that would not be detrimental to enzyme function, but may prevent escape of volatile DMS, would allow use of this assay for quantitative DMS analysis.

Various analytical assays used to measure terminal reductase activity have different detection limits. Optical spectroscopy has a lower detection limit of 100 nmoles of product; this is similar to the detection limit for the TMA-specific electrode, and picrate titration method of TMA [10]. NMR has a detection limit of 10 nmoles of product (TMA), similar to that found for gas chromatography analysis of DMSO/DMS [22]. Advantages of NMR spectroscopy are, the detection limit is increased 10 fold compared to optical spectroscopy assays, and it does not suffer with overlapping absorption bands as is observed for some Q analogue assays. (A recent alternative is provided using lapachol and plumbagin where overlapping absorption bands are not a problem [43]). However, NMR spectroscopy is still not sensitive enough to measure the K_m for BV. It appears to be less than 0.02 mM. This would require measurement of approximately 100 pmoles of product. This analysis appears to require the use of MEKC which has a lower detection limit of 0.5 pmoles [48].

5.5. References

1. Andrea, M.O. (1980) Determination of trace quantities of dimethylsulfoxide in aqueous solutions. Anal. Chem. 52, 150-153.

2. Andreae, M.O. and Crutzen, P.J. (1997) Atmospheric aerosols: biogeochemical sources and role in atmospheric chemistry. Science 276, 1052-1057.

3. Bennett, B., Benson, N., McEwan, A.G. and Bray, R.C. (1994) Multiple states of the molybdenum center of dimethylsulphoxide reductase from *Rhodobacter capsulatus* revealed by EPR spectroscopy. Eur. J. Biochem. 225, 321-331.

4. Berresheim, H., Tanner, D.J. and Eisele, F.L. (1993) Real-time measurement of dimethylsulfoxide in ambient air. Anal. Chem. 65, 84-86.

5. Bilous, P.T. and Weiner, J.H. (1985) Dimethyl sulfoxide reductase activity by anaerobically grown *Escherichia coli*. J. Bacteriol. 162, 1151-1155.

6. Boyer, H.W. and Roulland-Dussoix, D. (1969) A complementary analysis of the restriction and modification of DNA in *Escherichia coli*. J. Mol. Biol. 41, 459.

7. Bray, R.C., Gutteridge, S., Lamy, M.T. and Wilkinson, T. (1983) Equilibria amongst different molybdenum (V)-containing species from sulphite oxidase. Biochem. J. 211, 227-236.

8. Cammack, R. and Weiner, J.H. (1990) Electron paramagnetic resonance spectroscopic characterization of dimethyl sulfoxide reductase of *Escherichia coli*. Biochemistry 29, 8410-8416.

9. Cecchini, G., Ackrell, B.A.C., Deshler, J.O. and Gunsalus, R.P. (1986) Reconstitution of quinone reduction and characterization of *Escherichia coli* fumarate reductase activity. J. Biol. Chem. 261, 1808-1814.

10. Chang, G.W., Chang, W.L. and Lew, K.B.K. (1976) A trimethylamine-specific electrode for fish quality control. J. Food Sci. 41, 723-724.

11. Craske, A. and Ferguson, S.J. (1986) The respiratory nitrate reductase from *Paracoccus denitrificans*. Molecular characterisation and kinetic properties. Eur. J. Biochem. 158, 429-436.

12. Easter, M.C., Gibson, D.M. and Ward, F.B. (1982) A conductance method for the assay and study of bacterial trimethylamine oxide reduction. J. Appl. Bact. 52, 357-365.

13. Fato, R., Castelluccio, C., Palmer, G. and Lenaz, G. (1988) A simple method for the determination of the kinetic constants of membrane enzymes utilizing hydrophobic substrates: ubiquinol cytochrome *c* reductase. Biochim. Biophys. Acta 932, 216-222.

14. Fersht, A. (1977) Chapter 10: Enzyme-substrate complementarity and theories of enzyme catalysis, in Enzyme structure and mechanism. 1st ed., p. 244-271, W. H. Freeman, San Francisco.

15. Finnegan, M.G., Hilton, J., Rajagopalan, K.V. and Johnson, M.K. (1993) Optical transitions of molybdenum (V) in glycerol-inhibited DMSO reductase from *Rhodobacter sphaeroides*. Inorg. Chem. 32, 2616-2617.

16. Fish, K.M., Massey, V., Sands, R.H. and Dunham, W.R. (1990) The interaction of bisulfite with milk xanthine oxidase. J. Biol. Chem. 265, 19665-19671.

17. George, G.N., Bray, R.C., Morpeth, F.F. and Boxer, D.H. (1985) Complexes with halide and other anions of the molybdenum center of nitrate reductase from *Escherichia coli*. Biochem. J. 277, 925-931.

18. George, G.N., Hilton, J. and Rajagopalan, K.V. (1996) X-ray absorption spectroscopy of dimethyl sulfoxide reductase from *Rhodobacter sphaeroides*. J. Am. Chem. Soc. 118, 1113-1117.

19. George, G.N., Turner, N.A., Bray, R.C., Morpeth, F.F., Boxer, D.H. and Cramer, S.P. (1989) Xray-absorption and electron-paramagnetic resonance spectroscopic studies of the environment of molybdenum in high-pH and low-pH forms of *Escherichia coli* nitrate reductase. Biochem. J. 259, 693-700.

20. Gibson, J.A.E., Garrick, R.C., Burton, H.R. and McTaggart, A.R. (1990) Dimethylsulfide and the algae *Phaeocyctis pouchetii*. Mar. Biol. 104, 339-346.

21. Gutman, M., Schejter, A. and Avi-Dor, Y. (1968) The preparation and properties of the membranal DPNH dehydrogenase from *Escherichia coli*. Biochim. Biophys. Acta 162, 506-517.

22. Hatton, A.D., Malin, G., McEwan, A.G. and Liss, P.S. (1994) Determination of dimethyl sulfoxide in aqueous solution by an enzyme-linked method. Anal. Chem. 66, 4093-4096.

23. Huber, C., Skopan, H., Feicht, R., White, H. and Simon, H. (1995) Pterin cofactor, substrate specificity, and observations on the kinetics of the reversible tungsten-containing aldehyde oxidoreductase from *Clostridium thermoaceticum.* Arch. Microbiol. 164, 110-118.

24. Jones, R.W. and Garland, P.B. (1977) Sites and specificity of bipyridylium compounds with anaerobic respiratory enzymes of *Escherichia coli* Effects of permeability barriers imposed by the cytoplasmic membrane. Biochem. J. 164, 199-211.

25. Kauten, R., Tsai, A.-L. and Palmer, G. (1987) The kinetics of reduction of yeast complex III by substrate analog. J. Biol. Chem. 262, 8658-8667.

26. King, G.F., Richardson, D.J., Jackson, J.B. and Ferguson, S.J. (1987) Dimethylsulphoxide and trimethylamine-N-oxide as bacterial electron transport acceptors: use of nuclear magnetic resonance to assay and characterise the reductase system in *Rhodobacter capsulatus*. Arch. Microbiol. 149, 47-51.

27. Kroger, A., Dorrer, E. and Winkler, E. (1980) The orientation of the substrate sites of formate dehydrogenase and fumarate reductase in the membrane of *Vibrio succinogenes.* Biochim. Biophys. Acta 589, 118-136.

28. Laemmli, U.K. (1970) Cleavage of structural proteins during the assembly of the head of bacteriophage T4. Nature 227, 680-685.

29. Lamy, M.T., Gutteridge, S. and Bray, R.C. (1980) Electron-paramagnetic-resonance parameters of molybdenum (V) in sulphite oxidase from chicken liver. Biochem. J. 185, 397-403.

30. Lemire, B.D., Robinson, J.J. and Weiner, J.H. (1982) Identification of membrane anchor polypeptides of *Escherichia coli* fumarate reductase. J. Bacteriol. 152, 1126-1131.

31. Lemma, E., Simon, J., Schagger, H. and Kroger, A. (1995) Properties of the menaquinol oxidase (Qox) and of *qox* deletion mutants of *Bacillus subtilis.* Arch. Microbiol. 163, 432-438.

32. Lemma, E., Unden, G. and Kroger, A. (1990) Menaquinone is an obligatory component of the chain catalyzing succinate respiration in *Bacillus subtilis.* Arch. Microbiol. 155, 62-67.

33. Markwell, M.A.D., Haas, S.M., Bieber, L.L. and Tolbert, N.E. (1978) A modification of the Lowry procedure to simplify protein determination in membrane and lipoprotein samples. Anal. Biochem. 87, 206-210.

34. Matsushita, K., Ohnishi, T. and Kaback, H.R. (1987) NADH-ubiquinone oxidoreductase of the *Escherichia coli* aerobic respiratory chain. Biochem. 26, 7732-7737.

35. Morpeth, F.F. and Boxer, D.H. (1985) Kinetic analysis of respiratory nitrate reductase from *Escherichia coli* K12. Biochem. 24, 40-46.

36. Murray, C.K. and Gibson, D.M. (1972) An investigation of the method of determining trimethylamine in fish muscle extracts by the formation of its picrate salt-part1. J. Fd. Technol. 7, 35-46.

37. Neugebauer, J.M. (1990) Detergents : An overview, in Guide to protein purification. Methods in Enzymology, (Deutscher, M.P., ed.), Vol. 182, First ed., p. 258, Academic Press, Inc., Toronto.

38. Neumann, S. and Simon, H. (1984) On a non-pyridine nucleotide dependent 2-oxo-acid reductase of broad substrate specificity from two *Proteus* species. FEBS Lett. 167, 29-32.

39. Norris, E.R. and Benoit, G.J. (1944) Studies on trimethylamine oxide. I. Occurrence of trimethylamine oxide in marine organisms. J. Biol. Chem. 158, 433-438.

40. Oren, A. and Truper, H.G. (1990) Anaerobic growth of halophilic archaebacteria by reduction of dimethylsulfoxide and trimethylamine N-oxide. FEMS Microbiol. Lett. 70, 33-36.

41. Owens, J.D., Miskin, D.R., Wacher-Viveros, M.C. and Benge, L.C.A. (1985) Sources of conductance changes during bacterial reduction of trimethylamine oxide to trimethylammonium in phosphate buffer. J. Gen. Micro. 131, 1357-1361.

42. Ritskes, T.M. (1975) The gas chromatographic determination of trimethylamine and dimethylamine in fish, fishery products and other foodstuffs. J. Fd. Technol. 10, 221-228.

43. Rothery, R., Chatterjee, I., Kiema, G., McDermott, M.T. and Wiener, J.H. (1998) Hydroxylated napthoquinones as substrates for *Escherichia coli* anaerobic reductases. Submitted. Biochem. J.

44. Rothery, R.A., Simala-Grant, J.L., Johnson, J.L., Rajagopalan, K.V. and Weiner, J.H. (1995) Association of molybdopterin guanine dinucleotide with *Escherichia coli* dimethylsulfoxide reductase : Effect of tungstate and a *mob* mutant. J. Bacteriol. 177, 2057-2063.

45. Rothery, R.A. and Weiner, J.H. (1991) Alteration of the iron-sulfur cluster composition of *Escherichia coli* dimethyl sulfoxide reductase by site-specific mutagenesis. Biochemistry 30, 8296-8305.

46. Sambasivarao, D. and Weiner, J.H. (1991) Dimethylsulfoxide reductase of *Escherichia coli* : an investigation of function and assembly by use of *in vivo* complementation. J. Bacteriol. 173, 5935-5943.

47. Sambrook, J., Fritsch, E.F. and Maniatis, T. (1989) Molecular cloning : A laboratory manual. Cold Spring Harbor Laboratory Press, Cold Spring Harbor, N.Y.

48. Tachibana, M., Onoe, H., Okubo, A. and Yamazaki, S. (1995) Application of micellar electrokinetic chromatography as a novel assay method for dimethyl sulfoxide reductase. Biosci. Biotech. Biochem. 59, 282-284.

49. Thanos, I., Bader, J., Gunther, H., Neumann, S., Krauss, F. and Simon, H. (1987) Electroenzymatic and electromicrobial reduction: Preparation of chiral compounds. Meth. Enzymol. 136, 302-317.

50. Trieber, C.A., Rothery, R.A. and Weiner, J.H. (1994) Multiple pathways of electron transfer in dimethyl sulfoxide reductase of *Escherichia coli.* J. Biol. Chem. 269, 7103-7109.

51. Unden, G., Hackenberg, H. and Kroger, A. (1980) Isolation and functional aspects of the fumarate reductase involved in the phosphorylative electron transport of *Vibrio succinogenes*. Biochim. Biophys. Acta 591, 275-288.

52. Weiner, J.H., MacIsacc, D.P., Bishop, R.E. and Bilous, P.T. (1988) Purification and properties of *Escherichia coli* dimethyl sulfoxide reductase, an iron-sulfur molybdoenzyme with broad substrate specificity. J. Bacteriol. 170, 1505-1510.

53. Wissenbach, U., Kroger, A. and Unden, G. (1990) The specific functions of menaquinone and demethylquinone in anaerobic respiration with fumarate, dimethylsulfoxide, trimethylamine N-oxide and nitrate by *Escherichia coli.* Arch. Microbiol. 154, 60-66.

54. Yamamoto, I., Hohmura, M. and Ishimoto, M. (1989) A novel gene, ***torB***, for trimethylamine N-oxide reductase in *Escherichia coli*. J. Gen. Appl. Microbiol. 35, 95-105.

55. Yamamoto, I., Okubo, M. and Ishimoto, M. (1986) Further characterization of trimethylamine N-oxide reductase from *Escherichia coli* a molybdoprotein. J. Biochem. 99, 1773-1779.

Chapter 6 : Analysis of the Substrate Specificity of DmsABC*

6.1. Introduction

Respiratory growth of *E. coli* on several S- and N-oxides has been established, and these studies have demonstrated that the terminal reductases, DmsABC and TorA, play important roles in this process [33]. While only DmsABC is responsible for anaerobic growth on DMSO, both DmsABC and TorA are responsible for anaerobic growth on TMAO [33]. The widespread occurrence in nature of DMSO and TMAO suggests that these compounds serve as true physiological substrates for the reductases [3, 14, 15]. The amino acid sequences of DmsABC and TorA are highly homologous, and it might be predicted the enzymes would share similar substrate profiles [25]. However, Chapter 9 shows TorA is restricted in its substrate spectrum [13], while DmsABC has a broad substrate specificity [41]. Previous kinetic analysis of DmsABC examined only a few substrates, therefore, it has not been possible to make conclusions regarding substrate binding, active site structure and catalysis.

In this study we have performed kinetic analysis of DmsABC using a variety of S- and N-oxides, inorganic anions, and miscellaneous compounds, in order to gain an understanding of the parameters affecting substrate binding and turnover. We have determined the toxicity of a range of DmsABC substrates, and monitored the ability of

---

[*] A version of this chapter has been published. Simala-Grant, J. L. and Weiner, J. H. (1996) Kinetic analysis and substrate specificity of *Escherichia coli* dimethylsulfoxide reductase. Microbiol. 142, 3231-3239. Data from Figure 2 initiated our interest in assay characterization, and is found in chapter 5. Figure 3 from this paper alludes to the presence of a previously unidentified S- and N-oxide reductase, and is found in chapter 8.

these substrates to serve as anaerobic terminal electron acceptor in wild-type cells.

6.2. Materials and Methods

6.2.1. Materials

Potential substrates (Figure 6.1.) of DmsABC were purchased from Sigma or Aldrich, except for the following. D- and L-biotin sulfoxide was synthesized from biotin [26], DMSO was obtained from Fisher Scientific Ltd., and S-nitroso-D/L-acetylpenacillamine (SNAP) was a generous gift from Marek Radomski, University of Alberta, and Wellcome Labs. For substituted PNO's, all compounds with substituents in the 2, 3, and 4 position were obtained whenever possible.

6.2.2. Strains and Plasmids

E. coli strain HB101 (*supE*44 *hsdS*20($r_B^-m_B^-$) *recA*13 *ara*-14 *procA*2 *lacY*1 [5]) and plasmid pDMS160 (pBR322 Amp^R (*dmsABC*)$^+$ [32]) were used in this study. HB101 was transformed with pDMS160, for overexpression of DmsABC. All manipulations of plasmids and strains were carried out essentially as described by Sambrook *et al.* [35].

6.2.3. Media and Growth Conditions

Strains were grown aerobically in LB or Terrific Broth [35] overnight, and these cultures were used as 1% inocula for minimal media [4]. Bacteria were grown anaerobically on minimal media for 48 hours, at 37°C [4], with the following exceptions. 0.16% peptone was substituted for casamino acids, and streptomycin sulfate was not included in the growth medium. As necessary, appropriate amino acids and vitamins were included at a final concentration of 0.005%. When appropriate, 50-100 µg/mL ampicillin, and 40 µg/mL kanamycin were included in the growth medium. The terminal electron acceptors fumarate, TMAO, DMSO, and PNO, were autoclaved prior to use, while

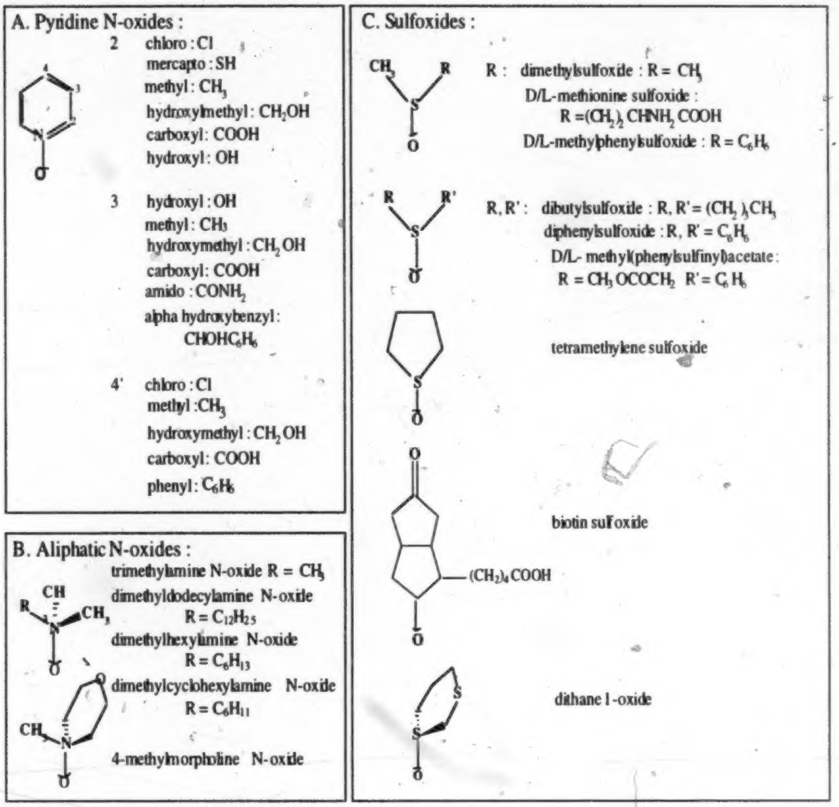
A. Pyridine N-oxides :
2 chloro : Cl
mercapto : SH
methyl : CH_3
hydroxylmethyl : CH_2OH
carboxyl : COOH
hydroxyl : OH
3 hydroxyl : OH
methyl : CH_3
hydroxymethyl : CH_2OH
carboxyl : COOH
amido : $CONH_2$
alpha hydroxybenzyl : $CHOHC_6H_6$
4' chloro : Cl
methyl : CH_3
hydroxymethyl : CH_2OH
carboxyl : COOH
phenyl : C_6H_6
4
3
2
N
O
B. Aliphatic N-oxides :
trimethylamine N-oxide R = CH_3
dimethyldodecylamine N-oxide R = $C_{12}H_{25}$
dimethylhexylamine N-oxide R = C_6H_{13}
dimethylcyclohexylamine N-oxide R = C_6H_{11}
4-methylmorpholine N-oxide
CH
R
CH_3
N
O
CH_3
C. Sulfoxides :
R : dimethylsulfoxide : R = CH_3
D/L-methionine sulfoxide : R = $(CH_2)_2CHNH_2COOH$
D/L-methylphenylsulfoxide : R = C_6H_5
R, R' : dibutylsulfoxide : R, R' = $(CH_2)_3CH_3$
diphenylsulfoxide : R, R' = C_6H_5
D/L- methyl(phenylsulfinyl)acetate : R = CH_3OCOCH_2 R' = C_6H_5
tetramethylene sulfoxide
biotin sulfoxide
dithane 1-oxide
CH_3
R
R'
S
O
$(CH_2)_4COOH$

Figure 6.1.

Structures of Various S- and N-oxides

all other S- and N-oxides were filter-sterilized. To assess the ability of various S- and N-oxides to sustain growth on minimal media in the presence of glycerol, cells were grown in sealed screw capped tubes, containing a small air bubble, to allow mixing using a continuously rotating wheel.

6.2.4. Toxicity of DmsABC Substrates as Indicated by Inhibition of Anaerobic Growth

HB101 grown overnight in LB was used as a 1% inocula for 3 mL of unsolidified 45°C LB top agar (0.7%). This sample was mixed, and poured onto 37°C LB agar plates (1.5%). Sterilized filters were dipped into filter sterilized substrate, just to the point of saturation, and placed on LB agar plates overlaid with LB top agar containing bacteria. All potential DmsABC substrates were used at 300 mM, except 4-nitropyridine N-oxide (150 mM), and 3-amidopyridine N-oxide (100 mM). Platinum catalyst and plates were placed in anaerobic jars that were subsequently repeatedly evacuated, and filled with H_2/CO_2 gas. After seventy-two hours at 37°C, the diameter of the zone of clearing (absence of growth), around the substrate soaked filters, was measured. Fumarate and nitrate were used as non-toxic controls. K_2CrO_4 and ampicillin were used as positive toxic controls.

6.2.5. Purification of DmsABC

HB101/pDMS160 was grown at 37°C, for 48 hours, in 19 L carboys, on Gly/Fum. Cells were harvested using a Pellicon membrane system equipped with a Millipore polysulfone PTNK filter. The concentrated cell mixture was then centrifuged at 9,500 x g for 10 minutes, and subsequently resuspended in buffer [32]. Everted envelopes were prepared [4], and membrane fractions were extracted with Triton X-100 [7]. DmsABC was purified from solubilized membrane proteins on either a DEAE-cellulose (Whatman DE-52) column as indicated previously [41], except that a 0-0.2 M KCl gradient was used, equivalent to ten column volumes, or on a DEAE-Sepharose

CL-6B column with a 50-300 mM NaCl gradient, equivalent to two column volumes.

6.2.6. Kinetic Analysis

Substrate-dependent oxidation of $BVH^{\cdot+}$, was monitored at 570 nm using a Gilford 250 spectrophotometer. 50 mM MOPS pH 7.0 was used as the buffer for all assays unless otherwise indicated, and electron acceptor (substrate) was varied as necessary. Closed cuvette assays (stoppered) were performed using degassed buffer, subsequently bubbled with N_2. Buffer was transferred to a cuvette, that was subsequently stoppered. Hamilton syringes were used for the ordered addition of : BV^{2+}, substrate, dithionite, and enzyme. A stable baseline was confirmed prior to addition of enzyme. BV was used at a final concentration of 0.2 mM, and dithionite was added to approximately 0.1 mM, to give an absorbance of about 1.0 OD. All assays were performed at 30°C using equilibrated buffer and a jacketed cuvette holder. 1 unit of enzyme activity corresponds to 1 μmol of $BVH^{\cdot+}$ oxidized per minute, or 0.5 μmol of S- or N-oxide reduced per minute. Between 3 and 9 assays were performed at each substrate concentration, and 5-8 different substrate concentrations were examined to determine each K_m. Whenever possible, a range of substrate concentrations was chosen that varied from at least two times less than the K_m, to five times greater than the K_m. This range of substrate concentration could not be achieved in some instances due to limitations resulting from the minimum concentration of substrate that can be used in the assay, or substrate inhibition. We ensured only a small fraction of substrate was consumed during the experiment. K_m and V_{max} values were determined from Eadie-Hofstee plots [11]. K_m values obtained, are apparent K_m values, using a saturating concentration of $BVH^{\cdot+}$. k_{cat} values were determined by estimating enzyme purity from PAGE analysis, as indicated in analytical techniques. Assays were performed on freshly diluted enzyme previously beaded into liquid N_2, and stored at -70°C for kinetic analysis, or intact or toluene permeabilized cells to determine membrane permeability of substrates. Bacteria were permeabilized by the addition of 1/100th volume of toluene, and incubation at 30°C for 10 minutes. Diluted sample was stored on ice and used during the day for kinetics to obtain reproducible results. Compounds not found to be substrates were tested for their ability to inhibit the transfer of electrons from reduced DmsABC to TMAO, by inclusion in the cuvette at a concentration equal to TMAO.

6.2.7. Analytical Techniques

Protein concentrations were determined [22] prior to performing PAGE using the BioRad mini-gel system, with a discontinuous SDS buffer system [18]. Gels were stained with Coomassie blue, destained [20], and scanned with a Joyce-Loebel Chromoscan 3 densitometer, to determine the purity of DmsABC. Confirmation of bands on the polyacrylamide gel corresponding to DmsA and B was determined by Western blotting [34]. DmsA and B polyclonal antibodies were used separately. ECL western blotting detection reagents from Amersham Life Sciences were used for blot development. No antibody has been successfully raised against DmsC. This subunit's position was estimated from its known molecular weight, and migration as compared with previously purified DmsABC.

6.3. Results

6.3.1. Utilization of N-oxides by DmsABC

A wide variety of N-oxides (Figure 6.1.) were examined for their ability to act as electron acceptors. The apparent K_m and k_{cat} values obtained under closed cuvette conditions are listed in Table 6.1.

Examination of a group of substituted PNO's led to some interesting findings about DmsABC substrate specificity. First, substitution at the 2 and 3 position did not appear to alter K_m or k_{cat} significantly. Unsubstituted PNO has a K_m of 0.094 mM. Next,

Table 6.1.

Kinetic Parameters for N-oxide Substrates of DmsABC, and Their Ability to Support or Inhibit Growth

Substrate	k_{cat} / K_m	K_m	k_{cat}	Growth	Inhibition
2-chloropyridine N-oxide	7130	0.043	307	++	No
3-amidopyridine N-oxide	5280	0.045	237	++	No
3-methylpyridine N-oxide	2600	0.089	231	++	No
2-methylpyridine N-oxide	2690	0.092	247	++	No
3-hydroxymethylpyridine N-oxide	2280	0.094	214	++	No
PNO	2580	0.094	243	++	No
3α-hydroxybenzylpyridine N-oxide	1450	0.158	229	-	No
4-phenylpyridine N-oxide	1205	0.246	297	-	No
4-hydroxymethylpyridine N-oxide	607	0.372	226	++	No
4-methylpyridine N-oxide	592	0.452	268	++	No
4-chloropyridine N-oxide	413	0.513	212	+/-	No
dimethyldodecylamine N-oxide	287	0.83	239	-	Yes
3-hydroxypyridine N-oxide	135	3.17	429	++	No
3-carboxypyridine N-oxide	34	4.94	168	++	No
4-methylmorpholine N-oxide	52	11.1	573	++	No
TMAO	59	20.2	1203	++	No
2-hydroxymethylpyridine N-oxide	ND	ND	89.3	+	ND
4-carboxypyridine N-oxide	ND	ND	30.3	++	No
2-mercaptopyridine N-oxide	ND	ND	8.0	-	No
2-carboxypyridine N-oxide	ND	ND	8.0	+/-	No

All assays were performed using the closed cuvette assay. K_m values were calculated for those substrates with a reasonable k_{cat}. K_m values are listed in mM, k_{cat}'s in s^{-1}, and k_{cat} / K_m's in s^{-1} mM^{-1}. For those compounds where K_m's were not determined, k_{cat}'s were estimated using excess substrate concentration. Anaerobic growth on these compounds (30 mM) in the presence of glycerol, was assessed visually as (-) no growth, (+/-) very poor growth, (+) growth, or (++) good growth. Bacteria grown in minimal media with no terminal electron acceptor was used as the negative control, and with fumarate as the positive control. ND indicates the parameter was not determined. Inhibition of bacterial growth was indicated by zones of clearing around substrate soaked filters incubated anaerobically on a lawn of HB101.

hydrophobic substituents, CH_3, CH_2OH, and amido groups are preferred (low K_m), whereas hydroxy and carboxy groups are not accepted, resulting in lower k_{cat} and very high K_m values. Finally substitution at the 4 position generally increased the K_m (0.25-0.5 mM), but had little effect on k_{cat}, resulting in intermediate k_{cat}/K_m values.

The K_m and inhibition characteristics of 2-hydroxypyridine N-oxide was not determined due to its ability to accept electrons directly from $BVH^{\cdot +}$ at high substrate concentrations.

Only a few aliphatic N-oxides were available. 4-methylmorpholine N-oxide and TMAO have relatively low k_{cat}/K_m values. They have substantially higher turnover numbers compared to the other compounds tested, and substantially higher K_m values. The detergent dimethyldodecylamine N-oxide (LDAO) was a reasonable substrate, although this compound forms micelles at a concentration of 2.1 mM [27]. The K_m was lower than the critical micelle concentration, however, there was no break in the Eadie-Hofstee plot at the critical micelle concentration. This suggests DmsABC is capable of reducing substrate that is part of a micelle. The K_m for LDAO was substantially lower than the other aliphatic N-oxides, possibly due to multiple interactions between the dodecyl alkyl sidechain and the enzyme, or partitioning of the substrate into Triton X-100 protein micelles.

6.3.2. Utilization of S-oxides

In general, the sulfoxides had similar K_m's to PNO, and PNO's substituted at the 2 and 3 position, and k_{cat} values near 100 (Table 6.2.). Because the sulfoxides have lower k_{cat} values than the PNO compounds, some of the substituted PNO's are the best substrates on the basis of k_{cat}/K_m values.

DmsABC may be enantioselective, as has been found for DMSOR, where the S enantiomer is reduced predominantly [1, 2]. The substrates D/L-methylphenyl sulfoxide and D/L-methionine sulfoxide present the enzyme with both enantiomers. Since neither of these

Table 6.2.

Kinetic Parameters for S-oxide Substrates of DmsABC, and Their Ability to Support or Inhibit Growth

Substrate	k_{cat} / K_m	K_m	k_{cat}	Growth	Inhibition
tetramethylene sulfoxide	2080	0.06	119	++	No
methionine sulfoxide	663	0.09	61.1	++	No
D/L-methylphenyl sulfoxide	483	0.21	99.6	+	No
DMSO	455	0.18	79.9	++	No
dithane 1-oxide	ND	ND	28.4	ND	No
dibutyl sulfoxide	ND	ND	<4	-	No
D-biotin sulfoxide	ND	ND	<4	+/-	No
D/L-methyl(phenylsulfinyl)acetate	ND	ND	<4	-	No
diphenyl sulfoxide	ND	ND	<4	-	Yes

Measurements as described in the legend to Table 6.1. All assays were performed using the closed cuvette assay.

compounds is reduced to any great extent, it is not possible to determine whether DmsABC is enantioselective. The answer is being pursued (by Pavel Badelov) using polarimetry, and R- and S-methyl-p-tolyl sulfoxide.

6.3.3. Utilization of Inorganic Anions and Miscellaneous Substrates

Some miscellaneous compounds were tested for their ability to act as DmsABC substrates. Interestingly, hydroxylamine (K_m 47.5 mM, k_{cat} 431 s^{-1}) and diethylhydroxylamine (k_{cat} >389 s^{-1}) were substrates, although high concentrations of hydroxylamine inhibited enzyme activity. The K_m for diethylhydroxylamine could not be determined, since it accepts electrons directly from $BVH^{\cdot+}$ at high substrate concentrations. ANO was not reduced by DmsABC when MOPS was employed as the buffer. However, when 50 mM potassium acetate buffer pH 5.5 was used, low activity was observed (k_{cat} 10 s^{-1}). Dimethylsulfone and triethanolamine are substrates with a k_{cat}'s of 12.8 s^{-1} and 4.2 s^{-1}, respectively. SNAP immediately produces nitric oxide to a concentration of at least 0.1 mM. The use of SNAP in the cuvette did not result in any BV^{2+}, indicating that nitric oxide is not a substrate. The sodium anions of arsenate, arsenite, carbonate, molybdate, nitrate, tellurate, and tellurite were not reduced by DmsABC. However, bromate was a reasonable substrate with K_m and k_{cat} of 31.3 mM and 401s^{-1} respectively. Chlorate showed a k_{cat} of 7.3 s^{-1}. The K_m for chlorate could not be determined due to its low k_{cat}. A number of additional compounds were examined, but triethylamine N-oxide picrate, K_2CrO_4, $NaSeO_3$, 5-chlorobenzofurazan 3-oxide, 4-nitropyridine N-oxide, and 4-nitroquinoline N-oxide accept electrons directly from $BVH^{\cdot+}$, and thus could not be tested as substrates of DmsABC.

6.3.4. Inhibition of DmsABC Activity

Compounds found to be poor substrates, were tested for their ability to act as inhibitors of DmsABC activity with TMAO as substrate. Because TMAO has a high K_m, non-substrates would not need to have particularly low K_i's to inhibit enzyme activity. Dibutyl sulfoxide, D/L-methyl(phenylsulfinyl)acetate, diphenyl sulfoxide, 2-mercaptopyridine N-oxide, triethanolamine borate, chlorate, and 2-carboxypyridine N-oxide, were not able to inhibit DmsABC activity. The following compounds were found to be weak inhibitors of DmsABC activity (% inhibition): D-biotin sulfoxide (33.5%); dimethylsulfone (12.4%). 3-carboxypyridine, the product of 3-carboxypyridine N-oxide reduction, was also a poor inhibitor (27.3%).

6.3.5. Growth Inhibition by S- and N-oxides

We thought it possible that DmsABC may play a role in the detoxification of various S- and N-oxides encountered in the environment, providing a selective advantage for the organism. As a result, we determined the toxicity of our collection of substrates to anaerobic growth of *E. coli*. Under the conditions described in methods section 6.2.4, most DmsABC substrates were not toxic to anaerobically growing *E. coli* (Tables 6.1. and 6.2.). However, hydroxylamine - a protein modifier, LDAO - a detergent, and diphenylsulfoxide did cause zones of clearing around the substrate soaked filters.

6.3.6. Ability of S- and N-oxides to Act as Terminal Electron Acceptors

These compounds were also tested for their ability to support anaerobic growth of *E. coli* with glycerol as carbon and energy source (Table 6.1 and 6.2). Most of the N-oxides tested could be used by *E. coli* as a terminal electron acceptor for anaerobic growth. Exceptions were 2-mercapto-, 4-phenyl-, 3α-hydroxybenzyl, and 4-nitropyridine N-oxide, and LDAO. The latter inhibited anaerobic growth, presumably due to its detergent properties. The S-oxide compounds reduced by DmsABC were able to support anaerobic growth, whereas those not reduced by DmsABC did not support growth. Only diphenyl sulfoxide was an inhibitor of growth. Of the miscellaneous compounds diethylhydroxylamine and ANO were capable of supporting anaerobic growth, while hydroxylamine, triethanolamine borate, dimethylsulfone, bromate, and chlorate were not.

6.3.7. Membrane Permeability of Non-toxic DmsABC Substrates Unable to Support Anaerobic Growth on Glycerol

4-phenylpyridine N-oxide and 3-α-hydroxybenzylpyridine N-oxide were tested for their ability to cross the membrane, as they were the only non-toxic DmsABC substrates unable to support growth. When either compound was used as a substrate with intact, or toluene permeabilized cells, equal levels of activity with DmsABC were observed, indicating the these substrates are able to cross the membrane.

6.4. Discussion

This work agrees with earlier conclusions, that DmsABC has a very broad substrate specificity, and analysis of the data gives us a better understanding of the parameters which affect substrate binding and turnover. K_m values vary 470 fold, while k_{cat} values vary only 20 fold, implicating K_m as the major determinant of k_{cat}/K_m values. Finally, we conclude that DmsABC plays an important role in the utilization of S- and N-oxides.

Two classes of S- and N-oxide reductases have been identified [13]. One class has broad substrate specificity, and includes the periplasmic DMSO reductases from *R. sphaeroides* [36] and *capsulatus* [21]. The second class has much more limited substrate specificity, and includes the TMAO reductases of *Shewanella* and *E. coli* [10, 13]. DmsABC is a membrane bound, heterotrimeric enzyme, with its active site exposed to the cytoplasm. Kinetic analysis suggest it is most similar to the *R.* enzymes.

If we compare all the substrates solely on the basis of k_{cat}, we can identify three compounds (TMAO, 4-methylmorpholine N-oxide and 3-

hydroxypyridine N-oxide) with substantially higher k_{cat} values, than all the other compounds tested (Table 6.1. and Figure 6.2.). These compounds also have the highest K_m values, and therefore relatively poor k_{cat}/K_m values, suggesting that they are poor substrates. (Figure 6.3.). This is obviously not the case, as cells grow well on these compounds as terminal electron acceptors. Two of these compounds are aliphatic, whereas the third is aromatic. Most substituted PNO's have k_{cat} values between 200 and 300 s^{-1} (Table 6.1 and Figure 6.2), and sulfoxides have k_{cat} values between 60 and 120 s^{-1} (Table 6.2 and Figure 6.2). For these compounds, a very large range of K_m values was observed indicating that substrate affinity has a primary role in determining enzyme specificity (Figure 6.2.). This can be observed more clearly in Figure 6.3. where K_m are plotted in descending order against the corresponding k_{cat}/K_m for DmsABC substrates

Redox potential would be expected to affect k_{cat} much more than K_m. PNO's have lower redox potentials, and are more difficult to reduce than aliphatic N-oxides because the electrons from the oxygen are in resonance with the aromatic ring, stabilizing the unstable N-O bond [28, 29]. It is possible that the lower redox potentials of PNO's could be an influencing factor in the lower k_{cat} values observed for these compounds.

Substituents added to the PNO ring will raise or lower the redox potential of the compound, depending on whether the substituents are electron withdrawing or electron donating [12, 17, 30]. A comparison of redox potential versus K_m or k_{cat} for the substituted PNO's, did not show any correlation.

However, a pattern is observed when the K_m values are examined. The K_m values are approximately equivalent for PNO, and PNO's substituted in the 2 and 3 position (Figure 6.4.). PNO's substituted in the 4 position have higher K_m values. Carboxysubstituted PNO's do not follow the rule above, and are not good substrates. This is presumably due to their negative charge.

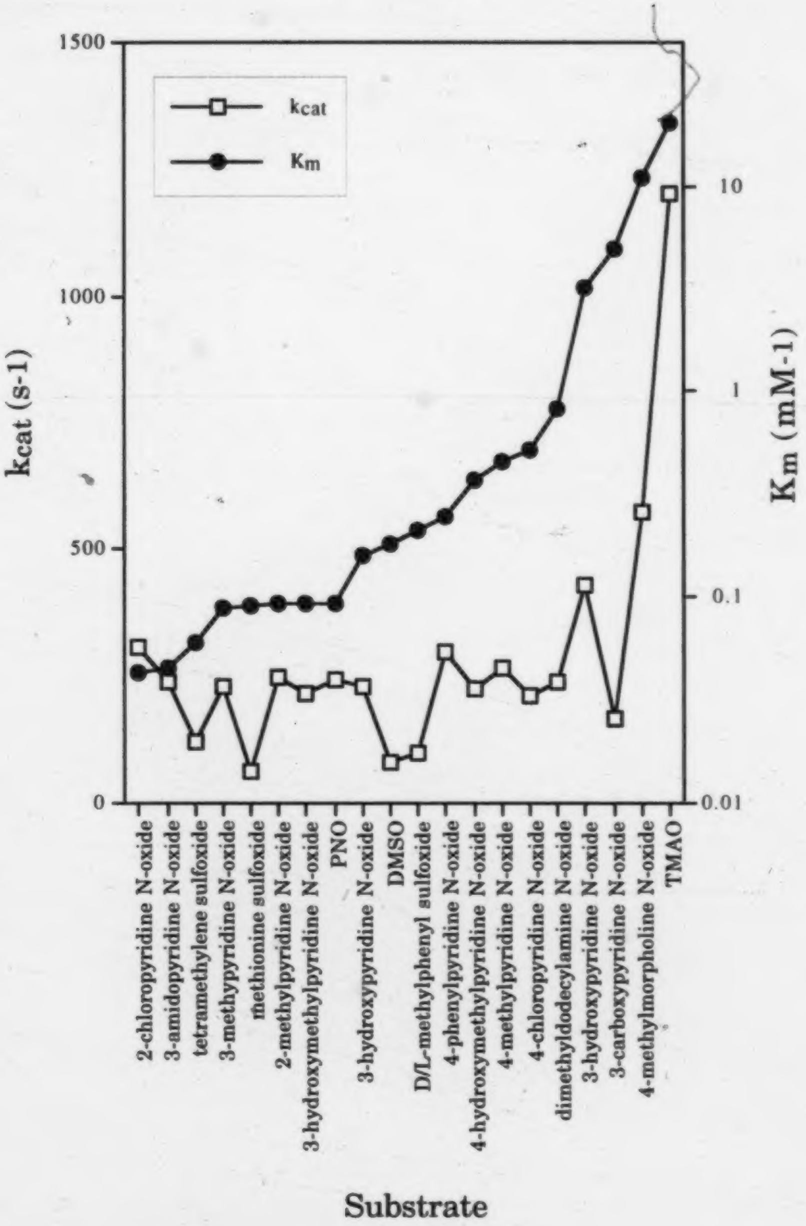

Figure 6.2.

K_m Versus k_{cat} for DmsABC Substrates

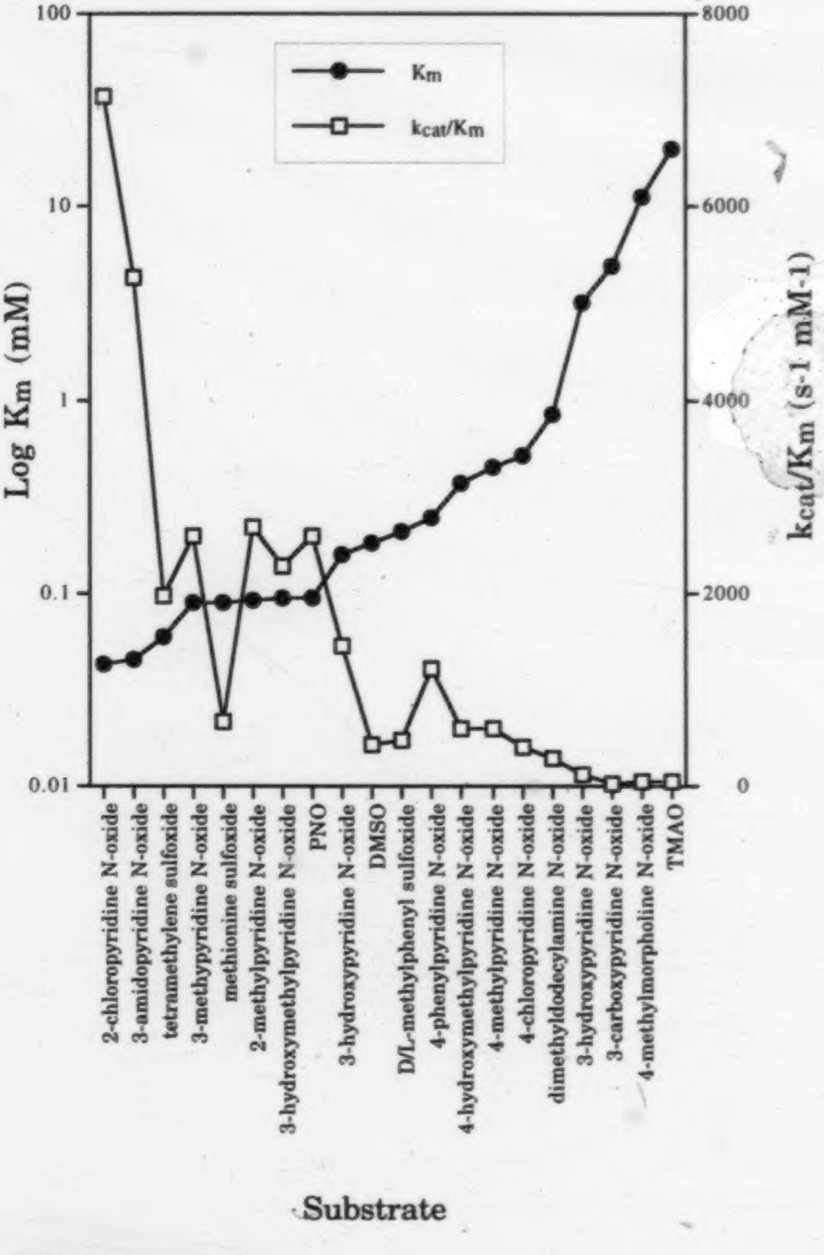

Figure 6.3.

K_m Versus k_{cat}/K_m for Substrates of DmsABC

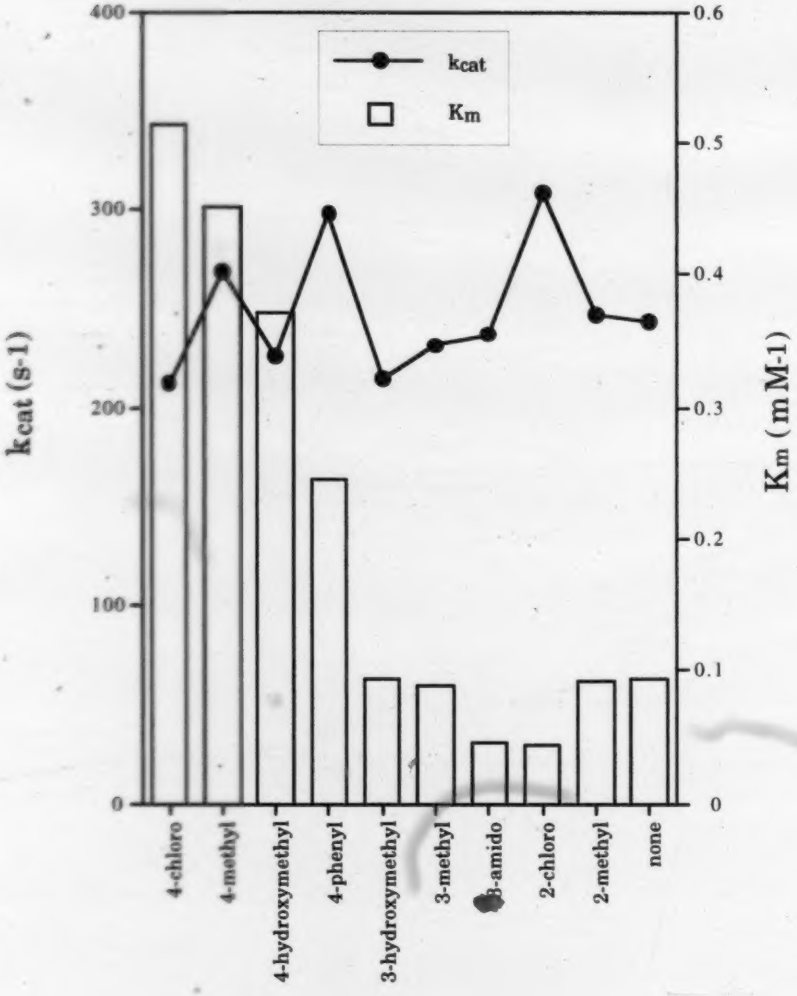

Substituent Added to PNO

Figure 6.4.

Comparison of Km and kcat Values for Various PNO Substrates of DmsABC

The K_m values for the PNO's and sulfoxides are observed to be lower than the aliphatic N-oxides. This may be for steric reasons, suggesting the enzyme may be willing to accept compounds with two substituents more easily than those with three substituents. The only aliphatic N-oxide that does not follow this rule is LDAO, possibly for the reasons mentioned in the results section.

Compact sulfoxides (DMSO and tetramethylene sulfoxide), or those with one extended substituent are accommodated by the enzyme (D/L-methionine sulfoxide and D/L-methylphenyl sulfoxide). However, those that are bulky, and those with two extended substituents are not (dibutyl sulfoxide, D/L-methyl(phenylsulfinyl)acetate, diphenyl sulfoxide, and D- and L-biotin sulfoxide). This agrees with X-ray structures of molybdopterin- and tungstopterin-containing aldehyde oxidoreductases, and molybdopterin containing DMSO reductase of *R. sphaeroides* and *capsulatus*, and FdhF. All show the active site accessible only through a narrow tunnel [6, 9, 16, 23, 24, 31, 37, 38]. The tunnel would restrict entry of substrates that are too wide. One can imagine the S- or N-oxide portion of the substrate deep within the tunnel, with one of the sidechains extending out the tunnel (i.e. LDAO).

We know that lack of reduction of diphenylsulfoxide is not due to difficulty of reduction, as compared to D/L-methylphenyl sulfoxide, but rather due to substrate bulkiness, as the former compound has a more positive redox potential than the latter [8, 40].

The compounds in Tables 6.1. and 6.2. incapable of supporting anaerobic growth are either toxic to *E. coli*, or are extremely poor substrates of DmsABC. Two compounds do not fit this generalization: 3α–hydroxybenzylpyridine N-oxide, and 4-phenylpyridine N-oxide. The reason for this is unknown, as these compounds are substrates of DmsABC, are not toxic to *E. coli*, and are able to cross the membrane.

We have demonstrated that *E. coli* has the ability to use a wide variety of S- and N-oxides as terminal electron acceptors, resulting in anaerobic growth in the presence of glycerol. TMAO has widespread occurrence in nature as an osmostabilizer in salt water fish, and DMSO is found in sea water as part of the global sulfur cycle [3, 14, 15]. Many of these compounds also are manmade. DMSO is used as a solvent and is found as an effluent from wood pulp mills [42]. PNO's are found as soil contaminants, in crude petroleum, in coal tar, and are used as organic solvents and drugs [39]. DmsABC is a key enzyme in utilization of these compounds as shown by the work reported herein. The presence of DmsABC in *E. coli,* may result in a selective advantage for the organism to use a wide variety of S- and N-oxides as they are encountered in the environment, including utilizing S-oxide drugs found in the intestine [19].

6.5. References

1. Abo, M., Tachibana, M., Okubo, A. and Yamazaki, S. (1994) Enantioselective reduction of the sulfoxide to sulfide in methyl phenyl sulfoxide by dimethyl sulfoxide reductase from *Rhodobacter sphaeroides* f. s. *denitrificans*. Biosci. Biotech. Biochem. 58, 596-597.

2. Abo, M., Tachibana, M., Okubo, A. and Yamazaki, S. (1995) Enantioselective deoxygenation of alkyl aryl sulfoxides by DMSO reductase from *Rhodobacter sphaeroides* f.s. *denitrificans*. Bioorg. Med. Chem. 3, 109-112.

3. Barrett, E.L. and Kwan, H.S. (1985) Bacterial reduction of trimethylamine oxide. Ann. Rev. Microbiol. 39, 131-49.

4. Bilous, P.T. and Weiner, J.H. (1985) Dimethyl sulfoxide reductase activity by anaerobically grown *Escherichia coli*. J. Bacteriol. 162, 1151-1155.

5. Boyer, H.W. and Roulland-Dussoix, D. (1969) A complementary analysis of the restriction and modification of DNA in *Escherichia coli*. J. Mol. Biol. 41, 459.

6. Boyington, J.C., Gladyshev, V.N., Khangulov, S.V., Stadtman, T.C. and Sun, P.D. (1997) Crystal structure of formate dehydrogenase H: catalysis involving Mo, molybdopterin, selenocysteine, and Fe_4S_4 cluster. Science 275, 1305-1308.

7. Cammack, R. and Weiner, J.H. (1990) Electron paramagnetic resonance spectroscopic characterization of dimethyl sulfoxide reductase of *Escherichia coli*. Biochemistry 29, 8410-8416.

8. Chambers, J.Q. (1978) Chapter XII-3 Organic sulfur compounds, in Encyclopedia of electrochemistry of the elements. (Bard, A.J. and Lund, H., eds.), p. 329-493, Dekker, New York.

9. Chan, M.K., Mukund, S., Kletzin, A., Adams, M.W.W. and Rees, D.C. (1995) Structure of a hyperthermophilic tungstopterin enzyme, aldehyde ferredoxin oxidoreductase. Science 267, 1463-1469.

10. Clarke, G.J. and Ward, F.B. (1988) Purification and properties of trimethylamine N-oxide reductase from *Shewanella* sp. NCMB 400. J. Gen. Microbiol. 133, 379-386.

11. Fersht, A. (1977) Chapter 10: Enzyme-substrate complementarity and theories of enzyme catalysis, in Enzyme structure and mechanism. 1st ed., p. 244-271, W. H. Freeman, San Francisco.

12. Fieser, L.F. and Fieser, M. (1956) Oxidation-reduction potentials, in Organic Chemistry. 3rd ed., p. 711, Reinhold Publishing Corporation, London.

13. Iobbi-Nivol, C., Pommier, J., Simala-Grant, J.L., Mejean, V. and Giordano, G. (1996) High substrate specificity and induction characteristics of trimethylamine N-oxide reductase of *Escherichia coli*. Biochim. Biophys. Acta 1294, 77-82.

14. Kelly, D.P. and Baker, S.C. (1990) The organosulphur cycle : aerobic and anaerobic processes leading to turnover of C_1 sulphur compounds. FEMS Micro. Rev. 87, 241-246.

15. Kiene, R.P. and Bates, T.S. (1990) Biological removal of dimethylsulphide from sea water. Nature 345, 702-705.

16. Knablein, J., Dobbek, H., Ehlert, S. and Schneider, F. (1997) Isolation, cloning, sequence analysis and X-ray structure of dimethyl sulfoxide/trimethylamine N-oxide reductase from *Rhodobacter sphaeroides*. Biol. Chem. 378, 293-302.

17. Kolthoff, I.M. and Lingane, J.J. (1941) Organic Polarography, in Polarography. Vol. 1, 2nd ed., p. 631-633, Interscience Publishers Inc., New York.

18. Laemmli, U.K. (1970) Cleavage of structural proteins during the assembly of the head of bacteriophage T4. Nature 227, 680-685.

19. Lee, S.C. and Renwick, A.G. (1995) Sulfoxide reduction by rat intestinal flora and by *Escherichia coli in vitro*. Biochem. Pharmacol. 49, 1567-1576.

20. Lemire, B.D., Robinson, J.J. and Weiner, J.H. (1982) Identification of membrane anchor polypeptides of *Escherichia coli* fumarate reductase. J. Bacteriol. 152, 1126-1131.

21. MacEwan, A.G., Wetstein, H.G., Meyer, O., Jackson, J.B. and Ferguson, S.J. (1987) The periplasmic nitrate reductase of *Rhodobacter capsulatus*; purification, characterisation and distinction from a single reductase for trimethylamine-N-oxide dimethylsulphoxide and chlorate. Arch. Microbiol. 147, 340-345.

22. Markwell, M.A.D., Haas, S.M., Bieber, L.L. and Tolbert, N.E. (1978) A modification of the Lowry procedure to simplify protein determination in membrane and lipoprotein samples. Anal. Biochem. 87, 206-210.

23. McAlpine, A.S., McEwan, A.G. and Bailey, S. (1998) The high resolution crystal structure of DMSO reductase in complex with DMSO. J. Mol. Biol. In press.

24. McAlpine, A.S., McEwan, A.G., Shaw, A.L. and Bailey, S. (1998) Molybdenum active center of DMSO reductase from *Rhodobacter capsulatus* : crystal structure of the oxidised enzyme at 1.82Å resolution and the dithionite-reduced enzyme at 2.8Å resolution. J. Biol. Inorg. Chem. In press.

25. Mejean, V., Iobbi-Nivol, C., Lepelletier, M., Giordano, G., Chippaux, M. and Pascal, M.-C. (1994) Trimethylamine N-oxide anaerobic respiration in *Escherichia coli* : involvement of the *tor* operon. Mol. Microbiol. 11, 1169-1179.

26. Melville, D.B. (1954) Biotin sulfoxide. J. Biol. Chem. 208, 495-501.

27. Neugebauer, J.M. (1990) Detergents : An overview, in Guide to protein purification. Methods in Enzymology (Deutscher, M.P., ed.), Vol. 182, 1st ed., p. 247-249, Academic Press, Toronto.

28. Ochaiai, E. (1953) Recent Japanese work on the chemistry of pyridine 1-oxide and related compounds. J. Org. Chem. 18, 534-551.

29. Ochaiai, E. (1967) Polarography, in Aromatic Amine Oxides. p. 91, Elsevier Publishing Company, Amsterdam.

30. Pozdeeva, A.G. and Novikov, E.G. (1969) Polarographic investigation of certain derivatives of the pyridine and quinoline series. Zh. Prikl. Kh. 42, 2626-2628.

31. Romao, M.J., Chan, M.K., Mukund, S., Kletzin, A., Adams, M.W.W. and Rees, D.C. (1995) Crystal structure of the xanthine oxidase-related aldehyde oxido-reductase from *D. gigas*. Science 270, 1170-1176.

32. Rothery, R.A. and Weiner, J.H. (1991) Alteration of the iron-sulfur cluster composition of *Escherichia coli* dimethyl sulfoxide reductase by site-specific mutagenesis. Biochemistry 30, 8296-8305.

33. Sambasivarao, D. and Weiner, J.H. (1991) Differentiation of the multiple S- and N-oxide reducing activities of *Escherichia coli*. Curr. Microbiol. 23, 105-110.

34. Sambasivarao, D. and Weiner, J.H. (1991) Dimethylsulfoxide reductase of *Escherichia coli* : an investigation of function and assembly by use of *in vivo* complementation. J. Bacteriol. 173, 5935-5943.

35. Sambrook, J., Fritsch, E.F. and Maniatis, T. (1989) Molecular cloning : A laboratory manual. Cold Spring Harbor Laboratory Press, Cold Spring Harbor, N.Y.

36. Satoh, T. and Kurihara, F.N. (1987) Purification and properties of dimethylsulfoxide reductase containing a molybdenum cofactor from a photodenitrifier, *Rhodopseudomonas sphaeroides* f.s. *denitrificans*. J. Biochem 102, 191-197.

37. Schindelin, H., Kisher, C., Hilton, J., Rajagopalan, K.V. and Rees, D.C. (1996) Crystal structure of DMSO reductase: Redox-linked changes in molybdopterin coordination. Science 272, 1615-1621.

38. Schneider, F., Lowe, J., Huber, R., Schindelin, H., Kisker, C. and Knablein, J. (1996) Crystal structure of dimethyl sulfoxide reductase from *Rhodobacter capsulatus* at 1.88 A resolution. J. Mol. Biol. 263, 53-69.

39. Shukla, O.P. (1984) Microbial transformation of pyridine derivatives. J. Sci. Ind. Res. 43, 98-116.

40. Suchelmelova, L. and Zyka, J. (1966) The effect of the structure of the alkyl group on the polarographic waves corresponding to catalytic hydrogen evolution by organic sulphoxides. J. Electroanal. Chem. 12, 194-198.

41. Weiner, J.H., MacIsacc, D.P., Bishop, R.E. and Bilous, P.T. (1988) Purification and properties of *Escherichia coli* dimethyl sulfoxide reductase, an iron-sulfur molybdoenzyme with broad substrate specificity. J. Bacteriol. 170, 1505-1510.

42. Wood, P.M. (1981) The redox potential for dimethyl sulphoxide reduction to dimethyl sulphide. FEBS Lett. 124, 11-14.

Chapter 7 : Modulation of the Substrate Specificity of DmsABC*

7.1. Introduction

DmsABC belongs to a family of homologous prokaryotic moco containing oxidoreductases [1, 34, 35]. This family is composed of reductases for S- and N-oxides, polysulfide, and nitrate, as well as formate dehydrogenases [1]. Each of the enzymes in the family possess a catalytic subunit that binds a moco. Multiple sequence alignments of the catalytic subunits reveal blocks of sequence homology, separated by sequence that differs in length and composition [1, 34, 35]. The alignments suggest the enzymes share a similar polypeptide fold and active site [28, 29, 35].

Two of the more closely related enzymes to DmsABC are the DMSO reductases from *R. sphaeroides* and *R. capsulatus*. The *R*. DMSO reductases are monomeric, soluble, and periplasmic. They have been crystallized, and their three-dimensional structures determined [11, 16, 17, 28, 29]. As a result of the sequence similarity between the three DMSO reductases, potentially interesting residues in DmsA, corresponding to structurally and/or functionally important residues revealed in the *R*. crystal structures, can be identified and targeted for mutation. Support for this approach comes from mutation of S147. The DMSO reductase crystal structures have shown this amino acid is a Mo ligand [28, 29]. Mutation of the homologous residue in DmsABC, S176, has a dynamic effect on the EPR lineshape and redox chemistry of the Mo [32].

---

* A version of this chapter has been published. Simala-Grant, J. L. and Weiner, J. H. (1998) Modulation of the substrate specificity of *Escherichia coli* DmsABC. Eur J. Biochem. 251, 510-515.

Three other moco containing enzymes have also been crystallized. They are the aldehyde oxidoreductases from *Pyrococcus furiosus* and *Desulfovibrio gigas* [5, 22], and FdhF [4]. Although the crystallized molybdoenzymes all catalyze similar reactions, oxo-group transfer between substrate and water, they possess slightly different forms of moco. In addition, these enzymes do not all share sequence homology, but rather fall into different moco containing oxido-reductase enzyme families. Nonetheless, there are some striking features shared between the structures of these enzymes. One structural feature of importance to this chapter is a large depression or crevice, described as a funnel, tunnel, or channel, that leads from the surface of the protein to the Mo atom of the moco, located approximately in the center of the protein. The substrate must travel 25Å down the tunnel, to reach the active site where catalysis occurs [29]. As a result, the amino acids lining this funnel will influence the enzyme's substrate specificity, either sterically, by hydrogen bonds, or hydrophobic and electrostatic interactions. For example, hydrophobic residues lining the bottom of the active site channel may facilitate binding of uncharged non-polar S- and N-oxides in the active site of *R. capsulatus* DMSO reductase [16, 17, 29].

With the objective of identifying key residues for substrate recognition in DmsA, we employed site-directed mutagenesis to alter amino acids potentially situated at the bottom of the active site funnel. To select amino acids for mutation, the DMSOR structure was examined to determine those residues located at the bottom of the funnel. Next, corresponding residues in DmsABC were identified by comparing the amino acid sequence of DmsABC with the two *R.* DMSO reductase enzymes. Sixteen mutants were constructed and analyzed.

7.2. Materials and Methods

7.2.1. Materials

Oligonucleotides were purchased from Ransom Hill Bioscience, Ramona, CA. Restriction endonucleases and modifying enzymes were obtained from Life Technologies Inc., and the Sculptor^{TM} *in vitro* mutagenesis kit was obtained from Amersham Corp. All other materials were reagent grade, and were obtained from commercial sources.

7.2.2. Strains and Plasmids

E. coli strains and plasmids used in this study are listed in Table 7.1. Chromosomal expression of DmsABC was examined in HB101 without plasmid. TG1 was used for routine DNA manipulation, and DSS301 for plasmid overexpression of wild-type and mutant DmsABC. Plasmid overexpression was performed using pDMS170. This plasmid was constructed by cloning the 4.83 kbp *Eco*RI-*Sal*I fragment, containing the *dmsABC* operon from pDMS223 [23], into pBR322, that had been previously cut with *Pvu*II and *Nru*I, and self ligated to destroy these sites (Table 7.1.).

7.2.3. Sequence Analysis

Sequence alignments were performed with the software package by Genetics Computer Group, Inc. Multiple sequence alignments were performed with PILEUP [8], and pair-wise sequence alignments were performed with GAP [7, 20]. PILEUP used the sequences from *E. coli* for DMSO reductase (*dmsA*), both biotin sulfoxide reductases (*bisC* and *bisZ*), and TMAO reductase (*torA*), and the DMSO reductases from *H. influenza* (*dmsA*), and *R. sphaeroides* (*DMSOR*). GAP used only the DMSO reductase sequences from *E. coli* and *R. sphaeroides*.

7.2.4. Molecular Modeling

Rasmol version 2.5, by RasMac Molecular Graphics Macintosh,

Table 7.1.

Bacterial Strains and Plasmids

Strain or Plasmid	Description	Source
***E. coli* strains**		
HB101	*supE*44 *hsdS*20($r_B^-m_B^-$) *recA*13 *ara*-14 *procA*2 *lacY*1	[3]
TG1	*supE*44 *hsdS*20($r_B^-m_B^-$) *recA*13 *ara*-14 *proA*2 *lacY*1 *galK*2 *rpsL*20*xyl*-5 *mtl*-1	Amersham
DSS301	TG1 Δ*dmsABC*	[25]
Plasmids		
pTZ18R	Amp^R *lacZ*	Pharmacia
pBR222	Tet ^{R} Amp^R	Pharmacia
pDMS170	pBR322 Amp^R (*dmsABC*)$^+$	This study
pDMS170 M147L	pBR322 Amp^R (*dmsA*[M^{147}→L^{147}]*BC*)$^+$	This study
pDMS170 M147I	pBR322 Amp^R (*dmsA*[M^{147}→I^{147}]*BC*)$^+$	This study
pDMS170 T148S	pBR322 Amp^R (*dmsA*[T^{148}→S^{148}]*BC*)$^+$	This study
pDMS170 R149C	pBR322 Amp^R (*dmsA*[R^{149}→C^{149}]*BC*)$^+$	This study
pDMS170 G167N	pBR322 Amp^R (*dmsA*[G^{167}→N^{167}]*BC*)$^+$	This study
pDMS170 A178Q	pBR322 Amp^R (*dmsA*[A^{178}→Q^{178}]*BC*)$^+$	This study
pDMS170 Q179I	pBR322 Amp^R (*dmsA*[Q^{179}→I^{179}]*BC*)$^+$	This study
pDMS170 A181T	pBR322 Amp^R (*dmsA*[A^{181}→T^{181}]*BC*)$^+$	This study
pDMS170 A181P	pBR322 Amp^R (*dmsA*[A^{181}→P^{181}]*BC*)$^+$	This study
pDMS170 G190V	pBR322 Amp^R (*dmsA*[G^{190}→V^{190}]*BC*)$^+$	This study
pDMS170 G190D	pBR322 Amp^R (*dmsA*[G^{190}→D^{190}]*BC*)$^+$	This study
pDMS170 W191G	pBR322 Amp^R (*dmsA*[W^{191}→G^{191}]*BC*)$^+$	This study
pDMS170 W357Y	pBR322 Amp^R (*dmsA*[W^{357}→Y^{357}]*BC*)$^+$	This study
pDMS170 W357C	pBR322 Amp^R (*dmsA*[W^{357}→C^{357}]*BC*)$^+$	This study
pDMS170 W357F	pBR322 Amp^R (*dmsA*[W^{357}→F^{357}]*BC*)$^+$	This study
Phage		
M13K07	Kan^R	Pharmacia

was used to examine the coordinates of *R. sphaeroides* DMSO reductase provided by H. Schindelin.

7.2.5. Site-directed Mutagenesis

All manipulations of plasmids and strains were carried out essentially as described by Sambrook *et al.* [26]. The mutants were generated by site-directed mutagenesis of single stranded pDMS223 [23], using the Sculptor^{TM} kit (Amersham), and mutagenic primers. The seven primers used for mutagenesis are listed in Table 7.2. Two primers allowed mutation of a single amino acid residue to only one other. Three primers allowed mutation of a single amino acid residue to several others, due to mixed bases being incorporated in the oligonucleotide at the site of mutation. Two primers were doped with 5% random nucleotide incorporation over the entire sequence, allowing potential mutations to occur over the entire primer sequence. Mutant DNA was subcloned into pDMS170 using *Bgl*II and *Eco*RI, and resequenced to confirm the mutation. DNA sequencing was carried out in the Department of Biochemistry DNA Core facility at the University of Alberta, using an Applied Biosystems model 373A DNA sequencer.

7.2.6. Media and Growth Conditions

Bacteria were grown anaerobically on minimal media [30]. Quantitative growth experiments were performed in Klett flasks using either fumarate (positive control), or DMSO as the electron acceptor [24].

7.2.7. Membrane Preparation

DSS301 with or without wild-type or mutant plasmid pDMS170 (Table 7.1), and HB101, were grown in 19 L carboys on Gly/Fum, and harvested using a Pellicon membrane system [33]. The cell paste was resuspended in buffer [23], and everted envelopes were prepared by French Pressure lysis [2]. Membranes were washed once with 50 mM MOPS pH 7.0, prior to use.

Table 7.2.

Primers for Site-directed Mutagenesis, Mutants Obtained in DmsA, and the Corresponding Residues in DMSOR

Primer	DmsA Mutants Obtained	Residue in DMSOR
5' GAACTGCTGCGGCAACTATCTGAACC 3'	G167N	G138
5' CCTACGGCGHCTGGGCAG 3'	G190V	L162
	G190D	L162
5' CCTACGGCGGCGGGGCAGATGG 3'	W191G	L162
5' GGCGAAACGCHAATGAGTGGC 3'	R217Q	W196
5' CAGCCAGGGATNTGGCCCGCAG 3'	W357Y	W322
	W357C	W322
	W357F	W322
Primer - doped with 5%N over the entire sequence		
5' GGTACGCTGGGCGGCACCATGACCCGCCGCTCCTGGCC 3'	M147L	Y114
	M147I	Y114
	T148S	G115
	R149C	W116
5' CCATTACGGCGACTACTCCTCCGCGCAAATTGCGG 3'	A178Q	A149
	Q179I	A150
	A181T	Q152
	A181P	Q152

Nucleotides altered from the native DmsABC sequence are underlined. H = A, T and C; N = A, T, G, and C; in equimolar ratios.

7.2.8. Kinetic Analysis

DMSO dependent oxidation of $DMNH_2$, was measured by following the oxidation of dithionite using saturating concentrations of DMSO and DMN ($\varepsilon = 8x10^{-3}$ L mol^{-1} cm^{-1}) [36].

S- or N-oxide dependent oxidation of BVH$\cdot^{+}$ ($\varepsilon = 7.8x10^{-3}$ L mol^{-1} cm^{-1}), was followed using the closed cuvette assay [30].

For determination of kinetic constants, between 3 and 9 assays were performed at each substrate concentration, and 5-8 different substrate concentrations were examined to determine each K_m. The values used were the means. In all cases, the standard deviation of the means was less than 10%. A range of substrate concentrations was chosen that varied from at least two times less than the K_m to five times greater than the K_m. We ensured only a small fraction of substrate was utilized during the experiment. K_m and V_{max} values were determined from Eadie-Hofstee plots [9].

k_{cat} values were determined by estimating accumulation of DmsABC in membrane samples, from SDS-PAGE analysis, as indicated below. Assays were performed on freshly diluted washed DSS301 membranes, previously aliquoted into liquid N_2, and stored at $^-70$°C. Diluted sample was stored on ice, and used during the day to obtain reproducible results.

7.2.9. Analytical Techniques

Protein concentrations were determined [15], and SDS-PAGE was performed [12], using BioRad Protean IIxi 20 cm slab gels. Coomassie blue stained gels [13] were scanned with a LKB/Bromma Ultroscan XL laser densitometer. % accumulation of DmsABC in membranes, was determined by comparing the intensity of DmsA bands in membrane and purified samples. A minimum of four concentrations of membrane and purified samples were used. Accumulation values reported are the mean of several experiments. The location of DmsA and DmsB bands was confirmed by Western blotting [25]. DmsA and DmsB polyclonal antibodies were used separately. ECL Western blotting detection reagents from Amersham Life Sciences were used for blot development. No antibody has been successfully raised against DmsC. For those mutants with poor expression (R149C, G167N, A178Q, and Q179I), and HB101 membranes (normal non-overexpressed levels), % accumulation of DmsABC in membrane samples was determined by comparing the intensity of DmsA bands from membranes to known amounts of DmsA on Western blots.

7.3. Results

7.3.1. Sequence Analysis, Molecular Modeling, and Primer Design

Multiple sequence alignment of prokaryotic moco containing enzymes has defined segments of sequence homology, separated by sequence that differs in length and composition [1, 33, 35]. Segment 3, (DmsA residues 142-197 (Figure 7.1.)), may be important for substrate binding, as sequence similarity in this region is only observed between enzymes using similar types of substrate, for example, those enzymes reducing S- and N-oxides.

The molecular graphics program Rasmol was used to examine the three-dimensional structure of DMSOR [28]. Residues forming the active site funnel can be defined either by the secondary structural unit they help compose, or in relation to other amino acids found on the surface of the active site funnel, and the Mo of the moco. In the latter definition, they can be considered to be approximately in the first to Xth concentric layer from the active site Mo. Residues Y114, G115, and W116, are found in the secondary structure following β-sheet 6. These residues compose almost one half of the bottom layer of the funnel,

dmsA	^{141}GTLGGT$\underline{\text{MTR}}$S	^{151}WPP....GNT	^{157}LVARLMNCCG	^{167}$\underline{\text{G}}$YLNHYGDYS
DMSOR	^{108}GTFGGS$\underline{\text{YGW}}$K	^{118}SPGRLHNCQV	^{128}LMRRALNLAG	^{138}GFV$\underline{\text{NSSGDYS}}$
dmsA	^{177}S$\underline{\text{AQ}}$I$\underline{\text{A}}$EGLNY	^{187}TYG$\underline{\text{GW}}$....A	^{193}DGNSPSDIEN	^{203}SKLVVLFGNN
DMSOR	^{148}$\underline{\text{TAAAQ}}$IIMPH	^{158}VMGT$\underline{\text{L}}$EV$\underline{\text{Y}}$EQ	^{168}QTAWPVVVEN	^{178}TDLMVFWAAD
dmsA	^{213}PGET....$\underline{\text{R}}$M	^{219}SGGGVTYYLE	^{229}QARQKSNARM	^{239}IIIDPRYTDT
DMSOR	^{188}PMKTNEIG$\underline{\text{W}}$V	^{198}IPDHGAYAGM	^{208}KALKEKGTRV	^{218}ICINPVRTET
dmsA	^{249}GAGREDEWIP	^{259}IRPGTDAALV	^{269}NGLAYVMITE	^{279}NLVDQAFLDK
DMSOR	^{228}ADYFGADVVS	^{238}PRPQTDVALM	^{248}LGMAHTLYSE	^{258}DLHDKDFLEN
dmsA	^{289}YCVGYDEKTL	^{299}PASAPKNGHY	^{309}KAYILGEGPD	^{319}GVAKTPEWAS
DMSOR	^{268}CTTGFD....	^{274}........LF	^{276}AAYLTGES.D	^{285}GTPKTAEWAA
dmsA	^{329}QITGVPADKI	^{339}IKLAREIGST	^{349}KPAFISQG$\underline{\text{W}}$G	^{359}PQRHANGEIA
DMSOR	^{295}EICGLPAEQI	^{305}RELARSFVAG	^{315}R.TMLAAG$\underline{\text{W}}$S	^{324}IQRMHHGEQA
dmsA	^{369}TRAISMLAIL	^{379}TGNVGINGGN	^{389}.......	
DMSOR	^{334}HWMLVTLASM	^{344}IGQIGLPGGG	^{354}FGLSYH$\underline{\text{Y}}$	

Figure 7.1.

Sequence Alignment of *E. coli* (*dmsA*) and *R. sphaeroides* (*DMSOR*) DMSO Reductases using GAP

Residues underlined are located at the bottom of active site funnel in DMSOR, and mutated in *dmsA*. Segment 3 has been defined as residues 142-197 in *dmsA*.

being found between approximately 4 and 8 Å from the Mo. Continuing around this imaginary concentric layer are residues Y360, Y165, W322 and S147, the Mo ligand. These residues are found to be between approximately 3 and 7 Å from the Mo. L162 is situated immediately above Y165, and W196 above W116. A large portion of the funnel, approximately 1/3, is composed of residues 141-152, forming β-sheet 7 and α-helix 5 [28]. Primers were made to mutate residues in DmsABC corresponding to four specific residues, and two segments including numerous amino acids (Table 7.2.). As there are no obvious counterparts to Y360 or Y165, the corresponding residues were not mutated (Figure 7.1). The DmsA residue equivalent to S147 in DMSOR (S176) has previously been mutated [32]. DmsA residue G167 was also selected for mutation, and an explanation for this will be given in the discussion.

7.3.2. Preparation of Mutants in DmsABC

Table 7.2. lists the sixteen single DmsA mutations obtained using the seven mutagenic oligonucleotides. Primers allowing mutation of an amino acid to several others at that site did not yield all possibilities. The same was observed when using the doped primers. In addition, mutational preference was observed at specific residues. Some double mutants were also obtained, but were only preliminary characterized, due to the inability to separate the effect of each of the mutations.

7.3.3. Accumulation of Wild-type and Mutant DmsABC in DSS301

All experiments were performed in the DmsABC deletion mutant DSS301. DSS301 was transformed with plasmids carrying either a mutant or wild-type copy of *dmsABC* (Table 7.1.). Expression from the plasmid provided the only DMSO reductase available to the cell. Following PAGE, DmsA and DmsB are easily stained and visualized as discrete bands at approximately 87 and 24 kDa. When over-expressed from pDMS170, wild-type DmsABC comprises approximately 25% of membrane protein compared with 3.5% when DmsABC is chromosomally-encoded. Expression of 15 of the 16 site-directed mutant enzymes resulted in expression levels from 3.7% to 17.9%. (Mutant A181P did not express and was not examined further (Table 7.3.)). Thus, all studied mutants accumulated to levels at least as great as chromosomally-encoded DmsABC, indicating there was enough DmsABC, if functional, to allow for wild-type growth. Interestingly, mutations in the range of amino acids 149 to 190 had the lowest expression.

7.3.4. Growth Characteristics of DSS301 Harboring Plasmid Containing Wild-type or Mutant DmsABC

DSS301 is unable to grow anaerobically with DMSO as the sole electron acceptor, due to deletion of *dmsABC* [24, 30]. This strain can be complemented by plasmids carrying *dmsABC* [25], and this provides a simple means to monitor functional activity of the mutant enzymes. As seen in Table 7.3., eleven of the mutations resulted in essentially normal doubling times, indicating that the DMSO reductase with these mutations was functional. R217Q had the longest doubling time, indicating this enzyme was significantly altered, but it could still support growth poorly. Mutations at G167, A178 and Q179 resulted in doubling times that were twice that of wild-type, suggesting this region of the protein was also functionally important. Although mutations in this region of the polypeptide resulted in proteins that expressed poorly compared to wild-type enzyme, their levels still exceeded that of chromosomally-encoded DmsABC. This confirms the increased doubling times were not a reflection of limiting amounts of enzyme.

7.3.5. Kinetic Characteristics of Mutant and Wild-type DmsABC with BV

In Table 7.4., we report the apparent K_m and k_{cat} values for the wild-type and mutant enzymes, using two distinctly different substrates, DMSO and PNO.

Table 7.3.

Growth Properties and Accumulation of DmsABC Mutants

Mutant	Doubling Time (hours)	% DmsABC in Membrane
M147L	5.4	14.8
M147I	7.8	12.2
T148S	7.3	10.3
R149C	7.9	4.2
G167N	13.5	6.0
A178Q	19.4	4.0
Q179I	18.0	4.0
A181T	6.2	3.7
A181P	NG	0
G190V	6.5	6.5
G190D	4.8	15.6
W191G	4.5	17.9
R217Q	40	14.2
W357Y	6.2	12.1
W357C	5.7	11.4
W357F	5.8	11.5
wild-type	5.1	24.7

Doubling times were determined from measurements of cell densities with DMSO as the sole terminal electron acceptor, using a Klett-Summerson spectrophotometer equipped with a number 66 filter. Doubling times and accumulation of wild-type and mutant DmsABC was determined in a DmsABC$^-$ strain. NG indicates no growth.

Table 7.4.

Kinetic Parameters for DmsABC Mutants with $BVH^{\bullet +}$ or $DMNH_2$ as Electron Donor

	$BVH^{\cdot +}$						$DMNH_2$
Mutant	DMSO			PNO			DMSO
	K_m (mM)	k_{cat} (s^{-1})	k_{cat}/K_m ($s^{-1}mM^{-1}$)	K_m (mM)	k_{cat} (s^{-1})	k_{cat}/K_m ($s^{-1}mM^{-1}$)	k_{cat} (s^{-1})
M147L	0.040	39	960	0.11	110	1000	3.8
M147I	0.020	27	1360	0.18	190	1100	7.6
T148S	0.11	370	3300	0.024	96	4000	21
R149C	0.076	68*	900*	0.12	95*	810*	12*
G167N	0.038	14*	370*	0.076	99*	1300*	1.9*
A178Q	<0.001	23*	23300*	<0.001	10.0*	>10000*	1.9*
Q179I	0.019	19*	1000*	0.034	36*	1100*	2.2*
A181T	0.039	210*	5500*	0.24	940*	4000*	39*
G190V	0.033	110	3400	0.12	260	2100	16
G190D	0.038	60	1600	0.15	190	1200	10
W191G	0.028	47	1600	0.048	99	2100	8.2
R217Q	1.1	55	50	3.8	120	33	6.3
W357Y	0.019	24	1300	0.028	33	1200	7.2
W357C	0.024	46	1900	0.095	100	1100	4.6
W357F	0.023	17	760	0.048	41	850	3.1
wild -type	0.032	61	1900	0.100	200	2000	10

All assays were performed on washed membranes, using saturating $BVH^{\bullet +}$ or $DMNH_2$ as electron donor, and as indicated, either DMSO or PNO as electron acceptor. For mutants with poor accumulation, k_{cat} and k_{cat}/K_m values are less accurate, and are indicated with a *.

The DMSO K_m for wild-type enzyme is about 0.03 mM. Twelve of the mutants had K_m values similar to wild-type enzyme. T148S had a 3.5-fold weaker K_m (0.11 mM), but a five-fold higher k_{cat}, resulting in a k_{cat}/K_m that was two-fold greater than the wild-type. G167N had a K_m for DMSO resembling wild-type enzyme, but the k_{cat} was greatly reduced resulting in a k_{cat}/K_m five-fold less than wild-type enzyme. R217Q had a K_m that was increased over 35-fold, while the k_{cat} was essentially wild-type, resulting in a very poor k_{cat}/K_m. This may account for the greatly increased doubling time of DSS301 harboring plasmid with this enzyme. A178Q was the most interesting mutation. The K_m for DMSO was greatly reduced in this mutant, to a level below 1 μM, and the k_{cat} was decreased by only about 50%. The k_{cat}/K_m for this mutant was thus greatly increased to over 23,000.

The results with PNO generally mirrored those seen with DMSO. The K_m for PNO was also greatly reduced in the A178Q mutation, and increased in the R217Q mutation. T148S, however, displayed a different phenotype. Where the K_m for DMSO was 3.5-fold higher for T148S, the K_m with PNO was four-fold lower. Additionally, the k_{cat} for this mutation increased six-fold with DMSO and decreased 50% for PNO. For the other mutations the changes in K_m and k_{cat} were within two fold of wild-type.

7.3.6. k_{cat} for Mutant and Wild-type DmsABC with Saturating $DMNH_2$ and DMSO

$DMNH_2$ is a Q analogue, and was employed to examine the kinetic characteristics of the mutant enzymes. $DMNH_2$ is a substrate sharing substantial structural similarity with MQH_2, the natural electron donor of DmsABC [6, 14, 19]. Washed membrane fractions from anaerobically grown DSS301, carrying mutant or wild-type plasmid, were assayed using $DMNH_2$ and DMSO as electron donor and acceptor, respectively. Assay limitations did not allow use of the extremely low concentrations of DMSO required to determine K_m's. However, k_{cat}'s could be determined (Table 7.4). The $DMNH_2$/DMSO

k_{cat}'s, although lower, paralleled very well those determined with $BVH^{\cdot +}$ as electron donor.

7.4. Discussion

We have previously characterized the broad substrate specificity of DmsABC [30]. Now we have extended our understanding of the activity of this enzyme, employing the three-dimensional structure of the related soluble periplasmic DMSOR. Residues forming the wall of the funnel leading to the active site Mo in DmsABC were predicted, and mutations were made in eleven individual amino acids, by a combination of random-primer mutagenesis, and site-directed mutagenesis. Our results suggest that T148, A178, and R217, are found in the active site funnel and are important in substrate binding, and/or specificity. Residues G167 and Q179 also appear to be important in DmsABC function, as mutation of these amino acids affects the ability of DmsABC to support anaerobic growth on Gly/DMSO medium. The six other amino acids that were mutated appear to have no affect on the function or activity of DmsABC. This suggests substantial flexibility in residues lining the active site tunnel.

Examination of the DMSOR crystal structure indicated residues causing a disturbance in enzyme function or activity, were not found to be spatially clustered [28].

Enzymes utilize electrostatic, steric, and non-polar interactions, as well as hydrogen bonds, to bind and orient substrate in the active site. S- and N-oxide substrates of molybdoenzyme, must travel down the active site funnel to reach the site of catalysis [28, 29, 35]. The S- and N-oxides substrates of DmsABC are quite non-polar, but do exhibit large permanent dipole moments [21]. The former characteristic allows hydrophobic interactions between substrate and active site residues. The latter allows formation of transient hydrogen bonds and/or electrostatic interactions.

Since S- and N-oxides are generally bulky uncharged molecules, Gly residues present in the segment conserved between molybdoenzymes with similar substrate specificities (segment 3 - Figure 7.1.) [1, 35], might be important in substrate binding and accessibility [1]. DMSO reductases from *E. coli, R. sphaeroides,* and *R. capsulatus,* show broader substrate specificity [18, 27, 30] than *E. coli* TMAO reductase [10]. It was predicted that Gly's in segment 3 of DmsA, replaced with bulkier residues in TorA, may restrict the substrate profile of TorA. G167 is conserved in the DMSO reductases, but is replaced by an Asn in TorA. Thus the G167N mutation was particularly interesting. This mutant displayed decreased k_{cat} values, and an increased doubling time, but it did not show major kinetic differences between the substrates DMSO and PNO. The DMSOR crystal structure shows the analogous residue G138 is exposed on the funnel surface, but is found approximately 24.9 Å from the active site Mo [28].

The observed changes in K_m for the mutants A178Q and R217Q, may be the result, of increased ability to form hydrophobic interactions and hydrogen bonds (A178Q), and the decreased ability to form electrostatic and hydrophobic interactions (R217Q), with substrate in the active site funnel. Homologous residues in DMSOR (A149 and W196), are found exposed on opposite sides of the funnel, at distances of 9.1 and 7.1 Å from the Mo, respectively (+.).

Changing T148 to Ser had different effects on the kinetic parameters for PNO and DMSO. It is possible that the decreased bulkiness of Ser results in poorer binding and catalysis for DMSO, whereas PNO finds this change a helpful enlargement of the active site funnel. G115, the homologous residue in DMSOR, is surface exposed, being approximately 8.4 Å from the Mo (Figure 7.2.).

M147, T148 and R149 potentially form a large portion of the bottom layer of the funnel. M147 and R149 of DmsABC (Y115 and W117 in DMSOR), are also in close proximity to the Mo, yet mutation of these amino acids did not significantly alter the kinetic properties of the

Figure 7.2.

Modeling of DMSOR Active Site Residues

The α-carbon backbone for residues 113-197 is shown in red, and the amino and carboxyl termini are numbered. The moco is shown, with the Mo as a sphere in turquoise, and the oxo ligand in orange The side chains for residues in DMSOR, homologous to those residues in DmsA showing alterations in function, are indicated. DMSOR residues G138, G115, W196, A149, and A150, are homologous to residues G167, T148, R217, A178, and Q179, respectively.

enzyme.

It has previously been documented that multiple paths of electron transfer exist within DmsABC, and the path of electron flow depends on the electron donor [31]. G167N and Q179I showed decreased ability to support growth on Gly/DMSO, although the kinetic parameters appeared within normal limits using $BVH^{\cdot +}$ as electron donor. The k_{cat} using $DMNH_2$ was very low. This suggests electron transfer from the endogenous Q pool has been deleteriously. The homologous residues in DMSOR (G138 and A150 respectively) are further from the Mo than any of the other mutants with altered activity, 24.9 and 11.9 Å respectively (Figure 7.2.). They are found in the same region of the funnel, but G138 is surface exposed, while A150 is not.

We have demonstrated the ability to change kinetic parameters and substrate specificity by altering amino acids potentially located in the active site tunnel of DmsABC. More extensive mutation of active site residues may reveal other residues, besides T148, A178, and R217, specifically involved in substrate binding and/or catalysis.

7.4. References

1. Berks, B.C., Ferguson, S.J., Moir, J.W.B. and Richardson, D.J. (1995) Enzymes and associated electron transport systems that catalyze the respiratory reduction of nitrogen oxides and oxyanions. Biochim. Biophys. Acta 1232, 97 - 123.

2. Bilous, P.T. and Weiner, J.H. (1985) Dimethyl sulfoxide reductase activity by anaerobically grown *Escherichia coli*. J. Bacteriol. 162, 1151 - 1155.

3. Boyer, H.W. and Roulland-Dussoix, D. (1969) A complementary analysis of the restriction and modification of DNA in *Escherichia coli*. J. Mol. Biol. 41, 459.

4. Boyington, J.C., Gladyshev, V.N., Khangulov, S.V., Stadtman, T.C. and Sun, P.D. (1997) Crystal structure of formate

dehydrogenase H: catalysis involving Mo, molybdopterin, selenocysteine, and Fe_4S_4 cluster. Science 275, 1305 - 1308.

5. Chan, M.K., Mukund, S., Kletzin, A., Adams, M.W.W. and Rees, D.C. (1995) Structure of a hyperthermophilic tungstopterin enzyme, aldehyde ferredoxin oxidoreductase. Science 267, 1463 - 1469.

6. Cox, J.C. and Knight, R. (1981) Trimethylamine N-oxide (TMAO) reductase activity in chlorate-resistant or respiration-deficient mutants of *Escherichia coli*. FEMS Microbiol. Lett. 12, 249-252.

7. Devereux, J., Haeberli, P. and Smithies, O. (1984) A comprehensive set of sequence analysis programs for the VAX. Nucleic Acids Res. 12, 387 - 395.

8. Feng, D.F. and Doolittle, R.F. (1987) Progressive sequence alignment as a prerequisite to correct phylogenetic trees. J. Mol. Evol. 35, 351 - 360.

9. Fersht, A. (1977) Chapter 10: Enzyme-substrate complementarity and theories of enzyme catalysis, in Enzyme structure and mechanism. p. 244-271, W. H. Freeman, San Francisco.

10. Iobbi-Nivol, C., Pommier, J., Simala-Grant, J.L., Mejean, V. and Giordano, G. (1996) High substrate specificity and induction characteristics of trimethylamine N-oxide reductase of *Escherichia coli*. Biochim. Biophys. Acta 1294, 77 - 82.

11. Knablein, J., Dobbek, H., Ehlert, S. and Schneider, F. (1997) Isolation, cloning, sequence analysis and X-ray structure of dimethyl sulfoxide/trimethylamine N-oxide reductase from *Rhodobacter sphaeroides*. Biol. Chem. 378, 293-302.

12. Laemmli, U.K. (1970) Cleavage of structural proteins during the assembly of the head of bacteriophage T4. Nature 227, 680 - 685.

13. Lemire, B.D., Robinson, J.J. and Weiner, J.H. (1982) Identification of membrane anchor polypeptides of *Escherichia coli* fumarate reductase. J. Bacteriol. 152, 1126 - 1131.

14. MacEwan, A.G., Wetstein, H.G., Meyer, O., Jackson, J.B. and Ferguson, S.J. (1987) The periplasmic nitrate reductase of *Rhodobacter capsulatus*; purification, characterisation and distinction from a single reductase for trimethylamine-N-oxide dimethylsulphoxide and chlorate. Arch. Microbiol. 147, 340-345.

15. Markwell, M.A.D., Haas, S.M., Bieber, L.L. and Tolbert, N.E. (1978) A modification of the Lowry procedure to simplify protein determination in membrane and lipoprotein samples. Anal. Biochem. 87, 206 - 210.

16. McAlpine, A.S., McEwan, A.G. and Bailey, S. (1998) The high resolution crystal structure of DMSO reductase in complex with DMSO. J. Mol. Biol. In press.

17. McAlpine, A.S., McEwan, A.G., Shaw, A.L. and Bailey, S. (1998) Molybdenum active center of DMSO reductase from *Rhodobacter capsulatus* : crystal structure of the oxidised enzyme at 1.82Å resolution and the dithionite-reduced enzyme at 2.8Å resolution. J. Biol. Inorg. Chem. In press.

18. McEwan, A.G., Wetzstein, H.G., Ferguson, S.J. and Jackson, J.B. (1985) Periplasmic location of the terminal reductase in trimethylamine N-oxide and dimethylsulphoxide respiration in the photosynthetic bacterium *Rhodopseudomonas capsulata*. Biochim. Biophys. Acta 806, 410 - 417.

19. Meganathan, R. (1984) Inability of *men* mutants of *Escherichia coli* to use trimethylamine-N-oxide as an electron acceptor. FEMS Microbiol. Lett. 24, 57-62.

20. Needleman, S.B. and Wunsch, C.D. (1970) A general method applicable to the search for similarities in the amino acid sequence of two proteins. J. Mol. Biol. 48, 443 - 453.

21. Ochaiai, E. (1967) Aromatic Amine Oxides. Elsevier Publishing Company, Amsterdam.

22. Romao, M.J., Chan, M.K., Mukund, S., Kletzin, A., Adams, M.W.W. and Rees, D.C. (1995) Crystal structure of the xanthine oxidase-related aldehyde oxido-reductase from *D. gigas*. Science 270, 1170-1176.

23. Rothery, R.A. and Weiner, J.H. (1991) Alteration of the iron-sulfur cluster composition of *Escherichia coli* dimethyl sulfoxide reductase by site-specific mutagenesis. Biochemistry 30, 8296 - 8305.

24. Sambasivarao, D. and Weiner, J.H. (1991) Differentiation of the multiple S- and N-oxide reducing activities of *Escherichia coli*. Curr. Microbiol. 23, 105 - 110.

25. Sambasivarao, D. and Weiner, J.H. (1991) Dimethylsulfoxide reductase of *Escherichia coli* : an investigation of function and

assembly by use of *in vivo* complementation. J. Bacteriol. 173, 5935 - 5943.

26. Sambrook, J., Fritsch, E.F. and Maniatis, T. (1989) Molecular cloning : A laboratory manual. Cold Spring Harbor Laboratory Press, Cold Spring Harbor, N.Y.

27. Satoh, T. and Kurihara, F.N. (1987) Purification and properties of dimethylsulfoxide reductase containing a molybdenum cofactor from a photodenitrifier *Rhodopseudomonas sphaeroides* f.s. *denitrificans*. J. Biochem. 102, 191 - 197.

28. Schindelin, H., Kisher, C., Hilton, J., Rajagopalan, K.V. and Rees, D.C. (1996) Crystal structure of DMSO reductase: Redox-linked changes in molybdopterin coordination. Science 272, 1615 - 1621.

29. Schneider, F., Lowe, J., Huber, R., Schindelin, H., Kisker, C. and Knablein, J. (1996) Crystal structure of dimethyl sulfoxide reductase from *Rhodobacter capsulatus* at 1.88 A resolution. J. Mol. Biol. 263, 53 - 69.

30. Simala-Grant, J.L. and Weiner, J.H. (1996) Kinetic analysis and substrate specificity of *Escherichia coli* dimethyl sulfoxide reductase. Microbiol. 142, 3231 - 3239.

31. Trieber, C.A., Rothery, R.A. and Weiner, J.H. (1994) Multiple pathways of electron transfer in dimethyl sulfoxide reductase of *Escherichia coli*. J. Biol. Chem. 269, 7103 - 7109.

32. Trieber, C.A., Rothery, R.A. and Weiner, J.H. (1996) Consequences of removal of a molybdenum ligand (DmsA-Ser-176) of *Escherichia coli* dimethyl sulfoxide reductase. J. Biol. Chem. 271, 27339 - 27345.

33. Weiner, J.H., MacIsacc, D.P., Bishop, R.E. and Bilous, P.T. (1988) Purification and properties of *Escherichia coli* dimethyl sulfoxide reductase, an iron-sulfur molybdoenzyme with broad substrate specificity. J. Bacteriol. 170, 1505 - 1510.

34. Weiner, J.H., Rothery, R.A., Sambasivarao, D. and Trieber, C.A. (1992) Molecular analysis of dimethylsulfoxide reductase : a complex iron-sulfur molybdoenzyme of *Escherichia coli*. Biochim. Biophys. Acta 1102, 1 - 18.

35. Wootton, J.C., Nicolson, R.E., Cock, J.M., Walters, D.E., Burke, J.F., Doyle, W.A. and Bray, R.C. (1991) Enzymes depending on the pterin molybdenum cofactor : sequence families, spectroscopic

properties of molybdenum and possible cofactor-binding domains. Biochim. Biophys. Acta 1057, 157 - 185.

36. Yamamoto, I., Okubo, M. and Ishimoto, M. (1986) Further characterization of trimethylamine N-oxide reductase from *Escherichia coli* a molybdoprotein. J. Biochem. 99, 1773 - 1779.

Chapter 8 : Elucidation and Identification of a Previously Uncharacterized Terminal N-oxide Reductase*

8.1. Introduction

Five S- and N-oxide reductases have been characterized, cloned and sequenced from *E. coli* : DmsABC (DMSO reductase) [5], TorA (TMAO reductase) [39], BisC (biotin sulfoxide reductase) [43], BisZ (alternative biotin sulfoxide reductase) [21], and MsrA (methionine sulfoxide peptide reductase) [12, 44]. MsrA does not share sequence homology with the former four [4], and is not a molybdoenzyme [44]. While biotin and methionine sulfoxide reductases are responsible for reducing oxidized biotin and methionine, respectively, in a repair or scavenging mechanism [43, 44], DmsABC and TorA are terminal reductases that support anaerobic growth in the presence of electron donor, carbon source, and their respective substrates [48]. BisC, BisZ and MsrA reductases are expressed under aerobic growth conditions [11, 22]. Expression of BisC increases due to oxidative stress [14], while MsrA expression increases during mid-log to stationary phase [40]. In contrast, DmsABC and TorA are expressed under specific anaerobic growth conditions [18, 42].

Kinetic analysis shows DmsABC has a very broad substrate specificity, utilizing a wide variety of S- and N-oxides (Chapter 6), while TorA has a narrower substrate specificity, reducing a smaller variety of

---

* A portion of this chapter has been published. Simala-Grant, J. L. and Weiner, J. H. (1996) Kinetic analysis and substrate specificity of *Escherichia coli* dimethylsulfoxide reductase. Microbiol. 142, 3231-3239. This chapter includes Figure 3 from this paper, as well as previously unpublished data. Figure 2 from this paper is found in Chapter 5, while the rest of the data is found in Chapter 6.

N-oxides, and no S-oxides (Chapter 9). Growth experiments demonstrated many of these S- and N-oxide substrates supported anaerobic growth in the presence of glycerol as carbon source and electron donor (Chapter 6). It was not known whether growth on these S- and N-oxides was due to one or both of DmsABC and TorA, or whether another as yet unidentified terminal reductase also contributed to growth on these S- and N-oxides. To answer this question we examined the ability of wild-type and mutant *E. coli* strains, unable to express one or both of DmsABC and TorA, to conserve the energy of S- and N-oxide reduction, as observed by anaerobic growth in the presence of glycerol and a variety of S- and N-oxides.

In this study *E. coli* is demonstrated to express at least one additional anaerobically expressed energy conserving terminal reductase, that allows anaerobic growth on substituted PNO's in the presence of glycerol. Substituted PNO reductase activity can be found in *E. coli* lacking both DmsABC or TorA, and we have characterized the subcellular location and expression of this enzyme. This protein is not recognized by DmsA or DmsB antibody, and appears to be a molybdoenzyme. The protein responsible has been designated PNO reductase (PNOR). Conditions for optimal activity have been established, and a preliminary purification procedure is outlined. In addition a mutant with increased PNOR activity was isolated.

8.2. Materials and Methods

8.2.1. Materials

DMN was a gift from A. Kroger, J. W. Goethe University, Frankfurt, Germany. All other materials were reagent grade and were purchased from commercial sources.

8.2.2. Strains and Plasmids

E. coli strains TG1, MC4100, LCB128, DSS401, and DSS501, used in this study, are described in Table 8.1. MC4100 is wild-type, LCB128 does not express TorA, DSS401 does not express DmsABC, and DSS501 does not express either TorA or DmsABC. TG1 was used for initial cloning experiments. All manipulations of strains were carried out essentially as described by Sambrook [50].

8.2.3. Media and Growth Conditions

Strains were grown aerobically in LB or Terrific Broth [50] overnight, and these cultures were used as 1% inocula.

Glycerol minimal media was used as indicated previously [6], except 0.16% peptone was substituted for casamino acids, streptomycin sulfate was not included in the growth medium, and a variety of electron acceptors were used at the concentrations listed below in mM, unless otherwise indicated in the text, or Figure and Table legends : fumarate, 40; TMAO, 70; PNO, 25; 3-carboxypyridine N-oxide, 25; 4-methylpyridine N-oxide, 25; and 3-hydroxypyridine N-oxide, 25; tetramethylene sulfoxide, 25; and DMSO, 30. Gly/Fum and Gly/PNO indicate glycerol minimal media with fumarate and PNO as terminal electron acceptor.

M9 minimal media with glucose [50], was used for anaerobic growth [48], with or without the addition of 20 mM PNO.

For anaerobic growth, bacteria were grown in 19 L carboys, 1 L flasks, or Klett flasks, filled to the top, and sealed to exclude O_2. Stir bars were employed to mix the culture during growth, for 48 hours, unless otherwise indicated in the text or Figure and Table legends.

To examine aerobically grown cells, 150 mL's of Gly/Fum (plus 5 mM PNO), in a 1 L flask, was shaken for 22 hours.

Table 8.1.

E. coli Strains Used in this Study

Strain	Description	Source
TG1	*supE*44 *hsdS*20($r_B^- m_B^-$) *recA*13 *ara*-14 *proA*2 *lacY*1 *gal*K2 *rpsL*20*xyl*-5 *mtl*-1	Amersham
MC4100	*ara*D139 (*lac*IPOZYA-*arg*F)U169 *rps*L *thi*	[15]
LCB128	as MC4100 *torA*::Mud1 (Amp^r-*lac*)	M. Chippaux, Marsaille, France
DSS401	as MC4100 Δ*dms* Kan^R	[48]
DSS501	as LCB128 Δ*dms* Kan^R	[48]
DSS501-3	as LCB128 Δ*dms* Kan^R (increased expression of FrdABCD and PNOR - mutation unknown)	This study.

Cells were grown at 30°C, and antibiotics were added to the growth medium when necessary in μg/mL : 50-100, ampicillin; 40, kanamycin; and 25, chloramphenicol.

100 mM sodium tungstate, was included in the growth media when indicated.

8.2.4. Preparation of Membrane and Supernatant Fractions

Large cell volumes were harvested using a Pellicon membrane system equipped with a Millipore polysulfone PTNK filter. Bacterial cells were pelleted by centrifugation at 9,500 x g for 10 minutes. Cell pellets were resuspended in 50 mM MOPS pH 7.0, with 5 mM EDTA, and the bacteria were broken by French pressure lysis unless otherwise indicated. Membrane and supernatant fractions were separated by centrifugation [6].

To compare the effect of different cell disruption techniques on enzyme activity, DSS501 grown on Gly/Fum (with 5 mM PNO), were lysed either by French Press [6], or the lysozyme freeze/thaw method [19].

8.2.5. Enzyme Assays

Fifty mM MOPS pH 7.0 was used for all assays unless otherwise indicated. Spectrophotometric changes were measured using a Gilford 250 spectrophotometer.

One unit of enzyme activity corresponds to 2 μmol of $BVH^{\cdot +}$ or $MVH^{\cdot +}$, 1 μmol NADH, NADPH, $FADH_2$, or $FMNH_2$ oxidized per minute, or 1 μmole of S- or N-oxide reduced per minute. The values used were the means. Unless otherwise indicated, the standard deviation of the means was less than 10%.

8.2.5.1. Assays for Reductase Activity

Substrate-dependent oxidation of BVH·+, or MVH·+ was monitored at 570 and 600 nm, respectively, using degassed and N_2 bubbled 50 mM MOPS unless otherwise indicated. Fifty mM sodium acetate pH 5.5 was used with the electron acceptor ANO.

For optimization of PNOR assays with BVH·+, the following "Good" buffers were tested at 50 mM : MES, pH 6.2 (pKa 6.1); bis-[2-hydroxyethyl]imino-tris[hydroxymethyl]methane; 2-bis[2hydroxyethyl]amino-2hydroxymethyl]-1,3propanediol (BIS-TRIS), pH 6.45 (pKa 6.5); N-[2-hydroxyethyl]piperazine-N'-[2-ethanesulfonic acid] (HEPES), pH 7.57 (pKa 7.5); BICINE, pH 8.4 (pKa 8.35); or "Other" buffers at 100 mM : sodium citrate, pH 6.2,; 3,diaza-2,4-cyclopentadiene (imidazole), pH 6.95; potassium phosphate, pH 8.0; tris[hydroxymethyl]aminomethane (TRIS), pH 8.6; glycine, pH 9.2.

To examine the effects of various compounds on enzyme activity, when indicated, each of the following compounds were included individually in the assay at the following concentrations : selenite, 2.33 mM; dithiothreitol (DTT), 1.67 mM; EDTA, 0.83 mM; NaCl, 25 mM; and glycerol, 2.67%. When metal mix was added to the assay, metals were at the following final concentrations in µM : $MgSO_4$, 65; $MnSO_4$, 8.2; $Fe_2(SO_4)_3$, 0.36; $CaCl_2$,1.2.

Open cuvette (non-stoppered) assays, were performed using BV^{2+} or oxidized MV (MV^{2+}) at a final concentration of 0.2 mM, and sodium dithionite (dithionite) at 0.33 mM. The order of addition was : BV^{2+}/ MV^{2+}, S- or N-oxide, dithionite, and enzyme.

8.2.5.2. Assays for Electron Donor Activity

NADH, and NADPH electron donor activity, was measured as per published procedures [32, 59]. Briefly, electron donor was added to approximately 16-26 µmolar, to obtain an initial OD of 0.3-0.5 at 340 nm. Oxidation was followed by loss of absorbance at 340 nm.

$FADH_2$, and $FMNH_2$ electron donor activity, was measured using 0.2 mM dithionite to reduce electron donor. Oxidation was measured by following an increase in the absorbance at 450 nm [1].

Oxidation of dithionite reduced DMN (0.2 mM) was measured following the oxidation of dithionite at 317 nm ($\varepsilon = 8x10^{-3}$ L mol^{-1} cm^{-1}) [66].

8.2.5.3. β-lactamase Assays

β-lactamase activity was measured following the decrease in absorbance at 570 nM using 50 μg/mL 7-(thienyl-2-acetamido)-3-[2-(4-N,N-dimethylaminophenyl-azo)-pyridinium methyl]-3-cepham-4-carboxylic acid (PADAC).

8.2.6. Localization of PNOR Activity

DSS501 was grown in a 19 L carboy containing Gly/Fum plus 5 mM PNO for 30.5 hours. The cell pellet obtained was washed twice with 4°C TRIS-HCl pH 7.3 containing 30 mM NaCl. Cells were resuspended in 80 volumes (weight/volume) 0.033 M TRIS-HCl pH 7.3 containing 20% sucrose and 0.1 EDTA at 23°C. Cells were swirled for 5 minutes, and centrifuged at 9,500 x g for 10 minutes. The cell pellet was suspended in 80 volumes (weight/volume) 0.5 mM $MgCl_2$, and swirled for 10 minutes. Cells were centrifuged at 9,500 x g for 10 minutes. The supernatant was considered the osmotic shock fluid, or periplasm, and was concentrated by ultrafiltration using an Amicon model 410 ultrafiltration cell, equipped with a UM-10 membrane. Intact cells were separated into membrane and cytoplasmic fractions as indicated in section 8.2.4. Preparation of Membrane and Supernatant Fractions. All three fractions were tested for β-lactamase, PNOR, and FrdABCD activity, as well as protein concentration.

8.2.7. Stability of PNOR Activity

When protease inhibitor cocktail was added to supernatant, the final concentrations of protease inhibitors in µg/mL were : aprotinin, 0.1; phosphoramidon, 0.1; TLCK-HCl, 0.1; TPCK, 0.2; A-PMSF, 0.1; E-64, 0.1; leupeptin, 0.05; pepstatin 0.01.

8.2.7.1. Stability at 4°C

DSS501 supernatant from cells grown anaerobically on Gly/Fum, was incubated for 21 hours at 4°C after addition of one of the following compounds to each sample : 10 mM PNO, 2 mM PMSF, 1 mM EDTA, 1 mM ascorbic acid, 2 mM DTT, 10% glycerol, protease inhibitor cocktail, or metal mix. When metal mix was added, metals were at the following final concentrations in µM : $MgSO_4$, 65; $MnSO_4$, 8.2; $Fe_2(SO_4)_3$, 0.36; $CaCl_2$, 1.2. BV/PNOR activity was measured before and after incubation at 4°C.

8.2.7.2. Stability to Freeze/Thaw

DSS501 Gly/Fum supernatant was precipitated using two volumes of saturated ammonium sulfate, as indicated in section 8.2.9.2. Ammonium Sulfate Precipitation. The pellet was either frozen to $^-70$°C before or after being resuspended in 50 mM MOPS. The thawed samples were analyzed for BV/PNOR activity using 66.6 mM PNO.

Alternatively, protease inhibitor cocktail was added to one of two supernatant samples. These samples were frozen in liquid N_2 and thawed multiple times. All samples were assayed for BV/PNOR activity using 66 mM PNO.

8.2.8. PNOR Activity Staining of Native-Polyacrylamide Gels

Supernatant from DSS501 grown anaerobically on Gly/Fum was loaded onto a native-polyacrylamide gel, and electrophoresed as indicated in section 8.2.12. Analytical Techniques. The native-polyacrylamide gel was soaked in 50 mM MOPS pH 7.0, and 2 mM

MV^{2+}, in a covered petri dish bubbled with N_2. MV^{2+} was reduced by the addition of dithionite crystals. Once the gel was uniformly stained with $MVH^{\cdot +}$, it was transferred to a petri dish with 50 mM MOPS, and 66.6 mM substituted PNO.

Bands of activity on the native-polyacrylamide gel were cut out, crushed, and incubated with 2% SDS, 0.01% bromphenol blue, 32% glycerol, and 100 mM DTT overnight.

8.2.9. Purification of PNOR

Purification of PNOR was carried out using DSS501 supernatant from carboys grown anaerobically on Gly/Fum with 5 mM PNO.

8.2.9.1. Heat Treatment

EDTA and DTT were added to supernatant to achieve final concentrations of 2 and 5 mM, respectively. Supernatant was incubated in 1 mL aliquots, in Eppendorf tubes, at 70°C, for 2.3 minutes. Heated tubes were placed on ice for 10 minutes, and centrifuged at 15,000 x g for 10 minutes to remove coagulated protein. The pellet was resuspended in 175 uL 50 mM MOPS with protease inhibitor cocktail (concentration of protease inhibitors as indicated in Materials and Methods section 8.2.7.), and centrifuged as indicated above. The combined supernatant fraction was assayed for BV/PNOR activity and protein concentration.

8.2.9.2. Ammonium Sulfate Precipitation

Heat purified supernatant was diluted to a protein concentration of 5 mg/mL, brought to the desired ammonium sulfate saturation, let sit on ice for 30 minutes with occasional mixing, and centrifuged at 9,500 x g for 10 minutes. The supernatant at X% ammonium sulfate saturation was subsequently brought to the next ammonium sulfate saturation as necessary, and the above procedure repeated. For purification, the 50-60% ammonium sulfate pellet was saved. It was assayed for BV/PNOR activity and protein concentration.

For the ammonium sulfate backwash technique, supernatant was brought to 60% ammonium sulfate saturation. After incubation for 30 minutes on ice, protein was pelleted by centrifugation at 9,500 x g for 10 minutes. The drained and dried pellet was resuspended with decreasing concentrations of saturated ammonium sulfate, and the above procedure was repeated. The final pellet was resuspended with 50 mM MOPS pH 7.0. Each fraction was assayed for BV/PNOR activity and protein concentration.

8.2.9.3. Desalting

A 5 mL Sephadex G-25 column was used to desalt the 50-60% ammonium sulfate fraction. The conductivity of the eluted protein fraction was measured to ensure sufficient salt had been removed.

8.2.9.4. MonoQ FPLC

20 mM TRIS pH 8.0 was pumped through the MonoQ column at a rate of 1 mL per minute. Elution was performed using a NaCl gradient as indicated : 0-17 minutes 0 mM NaCl, 17-25 minutes 0-180 mM NaCl, 25-35 minutes 180 mM NaCl, 35-55 minutes 180-240 mM NaCl, 55-105 minutes 240-400 mM NaCl. 1 mL fractions were collected, and analyzed for BV/PNOR activity and protein concentration.

8.2.10. Isolation and Analysis of DSS501-3

DSS501 was streaked on Gly/PNO agar plates [50]. Plates were incubated in gas tight jars repeatedly evacuated to remove O_2, and filled with 90% H_2/10% CO_2. Within 4 hours palladium catalyst (Becton Dickinson) converted any O_2 remaining to water. Plates were incubated for 6 days at 30°C. One of the largest colonies was selected and the process indicated above was repeated two more times to obtain DSS501-3.

DSS501 and DSS501-3 were grown anaerobically on Gly/Fum with 5 mM PNO in 1 L flasks. The supernatant fraction from these cultures, was assayed for BV/PNOR activity and protein concentration.

DSS501 and DSS501-3 were grown anaerobically on Gly/PNO in Klett flasks as indicated in section Materials and Methods section 8.2.3, and their doubling times and maximal cell yield was compared.

8.2.11. DNA Sequence Analysis

A BLAST search was performed against the *E. coli* chromosome, using the DmsA sequence [2], to obtain the identity/sequence of any homologous enzymes.

The sequences coding for orf808A, orf808B, orf205, and orf284 from 35.69 minutes on the *E. coli* chromosome, were analyzed using MacVector 6.0.1 (Oxford Molecular Group PLC), and compared to the sequences for DmsA, DmsB and DmsC.

8.2.12. Analytical Techniques

Protein concentrations were determined as indicated previously [38]. PAGE was performed using the BioRad mini-gel, or Protean IIxi 20 cm slab gel system, with a discontinuous SDS buffer system [36] (SDS-PAGE) or the same buffer system without SDS (native-PAGE). Gels were stained with Coomassie blue and destained [37]. DmsA and B polyclonal antibodies were used separately for Western blotting [49], using ECL Western blotting detection reagents from Amersham Life Sciences for blot development. No antibody has been successfully raised against DmsC.

8.3. Results

8.3.1. Ability of Wild-type and Mutant *E. coli* to grow on S- and N-oxides in the Presence of Glycerol

Wild-type and mutant *E. coli* were examined for growth using glycerol as the carbon and energy source, and a variety of S- and N-oxides as sole terminal electron acceptor. All strains grew on the positive control, fumarate. Anaerobic growth curves for *E. coli* MC4100, grown on selected S- and N- oxides, are shown in Figure 8.1. (a). TMAO, 3-carboxypyridine N-oxide and 4-methylpyridine N-oxide, supported essentially identical growth, and these were comparable to growth with PNO and 3-hydroxypyridine N-oxide as terminal acceptor (data not shown). MC4100 grows well on DMSO, but a longer lag precedes exponential growth. Stationary phase was reached in about 20 hours. Tetramethylene sulfoxide supported very limited growth (data not shown).

As reported previously [48], *E. coli* DSS401, deleted for *dmsABC*, grew well on TMAO, whereas no growth was observed on DMSO. This strain exhibited slower growth on 3-carboxypyridine N-oxide and 4-methylpyridine N-oxide (Figure 8.1. (b)), PNO, and 3-hydroxypyridine N-oxide (data not shown). No growth was observed on tetramethylene sulfoxide (data not shown). This data indicates DmsABC is solely responsible for growth on S-oxides.

E. coli LCB128, lacking functional *torA*, grew well on all substrates tested (Figure 8.1. (c)), including PNO and 3-hydroxypyridine N-oxide, except tetramethylene sulfoxide, where very poor growth was observed (data not shown).

E. coli lacking functional *torA* and *dmsABC* (DSS501), was unable to grow on sulfoxides and TMAO, but surprisingly, maintained the ability to grown on 3-carboxypyridine N-oxide (Figure 8.1. (d)), PNO, and 3-hydroxypyridine N-oxide (data not shown). Growth was not

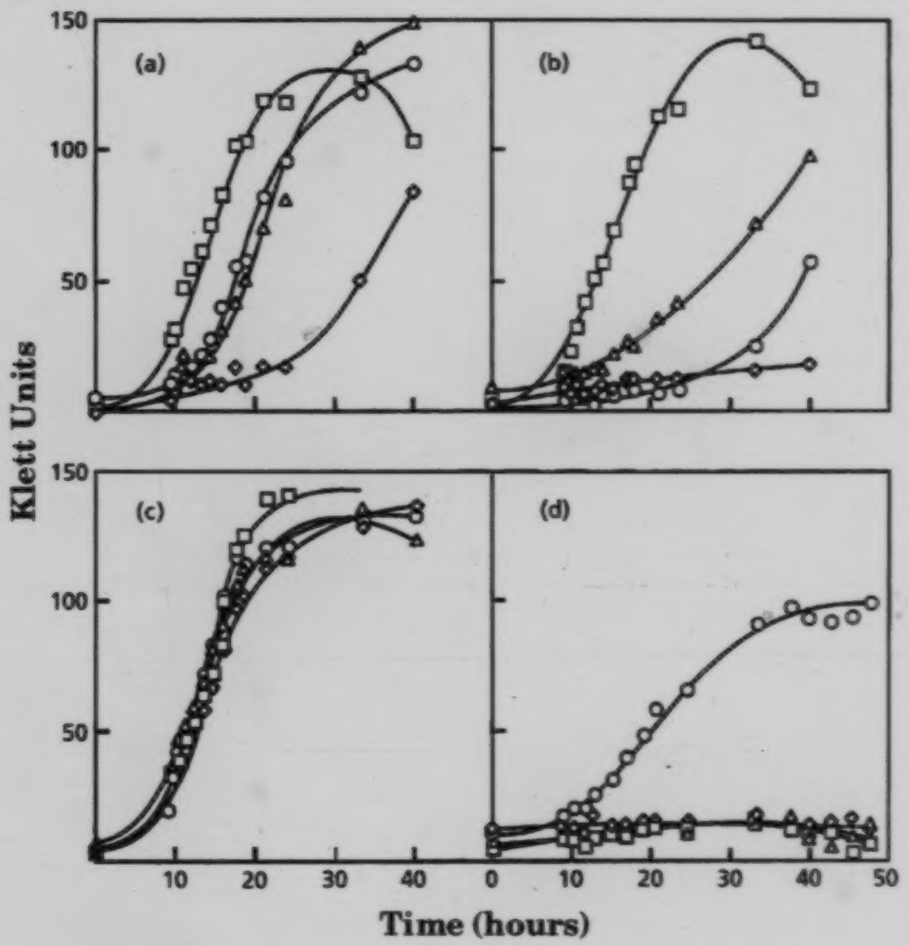

Figure 8.1.

Anaerobic Growth of Wild-Type *E. coli* and Selected Mutants on S- and N-oxide Substrates with Glycerol as the Electron Donor and Carbon Source at 30°C

(a) MC4100 wildtype; (b) DSS401 Δ*dmsABC*; (c) LCB128 *torA*$^-$; (d) DSS501 Δ*dmsABC torA*$^-$. Terminal electron acceptors used were as follows : 70 mM TMAO (□); 30 mM DMSO (◇); 70 mM 3-carboxypyridine N-oxide (○); 25 mM 4-methylpyridine N-oxide (Δ). Growth readings were taken as necessary with a Klett-Summerson spectrophotometer equipped with a number 66 filter, using minimal media as a blank.

observed for DSS501 on anaerobic minimal media if either PNO or glycerol were absent.

These results indicate an alternate terminal reductase, previously unidentified, conserves the redox energy of these substituted PNO's in *E. coli* , in the absence of functional *dmsABC* and *torA* . Growth on substituted PNO's is better in strains bearing a wild-type copy of DmsABC, indicating DmsABC also contributes to growth on substituted PNO's in wild-type cells. As a result, examination of this new terminal reductase (PNOR), capable of using substituted PNO's, must occur in a *dmsABC*$^-$ strain, to prevent masking of PNOR by DmsABC.

8.3.2. Anaerobic Growth of DSS501 on Gly/PNO is Abolished by the Addition of Tungstate

Tungstate is known to be a molybdate antagonist, and its inclusion in the growth media is known to inhibit molybdoenzymes [26].

Anaerobic growth of DSS501 on Gly/PNO was abolished when tungstate was included in the growth media, suggesting one of the proteins necessary for growth on Gly/PNO is a molybdoenzyme [46].

8.3.3. PNO Does Not Act as an Electron Sink During Growth on Glucose

DSS501 grown anaerobically on glucose minimal media with or without PNO, is shown in Figure 8.2. This single experiment revealed equivalent doubling times in exponential phase, and maximal cell density for all cultures. This indicates PNO cannot act as an electron sink when grown on glucose.

8.3.4. Expression of PNOR Activity

DSS501 was assayed for the ability to reduce PNO using BVH$^{\cdot +}$. DSS501 showed a ten fold higher specific activity for PNOR when grown anaerobically versus aerobically on Gly/Fum (with 5 mM PNO) (data not

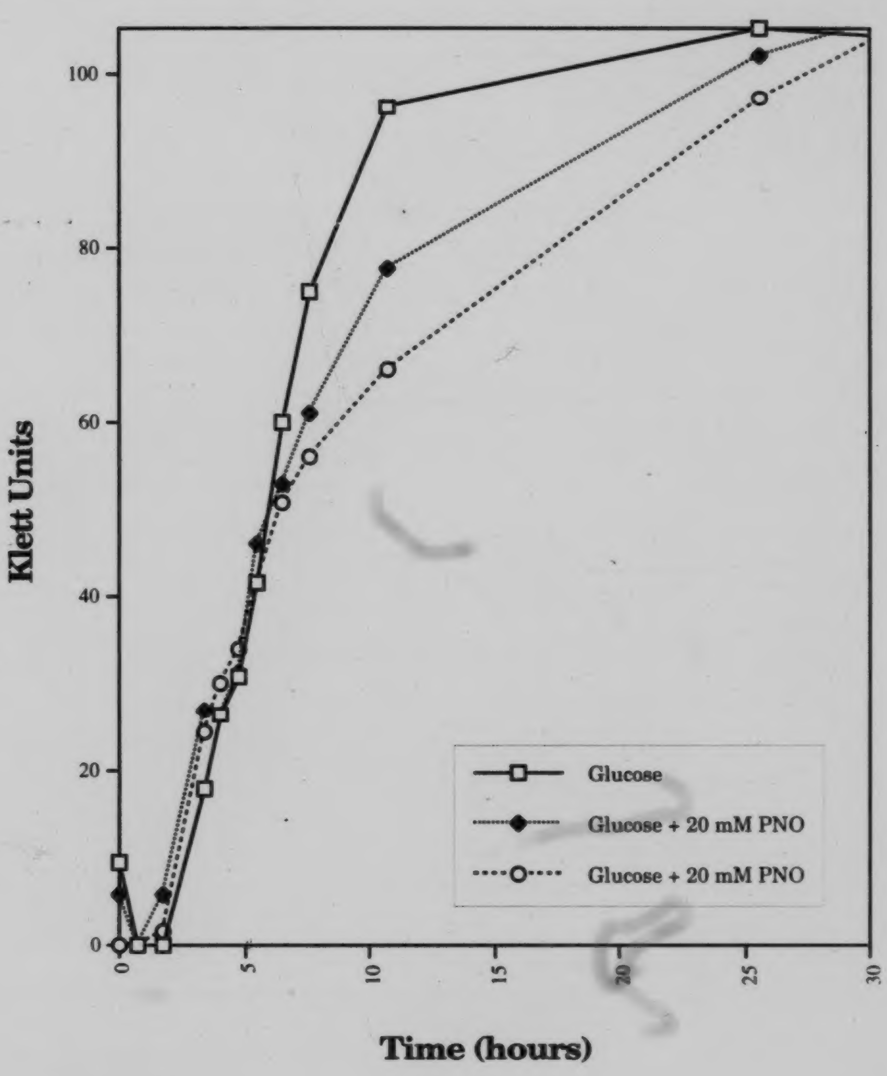

Figure 8.2.

Anaerobic Growth of DSS501 on Glucose Minimal Media +/- PNO at 30°C

Growth readings were taken as necessary with a Klett-Summerson spectrophotometer equipped with a number 66 filter, using minimal media as a blank.

shown). This result suggests PNOR is induced under anaerobic conditions.

PNOR activity was examined from cells grown for varying lengths of time. PNOR activity was found in DSS501 grown anaerobically on Gly/Fum from 23.5 to 71.5 hours. Table 8.2. shows PNOR specific activity increases between 0 and 29.5 hours, and then plateaus, indicating examination of cells 29.5 hours or older would be most useful.

PNOR activity was found in DSS501 grown anaerobically on glycerol minimal media with the following terminal electron acceptors : fumarate, 3-carboxypyridine N-oxide, PNO, and 3-hydroxypyridine N-oxide (data not shown). Induction of PNOR was examined by including substituted PNO's in the anaerobic growth media. The specific activity for PNOR increased slightly (83% maximum increase for 5 mM carboxypyridine N-oxide), with the inclusion of various substituted PNO's in the media (Table 8.3.). However, the increase was minimal, and inclusion of substituted PNO's also resulted in better cell growth. This suggests PNOR is expressed constitutively under anaerobic conditions.

PNOR and FrdABCD activity were examined in 1 L cultures grown anaerobically on Gly/Fum with or without tungstate, to determine whether PNOR is a molybdoenzyme. FrdABCD is not a molybdoenzyme. As a result, the specific activity for FrdABCD decreased only 2% on inclusion of tungstate in the growth media, while PNOR specific activity decreased 91%. This suggests PNOR is a molybdoenzyme.

8.3.5. Localization of PNOR Activity

To determine the location of PNOR activity, osmotic shock was performed to obtain the periplasmic fraction. The cytoplasmic and membrane fractions were subsequently separated. PNOR activity was

Table 8.2.

PNOR Specific Activity in DSS501 Grown Anaerobically on Gly/Fum for Increasing Amounts of Time

Time of Anaerobic Growth (hours)	Specific Activity (u/mg) +/- Standard Deviation
23.5	0.017 +/-0.0003
29.5	0.028 +/-0.001
49.5	0.025 +/-0.005
71.5	0.027 +/-0.0

DSS501 was grown anaerobically on Gly/Fum with 5 mM PNO, in 1L flasks. Reductase activity was measured using BV, and 66.6 mM PNO. One u (unit) of enzyme activity is equal to 2 µmole of BVH $^{+}$ oxidized or 1 µole of PNO reduced per minute.

Table 8.3.

Effect of the Inclusion of Substituted PNO's on PNOR Activity in DSS501 Grown Anaerobically on Gly/Fum

	* Specific Activity (u/mg) +/- Standard Deviation		
Substituted PNO (5 mm)	**PNOR**	**FrdABCD**	**% Increase* for PNOR**
None	0.009+/-0.013	0.023+/-0.00056	-
4-methylpyridine N-oxide	0.015+/-0.002	0.032+/-0.0056	47
PNO	0.016+/-0.006	0.028+/-0.0035	63
3-carboxypyridine N-oxide	0.018+/-0	0.028+/-0.0012	83

*% increase is for PNOR specific activity. It was calculated by dividing the % increase in specific activity for PNOR, by the % increase in specific activity for FrdABCD, to correct for better cell growth with the inclusion of substituted PNO's in the growth media. Reductase activity was measured using BV and 33 mM PNO. DSS501 was grown in 1 L flasks. One u (unit) of enzyme activity is equal to 2 μmole of BVH^{+} oxidized or 1 μole of PNO reduced per minute.

found solely in the cytoplasm, and not in the membrane or periplasmic fractions (Table 8.4.). β-lactamase (periplasmic) and FrdABCD (membrane bound) were used as controls to demonstrate the fractions were separated as indicated. A small amount of FrdABCD activity should have been observed in the cytoplasmic fraction due to incomplete separation of membrane and cytoplasmic fractions (as in Table 8.5.). However, this data still indicates PNOR activity is localized to the cytoplasm in broken cells.

8.2.6. Characterization of PNOR Activity

DSS501 supernatant is able to reduce PNO and substituted PNO's with the substituents : 3-carboxy, 3-hydroxy, and 4-methyl, in the presence of $BVH^{\cdot+}$. No DMSO or ANO reductase activity was observed (Table 8.5.). TMAO reductase activity was sometimes observed, but varied with the preparation.

Compounds known to occasionally increase enzyme activity, were added to the enzyme assay, to see if the low specific activity of PNOR in the supernatant could be increased. Substituted PNOR activity using $BVH^{\cdot+}$ as electron donor could not be increased by including any of the following in the assay : DTT, EDTA, NaCl, metal mix, selenite or glycerol. PNOR activity was found to increase with decreasing pH when using both "Good" and "other" buffers (Figure 8.3.). The pH of the buffer was not poised below 6, due to an increase in the endogenous rate of $BVH^{\cdot+}$ oxidation. The maximal activity observed for each of the two buffer systems ("Good" and "other") was equivalent within experimental error (8% difference).

PNOR activity was determined using alternate electron donors. $MVH^{\cdot+}$, NADH, and NADPH donated electrons with 23, 60, and 60% efficiency, respectively, compared to $BVH^{\cdot+}$. $FMNH_2$, $FADH_2$ and $DMNH_2$ could not donate electrons to PNOR.

Table 8.4.

Localization of Enzyme Activities in Anaerobically Grown DSS501

	% Total Activity for Each Enzyme		
Fraction	**PNOR**	**β-lactamase**	**FrdABCD**
Periplasm	0	80	0
Cytoplasm	100	20	0
Membrane	0	0	100

DSS501 was grown anaerobically in 19 L carboys for 30.5 hours on Gly/Fum plus 5 mM PNO. Reductase activity was measured using the BV, and 33.3 mM PNO, or 70 mM fumarate. β-lactamase activity was measured using PADAC.

Table 8.5.

PNOR Activity from Anaerobically Grown DSS501

Substrate Electron Acceptor	(mM)	Specific Activity (u/mg) Membrane	 Supernatant
Fumarate	70	0.74	0.12
TMAO	70	0	0*
DMSO	30	0	0
Tetramethylene sulfoxide	10	0	0
ANO	0.7	0	0
PNO	10	0	0.04
3-carboxypyridine N-oxide	10	0	0.1
3-hydroxypyridine N-oxide	10	0	0.04
4-methylpyridine N-oxide	10	0	0.04

DSS501 was grown anaerobically in 1 L flasks on Gly/Fum, and reductase activity was measured using BV. * For this experiment, no TMAO reductase activity was observed. However, activity generally averaged 50% that of PNOR activity. One u (unit) of enzyme activity is equal to 2 µmole of BVH^{+} oxidized or 1 µole of PNO reduced per minute.

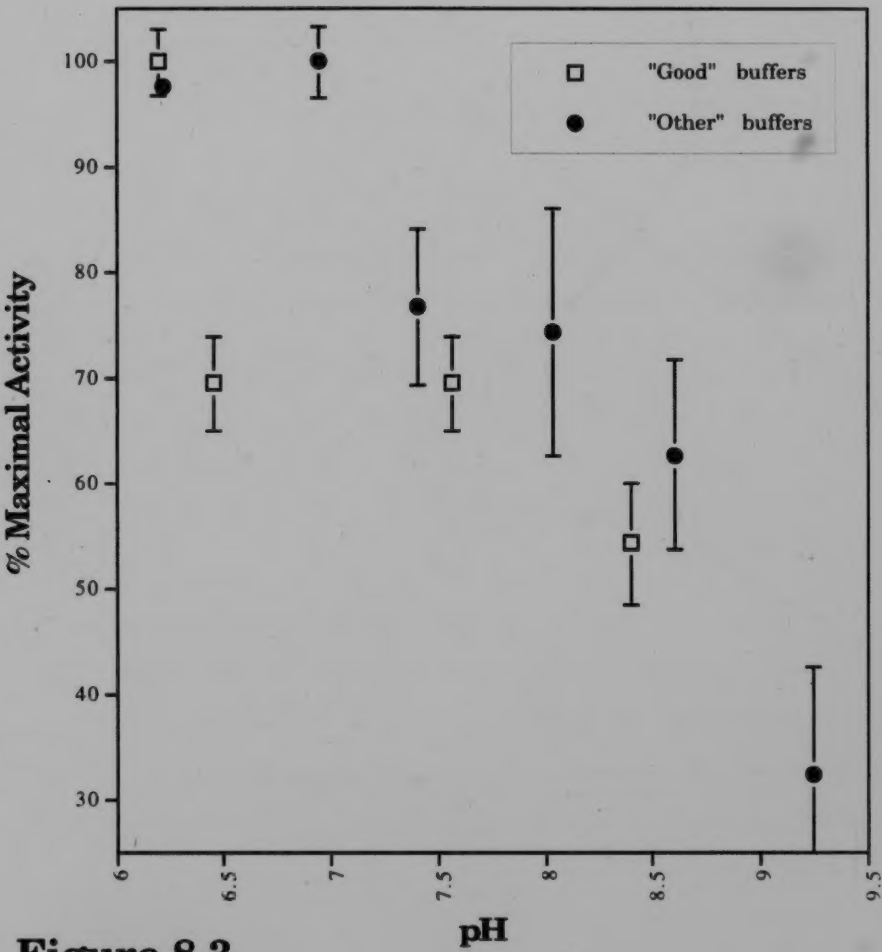

Figure 8.3

Optimization of PNOR Activity Using Various Buffers at Various pH's for the BV/PNOR Assay

DSS501 supernatant was examined for PNOR activity using BV, and 66.6 mM PNO. "Good", buffers used were : MES pH 6.2, BIS-TRIS pH 6.45, HEPES pH 7.57, BICINE pH 8.4. "Other" buffers used were : citrate pH 6.2, imidazole pH 6.95, phosphate pH 8.0, TRIS pH 8.6, and glycine pH 9.2. Maximal activity is PNOR activity at the optimal conditions used for each of the two buffer types (equivalent within experimental error). Error bars show the standard deviation.

8.3.7. Stability of PNOR Activity

After 21 hours at 4°C, 62% of PNOR activity remained in DSS501 supernatant grown anaerobically on Gly/Fum. Various compounds were added to try and increase the stability of PNOR at 4°C (Table 8.6). Most compounds had little if any effect on the stability of PNOR activity. However, inclusion of protease inhibitor cocktail resulted in no loss of activity during this incubation.

PNOR activity was also lost during a freeze/thaw of DSS501 supernatant grown anaerobically on Gly/Fum. Only 60% of PNOR activity remained after freezing to $^{-}$70°C. However, a minimal amount of activity was lost on subsequent freeze/thaws. (<10% of PNOR activity was lost on freeze/thaws two and three.) Inclusion of protease inhibitor cocktail did not prevent the loss of PNOR activity, suggesting that loss of activity was due to the freezing process, and not due to protease digestion on thawing. However, if supernatant was frozen as an ammonium sulfate pellet, 84% of PNOR activity remained after thawing.

8.3.8. PNOR Activity is Protein Mediated and is Distinct from DmsABC

Native-polyacrylamide gels can be stained for oxidation of $MVH^{\cdot +}$. Lanes from the native-polyacrylamide gel are incubated with $MVH^{\cdot +}$ until uniformly stained, and then transferred to buffer containing the substrate to be reduced. As the $MVH^{\cdot +}$ becomes oxidized by protein, bands of clearing can be observed.

Supernatant from DSS501 grown anaerobically on Gly/Fum shows three equally spaced bands of clearing, on a native polyacrylamide gel stained for PNOR activity (Figure 8.4. A.). The middle band is faint, and difficult to see. Bands of $MVH^{\cdot +}$ oxidation activity can be visualized using PNO, 3-carboxypyridine N-oxide, or 4-

Table 8.6.

% PNOR Activity Remaining After 21 Hours at 4°C

Compounds Added (mM)	% Activity Remaining
Nothing (50 mM MOPS pH 7.0)	62
PNO (10)	75
EDTA (1)	62
Ascorbic acid (1)	62
Metal mix*	67
DTT (2)	62
Protease inhibitor cocktail*	110
NaCl (25)	67

DSS501 was grown anaerobically on Gly/Fum plus 5 mM PNO. Supernatant was incubated for 21 hours at 4°C in the presence of the compounds listed above. *When metal mix was added, metals were included at the following final concentrations in µM : $MgSO_4$, 65; $MnSO_4$, 8.2; $Fe_2(SO_4)_3$, 0.36; $CaCl_2$, 1.2. When protease inhibitor cocktail was added, the final concentrations of protease inhibitors in µg/mL were : aprotinin, 0.1; phosphoramidon, 0.1; TLCK-HCl, 0.1; TPCK, 0.2; A-PMSF, 0.1; E-64, 0.1; leupeptin, 0.05; pepstatin 0.01. Reductase activity was measured using BV and 66.6 mM PNO.

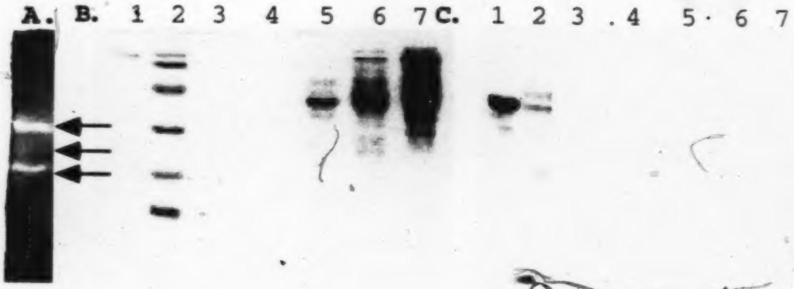

Figure 8.4.

Native-PAGE, SDS-PAGE, and Western Blot Analysis of DSS501 Supernatant Grown Anaerobically on Gly/Fum

A. A 7.5% native-polyacrylamide gel of DSS501 supernatant stained with MVH·+ and 66.6 mM PNO. The arrows indicate the bands of clearing designated "top", "middle", and "bottom".

B. A 15% SDS-polyacrylamide gel stained with Coomassie blue of : 1. purified DmsABC; 2. low molecular weight standards (in kDa 97.4, 66.2, 45, 31, 21.5, 14.4); 3. and 4. blank; 5. 6. and 7. "bottom", "middle" and "top" activity bands, respectively, from the native-polyacrylamide gel.

C. Western blot of the 15% SDS-polyacrylamide gel in B. using DmsA antibody.

methylpyridine N-oxide (data not shown). This indicates PNOR activity is protein mediated. There appear to be multiple forms of PNOR. This could be due to degradation of PNOR, alternate modification, oligomerization with itself or other proteins, or the result of different proteins able to reduce PNOR in the presence of MVH·+.

The three bands of activity from the native-polyacrylamide gel ("bottom", "middle" and "top"), were cut out. Protein was extracted from the gel slices, and characterized by SDS-PAGE (Figure 8.4. B.) and Western blotting (Figure 8.4. C.). The SDS-polyacrylamide gel shows numerous protein bands in the lanes containing protein from the "top", "middle", and "bottom" native-polyacrylamide gel slices. Since PNOR activity in DSS501 supernatant is quite low, we would not expect the protein(s) responsible to be highly expressed, and although there are far less bands in the "bottom" native-polyacrylamide gel slice, it is notpossible to distinguish unequivocally which of the SDS-PAGE bands is responsible for the PNOR activity.

A Western blot of the SDS-polyacrylamide gel probed with DmsA (Figure 8.4. C.) or DmsB antibody (data not shown), shows that, as expected, DmsA and DmsB antibody does not recognize the protein band(s) responsible for PNOR activity from DSS501 supernatant. There were a few spurious bands in the lane with the low molecular weight standards. The Western blot indicates PNOR is immunologically distinct from DmsAB.

8.3.9. Purification of PNOR

To determine whether the method of cell breakage influenced PNOR specific activity, French pressure lysis, and lysozyme freeze/thaw cell breakage techniques were performed on DSS501 grown anaerobically on Gly/Fum with 5 mM PNO. Both techniques resulted in essentially identical specific activities (0.030 and 0.027 u/mg, respectively). Since French pressure lysis is easier to use for large cell volumes, it was selected as the optimal cell breakage technique.

A heat step was employed for purification of PNOR from the supernatant. Temperature (60°C and 70°C), time (1-3 minutes), volume (0.3-1.0 mL), protein concentration (5-45 mg/mL), and treatment of pellet, were varied to optimize purification. Fold purification and % activity recovered, for a 70°C, 2.3 minutes heat step, after coagulated protein was removed, varied between 1.4-2.5 fold and 70-140%, respectively.

Supernatant from the heat step was fractionated using saturated ammonium sulfate. The 50-60% ammonium sulfate cut was found to contain the PNOR activity. Fold purification and % activity recovered varied from 5-10 and 40-70%, respectively. The ammonium sulfate backwashing technique was employed in an attempt to increase fold purification and recovery of PNOR, however, this was not successful.

A Sephadex G-25 column was employed to remove excess salt from the resuspended ammonium sulfate pellet. 70 to 100% of PNOR activity was recovered.

Supernatant from the G-25 column was fractionated by MonoQ-FPLC. Purification conditions were optimized by varying the initial ionic strength of the column buffer, and gradient slope. Fold purification of the PNOR fraction obtained at 180 mM NaCl varied from 2.3-5.6. Approximately 25-65% of PNOR activity was recovered by this step. Unfortunately, when the PNOR activity from the Mono-Q column was analyzed by SDS-PAGE, numerous bands were observed, and it could not be unequivocally determined which band(s) was/were PNOR.

Using heat treatment, ammonium sulfate precipitation, and MonoQ-FPLC, the specific activity for PNOR was increased approximately 15 fold, with 10% of initial PNOR activity remaining.

8.3.10. Isolation of a Mutant with Increased PNOR Activity

Strains with increased PNOR activity would be useful for purification of PNOR. To increase the initial specific activity of PNOR in the supernatant of anaerobically grown cells, a selection procedure was developed. It was suspected that larger colony size on Gly/PNO plates incubated anaerobically, would be the result of higher PNOR activity.

The largest DSS501 colony from anaerobically grown Gly/PNO plates was selected, and this process was repeated twice more. The mutant colony obtained (named DSS501-3), was still unable to grow on Gly/DMSO or Gly/TMAO, indicating lack of functional *dmsABC* and *torA*. Examination of DSS501-3 growth on liquid media revealed no change in the doubling time for DSS501-3 grown anaerobically on Gly/PNO as compared to DSS501. Supernatant from DSS501-3 grown on Gly/Fum (plus 5 mM PNO), showed fumarate, TMAO, and PNO reductase activities that were 3.1, 2.1, and 2.2 fold greater, respectively, than DSS501. This suggests the increase in PNOR specific activity in DSS501-3 may be due to an increase in the accumulation of anaerobically expressed protein.

8.3.11. Sequence Analysis of the *E. coli* Chromosome for Previously Unidentified Molybdoenzymes

The loss in PNOR activity in DSS501 supernatant when tungstate was included in the growth media (8.3.4. Expression of PNOR Activity), suggests PNOR is a molybdoenzyme. Prokaryotic molybdoenzymes form a family of related proteins, where proteins with similar substrate profiles share greater sequence similarity [4, 61, 65]. If PNOR is a molybdoenzyme, it should share sequence similarity with other identified molybdoenzymes, and in particular other S- and N-oxide reductases. When this study began, there were no identified molybdoenzyme sequences in *E. coli* with unknown function. However, with the completion of the sequence of *E. coli* genome [9], it was possible to examine the genome for uncharacterized genes, sharing sequence similarity with other molybdoenzymes.

A BLAST search was performed using the DmsA sequence, a molybdoenzyme that shares overlapping substrate specificity with PNOR. Twelve sequences were obtained, that produced high-scoring segment pairs with DmsA (Table 8.7.). Ten of the sequences identified previously characterized molybdoenzymes. However, two sequences were novel : orf808A and orf808B. These sequences appear to be within an operon (see below) (orf1-4) at 35.69 minutes on the *E. coli* chromosome. This cluster of genes appears to initiate with orf808A, and is followed by orf808B, orf205, and orf284.

Comparison of the sequences for orf808A and orf808B with DmsA revealed 67% and 66% identity with DmsA, respectively (Figure 8.5.). The seven blocks of homology conserved between prokaryotic molybdoenzymes were also found in orf808A and orf808B [4, 61, 65]. Examination of the sequences revealed all residues found to be important in substrate binding or catalysis by DmsA (Chapter 7), are absolutely conserved in orf808A and orf808B. In addition, the double-arginine leader suggested to be important in targeting select molybdoenzymes, as well as other redox cofactor containing enzymes, is also conserved [4]. The observed sequence similarity between DmsA, orf808A, and orf808B suggests they share a similar function. Orf808A and orf808B are likely novel S- and N-oxide reductases.

Orf205 and orf284, found downstream of orf808A and orf808B, show 94% and 38% identity to DmsB and DmsC, respectively (Figure 8.6. and 8.7.). The Cys residues known to ligate the four [4Fe-4S] clusters in DmsB are conserved in orf205 [61] (Figure 8.6.), while the eight transmembrane segments in found in DmsC [62], appear to be conserved in orf284 (Figure 8.7.). Orf284 may have an extension at the N-terminus compared to DmsC and the analogous protein in *H. influenza* [23]. (The retrieved protein sequence is shown in Figure 8.7.,

Table 8.7.

Sequences from the Complete *E. coli* Genome Homologous to DmsA

E. coli Sequences Producing High-scoring Pairs with DmsA Using BLAST	P(N)	Reference Indicating Moco Binding
DmsA **Moco Containing Subunit of DMSO reductase**	0	[46]
orf808A **Previously Unidentified, Unknown Function**	0	None
orf808B **Previously Unidentified, Unknown Function**	0	None
BisC **Biotin Sulfoxide Reductase**	7.4e-74	[20]
TorA **TMAO Reductase**	2.0e-64	[66]
BisZ **Alternative Biotin Sulfoxide Reductase**	4.1e-6	[20]
FdhF **Moco Containing Subunit of Formate Dehydrogenase-H**	3.9e-34	[3]
NarG **Moco Containing Subunit of Nitrate Reductase-A**	1.2e-29	[8]
NarZ **Moco Containing Subunit of Nitrate Reductase-Z**	1.8e-24	[7]
FdoG **Moco Containing Subunit of Formate Dehydrogenase-O**	7.8e-22	[51]
FdnG **Moco Containing Subunit of Formate Dehydrogenase-N**	3.1e-19	[51]
Nap A **Moco Containing Subunit of Periplasmic Nitrate Reductase**	6.0e-16	None

P(N) is the probability of finding a segment pair with greater similarity.

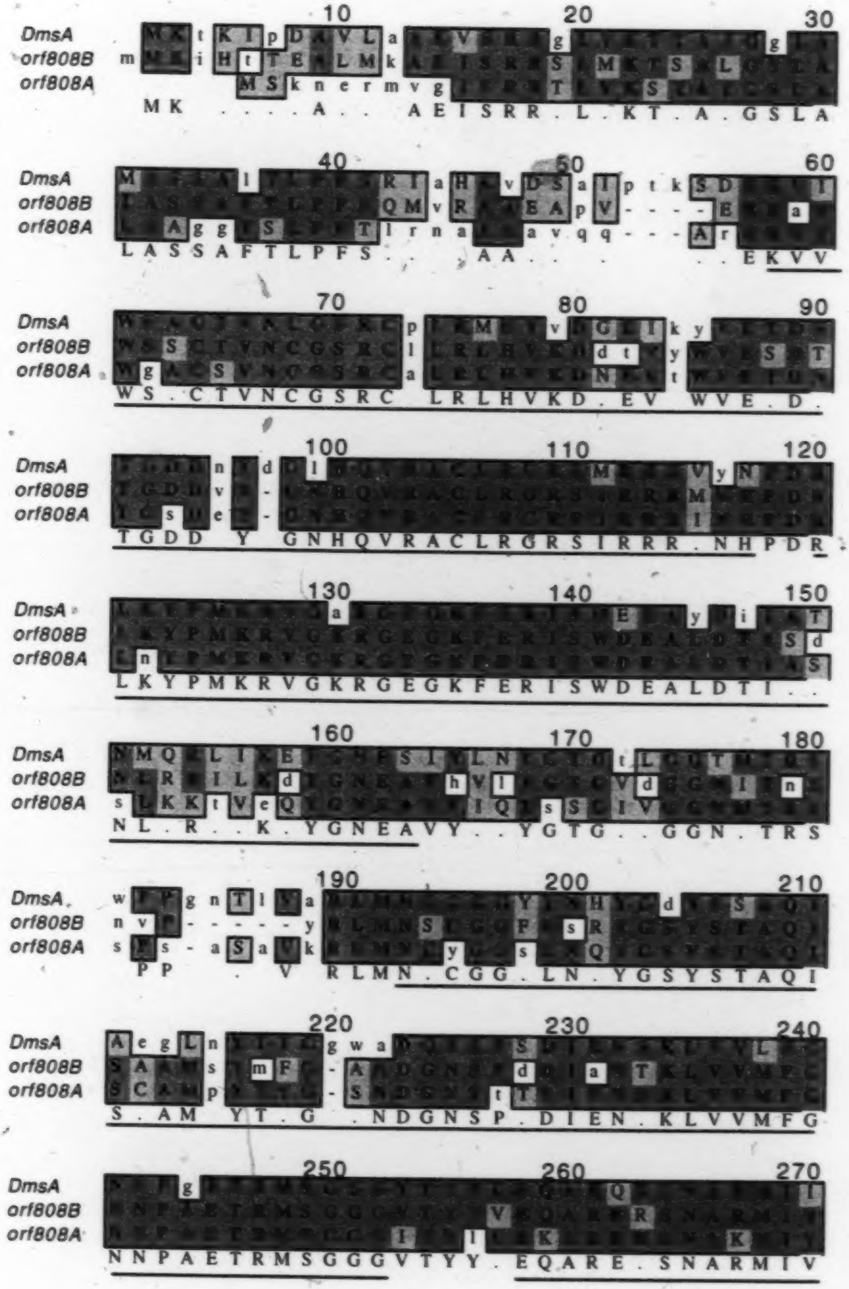
DmsA
orf808B
orf808A
MK . . . . A . . AEISRR . L . KT . A . GSLA
LASSAFTLPFS . . . AA . . . . EKVV
WS . CTVNCGSRC LRLHVKD . EV WVE . D .
TGDD Y GNHQVRACLRGRSIRRR . NHPDR
LKYPMKRVGKRGEGKFERISWDEALDTI . .
NL . R . . K . YGNEAVY . . YGTG . . GGN . TRS
PP . V RLMN . CGG . LN . YGSYSTAQI
S . AM YT . G . NDGNSP . DIEN . KLVVMFG
NNPAETRMSGGGVTYY . EQARE . SNARMIV

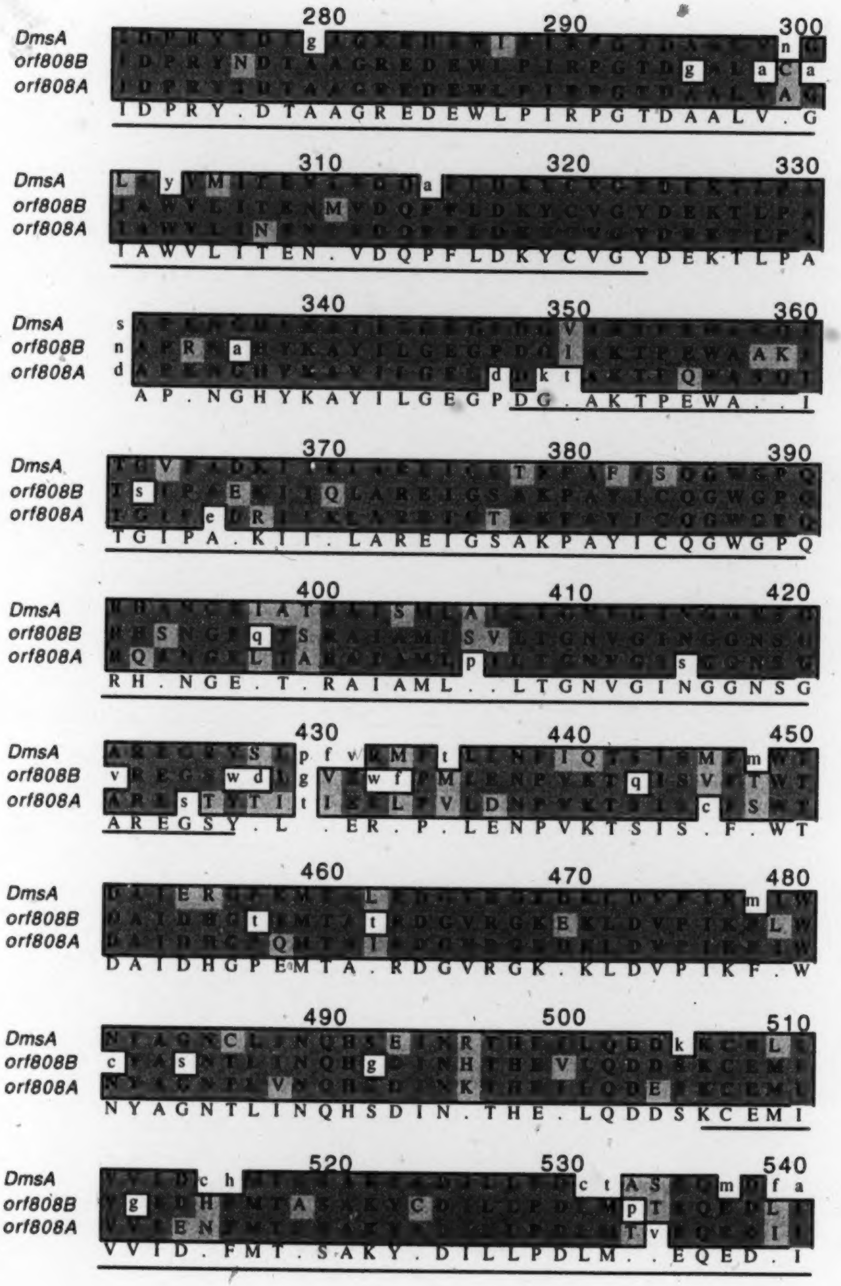
280
290
300
DmsA
orf808B
orf808A
I D P R Y . D T A A G R E D E W L P I R P G T D A A L V . G
310
320
330
DmsA
orf808B
orf808A
I A W V L I T E N . V D Q P F L D K Y C V G Y D E K T L P A
340
350
360
DmsA
orf808B
orf808A
A P . N G H Y K A Y I L G E G P D G . A K T P E W A . . I
370
380
390
DmsA
orf808B
orf808A
T G I P A . K I I . L A R E I G S A K P A Y I C Q G W G P Q
400
410
420
DmsA
orf808B
orf808A
R H . N G E . T . R A I A M L . . L T G N V G I N G G N S G
430
440
450
DmsA
orf808B
orf808A
A R E G S Y . L . E R . P . L E N P V K T S I S . F . W T
460
470
480
DmsA
orf808B
orf808A
D A I D H G P E M T A . R D G V R G K . K L D V P I K F . W
490
500
510
DmsA
orf808B
orf808A
N Y A G N T L I N Q H S D I N . T H E . L Q D D S K C E M I
520
530
540
DmsA
orf808B
orf808A
V V I D . F M T . S A K Y . D I L L P D L M . . E Q E D . I

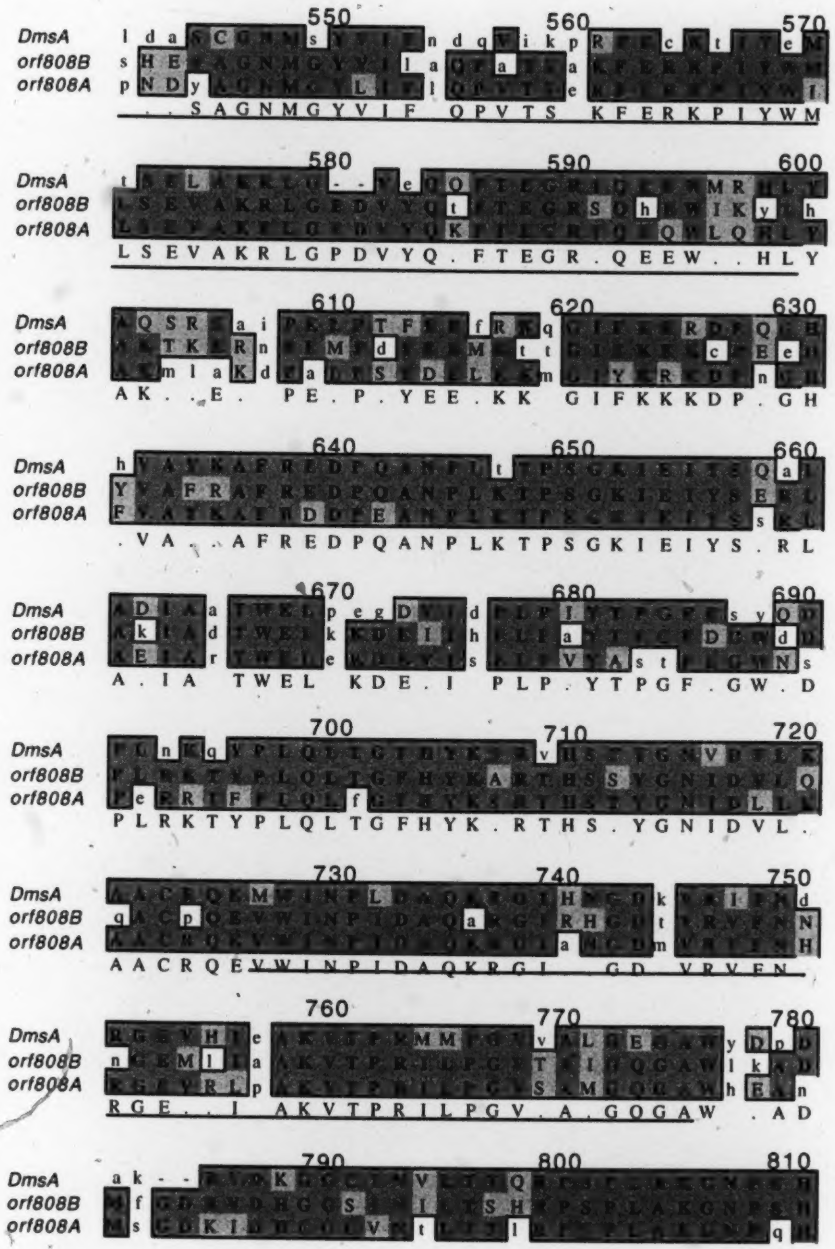

550 560 570
DmsA
orf808B
orf808A
. . SAGNMGYVIF QPVTS KFERKPIYWM
580 590 600
LSEVAKRLGPDVYQ.FTEGR.QEEW..HLY
610 620 630
AK..E. PE.P.YEE.KK GIFKKKDP.GH
640 650 660
.VA..AFREDPQANPLKTPSGKIEIYS.RL
670 680 690
A.IA TWEL KDE.I PLP.YTPGF.GW.D
700 710 720
PLRKTYPLQLTGFHYK.RTHS.YGNIDVL.
730 740 750
AACRQEVWINPIDAQKRGI GD VRVFN
760 770 780
RGE..I AKVTPRILPGV.A.GQGAW .AD
790 800 810

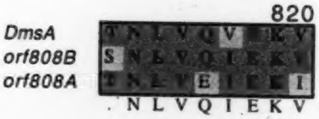
820
DmsA
orf808B
orf808A
T N L V Q V K V
S N L V Q I E K V
T N L V E I E K I
. N L V Q I E K V

Figure 8.5.

Alignment of the Amino Acid Sequences for DmsA, orf808A, and orf808B

The amino acid sequences for DmsA, orf808A, and orf808B were aligned using MacVector 6.0. The one letter amino acid codes are shown, with identical residues in dark grey, and conservative substitutions in light grey. Non-conserved residues are shown in lower case and are not shaded. The consensus sequence is identified below the alignment. Regions 1-7, the blocks of sequence homology shared between prokaryotic molybdoenzymes, are underlined

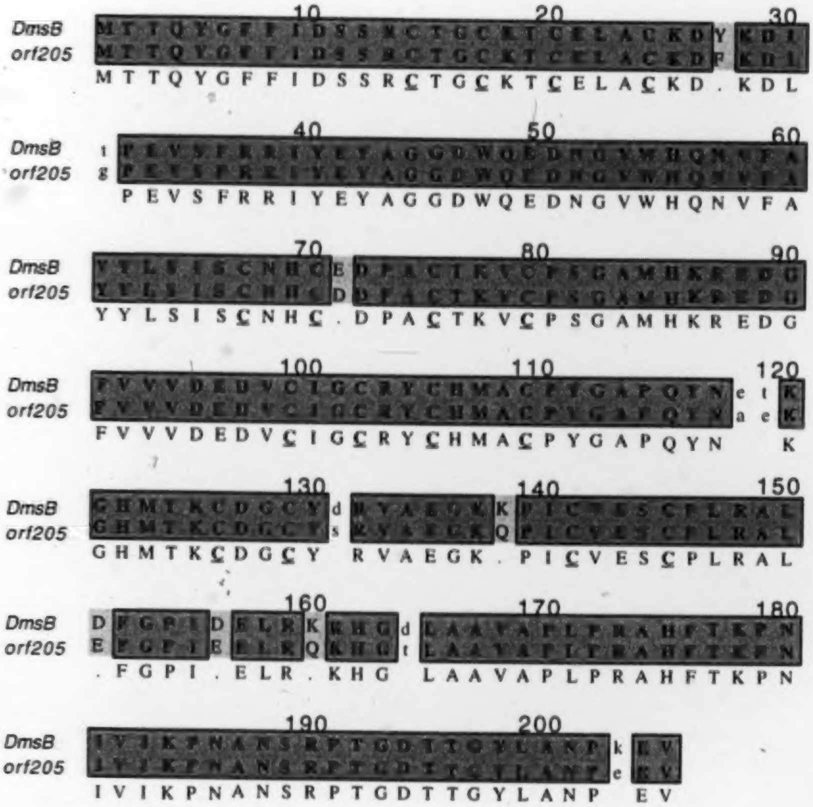

10 20 30
DmsB
orf205
M T T Q Y G F F I D S S R C T G C K T C E L A C K D . K D L
40 50 60
DmsB t
orf205 g
P E V S F R R I Y E Y A G G D W Q E D N G V W H Q N V F A
70 80 90
DmsB E
orf205 D
Y Y L S I S C N H C . D P A C T K V C P S G A M H K R E D G
100 110 120
DmsB e t
orf205 a e
F V V V D E D V C I G C R Y C H M A C P Y G A P Q Y N K
130 140 150
DmsB d K
orf205 s Q
G H M T K C D G C Y R V A E G K . P I C V E S C P L R A L
160 170 180
DmsB D D K d
orf205 E E Q t
. F G P I . E L R . K H G L A A V A P L P R A H F T K P N
190 200
DmsB k
orf205 e
I V I K P N A N S R P T G D T T G Y L A N P E V

Figure 8.6.

Alignment of the Amino Acid Sequences for DmsB and orf205

The amino acid sequences for DmsB and orf205 were aligned using MacVector 6.0. The one letter amino acid codes are shown, with identical residues shown in dark grey, and conservative substitutions in light grey. Non-conserved residues are shown in lower case and are not shaded. The consensus sequence is indicated below the alignment. Cys residues known to ligate the [4Fe-4S] clusters in DmsB are underlined and bolded in the consensus sequence.

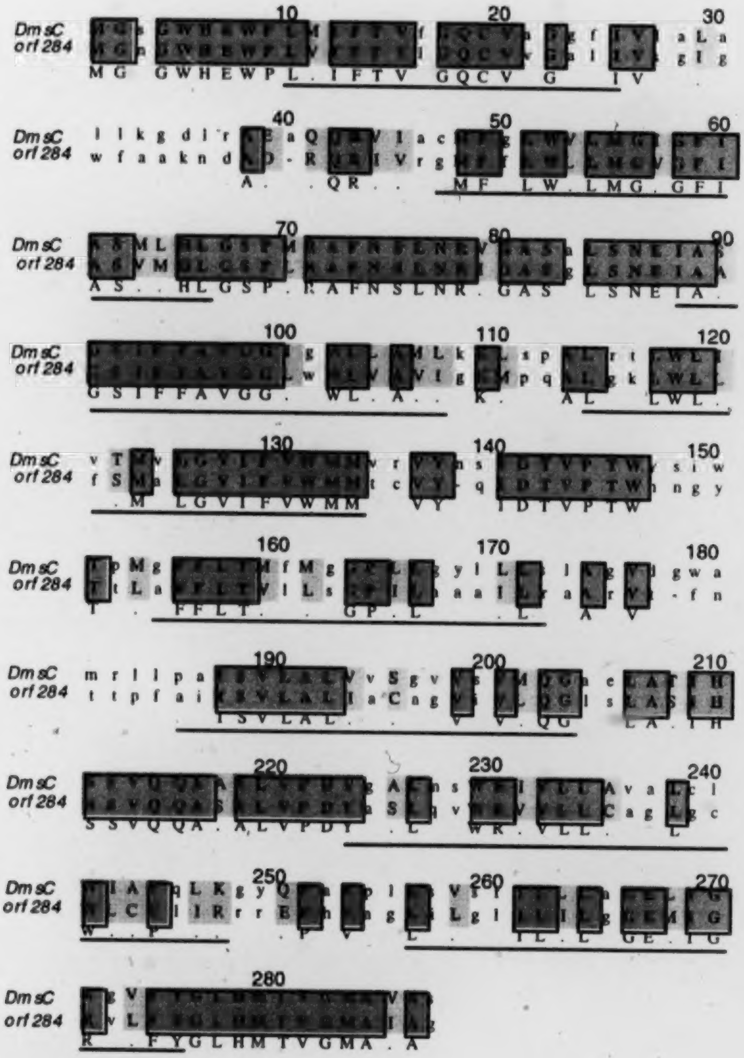
DmsC
orf284
10
20
30
40
50
60
70
80
90
100
110
120
130
140
150
160
170
180
190
200
210
220
230
240
250
260
270
280

Figure 8.7.

Alignment of the Amino Acid Sequences from DmsC and orf284

The amino acid sequences for DmsC and orf284 were aligned using MacVector 6.0. The one letter amino acid codes are shown, with identical residues in dark grey, and conservative substitutions in light grey. Identical and conservative substitutions are boxed. Non conserved residues are shown in lower case, and are unshaded. Putative transmembrane segments are underlined.

as a result the extension is not shown.) The sequence similarity between DmsB and DmsC, and orf205 and orf284, respectively, suggest the pairs of proteins share a similar functions. This would suggest orf1-4 expresses protein that composes an S- and N-oxide reductase that accepts electrons from the Q pool.

Analysis of the promoter region upstream of orf808A shows an FNR box very close to the consensus (TTGATNNNNATCAA) [56], suggesting anaerobic regulation of this operon (Figure 8.8). The 5' untranslated sequence also shows reasonable $^{-}35$ and $^{-}10$ promoter [57], and Shine Dalgarno sequences [57] (Figure 8.8). Anaerobic respiratory enzymes are often regulated by NarX/L / NarQ/P, to repress the synthesis of protein involved in less energetically favorable pathways than nitrate reduction [56]. As a result, the untranslated region of this operon was examined for NarL binding sites, although none were found [56].

Orf808A and orf808B, orf808B and orf205, and orf205 and orf284, are separated by 62, 13 and 2 nucleotides, respectively. Alternatively, orf284 may initiat upstream, overlapping 235 nucleotides with orf205. Examination of the upstream nucleotide sequence for orf808B, orf205 and orf284, also reveal Shine-Dalgarno sequences (Figure 8.8.) [57]. It seems unusual to have two such similar proteins as part of this operon (orf808A and orf808B). Since the Shine-Dalgarno sequence for orf808B is less like the consensus than orf808A, it is possible only the latter is expressed along with orf205 and orf284.

8.4. Discussion

Our results demonstrate *E. coli* expresses at least one previously unidentified anaerobically expressed energy conserving terminal reductase. This protein, PNOR, allows anaerobic growth on substituted PNO's in the presence of glycerol. PNOR appears to be a cytoplasmically localized molybdoenzyme, induced by anaerobiosis. It

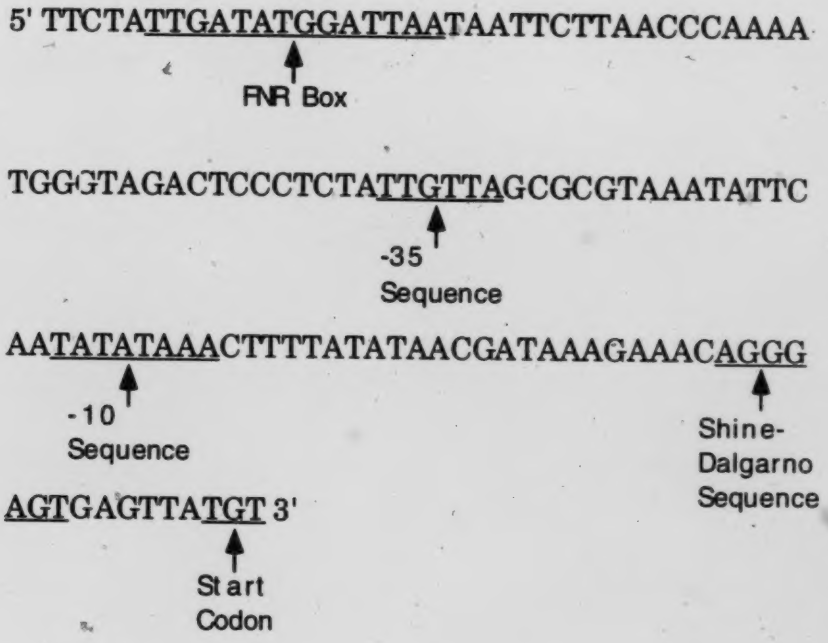
5' TTCTATTGATATGGATTAATAATTCTTAACCCAAAA
FNR Box
TGGGTAGACTCCCTCTATTGTTAGCGCGTAAATATTC
-35
Sequence
AATATATAAACTTTTATATAACGATAAAGAAACAGGG
-10
Sequence
Shine-
Dalgarno
Sequence
AGTGAGTTATGT 3'
Start
Codon

Figure 8.8.

5' Untranslated Region for orf1-4 at 35.69 Minutes on the *E. coli* Chromosome

Orf1-4 includes orf808A, orf808B, orf205, and orf207, respectively. The Shine-Dalgarno sequences for orf808B, orf205, and orf284, appear to be : AAGTGAG, AAGGAGT, and ACGAAGT/AGGAAGT, respectively. (See text for note regarding orf284 Shine-Dalgarno.)

is distinct from the other known anaerobic terminal S- and N-oxide reductases, DmsABC and TorA. Sequence analysis of the completed *E. coli* genome suggests the protein may be coded for by a gene cluster located at 35.69 minutes.

PNOR activity has previously been mentioned in the literature [34, 47]. However, analysis by both Kester et al., and Sagai et al., was performed when the proteins responsible for S- and N-oxide reduction had not been elucidated (DmsABC and TorA). As a result, *E. coli* bearing functional mutations at the *dmsABC* and *torA* loci were unavailable. It is now known DmsABC and TorA both reduce substituted PNO's (Chapter 6 and 9). PNO reduction by TorA would not interfere with measurement of PNOR activity in cells grown on minimal media if inducer was not present, or if cells were grown with aeration. Inducer (i.e., PNO) and anaerobiosis are both required for TorA expression [30, 33]. However, DmsABC is constitutively expressed under anaerobic conditions [18]. DmsAB is found in the supernatant fraction of wild-type cells, and has a specific activity with PNO sixteen fold greater than PNOR in DSS501 supernatant. Therefore, in a wild-type *E. coli* under anaerobic conditions, DmsAB rather than PNOR would be the dominant enzyme reducing PNO *in vitro*. Thus, use of strains functionally impaired for DmsABC are necessary when examining PNOR. None the less, Kester et al. did find the same electron donor profile and localization for PNOR as was found in this study even though use of a *dmsABC*$^-$ strain was not possible [34]. This is likely because their experiments were performed on aerobically grown cells, where DmsAB expression may be lower than that of PNOR. DmsABC expression increases 65 fold when cells become anaerobic [18], while PNOR activity increases only ten fold (results in this chapter). Since PNOR activity increases when cells are grown under anaerobic conditions, examination of PNOR using cells grown in this manner seems prudent. It has been possible to characterize PNOR activity in a strain functionally impaired at the *dmsABC*$^-$ and *torA*$^-$ loci (DSS501), allowing reduction of PNO by DmsABC and TorA to be ruled out, and enabling the study of PNOR in the absence of enzymes with overlapping substrate profiles. The Western blot of PNOR activity, using DmsA and DmsB antibody, demonstrates DSS501 is not expressing DmsA or DmsB, and indicates the PNOR activity observed in DSS501 is distinct from DmsA.

ANO reductase activity has also been observed in *E. coli* [47, 48]. This does not appear to be the same activity as the PNOR activity we have characterized, since the electron donor profile for ANO reductase activity is the exact opposite to that observed for PNOR. ANO reductase oxidizes $FMNH_2$ and $FADH_2$, but not NADH or NADPH [47]. PNOR will not oxidize $FMNH_2$ and $FADH_2$, but rather accepts electrons from $MVH\cdot^+$, $BVH\cdot^+$, NADH and NADPH. Also, ANO reductase activity appears to be split fifty-fifty between membrane and soluble fractions [48], contrary to observations for PNOR. It is not known whether the protein responsible for ANO reduction is a molybdoenzyme, as our results suggest for PNOR. DmsABC can poorly reduce ANO [55], while TorA cannot [25]. Once again, use of a DmsABC mutant would be prudent when studying and determining the identity of ANO reductase. No ANO reductase activity was observed in the extracts examined. However, conditions were not optimized for this activity. The literature indicates ANO reductase activity is quite low, and specific conditions are required for its detection [47, 48]. As a result, it is not particularly distressing that ANO reductase activity was not observed.

The PNOR activity characterized is not likely the result of BisC or BisZ for two reasons. One, PNOR activity is induced by anaerobiosis, while BisC and BisZ are not [14]. Two, PNOR does not appear to utilize S-oxides, further eliminating BisC, BisZ and MsrA. Also, MsrA is not a molybdoenzyme, as our results suggest for PNOR.

Growth of DSS501 on Gly/PNO was abolished when tungstate was included in the growth media, and cells grown in the presence of tungstate showed little PNOR activity. Together these results suggest PNOR is a molybdoenzyme. This could be confirmed by fluorescence studies analyzing partially purified PNOR for moco.

Since prokaryotic molybdoenzymes share sequence homology, and form a family of homologous enzymes [4, 61, 65], the recently released fully sequenced *E. coli* genome [9] was searched for sequences sharing homology with the molybdoenzyme DmsA. This search identified the ten previously identified molybdoenzymes, as well as two uncharacterized open reading frames (orf808A and orf808B), located at 35.69 minutes on the *E. coli* chromosome. By the method of elimination, the operon orf1-4 is the most likely candidate responsible for the PNOR activity observed. In fact, orf808A and orf808B are the only molybdoenzyme sequences with unclaimed function on the *E. coli* chromosome. As a result, efforts were made using PCR to clone orf1-4 into pTZ19R (Pharmacia), either in its entirety (6650 nucleotides), or in two pieces (3160 and 3490), later to be reconstructed into the native operon (J. Simala-Grant unpublished results). Although 3200 nucleotides was routinely amplified from the DmsABC operon, little amplified product was obtained during numerous attempts to PCR orf1-4. Cloning of orf1-4 from Clarke and Carbon clones [17] and ligation into pBC (Stratagene) using restriction enzyme digestion of purified DNA was pursued (J. Simala-Grant unpublished results). Once again, efforts were unsuccessful. Due to the reasoning above, cloning orf1-4 and overexpression of the proteins coded by this region, will need to be pursued. This will not only allow unequivocal determination of whether orf1-4 code for PNOR, but if correct, will facilitate greatly in future characterization of PNOR.

N-terminal sequencing of purified PNOR would also ascertain PNOR's nucleotide identity. Alternatively, growth and activity analysis of a gene knockout for orf1-4, using DSS501 as the parent strain, would reveal whether this region of DNA is responsible for the PNOR activity observed.

Growth analysis of DSS501 and subsequent characterization of PNOR activity in the supernatant suggest a cytoplasmically localized molybdoenzyme is responsible for the conservation of redox energy concomitant with PNO reduction. These results suggests PNOR either transiently localizes to the membrane, or is localized to the membrane, but falls off the membrane on cell breakage. If purified PNOR was available, or the nucleotide sequence of PNOR was known, antibodies could be synthesized and used to identify PNOR's location *in vivo*, as its location may be altered as a result of cell breakage. These two suggestions are not without precedent. GlpAC is found in the cytoplasm in broken cells [53], but transfers reducing equivalents to the Q pool through membrane bound GlpB [60]. It is not known whether they transiently localize to the membrane *in vivo*, or membrane association is disrupted by cell breakage. In addition, cytoplasmically localized PutA [13, 64] and PoxB [27, 29] have also been shown to donate electrons to the Q pool. In the case of PutA, it has been shown its association with membranes is dependent on its redox state [13], while PoxB associates with the membrane in the presence of substrate and cofactor [27]. Whether PNOR's redox state or addition of substrate affects its interaction with membranes could be examined in future studies.

If PNOR is encoded by orf1-4, orf284 would likely be the membrane anchor, due to its homology with DmsC. Since we found PNOR activity in the supernatant it is possible either orf284 is not expressed , or the catalytic portion of PNOR may have dissociated from the membrane portion during cell breakage. Alternatively, one of orf808A or orf808B may exist in the cytoplasm, and may be PNOR, while the other, in addition to orf205 and orf284, may form a membrane bound reductase that has not yet been characterized. There are difficulties with both hypotheses, as the former leaves open the question as to why two catalytic subunits (orf808A and orf808B) are necessary. The latter hypothesis leaves the unanswered question : how is PNO reduction coupled to the pmf?

Figure 8.1. demonstrates the energy of PNO reduction is conserved *in vivo*. However, PNOR does not accept electrons from the Q analogue $DMNH_2$. This suggests the PNOR activity characterized from the supernatant likely interacts with the Q pool via another protein *in vivo*, for example orf284. However, since PNOR activity was found in the cytoplasm this suggests it has dissociated from the membrane anchor. Another possibility it that PNOR interacts with an additional protein in a manner similar to the soluble and periplasmic TorA [54]. The energy of TMAO reduction is conserved by TorA via its interaction with TorC, a membrane localized *c*-type cytochrome [10, 39].

It is possible the multiple PNOR activity bands observed on the native-polyacrylamide gel (Figure 8.4.) are the result of multiple forms of PNOR, dependent on its interaction with other subunits necessary for the conservation of redox energy during the reduction of PNO. If PNOR corresponds to orf1-4, there are bands on the SDS-PAGE that could theoretically correspond to orf808A, orf808B, orf205 and orf284. Since PNOR activity was characterized in the supernatant the absence of orf284 would be expected.

Since reducing equivalents appear to be proceeding from gly-3-P to PNO *in vivo*, it is surprising that addition of PNO to glucose minimal media did not increase cell yield. Terminal reductant (PNO) would be expected to increase cell yield under anaerobic conditions, since redox balance could be achieved using more energy efficient pathways [16]. However, repression of some anaerobic enzymes has been observed to be dependent on carbon source [18, 45, 63], and this may be the phenomena observed here. The hypothesis that PNOR is repressed by the presence of glucose in the growth media could be examined in future studies by growth of DSS501 on fructose, a non-repressing sugar [45], in the presence and absence of PNO. In this case the addition of PNO to fructose minimal media would be expected to increase cell yield.

DSS501 was shown to grow on glycerol minimal media in the presence of PNO, 3-carboxypyridine N-oxide, and 3-hydroxypyridine N-oxide, but not 4-methylpyridine N-oxide. However, in contradiction, all of these compounds were substrates for PNOR in DSS501 supernatant. The explanation for this is at present a mystery.

While the electron acceptor profile indicates PNOR is able to reduce a variety of substituted PNO's, the electron donor profile was narrower. PNOR only accepted electrons from those electron donors tested that possess the lowest redox potentials. NADH was the electron donor with the highest $E_{m,7}$ used by PNOR ($^-320$ mV) [24, 58]. However, it was not observed that decreasing redox potential resulted in increased PNOR activity. A graph of PNOR activity versus redox potential of electron donor approximates a bell shaped curve, where maximal PNOR activity is observed with an electron donor potential of $^-350$ mV. Nonetheless, structural requirements may impede electron transfer from non-utilized electron donors. The electron donor profile for PNOR is different from that observed for DmsABC [61]. Although both are able to oxidize $BVH^{\cdot+}$ and $MVH^{\cdot+}$, PNOR also oxidizes NADH and NADPH, while DmsABC oxidizes $FADH_2$ and $FMNH_2$.

Reduction of N-oxides has been suggested to occur after protonation [35, 41], thus it is possible that increased PNOR activity with decreasing pH is the result of electron acceptor protonation.

A number of compounds were added to DSS501 supernatant in an attempt to stimulate PNOR due to the low reductase activity observed. Since the compounds added did not increase activity, this suggested disruptive disulfides had not formed, and that additional metal ions were both not needed, and were not inhibiting PNOR activity. Future studies may examine whether lipids or detergents activate PNOR as has been observed for PoxB [27].

PNOR activity was observed to increase ten fold when O_2 was excluded from the growth media. The induction of PNOR due to anaerobiosis appears to be within a reasonable range, since similar conditions result in 6.4 and 65 fold increases in expression of FrdABCD and DmsABC, respectively [18, 31]. The nucleotide sequence upstream orf808A shows an FNR binding site, suggesting operon orf1-4 likely shows increased expression under anaerobic conditions due to FNR binding.

Induction of expression by substituted PNO's was rather small compared to that observed for NarGHI, as nitrate reductase activity increases thirteen fold on inclusion of nitrate under anaerobic growth conditions [31]. This suggests the small increase in expression on inclusion of PNO's in the growth media, may be a function of better growth in the presence of PNO's. However, the calculations attempted to correct for this factor.

Partial purification of PNOR resulted in a fifteen fold increase in specific activity, with 10% of initial activity remaining. Difficulty in purifying other reductases has been observed previously [52]. To obtain pure protein, further purification steps are needed. Preparative-PAGE or gel filtration are good candidates for additional purification steps. Use of a fast purification procedure may prevent significant deterioration of PNOR during purification. Particularly useful would be PNOR with an engineered affinity tag [28]. This naturally requires the DNA sequence for PNOR, and emphasizes the need to clone orf1-4. Purified protein could be used to obtain an N-terminal sequence. This would unequivocally reveal the nucleotide identity of PNOR.

A mutant strain was obtained by repeated selection of larger colonies on Gly/PNO plates. DSS501-3 showed greater PNOR specific activity than its parent, DSS501. Use of this mutant strain for purification of PNOR may be useful, until strains overexpressing PNOR from plasmid are available.

This study has elucidated the presence of a previously unidentified anaerobically expressed terminal reductase, PNOR. These results suggest PNOR is a molybdoenzyme distinct from DmsABC and TorA. Utilization of procedures developed for the purification of PNOR will facilitate future studies in the characterization of this newly identified terminal reductase. Examination of the *E. coli* genome has revealed a cluster of genes at 35.69 minutes that may be responsible for PNOR activity. It will be important to determine whether orf1-4 codes for PNOR. With this dispute resolved, it will be possible to proceed with determining the proteins involved in PNO reduction, and their role in electron transfer.

8.5. References

1. Adams, M.W.W. and Mortenson, L.E. (1982) The effect of cyanide and ferricyanide on the activity of the dissimilatory nitrate reductase of *Escherichia coli*. J. Biol. Chem. 257, 1791-1799.

2. Altschul, S.F., Gish, W., Miller, W., Myers, E.W. and Lipman, D.J. (1990) Basic local alignment search tool. J. Mol. Biol. 215, 403-410.

3. Axley, M.J., Grahame, D.A. and Stadtman, T.C. (1990) *Escherichia coli* formate-hydrogen lyase. Purification and properties of the selenium-dependent formate dehydrogenase component. J. Biol. Chem. 265, 18213-18218.

4. Berks, B.C., Ferguson, S.J., Moir, J.W.B. and Richardson, D.J. (1995) Enzymes and associated electron transport systems that catalyze the respiratory reduction of nitrogen oxides and oxyanions. Biochim. Biophys. Acta 1232, 97-123.

5. Bilous, P.T., Cole, S.T., Anderson, W.F. and Weiner, J.H. (1988) Nucleotide sequence of the *dmsABC* operon encoding the anaerobic dimethylsulphoxide reductase of *Escherichia coli*. Mol. Micro. 2, 785-795.

6. Bilous, P.T. and Weiner, J.H. (1985) Dimethyl sulfoxide reductase activity by anaerobically grown *Escherichia coli*. J. Bacteriol. 162, 1151-1155.

7. Blasco, F., Iobbi, C., Ratouchniak, J., Bonnefoy, V. and Chippaux, M. (1990) Nitrate reductases of *Escherichia coli*: sequence of the second nitrate reductase and comparison with that encoded by the *narGHJI* operon. Mol. Gen. Genet. 222, 104-111.

8. Blasco, F., Pommier, J., Augier, V., Chippaux, M. and Giordano, G. (1992) Involvement of the *narJ* or *narW* gene product in the

formation of active nitrate reductase in *Escherichia coli.* Mol. Micro. 6, 221-230.

9. Blattner, F.R., Plunkett-III, G., Bloch, C.A., Perna, N.T., Burland, V., Riley, M., Collado-Vides, J., Glasner, J.D., Rode, C.K., Mayhew, G.F., Gregor, J., Davis, N.W., Kirkpatrick, H.A., Goeden, M.A., Rose, D.J., Mau, B. and Shau, Y. (1997) The complete genome sequence of *E. coli* K-12. Science 277, 1453-1468.

10. Bragg, P.D. and Hackett, N.R. (1983) Cytochromes of the trimethylamine N-oxide anaerobic respiratory pathway of *Escherichia coli.* Biochim. Biophys. Acta 725, 168-177.

11. Brot, N., Fliss, H., Coleman, T. and Weissbach, H. (1984) Enzymatic reduction of methionine sulfoxide residues in proteins and peptides. Meth. Enzymol. 107, 352-360.

12. Brot, N., Rahman, M.A., Moskovitz, J. and Weissbach, H. (1995) *Escherichia coli* peptide methionine sulfoxide reductase cloning, high expression, and purification. Meth. Enzymol. 251, 462-470.

13. Brown, E.D. and Wood, J.M. (1993) Conformational change and membrane association of the PutA protein are coincident with reduction of its FAD cofactor by proline. J. Biol. Chem. 268, 8972-8979.

14. Campbell, A. Personal communication.

15. Casadaban, M.J. (1976) Transposition and fusion of the *lac* genes to selected promoters in *Escherichia coli* using bacteriophage lambda and Mu. Mol. Biol. 104, S41-S55.

16. Clarke, D.P. (1989) The fermentation pathways of *Escherichia coli.* FEMS Microbiol. Rev. 63, 223-234.

17. Clarke, L. and Carbon, J. (1976) A colony bank containing synthetic colE1 hybrid plasmids representative of the entire *E. coli* genome. Cell 9, 91-99.

18. Cotter, P.A. and Gunsalus, R.P. (1989) Oxygen, nitrate, and molybdenum regulation of *dmsABC* gene expression in *Escherichia coli.* J. Bact. 171, 3817-3823.

19. Cull, M. and McHenry, C.S. (1990) Preparation of extracts from prokaryotes, in Guide to protein purification. (Deutscher, M.P., ed.), Vol. 182, p. 150-151, Academic Press, Inc., Toronto.

20. delCampillo-Campbell, A. and Campbell, A. (1982) Molybdenum cofactor requirement for biotin sulfoxide reduction in *Escherichia coli.* J. Bact. 149, 469-478.

21. delCampillo-Campbell, A. and Campbell, A. (1996) Alternative gene for biotin sulfoxide reduction in *Escherichia coli* K-12. J. Mol. Evol. 42, 85-90.

22. delCampillo-Campbell, A., Dykhuizen, D. and Cleary, P. (1979) Enzymic reduction of d-biotin d-sulfoxide to d-biotin. Meth. Enzymol. 62, 379-385.

23. Fleischmann, R.D., Adams, M.D., White, O., Clayton, R.A., Kirkness, E.F., Kerlavage, A.R., Bult, C.J., Tomb, J.-F., Dougtety, B.A., Merrck, J.M., McKenney, K., Sutton, G., FitzHugh, W., Fields, C., Gocayne, J.D., Scott, J., Shirley, R., Liu, L.-I., Glodek, A., Kelley, J.M., Weidman, J.F., Phillips, C.A., Sprigs, T., Hedblom, E., Cotton, M.D., Utterback, T.R., Hanna, M.C., Nguyen, D.T., Saudek, D.M., Brandon, R.C., Fine, L.D., Fritchman, J.L., Fuhrmann, J.L., Geoghagen, N.S.M., Gnehm, C.L., McDonald, L.A., Small, K.V., Fraser, C.M., Smith, H.O. and Venter, J.C. (1995) Whole-genome random sequencing and assembly of *Haemophilus influenza* Rd. Science 269, 496-512.

24. Gennis, R. and Stewart, V. (1996) Respiration, in *Escherichia coli* and *Salmonella* cellular and molecular biology. (Neidhardt, F.C., ed.), Vol. 1, p. 217-261, ASM Press, Washington.

25. Giordano, G. Personal Communication.

26. Giordano, G., Violet, M., Medani, C.-L. and Pommier, J. (1984) A common pathway for the activation of several molybdoenzymes in *Escherichia coli* K-12. Biochim. Biophys. Acta 798, 216-225.

27. Grabau, C., Chang, Y. and J. E. Cronan, J. (1989) Lipid binding by *Escherichia coli* pyruvate oxidase is disrupted by small alterations of the carboxy-terminal region. J. Biol. Chem. 264, 12510-12519.

28. Grisshammer, R. and Tate, C.G. (1995) Overexpression of integral membrane proteins for structural studies. Quart. Rev. Phys. 28, 315-422.

29. Ingeldew, W.J. and Poole, R.K. (1984) The respiratory chains of *Escherichia coli.* Microbiol. Rev. 48, 222-271.

30. Iobbi-Nivol, C., Pommier, J., Simala-Grant, J.L., Mejean, V. and Giordano, G. (1996) High substrate specificity and induction

characteristics of trimethylamine N-oxide reductase of *Escherichia coli*. Biochim. Biophys. Acta 1294, 77-82.

31. Iuchi, S. and Lin, E.C.C. (1987) The *narL* gene product activates the nitrate reductase operon and represses the fumarate reductase and trimethylamine-oxide reductase operons in *Escherichia coli*. Proc. Natl. Acad. Sci. 84, 3901-3905.

32. Jarabak, J. and Harvey, R.G. (1993) Studies on three reductases which have polycyclic aromatic hydrocarbons quinones as substrates. Arch. Biochem. Biophys. 303, 394-401.

33. Jourlin, C., Bengrine, A., Chippaux, M. and Mejean, V. (1996) An unorthodox sensor protein (TorS) mediates the induction of the *tor* structural genes in response to trimethylamine N-oxide in *Escherichia coli*. Mol. Micro. 20, 1297-1306.

34. Kester, M. and Norton, S.J. (1972) *Escherichia coli* pyridine N-oxide reductase. Biochim. Biophys. Acta 258, 709-718.

35. Kubota, T. and Miyazaki, H. (1962) Polarography of pyridine N-oxide and its alkyl derivatives. Bull. Chem. Soc. Jap. 35, 1549-1551.

36. Laemmli, U.K. (1970) Cleavage of structural proteins during the assembly of the head of bacteriophage T4. Nature 227, 680-685.

37. Lemire, B.D., Robinson, J.J. and Weiner, J.H. (1982) Identification of membrane anchor polypeptides of *Escherichia coli* fumarate reductase. J. Bacteriol. 152, 1126-1131.

38. Markwell, M.A.D., Haas, S.M., Bieber, L.L. and Tolbert, N.E. (1978) A modification of the Lowry procedure to simplify protein determination in membrane and lipoprotein samples. Anal. Biochem. 87, 206-210.

39. Mejean, V., Iobbi-Nivol, C., Lepelletier, M., Giordano, G., Chippaux, M. and Pascal, M.-C. (1994) Trimethylamine N-oxide anaerobic respiration in *Escherichia coli* : involvement of the *tor* operon. Mol. Microbiol. 11, 1169-1179.

40. Moskovitz, J., Rahman, A., Strassman, J., Yancey, S.O., Kushner, S.R., Brot, N. and Weissbach, H. (1995) *Escherichia coli* peptide methionine sulfoxide reductase gene: regulation of expression and role in protecting against oxidative damage. J. Bact. 177, 502-507.

41. Ochaiai, E. (1967) Polarography, in Aromatic Amine Oxides. 1st ed., p. 91, Elsevier Publishing Company, Amsterdam.

42. Pascal, M.-C., Burini, J.-F. and Chippaux, M. (1984) Regulation of the trimethylamine N-oxide (TMAO) reductase in *Escherichia coli* : Analysis of *tor*:Mud1 operon fusion. Mol. Gen. Genet. 195, 351-355.

43. Pierson, D.E. and Campbell, A. (1990) Cloning and nucleotide sequence of *bisC*, the structural gene for biotin sulfoxide reductase in *Escherichia coli*. J. Bact. 172, 2194-2198.

44. Rahman, M.A., Nelson, H., Weissbach, H. and Brot, N. (1992) Cloning, sequencing, and expression of the *Escherichia coli* peptide methionine sulfoxide reductase gene. J. Biol. Chem. 267, 15549-15551.

45. Reams, S.G. and Clark, D.P. (1988) Glucose repression of anaerobic genes of *Escherichia coli* is independent of cyclic AMP. FEMS Microbiol. Lett. 56, 231-236.

46. Rothery, R.A., Simala-Grant, J.L., Johnson, J.L., Rajagopalan, K.V. and Weiner, J.H. (1995) Association of molybdopterin guanine dinucleotide with *Escherichia coli* dimethylsulfoxide reductase : Effect of tungstate and a *mob* mutant. J. Bacteriol. 177, 2057-2063.

47. Sagai, M. and Ishimoto, M. (1973) An enzyme reducing adenosine N-oxide in *Escherichia coli*, amine N-oxide reductase. J. Biochem. 73, 843-859.

48. Sambasivarao, D. and Weiner, J.H. (1991) Differentiation of the multiple S- and N-oxide reducing activities of *Escherichia coli*. Curr. Microbiol. 23, 105-110.

49. Sambasivarao, D. and Weiner, J.H. (1991) Dimethylsulfoxide reductase of *Escherichia coli* : an investigation of function and assembly by use of *in vivo* complementation. J. Bacteriol. 173, 5935-5943.

50. Sambrook, J., Fritsch, E.F. and Maniatis, T. (1989) Molecular cloning : A laboratory manual. Cold Spring Harbor Laboratory Press, Cold Spring Harbor, N.Y.

51. Sawers, G. (1994) The hydrogenases and formate dehydrogenases of *Escherichia coli*. Anton. Van Leeuwen. 66, 57-88.

52. Schroder, I., Kroger, A. and Macy, J.M. (1988) Isolation of the sulphur reductase and reconstitution of the sulphur respiration of *Wolinella succinogenes.* Arch. Microbiol. 149, 572-579.

53. Schryvers, A. and Weiner, J.H. (1981) The anaerobic sn-glycerol-3-phosphate dehydrogenase of *Escherichia coli.* J. Biol. Chem. 256, 9959-9965.

54. Silvestro, A., Pommier, J., Pascal, M.-C. and Giordano, G. (1989) The inducible trimethylamine N-oxide reductase of *Escherichia coli* K12: its localization and inducers. Biochim. Biophys. Acta 999, 208-216.

55. Simala-Grant, J.L. and Weiner, J.H. (1996) Kinetic analysis and substrate specificity of *Escherichia coli* dimethyl sulfoxide reductase. Microbiol. 142, 3231-3239.

56. Stewart, V. and Rabin, R.S. (1995) Dual sensors and dual response regulators interacts to control nitrate- and nitrite-responsive gene expression in *Escherichia coli,* in Two-component signal transduction. (Hoch, J.A. and Silhavy, T.J., eds.), Vol. 1, 1st ed., p. 233-252, ASM Press, Washington.

57. Stryer, L. (1988) Biochemistry. Vol. 1, 3rd ed., p. 753, W. H. Freeman and Company, New York.

58. Unden, G., Hackenberg, H. and Kroger, A. (1980) Isolation and functional aspects of the fumarate reductase involved in the phosphorylative electron transport of *Vibrio succinogenes.* Biochim. Biophys. Acta 591, 275-288.

59. Unemoto, T., Hayashi, M., Miyaki, K. and Hayashi, M. (1965) Intracellular localization and properties of trimethylamine-N-oxide reductase in *Vibrio parahaemolyticus.* Biochim. Biophys. Acta 110, 319-328.

60. Varga, M.E.R. and Weiner, J.H. (1995) Physiological role of GlpB of anaerobic glycerol-3-phosphate dehydrogenase of *Escherichia coli.* Biochem. Cell Biol. 73, 147-153.

61. Weiner, J.H., MacIsacc, D.P., Bishop, R.E. and Bilous, P.T. (1988) Purification and properties of *Escherichia coli* dimethyl sulfoxide reductase, an iron-sulfur molybdoenzyme with broad substrate specificity. J. Bacteriol. 170, 1505-1510.

62. Weiner, J.H., Shaw, G., Turner, R.J. and Trieber, C.A. (1993) The topology of the anchor subunit of dimethyl sulfoxide reductase of *Escherichia coli.* J. Biol. Chem. 268, 3238-3244.

63. Winkelman, J.W. and Clark, D.P. (1986) Anaerobically induced genes of *Escherichia coli*. J. Bact. 167, 362-367.

64. Wood, J.M. (1987) Membrane association of proline dehydrogenase in *Escherichia coli* is redox dependent. Proc. Natl. Acad. Sci 84, 373-377.

65. Wootton, J.C., Nicolson, R.E., Cock, J.M., Walters, D.E., Burke, J.F., Doyle, W.A. and Bray, R.C. (1991) Enzymes depending on the pterin molybdenum cofactor : sequence families, spectroscopic properties of molybdenum and possible cofactor-binding domains. Biochim. Biophys. Acta 1057, 157-185.

66. Yamamoto, I., Okubo, M. and Ishimoto, M. (1986) Further characterization of trimethylamine N-oxide reductase from *Escherichia coli* a molybdoprotein. J. Biochem. 99, 1773-1779.

Chapter 9 : Kinetic Analysis and Substrate Specificity of *E. coli* TorA *

9.1. Introduction

The facultative anaerobe *E. coli* is capable of anaerobic respiration using a variety of terminal electron acceptors. It has been demonstrated that two immunologically and genetically distinct enzymes, TorA and DmsABC, are involved in TMAO reduction in *E. coli* [1, 13, 15, 19]. TorA is inducible and periplasmic [20], while DmsABC is constitutive and membrane bound [23].

Several lines of evidence including analysis of activity-stained native gels, assays using high concentrations of substrate, or assays of crude extracts, suggested both TorA and DmsABC are able to reduce a large variety of N- and S-oxides [20, 23, 24]. Nevertheless, an unexpected result clearly showed deletion of the *dmsABC* operon totally abolished growth of *E. coli* on Gly/DMSO [15]. Previously, DMSO was shown to induce synthesis of TorA, and TorA appeared to have DMSO reductase activity in crude extracts [20]. These results indicate either, TorA does not reduce DMSO, or DMSO reduction by TorA is not coupled to energy-yielding reactions. A thorough kinetic study determining the kinetic parameters of purified TorA has not been performed.

---

* A version of this chapter has been published. Iobbi-Nivol, C., Pommier, J., Simala-Grant, J., Mejean, V., and Giordano, G. (1996) High substrate specificity and induction characteristics of trimethylamine N-oxide reductase of *Escherichia coli*. Biochim. Biophys. Acta 1294, 77-82.

The published paper contains additional data on induction characteristics of TorA, by the same compounds used for kinetic analysis. Induction data was not included in this chapter, as Joanne Simala-Grant was not involved in the planning or carrying out of those experiments, and it is not pertinent to the thesis subject. Joanne Simala-Grant initiated the kinetic study, and performed initial kinetic characterization of TorA using their selection of S- and N-oxides during a collaborative visit by Dr. Giordano. (The two labs involved in this work share a NATO grant.) The paper was written mostly by Joanne Simala-Grant and Dr. Giordano, during a subsequent visit.

The kinetic analysis of DmsABC using a variety of S- and N-oxides (Chapter 6), and scientific ties with Dr. G. Giordano at the CNRS in Marseille France, prompted a collaboration on the kinetic characterization of TorA. This study employed most of the same S- and N-oxides used in the kinetic study of DmsABC.

The kinetic characterization of purified TorA using a wide variety of N- and S-oxide's demonstrates TorA has a narrow substrate specificity. A kinetic comparison is made between the two *E. coli* S- and N-oxide reductases TorA and DmsABC.

9.2. Materials and Methods

9.2.1. Materials

N- and S-oxides were purchased from Sigma or Aldrich. Some compounds possess the N-oxide within a benzene ring. Substitution can occur in position 2, 3, or 4 (Figure 6.1. A). Other N-oxides are structurally similar to TMAO, and possess one or more substitutions of the methyl groups by aliphatic carbon chains or by hydrogen atoms. (Figure 6.1. B). The sulfoxides are similar in structure to DMSO, and possess one or two substitutions of the methyl groups by an aliphatic carbon chain, or phenyl group (Figure 6.1. C). 4-Methylmorpholine N-oxide, and tetramethylene sulfoxide, are compact molecules resulting from the cyclizing of two methyl groups. (Figure 6.1 B and C).

9.2.2 Strains

E. coli strain MC4100 was used in this study (*ara*D139 (*lac*IPOZYA-*arg*F)U169 *rps*L *thi* [2]).

9.2.3 Media Preparation and Crude Extracts

Bacteria were grown anaerobically [6] on basal medium supplemented with Difco yeast extract and Difco bacto-peptone (1 g/L of each). The carbon source was glucose (2 g/L), and 1 mM sodium molybdate was routinely included.

The cells were harvested at the end of exponential growth phase, washed in 40 mM TRIS (pH 7.6), containing 1 mM benzamidine-HCl, resuspended in the same buffer, and disrupted by French Press. The crude extracts were obtained after removal of cell debris by centrifugation, at 18,000 x g for 15 min. All procedures were performed at 4°C.

9.2.4. Purification of TorA

TorA was purified from 200 g of wet cells. The crude extracts were centrifuged twice at 170,000 x g for 90 minutes to prepare a soluble fraction. TorA was purified from the soluble fraction by a heat step, and DEAE-cellulose, Sephadex G-200, DEAE-Sepharose CL-6B, and hydroxylapatite columns [19]. The specific activity of purified enzyme was measured with TMAO, and gave a value of 105 μmole TMAO reduced min^{-1} mg^{-1} protein.

9.2.5. Enzyme Assays and Determination of Kinetic Parameters

TorA activity was measured spectrophotometrically at 37°C, following the oxidation of $BVH^{\cdot +}$ at 600 nm, coupled to the reduction of N- or S-oxide substrate [22]. K_m's were determined for each of the compounds showing reasonable V_{max} values. Four duplicates were performed at each of the eight different substrate concentrations. The values of V_{max} and K_m were estimated with the Newton Gauss algorithm [4]. Protein concentration was estimated [9], and used to determine k_{cat} values.

Inhibition of TorA by poor substrates was examined by adding 2-20 mM of poor substrate, in a reaction mixture containing 0.5 mM TMAO.

9.3. Results

9.3.1. Kinetic Analysis

The reduction of N- and S- oxides by TorA was examined (Table 9.1.). Twelve different N-oxides can be reduced by TorA. Of these, TMAO, 3-methylpyridine N-oxide, and LDAO, had high and similar k_{cat} values, with the rest in this group showing intermediate k_{cat}'s between 10 and 70% of TMAO. k_{cat} values for the other 8 N-oxides, and all S-oxides tested, could not be determined with any precision, as the reduction of these compounds by TorA was very poor. k_{cat}'s for these compounds were estimated to be no more that 2.5% of the value for TMAO. Increasing their concentration in the assay resulted in some cases, in an apparently non-enzymatic reduction. Others were not sufficiently soluble at the high concentrations required for the determination of k_{cat} value's.

Only two N-oxide's, TMAO, and 4-methylmorpholine N-oxide, showed low K_m values. 2- and 4-methylpyridine N-oxide have K_m's about 5 fold higher. The other substrates tested have much higher K_m's. It was impossible to obtain K_m's for 8 of the N-oxides and all S-oxide substrates, as reduction of these compounds by TorA is very poor (Table 9.1.).

We determined k_{cat}/K_m values to examine enzyme preference for the substrates tested (Table 9.1.). These value's take into account both the affinity of an enzyme for substrate, as well as substrate turnover, and determines enzyme specificity for competing substrates [5]. Only TMAO and 4-methylmorpholine N-oxide, structurally similar compounds, can be considered good substrates on this basis.

Table 9.1.

Kinetic Parameters for N- and S-oxide Substrates of TorA

Compound	k_{cat} (s^{-1})	K_m (mM)	k_{cat}/K_m (s^{-1} mM^{-1})	Relative k_{cat}/K_m
Aliphatic N-oxides				
TMAO	150.3	0.07	2150	100
4-methylmorpholine N-oxide	96.5	0.02	4825	224
LDAO	154.62	1.25	124	5.75
N,N-dimethylhexylamine N-oxide	13.77	1.14	12	0.56
hydroxylamine N-oxide	69.95	7.39	9	0.44
triethylamine N-oxide	<4	nd	-	-
Aromatic N-oxides				
2-methylpyridine N-oxide	102.3	0.26	393	18.3
4-methylpyridine N-oxide	49.55	0.32	155	7.2
3-hydroxypyridine N-oxide	49.24	0.75	66	3.05
2-chloropyridine N-oxide	100.95	2.01	50	2.33
4-chloropyridine N-oxide	66.68	2.15	31	1.44
PNO	53.45	1.86	29	1.34
3-methylpyridine N-oxide	136.81	5.43	25	1.17
4-carboxypyridine N-oxide	<4	nd	-	-
2-hydroxypyridine N-oxide	<4	nd	-	-
2-hydroxymethylpyridine N-oxide	<4	nd	-	-
2-carboxypyridine N-oxide	<4	nd	-	-
3-carboxypyridine N-oxide	<4	nd	-	-
3-amidopyridine N-oxide	<4	nd	-	-
S-oxides				
DMSO	<4	nd	-	-
D/L-methionine sulfoxide	<4	nd	-	-
tetramethylene sulfoxide	<4	nd	-	-
dibutyl sulfoxide	<4	nd	-	-
diphenyl sulfoxide	<4	nd	-	-

All assays were performed using the closed-cuvette assay. The relative k_{cat}/K_m ratio obtained for each compound, is expressed as a percentage of the value for TMAO. nd indicates not determined, as activity values were too low for a K_m determination. For structures of N- and S-oxides see Figure 6.1.

We looked for potential inhibition of TorA by several of the poor substrates : 2-hydroxypyridine N-oxide, 2-carboxypyridine N-oxide, DMSO, and tetramethylene sulfoxide. These compounds do not act as inhibitors of TorA activity using TMAO as substrate (Table 9.2.).

9.4. Discussion

Enzymes catalyzing the reduction of TMAO have been studied in several organisms. Enzymes that reduce N- and S-oxides fall into two categories. Enzymes that possess broad substrate specificity, include the DMSO reductases from *R. sphaeroides* [16], *R. capsulatus* [10], and *E. coli* (Chapter 6 and [21, 23]). The second class possess a narrower substrate specificity, and include *Shewanella* TMAO reductase [3].

Our study indicates that in contrast to DmsABC [21], TorA possesses very narrow substrate specificity. TorA shows high substrate specificity towards TMAO and 4-methylmorpholine N-oxide, and is unable to reduce any S-oxides.

The observation that TorA cannot utilize S-oxides explains why a DmsABC$^-$ mutant cannot grow on Gly/DMSO, even though DMSO induces TorA synthesis [7, 20]. It also suggests the N-oxide moiety is necessary for recognition by the enzyme.

Redox potential would be expected to affect k_{cat} much more than K_m. PNO's have lower redox potentials, and are more difficult to reduce than aliphatic N-oxides, because the electrons from the oxygen are in resonance with the aromatic ring, stabilizing the unstable N-O bond [14]. However, this does not appear to affect the k_{cat}'s observed, as the three highest k_{cat} values belong to both aliphatic and aromatic N-oxides.

The low K_m values toward TMAO and 4-methylmorpholine N-oxide, two compact aliphatic N-oxides, suggests TorA can distinguish these from the other larger aliphatic N-oxides, as well as from the

Table 9.2.

Ability of N- and S-oxide's to Inhibit Reduction of TMAO by TorA

Compound	Specific Activity (μM min^{-1} mg^{-1})
TMAO	34
TMAO + 2-hydroxypyridine N-oxide	33
TMAO + 2-carboxypyridine N-oxide	36
TMAO + DMSO	36
TMAO + tetramethylene sulfoxide	35

All assays were performed using the closed-cuvette assay with 0.5 mM TMAO and 20 mM tested compound.

smaller hydroxylamine. This suggests an optimal size for substrate, equivalent to the approximate volume of TMAO or 4-methylmorpholine N-oxide. Optimal substrate would allow positive interactions between enzyme and substrate, without steric hindrance.

Several aromatic N-oxides have 5-10 fold higher K_m values than TMAO, while others have substantially higher K_m values, or are not substrates at all. It appears that TorA will not utilize charged compounds, as aromatic substrates with ionizable substituents are not accepted.

Inhibition studies indicated the poor substrates examined were not inhibitors of TorA activity. This indicates absence of activity is firstly due to lack of binding to TorA.

A plot of TorA substrates, arranged in order of increasing K_m versus k_{cat} (Figure 9.1.), shows a fairly random relationship between the two. This is slightly different from what is observed for DmsABC, where k_{cat} values fall mostly within a narrower range, while the 3 aliphatic N-oxides show higher k_{cat} values. (Figure 6.2.).

Both TorA and DmsABC show very large variations in K_m values (370 and 470 fold, respectively), and only small variations in k_{cat} values (10 and 20 fold, respectively). As a result, K_m influences the value of k_{cat}/K_m much more than k_{cat}. This can be observed in Figure 9.2., where TorA substrates with low K_m values show high k_{cat}/K_m values and vice versa. k_{cat}/K_m values distinguish TMAO and 4-methylmorpholine N-oxide as the best TorA substrates.

DmsABC and TorA belong to a family of homologous prokaryotic molybdoenzymes, believed to share a similar polypeptide fold and active site. Two of the S- and N-oxide reductases in this family have been crystallized, and their three dimensional structures determined [8, 11, 12, 17, 18]. The structures of the DMSO reductases from *R. sphaeroides* and *R. capsulatus* show a narrow tunnel that extends from the surface of the protein to the Mo, where S- an N-oxide reduction occurs.

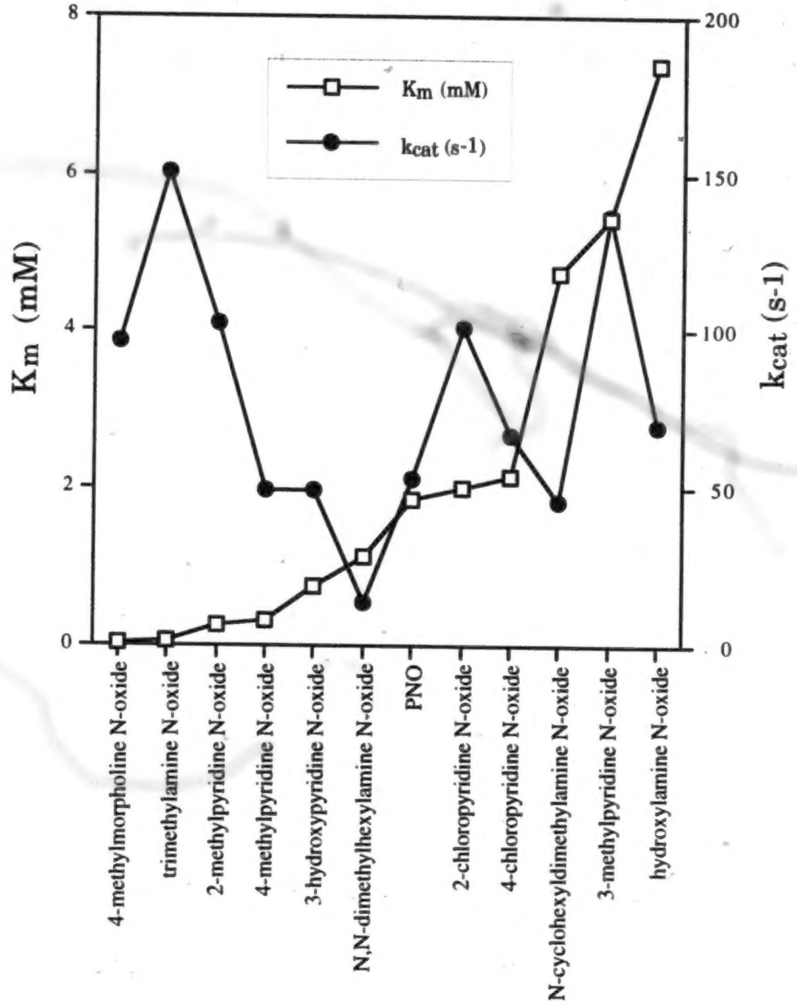

Substrate

Figure 9.1.

Substrates of TorA Arranged in Order of Increasing K_m Versus k_{cat} Value

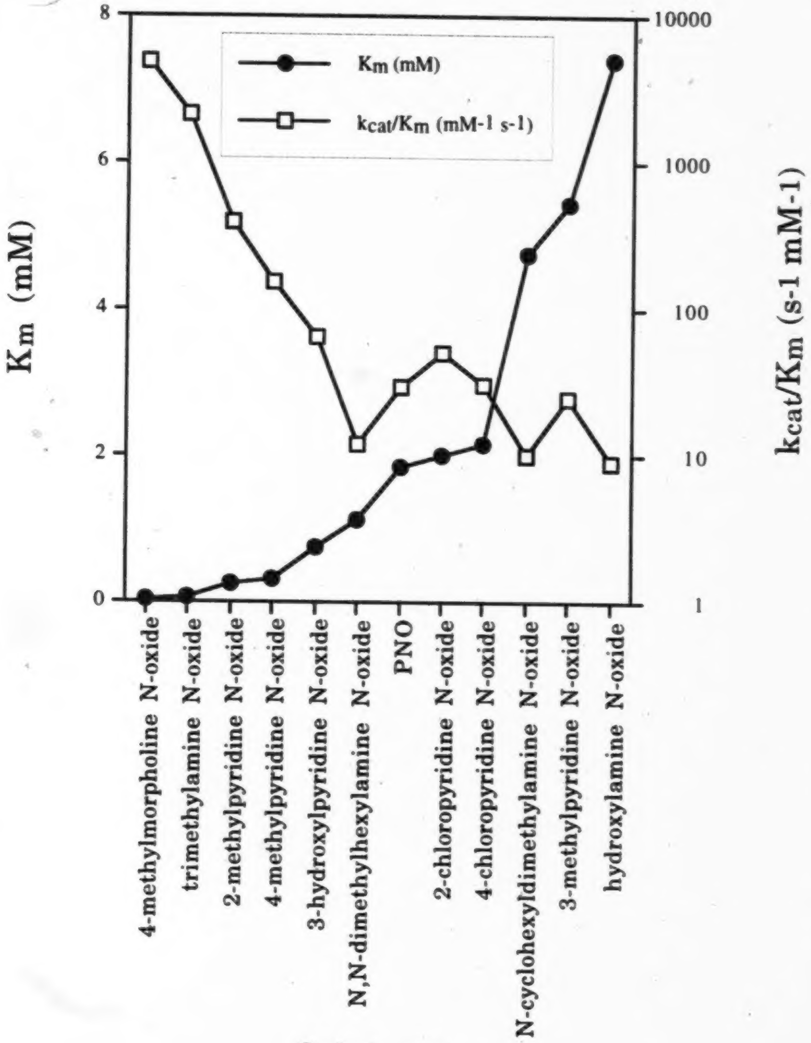

Figure 9.2.

Substrates of TorA Arranged in Order of Increasing K_m Versus k_{cat}/K_m Value

The narrow substrate specificity of TorA (Table 9.1.) contrasts the broad substrate specificity of DmsABC (Table 6.1. and 6.2.). Also, TorA prefers smaller compact N-oxides to larger ones. This preference is not seen in DmsABC. These observations suggest the active site funnel of TorA may be narrower. TorA may possess residues that could negatively interact with some of the aromatic PNO's excluding them from reduction by TorA, while still being accepted by DmsABC.

Although the substrate specificity of DmsABC overlaps with TorA, the poorest DmsABC substrates are the best TorA substrates, and vice versa. This may allow these proteins to play complementary roles in the cell.

These kinetic results leads to two major conclusions. First, TorA shows a narrow substrate specificity. It excludes reduction of all S-oxides and many N-oxides. TMAO and 4-methylmorpholine N-oxide are by far the best substrates. Second, the N-oxide appears essential for recognition by TorA, and smaller compact molecules appear to be preferred.

9.5. References

1. Bilous, P.T. and Weiner, J.H. (1988) Molecular cloning and expression of the *Escherichia coli* dimethyl sulfoxide reductase operon. J. Bacteriol. 170, 1511-1518.

2. Casadaban, M.J. (1976) Transposition and fusion of the *lac* genes to selected promoters in *Escherichia coli* using bacteriophage lambda and Mu. Mol. Biol. 104, S41-S55.

3. Clarke, G.J. and Ward, F.B. (1988) Purification and properties of trimethylamine N-oxide reductase from *Shewanella* sp. NCMB 400. J. Gen. Microbiol. 133, 379-386.

4. Cleland, W.W. (1967) The statistical analysis of enzyme kinetic data. Adv. Enzymol. 29, 1-32.

5. Fersht, A. (1985) Chapter 3: The basic equations of enzyme kinetics, in Enzyme structure and mechanism. 2nd ed., p. 98-120, W. H. Freeman, New York.

6. Giordano, G., Graham, A., Boxer, D.H., Haddock, B.A. and Azoulay, E. (1978) Characterization of the membrane-bound nitrate reductase activity of aerobically grown chlorate-sensitive mutants of *Escherichia coli* K12. FEBS Lett. 95, 290-294.

7. Iobbi-Nivol, C., Pommier, J., Simala-Grant, J.L., Mejean, V. and Giordano, G. (1996) High substrate specificity and induction characteristics of trimethylamine N-oxide reductase of *Escherichia coli*. Biochim. Biophys. Acta 1294, 77-82.

8. Knablein, J., Dobbek, H., Ehlert, S. and Schneider, F. (1997) Isolation, cloning, sequence analysis and X-ray structure of dimethyl sulfoxide/trimethylamine N-oxide reductase from *Rhodobacter sphaeroides*. Biol. Chem. 378, 293-302.

9. Lowry, O.H., Rosenbrough, N.J., Farr, A.L. and Randall, R.J. (1951) Protein measurement with the folin phenol reagent. J. Biol. Chem. 193, 265-275.

10. MacEwan, A.G., Wetstein, H.G., Meyer, O., Jackson, J.B. and Ferguson, S.J. (1987) The periplasmic nitrate reductase of *Rhodobacter capsulatus*; purification, characterisation and distinction from a single reductase for trimethylamine-N-oxide dimethylsulphoxide and chlorate. Arch. Microbiol. 147, 340-345.

11. McAlpine, A.S., McEwan, A.G. and Bailey, S. (1998) The high resolution crystal structure of DMSO reductase in complex with DMSO. J. Mol. Biol. In press.

12. McAlpine, A.S., McEwan, A.G., Shaw, A.L. and Bailey, S. (1998) Molybdenum active center of DMSO reductase from *Rhodobacter capsulatus* : crystal structure of the oxidised enzyme at 1.82Å resolution and the dithionite-reduced enzyme at 2.8Å resolution. J. Biol. Inorg. Chem. In press.

13. Mejean, V., Iobbi-Nivol, C., Lepelletier, M., Giordano, G., Chippaux, M. and Pascal, M.-C. (1994) Trimethylamine N-oxide anaerobic respiration in *Escherichia coli* : involvement of the *tor* operon. Mol. Microbiol. 11, 1169-1179.

14. Ochaiai, E. (1953) Recent Japanese work on the chemistry of pyridine 1-oxide and related compounds. J. Org. Chem. 18, 534-551.

15. Sambasivarao, D. and Weiner, J.H. (1991) Differentiation of the multiple S- and N-oxide reducing activities of *Escherichia coli.* Curr. Microbiol. 23, 105-110.

16. Satoh, T. and Kurihara, F.N. (1987) Purification and properties of dimethylsulfoxide reductase containing a molybdenum cofactor from a photodenitrifier, *Rhodopseudomonas sphaeroides* f.s. *denitrificans.* J. Biochem 102, 191-197.

17. Schindelin, H., Kisher, C., Hilton, J., Rajagopalan, K.V. and Rees, D.C. (1996) Crystal structure of DMSO reductase: Redox-linked changes in molybdopterin coordination. Science 272, 1615-1621.

18. Schneider, F., Lowe, J., Huber, R., Schindelin, H., Kisker, C. and Knablein, J. (1996) Crystal structure of dimethyl sulfoxide reductase from *Rhodobacter capsulatus* at 1.88 A resolution. J. Mol. Biol. 263, 53-69.

19. Silvestro, A., Pommier, J. and Giordano, G. (1988) The inducible trimethylamine *N*-oxide reductase of *Escherichia coli* K12 : biochemical and immunological studies. Biochim. Biophys. Acta. 954, 1-13.

20. Silvestro, A., Pommier, J., Pascal, M.-C. and Giordano, G. (1989) The inducible trimethylamine N-oxide reductase of *Escherichia coli* K12 : its localization and inducers. Biochim. Biophys. Acta 999, 208-216.

21. Simala-Grant, J.L. and Weiner, J.H. (1996) Kinetic analysis and substrate specificity of *Escherichia coli* dimethyl sulfoxide reductase. Microbiol. 142, 3231-3239.

22. Tagaki, H., Tsuchiya, T. and Ishimoto, M. (1981) Proton translocation coupled to trimethylamine N-oxide reduction in anaerobically grown *Escherichia coli.* J. Bacteriol. 148, 762-768.

23. Weiner, J.H., MacIsacc, D.P., Bishop, R.E. and Bilous, P.T. (1988) Purification and properties of *Escherichia coli* dimethyl sulfoxide reductase, an iron-sulfur molybdoenzyme with broad substrate specificity. J. Bacteriol. 170, 1505-1510.

24. Yamamoto, I., Okubo, M. and Ishimoto, M. (1986) Further characterization of trimethylamine N-oxide reductase from *Escherichia coli* a molybdoprotein. J. Biochem. 99, 1773-1779.

Chapter 10 : Conclusions, Discussion, and Future Directions

10.1. Conclusions

DmsABC is a complex multisubunit Fe-S molybdoenzyme. It allows for respiratory growth on S- and N-oxides, and is an excellent model system for studying both prokaryotic molybdoenzymes, and electron transport chain proteins. The studies undertaken in this thesis have elucidated some key features of DmsABC structure and function (Chapter 2, 3, 4, 5, 6, and 7), allowed kinetic comparison with another terminal reductase (TorA) (Chapter 9), and opened up a new avenue of research into the study of a novel terminal reductase (PNOR) (Chapter 8).

In an effort to obtain DmsABC in the absence of its membrane anchor subunit (DmsC), the cytoplasmic catalytic dimer (DmsAB) was examined. Examination revealed cytoplasmic DmsAB activity was easily lost in comparison with DmsABC activity, implicating DmsC in the stabilization of the membrane bound trimer. Glycerol was found to inhibit the loss of DmsAB activity, suggesting activity loss may have been the result of denaturation. An alternate process of activity loss was suggested for DmsABC, as substrate aided in the maintenance of DmsABC stability (Chapter 2).

Molybdoenzymes may bind moco with or without appended nucleotide (Figure 1.4.). Although the locus responsible for appending nucleotide to MPT (*mob*) was known to be necessary for DmsABC activity [6], it had not been demonstrated whether the moco in DmsA was MPT or a dinucleotide derivative. As a result, moco from DmsABC was examined. Absorption and fluorescence spectroscopy revealed DmsABC bind's MPT with GMP appended in a pyrophosphate linkage. This was the second *E. coli* molybdoenzyme found to bind MGD, suggesting all *E. coli* molybdoenzymes may bind this form of the moco (Chapter 3).

Recent sequence analysis of DmsA suggested the originally proposed initiating Met may be incorrect [3]. As a result, this was examined using a site-directed mutant and *tac* plasmid constructs of DmsA with altered initiating Met's. The constructs and mutant were examined for growth on Gly/DMSO and accumulation of DmsA (Chapter 4). In contrast to previously published data [5], a Met, 29 residues upstream of the originally proposed initiating Met was demonstrated to be the correct initiating codon for DmsA. The published amino acid numbering for DmsA begins 29 residues downstream from the Met, demonstrated to be the initiating codon, thus 29 residues are not numbered. In chapter 4 these residues were numbered with negative numbers ascending in the 5' direction (Figure 4.1.). However, these results suggest DmsA needs to be renumbered starting at $M^{-}29$. These results also indicated the DmsA-leader possesses a double-arginine consensus (Chapter 4), suggested to be important for the translocation of a subset of redox cofactor containing proteins [3]. Plasmid constructs with truncated and deleted leader, and the second Arg in the double-arginine consensus mutated to an Asp, were employed. The DmsA-leader was demonstrated to be necessary for production of functional DmsABC, as was the second Arg in the double-arginine consensus. In the absence of the leader, DmsAB was found attached to the membrane but was non-functional (Chapter 4). Since DmsAB binds to DmsC on the cytoplasmic face of the membrane [43, 45, 58], the double-arginine consensus was suggested to be necessary in addition to translocation [3], for functional membrane targeting (Figure 4.7. - Chapter 4).

To determine whether factors inherent to the assays employed influenced the kinetic constants for DmsABC, the commonly employed open and closed cuvette spectroscopic assays were examined. In addition, the usefulness of a NMR spectroscopy assay for the kinetic characterization of DmsABC was determined. All three assays employ dithionite to reduce the electron donor BV. The open cuvette assay was found to be problematic as it employs excess dithionite, and dithionite was shown to be a competitive inhibitor of DmsABC under turnover conditions. In addition, dithionite was an inhibitor of DmsABC if dithionite was incubated with DmsABC in the absence of substrate, indicating order of addition to the cuvette was important. The NMR spectroscopy assay was precluded as an optimal assay since DmsABC had a lower k_{cat} when employing the NMR spectroscopy assay. This may have been due to poor mixing as a result of narrow NMR tube width, resulting in contact between DmsABC and dithionite before substrate. These results suggested development of a novel assay for DmsABC not requiring dithionite would be prudent (Chapter 5).

In order to gain an understanding of the parameters affecting substrate binding and turnover, kinetic analysis of DmsABC was performed employing a wide variety of electron acceptors. DmsABC was demonstrated to possess a very broad substrate specificity, utilizing S- and N-oxides, and a variety of miscellaneous compounds (Chapter 6). In contrast, TorA showed a narrower substrate specificity for a few N-oxides (Chapter 9). For both enzymes, the K_m's varied widely compared to the k_{cat}, and as a result K_m was the primary determinant in the k_{cat}/K_m for a substrate.

Structures of molybdoenzymes as determined by X-ray crystallography, demonstrate they all possess a funnel that leads from the surface of the protein to the Mo at approximately the center of the protein where substrate is reduced [14, 18, 31, 35, 36, 40, 48]. As a result, substrate must pass down the funnel to reach the active site, and thus residues lining the funnel likely influence substrate binding and specificity. To identify key residues for substrate binding in DmsA, the crystal structure of DMSOR was examined for residues lining the funnel, and a comparison was made between the homologous DMSOR and DmsA sequences. This allowed potential DmsA funnel/active site residues to be targeted for mutation. Fifteen mutants were made, and examined for growth on Gly/DMSO, and kinetic analysis using two electron donors ($BVH^{\cdot+}$ and $DMNH_2$), and two electron acceptors

(DMSO and PNO). Analysis of site-directed mutants suggested DmsA residues T148, A178 and R217, are near the Mo, and influence the substrate specificity of DmsABC. T148 was observed to have an increased and decreased K_m for DMSO and PNO, respectively, while A178 and R217 had extremely low and high K_m's for both electron acceptors, respectively. Q179 and G167 showed decreased k_{cat}'s with the MQ analogue DMN, and an inability to grow on Gly/DMSO. This suggested their importance in electron transfer *in vivo* (Chapter 7). This was the first published use of the available molybdoenzyme crystal structures, to identify key functional residues for mutation. However, many similar projects will certainly be forthcoming.

Kinetic analysis of DmsABC demonstrated its ability to reduce a wide variety of S- and N-oxides and miscellaneous compounds. Examination revealed that most of these compounds could support anaerobic respiratory growth with a non-fermentative substrate (Chapter 6). In an effort to define the roles of DmsABC and TorA in respiratory growth on these compounds, growth was examined in single and double mutants for DmsABC and TorA. Respiratory growth on PNO's was maintained in the absence of DmsABC and TorA expression, indicating the presence of a previously unidentified terminal reductase. PNOR was characterized, and demonstrated to be an anaerobically expressed cytoplasmically localized molybdoenzyme. Potential PNOR gene sequences were identifed on the *E. coli* chromosome, but not confirmed (Chapter 8).

10.2. Discussion

10.2.1. The Role of S- and N-oxide Reductases in Respiratory Growth in *E. coli*

Three terminal S- and N-oxide reductases have been identified in *E. coli*. While DmsABC is solely responsible for growth on DMSO and tetramethylene sulfoxide, growth on TMAO is mediated by both

DmsABC and TorA. At the same time, growth on PNO is mediated by DmsABC, TorA, and PNOR. The extremely low *in vitro* activity of PNOR suggests it is of little importance for anaerobic growth on PNO. This may be due to poor use of *in vitro* electron donors, as *E. coli* grows on Gly/PNO in the absence of DmsABC and TorA (Chapter 8). In addition, growth on ANO is likely mediated almost exclusively by a fourth terminal reductase, ANO reductase, that has not been characterized [24, 46, 51]. This is another example of the apparent redundancy of the *E. coli* respiratory chain.

Kinetic analysis demonstrated DmsABC possesses a very broad substrate specificity for electron acceptors, although preference is observed for S-oxides and PNO's (Chapter 6). TorA shows a strong bias for aliphatic N-oxides, although it can reduce a few PNO's (Chapter 9). PNOR was demonstrated to reduce only PNO's (Chapter 8). Although the substrate specificity of these three terminal reductases overlap, they are different in their primary selectivity, providing *E. coli* with the ability to reduce a wide variety of S- and N-oxides present in the environment.

DmsABC, PNOR, and TorA, show alternate patterns of expression. DmsABC is expressed constitutively under anaerobic conditions, in the absence of nitrate [19]. PNOR is also expressed constitutively under anaerobic conditions, although it is not known whether expression of PNOR is repressed in the presence of nitrate (Chapter 8). TorA is induced by a variety of S- and N-oxides, and is not repressed by nitrate [28, 37]. The differential expression of these three terminal S- and N-oxide reductases in conjunction with their alternate but overlapping substrate specificities likely allows for optimal *E. coli* growth.

10.2.2. Stability of DmsABC

DmsC has been implicated in the stabilization of DmsAB (Chapter 2). Likewise, DmsA and DmsB also appear to stabilize each other. If DmsA is mutated such that it is no longer stable, both DmsA and DmsB are degraded (Chapter 4). In addition, it has not been possible to accumulate DmsA when expressed alone [50].

Although DmsABC is more stable than DmsAB, its stability contrasts that of DMSOR, TorA, and NarGHI. DmsABC was observed to lose moco during purification (Chapter 3), and is thermolabile [49]. These results contrast *R. capsulatus* DMSO reductase and DMSOR binding 0.80 and 0.93 moles of Mo per mole of purified enzyme, respectively [27, 52], and the thermostability of TorA [49] and NarGHI [1, 2]. It is not known whether the loss of moco from, and thermostability of DmsABC *in vitro*, are the result of two different processes. Substrate was shown to stabilize DmsABC activity *in vitro* at 21°C (Chapter 2). In addition, substrate has been demonstrated to stabilize interactions between DmsAB and DmsC *in vitro*, keeping the complex membrane-localized [45]. It is not known whether these two observations are connected. If so, it would suggest DmsABC is stable *in vitro*, but once binding of DmsAB to DmsC is lost, activity loss waslikely due to the instability of DmsAB (Chapter 2).

10.2.3. Assembly of Moco into DmsABC

NarGHI and NarZYV have been demonstrated to require NarJ and NarW, respectively, for correct assembly, and addition of the moco [8, 11]. These system-specific chaperones are found within the operons for nitrate reductase A and Z. No gene for a system-specific chaperone was found within the *dmsABC* operon [5]. A system-specific chaperone for DmsABC may exist elsewhere on the chromosome, although no evidence has been obtained to support this hypothesis.

NarGHI seems to possess a higher affinity for the moco, since NarGHI from aerobically grown cells binds stoichiometric quantities of moco, and anaerobically grown *moeB* mutant cells (see Figure 1.5.) bind enough moco to allow growth on Gly/nitrate. This is in contrast to DmsABC, where sub-stoichiometric amounts of moco are bound in aerobically grown cells, and no growth is observed on Gly/DMSO in a *moeB* mutant [4, 41]. In addition, reconstitution of DmsAB is very poor compared to NarGH (Chapter 2). It is likely the low reconstitution of DmsAB is at least partially due to its instability. However, narJ may be responsible for increasing the affinity of nitrate reductase A for moco under aerobic conditions, in a *moeB* mutant, and during reconstitution.

10.2.4. Double-Arginine Consensus

It has been suggested that periplasmic and membrane proteins binding a subset of redox cofactors, including the moco, have unique requirements for cofactor insertion and membrane targeting and translocation, and thus possess a double-arginine consensus. This consensus allows for their recognition by the MTT apparatus (Chapter 4 and [3, 20, 56]). Mutation of the double-arginine consensus in *Pseudomonas stutzeri* nitrous oxide reductase results in accumulation of apo-enzyme, suggesting the consensus is necessary for cofactor insertion [20].

DmsA possesses a double-arginine consensus, while it is missing from the molybdoenzymes BisC, FdhF, NarG, and NarZ [9, 10, 38, 60]. Since BisC is suggested to be cytoplasmic, the absence of a double-arginine consensus is expected. However, FdhF has been suggested to be attached to the periplasmic face of the membrane [12, 29], while NarG and NarZ are bound to the cytoplasmic face of the membrane [29]. If the double-arginine consensus is required for membrane targeting and translocation of molybdoenzymes, it is not obvious why DmsA would require a double-arginine consensus while FdhF, NarG and NarZ do not. Could NarJ and NarW fulfill the role of the double-arginine consensus for NarGHI and NarZYV by aiding in moco insertion? If so this would only leave the questionable absence of a double-arginine consensus, in addition to any kind of a leader, with FdhF [60].

10.3. Future Directions

10.3.1 DmsC

DmsC anchors DmsAB to the membrane, and is required for MQH_2 oxidation [45]. It serves to pass electrons from the Q pool to DmsB [44], and will be the important subunit in the generation of a pmf by DmsABC.

DmsC has been demonstrated to possess one Q_L site [59]. To identify the specificity of the Q_L site, and indicate the portions of MQH_2 specifically recognized by DmsC, a thorough kinetic analysis could be performed using the available Q analogues and inhibitors [32, 33].

H65 has been demonstrated to compose part of the Q_L site [44]. Additional residues important in MQH_2 binding could be identified, and this would help identify the location of the Q_L binding site with respect to the membrane. Site-directed mutagenesis, random mutagenesis in association with a selection procedure, or use of photoactivatable MQ analogues could be employed to achieve this end.

It would be interesting to determine whether DmsC also possesses a Q_H site, as has been found for CyoABCD [47]. The presence of Q_H site would aid in electron flow from DmsC to DmsB, but would be difficult to explain in light of the interaction observed between Fe-S cluster 1 and HOQNO bound to the Q_L site [44]. The presence of both Q_L and Q_H sites would support a determination that DmsABC generates a pmf, since the Q_L and Q_H sites would likely be found near the periplasmic and cytoplasmic sides of the membrane, respectively. If DmsC were determined to bind a non-dissociable Q, kinetic analysis of DmsABC in a MQ deficient strain would likely alter its kinetic parameters, but may provide information regarding electron transfer through DmsC [47].

Due to the present controversy [7, 13, 53], the involvement of DmsABC in generation of a pmf should be unequivocally determined by addition of reduced MQH_2 to DmsABC reconstituted into vesicles (as in [23]). If DmsABC were demonstrated to generate a pmf it would be important to determine whether this was via a scalar mechanism, or proton wire. Determination of the location of the Q_L binding site, and whether an additional Q_H site exists (as above), would help answer this question. If the Q_L binding site were localized to the periplasmic half of the membrane, or both Q_L and Q_H sites were found in DmsC, the simplest explanation would suggest DmsC uses a scalar mechanism to generate a pmf. If the Q_L binding site were localized to the cytoplasmic half of the membrane, or the H^+/e^- ratio was more than one, the simplest explanation would suggest DmsABC uses a proton wire to generate a pmf. In this last case, it would be important to determine the residues involved in proton translocation. Mutants obtained able to catalyze $BVH^{\cdot+}$ and $DMNH_2$ dependent reduction of DMSO, but unable to grow on Gly/DMSO, may indicated residues involved in proton conduction through DmsC.

10.3.2. DmsB

DmsB possesses four groups of Cys residues that bind four [4Fe-4S] clusters [16]. It is responsible for electron transfer from DmsC to DmsA [42].

Although Cys group III has been demonstrated to ligate cluster 1 (Figure 1.9) [42], the rest of the group-cluster pairings are speculative. In an effort to determine the remaining group-cluster pairings, the C_D Cys's from each of the four groups have been mutated, and will be examined by EPR. If the mutant enzymes do not assemble to the membrane, or if more than one of the Fe-S clusters are missing, as has been observed in other mutagenic studies [2, 34], mutation of other Cys residues could be attempted. Alternatively, residues adjacent to the Cys's could be mutated in an attempt to modulate the redox potential of the clusters, thereby aiding in their group pairing.

It has been determined that cluster 1 is the entry point for electrons into DmsB. However, the role of the other Fe-S clusters have not been determined. EPR and kinetic analysis of mutated enzymes with altered Fe-S cluster redox potentials or composition, will aid in determining whether all of the Fe-S clusters are important in electron transfer, or whether some of them play a structural or regulatory role.

10.3.3. DmsA

DmsA accepts electrons from DmsB [54], binds moco [16], and is the site of S- and N-oxide reduction [57].

DmsA binds MGD, and calculations suggest it is likely in the form of bis-MGD (Chapter 3). However, this could be unequivocally determined by analysis of phosphate versus Mo content of DmsABC [52].

Previous analysis has indicated S176 is a Mo ligand [55], and if DmsA binds two MGD's, the four dithiolene sulfurs bring the Mo ligands to five. This would leave only one unidentified ligand. Examination of the DMSOR crystal structure would suggest an additional oxo-ligand would complete the Mo ligand sphere [48]. However, this could be tested by extended-xray-fine-structure analysis. This technique gives information on the number and type of atoms surrounding the metal ion, as well as their distances [17].

It has been suggested the $E_{m,7}$ of the Mo may be influenced by the pterin redox state [39]. There have been only four studies looking at the oxidation state of MPT [21, 22, 30, 52], so there is little evidence to support this claim. However, once additional studies have accumulated, it may be possible to assess the role of MPT redox state in modulating the $E_{m,7}$ of the Mo. The pterin redox state in DmsA is unknown, but could be determined by absorption spectroscopy of moco from denatured protein, and comparison with pterin standards of known redox state. In addition, reduction of 2,6-dichloroindophenol by moco from DmsABC would determine the number of reducing equivalents in the moco corroborating absorption spectroscopy data [22, 39, 52].

Examination of the DMSOR crystal structure, and subsequent comparison of the sequences of DMSOR and DmsA, suggested important residues in DmsA to be mutated to alter substrate specificity (Chapter 7). Further examination of the crystal structures including those of FdhF, and *R. capsulatus* DMSO reductase, reveals other residues of interest [14, 31, 35, 36]. Mutation of the homologous residues in DmsA and examination of the mutants for growth on Gly/DMSO, and by kinetic analysis and EPR may reveal their role in the mechanism of DmsA .

The mechanism proposed for DMSOR (Figure 1.7.) indicates two one proton one electron donation steps (4 and 5). H643 has been suggested to be involved in electron transfer to the P-pterin prior to reduction of the Mo [31], while D145 has been suggested to be the proton donor in *R. capsulatus* DMSO reductase [31, 35]. The involvement of the homologous residues, H672 and D174 in DmsA, in electron transfer and proton donation, respectively, could be determined.

DmsABC was shown to possess a very broad electron acceptor specificity (Chapter 6). Additional kinetic analysis could determine the order of addition and release of substrate and product, and whether DmsABC is enantioselective. If DmsABC were enantioselective it would indicate broad substrate specificity (Chapter 6) is coupled with a requirement for the specific placement of substituents on the S- and N-oxides.

10.3.4. PNOR

E. coli has been shown to possess a novel terminal reductase (PNOR). Preliminary characterization of this enzyme has been performed (Chapter 8). However, the gene(s) responsible for this activity have not been determined. Their identity would significantly aid in future experiments, and result in the ability to address numerous questions, such as how many subunits are involved, and does this enzyme employ a similar mechanism to DmsABC. Growth on Gly/PNO in a *dmsABC⁻ tor⁻* mutant indicates a pmf is generated during PNO reduction, suggesting PNOR is coupled to the Q pool. However, since PNOR activity is found in the cytoplasm, it is not known how this occurs (Chapter 8). Determining the subunits involved, and their location *in vivo* would aid in answering this question. It would be interesting to examine whether binding of PNOR to the membrane is dependent on a decreased redox potential or the presence of substrate, in a manner similar to PutA or PoxB, respectively [15, 25, 26].

10.3.5. The Double-Arginine Consensus and the MTT Apparatus

Periplasmic and membrane proteins binding a subset of redox cofactors, possess a double-arginine consensus. This consensus allows for their recognition by the MTT apparatus and their subsequent membrane targeting or translocation (Figure 4.7. - Chapter 4 and [3, 20, 56]). It is believed that the MTT apparatus recognizes the double-arginine consensus, and is involved in their membrane targeting and translocation. Proteins composing the MTT apparatus have been identified. Their functions have been suggested to be a receptor for double-arginine leader proteins (MttC), a pore for translocation (MttB), and a gate for the pore (MttA) [56].

DmsA possesses a double-arginine consensus. It was found that leaderless-DmsA accumulated in the membrane but was non-functional (Chapter 4). The double-arginine consensus is suggested to be necessary for the insertion of redox cofactor [3, 20], and thus demonstration that non-functional leaderless-DmsA does not bind moco, would confirm this hypothesis.

One of the most intriguing hypotheses regarding the MTT machinery, is that it allows proteins to be translocated with bound cofactor, in the fully folded state [3]. This is in contrast to the translocation of unfolded protein by the Sec-system. Since β-galactosidase folds quickly in the cytoplasm, β-galactosidase with a fused Sec-leader can not be translocated by the Sec-system. Confirmation that the MTT machinery is responsible for translocating fully folded proteins could be obtained by demonstrating translocation of β-galactosidase with a fused double-arginine leader.

DmsABC is a complex multisubunit Fe-S molybdoenzyme. An understanding of this protein can be applied to both prokaryotic molybdoenzymes, and electron transport chain proteins. In addition, the newly identified PNOR and MTT apparatus have only preliminary characterized, and thus many interesting unanswered questions remain.

10.4. References

1. Augier, V., Asso, M., Guigliarelli, B., More, C., Bertrand, P., Santini, C.-L., Blasco, F., Chippaux, M. and Giordano, G. (1993) Removal of the high-potential [4Fe-4S] center of the b-subunit from *Escherichia coli* nitrate reductase. Physiological, biochemical, and EPR characterization of site-directed mutated enzymes. Biochem. 32, 5099-5108.

2. Augier, V., Guigliarelli, B., Asso, M., Bertrand, P., Frixon, C., Giordano, G., Chippaux, M. and Blasco, F. (1993) Site directed mutagenesis of conserved cysteine residues within the b-subunit of *Escherichia coli* nitrate reductase. Physiological, biochemical, and EPR characterization of site-directed mutated enzymes. Biochem. 32, 2013-2023.

3. Berks, B.C. (1996) A complex export pathway for proteins binding complex redox cofactors? Mol. Micro. 22, 393-404.

4. Bilous, P. and Weiner, J.H. Unpublished results.

5. Bilous, P.T., Cole, S.T., Anderson, W.F. and Weiner, J.H. (1988) Nucleotide sequence of the *dmsABC* operon encoding the

anaerobic dimethylsulphoxide reductase of *Escherichia coli.* Mol. Micro. 2, 785-795.

6. Bilous, P.T. and Weiner, J.H. (1985) Dimethyl sulfoxide reductase activity by anaerobically grown *Escherichia coli.* J. Bacteriol. 162, 1151-1155.

7. Bilous, P.T. and Weiner, J.H. (1985) Proton translocation coupled to dimethyl sulfoxide reduction in anaerobically grown *Escherichia coli* HB101. J. Bacteriol. 163, 369-375.

8. Blasco, F., Dos-Santos, J.-P., Magalon, A., Frixon, C., Guigliarelli, B., Santini, C.-L. and Giordano, G. (1998) NarJ is a specific chaperone required for molybdenum cofactor assembly in nitrate reductase A of *Escherichia coli.* Manuscript in preparation.

9. Blasco, F., Iobbi, C., Giordano, G., Chippaux, M. and Bonnefoy, V. (1989) Nitrate reductase of *Escherichia coli:* completion of the nucleotide sequence of the *nar* operon and reassessment of the role of the a and b subunits in iron binding and electron transfer. Mol. Gen. Genet. 218, 249-256.

10. Blasco, F., Iobbi, C., Ratouchniak, J., Bonnefoy, V. and Chippaux, M. (1990) Nitrate reductases of *Escherichia coli*: sequence of the second nitrate reductase and comparison with that encoded by the *narGHJI* operon. Mol. Gen. Genet. 222, 104-111.

11. Blasco, F., Pommier, J., Augier, V., Chippaux, M. and Giordano, G. (1992) Involvement of the *narJ* or *narW* gene product in the formation of active nitrate reductase in *Escherichia coli.* Mol. Micro. 6, 221-230.

12. Bock, A. and Sawers, G. (1996) Fermentation, in *Escherichia coli* and *Salmonella* Cellular and Molecular Biology. (Neidhardt, F.C., ed.), Vol. 1, p. 262-282, ASM Press, Washington.

13. Bogachev, A.V., Murtazina, R.A. and Skulachev, V.P. (1996) H+/e- stoichiometry for NADH dehydrogenase I and dimethyl sulfoxide reductase in anaerobically grown *Escherichia coli* cells. J. Bact. 178, 6233-6237.

14. Boyington, J.C., Gladyshev, V.N., Khangulov, S.V., Stadtman, T.C. and Sun, P.D. (1997) Crystal structure of formate dehydrogenase H: catalysis involving Mo, molybdopterin, selenocysteine, and an Fe_4S_4 cluster. Science 275, 1305-1308.

15. Brown, E.D. and Wood, J.M. (1993) Conformational change and membrane association of the PutA protein are coincident with

reduction of its FAD cofactor by proline. J. Biol. Chem. 268, 8972-8979.

16. Cammack, R. and Weiner, J.H. (1990) Electron paramagnetic resonance spectroscopic characterization of dimethyl sulfoxide reductase of *Escherichia coli*. Biochemistry 29, 8410-8416.

17. Campbell, I.C. and Dwek, R.A. (1984) Biological Spectroscopy, p. 338-339, Benjamin/Cummings Publishing Company, Inc., Menlo Park.

18. Chan, M.K., Mukund, S., Kletzin, A., Adams, M.W.W. and Rees, D.C. (1995) Structure of a hyperthermophilic tungstopterin enzyme, aldehyde ferredoxin oxidoreductase. Science 267, 1463-1469.

19. Cotter, P.A. and Gunsalus, R.P. (1989) Oxygen, nitrate, and molybdenum regulation of *dmsABC* gene expression in *Escherichia coli*. J. Bact. 171, 3817-3823.

20. Dreusch, A., Burgissser, D.M., Heizmann, C.W. and Zumft, W.G. (1997) Lack of copper insertion into unprocessed cytoplasmic nitrous oxide reductase generated by an R20D substitution in the arginine consensus motif of the signal peptide. Biochim. Biophys. Acta 1319, 311-318.

21. Gardlik, S. and Rajagopalan, K.V. (1991) The mechanism of inactivation of sulfite oxidase by periodate and arsenite. J. Biol. Chem. 266, 16627-16632.

22. Gardlik, S. and Rajagopalan, K.V. (1991) Oxidation of molybdopterin in sulfite oxidase by ferricyanide. J. Biol. Chem. 266, 4889-4895.

23. Geisler, V., Ullmann, R. and Kroger, A. (1994) The direction of the proton exchange associated with the redox reactions of menaquinone during electron transport in *Wolinella succinogenes*. Biochim. Biophys. Acta 1184, 219-226.

24. Giordano, G. Personal communication.

25. Grabau, C., Chang, Y. and J. E. Cronan, J. (1989) Lipid binding by *Escherichia coli* pyruvate oxidase is disrupted by small alterations of the carboxy-terminal region. J. Biol. Chem. 264, 12510-12519.

26. Grabau, C. and Cronan, J.E. (1986) *In vivo* function of *Escherichia coli* pyruvate oxidase specifically requires a functional lipid binding site. Biochem. 25, 3748-3751.

27. Hilton, J.C. and Rajagopalan, K.V. (1996) Identification of the molybdenum cofactor of dimethyl sulfoxide reductase from *Rhodobacter sphaeroides* f. sp. *denitrificans* as bis(molybdopterin guanine dinucleotide)molybdenum. Arch. Biochem. Biophys. 325, 139-143.

28. Iobbi-Nivol, C., Pommier, J., Simala-Grant, J.L., Mejean, V. and Giordano, G. (1996) High substrate specificity and induction characteristics of trimethylamine N-oxide reductase of *Escherichia coli*. Biochim. Biophys. Acta 1294, 77-82.

29. Jones, R.W. and Garland, P.B. (1977) Sites and specificity of the reaction of bipyridylium compounds with anaerobic respiratory enzymes of *Escherichia coli*. Biochem. J. 164, 199-211.

30. Kessler, D.L. and Rajagopalan, K.V. (1974) Hepatic sulfite oxidase. Identification of the molybdenum center as the site of irreversible inactivation by ferricyanide. Biochim. Biophys. Acta 370, 399-409.

31. Knablein, J., Dobbek, H., Ehlert, S. and Schneider, F. (1997) Isolation, cloning, sequence analysis and X-ray structure of dimethyl sulfoxide/trimethylamine N-oxide reductase from *Rhodobacter sphaeroides*. Biol. Chem. 378, 293-302.

32. Lemma, E., Hagerhall, C., Geisler, V., Brandt, U., vonJagow, G. and Kroger, A. (1991) Reactivity of the *Bacillus subtilis* succinate dehydrogenase complex with quinones. Biochim. Biophys. Acta 1059, 281-285.

33. Lemma, E., Unden, G. and Kroger, A. (1990) Menaquinone is an obligatory component of the chain catalyzing succinate respiration in *Bacillus subtilis*. Arch. Microbiol. 155, 62-67.

34. Manodori, A., Cecchini, G., Schroder, I., Gunsalus, R.P., Werth, M.T. and Johnson, M.K. (1992) [3Fe-4S] to [4Fe-S] cluster conversion in *Escherichia coli* fumarate reductase by site-directed mutagenesis. Biochemistry 31, 2703-2712.

35. McAlpine, A.S., McEwan, A.G. and Bailey, S. (1998) The high resolution crystal structure of DMSO reductase in complex with DMSO. J. Mol. Biol. In press.

36. McAlpine, A.S., McEwan, A.G., Shaw, A.L. and Bailey, S. (1998) Molybdenum active center of DMSO reductase from *Rhodobacter capsulatus* : crystal structure of the oxidised enzyme at 1.82Å resolution and the dithionite-reduced enzyme at 2.8Å resolution. J. Biol. Inorg. Chem. In press.

37. Pascal, M.-C., Burini, J.-F. and Chippaux, M. (1984) Regulation of the trimethylamine N-oxide (TMAO) reductase in *Escherichia coli* : Analysis of *tor*:Mud1 operon fusion. Mol. Gen. Genet. 195, 351-355.

38. Pearson, D.M., O'Reilly, C., Colby, J. and Black, G.W. (1994) DNA sequence of the *cut A, B* and *C* genes, encoding the molybdenum containing hydroxylase carbon monoxide dehydrogenase, from *Pseudomonas thermocarboxydovorans* strain C2. Biochim. Biophys. Acta 1188, 432-438.

39. Rajagopalan, K.V. (1991) Novel aspects of the biochemistry of the molybdenum cofactor. Adv. Enz. Rel. Areas Mol. Biol. 64, 215-289.

40. Romao, M.J., Chan, M.K., Mukund, S., Kletzin, A., Adams, M.W.W. and Rees, D.C. (1995) Crystal structure of the xanthine oxidase-related aldehyde oxido-reductase from *D. gigas*. Science 270, 1170-1176.

41. Rothery, R. and Weiner, J.H. Unpublished results.

42. Rothery, R.A. and Weiner, J.H. (1991) Alteration of the iron-sulfur cluster composition of *Escherichia coli* dimethyl sulfoxide reductase by site-specific mutagenesis. Biochemistry 30, 8296-8305.

43. Rothery, R.A. and Weiner, J.H. (1993) Topological characterization of *Escherichia coli* DMSO reductase by electron paramagnetic spectroscopy of an engineered [3Fe-4S] cluster. Biochem. 32, 5855-5861.

44. Rothery, R.A. and Weiner, J.H. (1996) Interaction of an engineered [3Fe-4S] cluster with a menaquinol binding site of *Escherichia coli* DMSO reductase. Biochem. 35, 3247-3257.

45. Sambasivarao, D., Scraba, D.G., Trieber, C. and Weiner, J.H. (1990) Organization of dimethyl sulfoxide reductase in the plasma membrane of *Escherichia coli*. J. Bacteriol 172, 5938-5948.

46. Sambasivarao, D. and Weiner, J.H. (1991) Differentiation of the multiple S- and N-oxide reducing activities of *Escherichia coli*. Curr. Microbiol. 23, 105-110.

47. Sato-Watanabe, M., Mogi, T., Ogura, T., Kitagawa, T., Miyoshi, H., Iwamura, H. and Anraku, Y. (1994) Identification of a novel quinone-binding site in the cytochrome *bo* complex from *Escherichia coli*. J. Biol. Chem. 46, 28908-28912.

48. Schindelin, H., Kisher, C., Hilton, J., Rajagopalan, K.V. and Rees, D.C. (1996) Crystal structure of DMSO reductase: Redox-linked changes in molybdopterin coordination. Science 272, 1615-1621.

49. Silvestro, A., Pommier, J., Pascal, M.-C. and Giordano, G. (1989) The inducible trimethylamine N-oxide reductase of *Escherichia coli* K12: its localization and inducers. Biochim. Biophys. Acta 999, 208-216.

50. Simala-Grant, J.L. and Weiner, J.H. Unpublished results.

51. Simala-Grant, J.L. and Weiner, J.H. (1996) Kinetic analysis and substrate specificity of *Escherichia coli* dimethyl sulfoxide reductase. Microbiol. 142, 3231-3239.

52. Solomon, P.S., Lane, I., Hanson, G. and McEwan, A.G. (1997) Characterisation of the pterin molybdenum cofactor in dimethylsulfoxide reductase of *Rhodobacter capsulatus*. Eur. J. Biochem. 246, 200-203.

53. Tran, Q.H., Bongaerts, J., Vlad, D. and Unden, G. (1997) Requirement for the proton-pumping NADH dehydrogenase I of *Escherichia coli* in respiration of NADH to fumarate and its bioenergetic implications. Eur. J. Biochem. 244, 155-160.

54. Trieber, C.A., Rothery, R.A. and Weiner, J.H. (1994) Multiple pathways of electron transfer in dimethyl sulfoxide reductase of *Escherichia coli*. J. Biol. Chem. 269, 7103-7109.

55. Trieber, C.A., Rothery, R.A. and Weiner, J.H. (1996) Consequences of removal of a molybdenum ligand (DmsA-Ser176) of *Escherichia coli* dimethyl sulfoxide reductase. J. Biol. Chem. 271, 27339-27345.

56. Weiner, J.H., Bilous, P.T., Shaw, G., Lubitz, S.P., Thomas, G.H., Cole, J.A. and Turner, R.J. (1998) Novel and ubiquitous system for the membrane targeting and translocation of proteins containing a double arginine leader. In press. Cell.

57. Weiner, J.H., Rothery, R.A., Sambasivarao, D. and Trieber, C.A. (1992) Molecular analysis of dimethylsulfoxide reductase : a complex iron-sulfur molybdoenzyme of *Escherichia coli*. Biochim. Biophys. Acta 1102, 1-18.

58. Weiner, J.H., Shaw, G., Turner, R.J. and Trieber, C.A. (1993) The topology of the anchor subunit of dimethyl sulfoxide reductase of *Escherichia coli*. J. Biol. Chem. 268, 3238-3244.

59. Zhao, Z. and Weiner, J.H. (1998) Interaction of HOQNO with dimethylsulfoxide reductase of *Escherichia coli*. Submitted.

60. Zinoni, F., Birkmann, A., Stadtman, T.C. and Bock, A. (1986) Nucleotide sequence and expression of the selenocysteine-containing polypeptide formate dehydrogenase (formate-hydrogen-lyase-linked) from *Escherichia coli*. Proc. Natl. Acad. Sci. 83, 4650-4654.

Appendix : Inability of BisC to Complement Deletion of DmsABC

A.1. Introduction

The molybdoenzyme [5, 8] BisC reduces d-biotin d-sulfoxide to d-biotin [6]. This enzyme may function either to scavenge biotin sulfoxide to be used as a source for biotin, or to reduce biotin sulfoxide bound to protein, that has spontaneously oxidized [8]. BisC shows sequence homology to DmsA [9], as well as other molybdoenzymes [1]. A second biotin sulfoxide reductase gene has been cloned (BisZ), this protein accounts for 4% of the biotin sulfoxide reductase activity in the cell [4].

The substrate specificity of BisC has not been examined, but reduction of other S- and N-oxides may be possible, as some molybdoenzymes have shown broad substrate specificity [7, 12-14].

Although BisC is soluble and cytoplasmic [6], it is possible that BisC could transiently associate with the membrane, accepting electrons from the MQH_2 either directly, or mediated by another protein. If this were the case, reduction of biotin sulfoxide could be coupled to formation of a pmf.

It was determined whether overproduction of BisC could complement deletion of DmsABC, by restoring growth on Gly/DMSO media. This would indicate BisC can reduce DMSO, and couple this reduction to energy conserving reactions.

A.2. Materials and Methods

A.2.1. Materials

All materials were reagent grade, and were purchased from commercial sources.

A.2.2. Strains and Plasmids

E. coli strains HB101 (*supE*44 *hsdS*20($r_B^- m_B^-$) *recA*13 *ara*-14 *procA*2 *lacY*1[3]) and DSS501 (*ara*D139 (*lac*IPOZYA-*arg*F)U169 *rps*L *thi* *torA*::Mud1 (Ap^r-*lac*) Δ*dms* Kan^R [10]), and plasmid pBRBISC352 (pBR322 Amp^S Tet^R (*bisC*)$^+$) are used in this study. The 5.8 kbp insert from pBISC352 [8], was subcloned using *Pst*I and *Eco*RI into pBR322, cut with the same restriction enzymes. This resulted in the Tet^R Amp^S clone pBRBISC352. DSS501 was transformed with pBRBISC352 for expression of BisC. All manipulations of plasmids and strains were carried out essentially as described by Sambrook et al. [11].

A.2.3. Media and Growth Conditions

HB101 and DSS501, with or without pBRBISC352, were grown aerobically in LB [11] overnight, and these cultures were used as 1% inocula for Gly/DMSO, as indicated previously [2], with the following exceptions. 0.16% peptone was substituted for casamino acids, and streptomycin sulfate was not included in the growth medium. Vitamin B1, proline, leucine, and arginine, were included at a final concentration of 0.005%. Fifty-100 μg/mL ampicillin, 40 μg/mL kanamycin, and 35 μg/mL tetracycline was included in the growth medium. Quantitative anaerobic growth experiments were performed in Klett flasks [10], filled to the top with Gly/DMSO, and sealed to exclude O_2. Magnetic stir bars were employed for mixing of the cultures during growth at 30°C.

A.3. Results

A.3.1 Anaerobic Growth of DSS501/ pBRBISC352 on Gly/DMSO

DmsABC is responsible for growth on Gly/DMSO media [10]. HB101 bears a chromosomal copy of DmsABC and is able to grow on Gly/DMSO. However, DSS501 is unable to grow on this media, as *dmsABC* is deleted from this strain. When pBRBISC352, bearing the BisC gene is transformed into DSS501, the strain is still unable to grow on Gly/DMSO media (Figure A.1.).

A.4. Discussion

The results indicate BisC overexpression does not complement deletion of DmsABC. Possible reasons for this observation are that BisC is unable to reduce DMSO, is not expressed to high enough levels, or reduction of DMSO is not coupled to energy yielding reactions.

A.5. References

1. Berks, B.C., Ferguson, S.J., Moir, J.W.B. and Richardson, D.J. (1995) Enzymes and associated electron transport systems that catalyze the respiratory reduction of nitrogen oxides and oxyanions. Biochim. Biophys. Acta 1232, 97-123.
2. Bilous, P.T. and Weiner, J.H. (1985) Dimethyl sulfoxide reductase activity by anaerobically grown *Escherichia coli*. J. Bacteriol. 162, 1151-1155.
3. Boyer, H.W. and Roulland-Dussoix, D. (1969) A complementary analysis of the restriction and modification of DNA in *Escherichia coli*. J. Mol. Biol. 41, 459.
4. delCampillo-Campbell, A. (1996) Alternative gene for biotin sulfoxide reduction in *Escherichia coli* K-12. J. Mol. Evol. 42, 85-90.

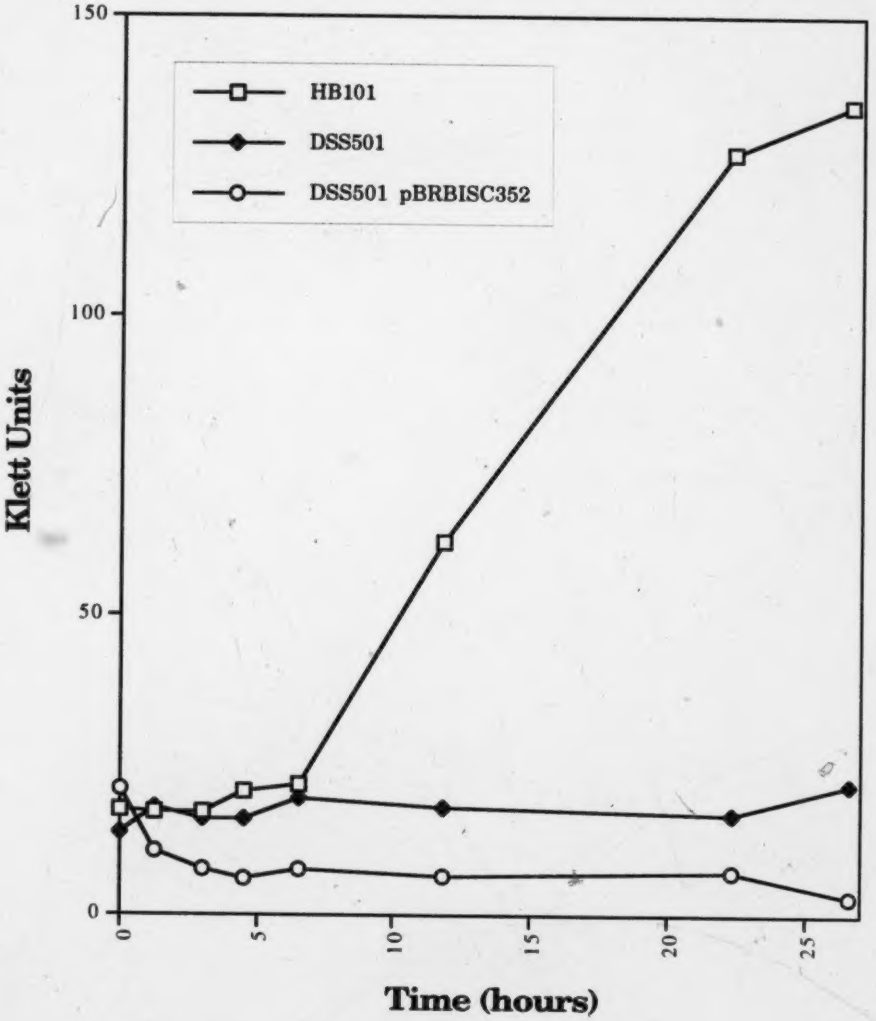

Figure A.1.

Anaerobic Growth of HB101 and DSS501, with or without pBRBISC352, on Gly/DMSO Media

Growth readings were taken, as necessary, with a Klett-Summerson spectrophotometer, equipped with a number 66 filter, using minimal media as a blank.

5. delCampillo-Campbell, A. and Campbell, A. (1982) Molybdenum cofactor requirement for biotin sulfoxide reduction in *Escherichia coli*. J. Bact. 149, 469-478.

6. delCampillo-Campbell, A., Dykhuizen, D. and Cleary, P. (1979) Enzymic reduction of d-biotin d-sulfoxide to d-biotin. Meth. Enzymol. 62, 379-385.

7. MacEwan, A.G., Wetstein, H.G., Meyer, O., Jackson, J.B. and Ferguson, S.J. (1987) The periplasmic nitrate reductase of *Rhodobacter capsulatus*; purification, characterisation and distinction from a single reductase for trimethylamine-N-oxide dimethylsulphoxide and chlorate. Arch. Microbiol. 147, 340-345.

8. Pierson, D.E. and Campbell, A. (1990) Cloning and nucleotide sequence of *bisC*, the structural gene for biotin sulfoxide reductase in *Escherichia coli*. J. Bact. 172, 2194-2198.

9. Pollock, V.V. and Barber, M.J. (1995) Molecular cloning and expression of biotin sulfoxide reductase from *Rhodobacter sphaeroides* forma sp. *denitrificans*. Arch. Biochem. Biophys. 318, 322-332.

10. Sambasivarao, D. and Weiner, J.H. (1991) Differentiation of the multiple S- and N-oxide reducing activities of *Escherichia coli*. Curr. Microbiol. 23, 105-110.

11. Sambrook, J., Fritsch, E.F. and Maniatis, T. (1989) Molecular cloning : A laboratory manual. Cold Spring Harbor Laboratory Press, Cold Spring Harbor, N.Y.

12. Satoh, T. and Kurihara, F.N. (1987) Purification and properties of dimethylsulfoxide reductase containing a molybdenum cofactor from a photodenitrifier, *Rhodopseudomonas sphaeroides* f.s. *denitrificans*. J. Biochem 102, 191-197.

13. Simala-Grant, J.L. and Weiner, J.H. (1996) Kinetic analysis and substrate specificity of *Escherichia coli* dimethyl sulfoxide reductase. Microbiol. 142, 3231-3239.

14. Weiner, J.H., MacIsacc, D.P., Bishop, R.E. and Bilous, P.T. (1988) Purification and properties of *Escherichia coli* dimethyl sulfoxide reductase, an iron-sulfur molybdoenzyme with broad substrate specificity. J. Bacteriol. 170, 1505-1510.